UNIVERSIDAD COMPLUTENSE DE MADRID

FACULTAD DE PSICOLOGÍA

Departamento de Psicobiología

TESIS DOCTORAL

Dopamine signaling is essential in cognitive process and motor performance

La señal dopaminérgica es esencial en los procesos cognitivos y la función motora

MEMORIA PARA OPTAR AL GRADO DE DOCTOR

PRESENTADA POR

Isabel Espadas Villanueva

Directora

Rosario Moratalla Villalba

Madrid, 2016

UNIVERSIDAD COMPLUTENSE DE MADRID
FACULTAD DE PSICOLOGIA
Departamento de Psicobiología

INSTITUTO CAJAL
CONSEJO SUPERIOR DE INVESTIGACIONES CIENTIFICAS

Dopamine signaling is essential in cognitive process and motor performance

TESIS DOCTORAL

Isabel Espadas Villanueva

MADRID, 2015

UNIVERSIDAD COMPLUTENSE DE MADRID
FACULTAD DE PSICOLOGIA
Departamento de Psicobiología

INSTITUTO CAJAL
CONSEJO SUPERIOR DE INVESTIGACIONES CIENTIFICAS

Dopamine signaling is essential in cognitive process and motor performance

Memoria presentada por Isabel Espadas Villanueva

para optar al título de Doctor,

elaborada a partir del trabajo realizado bajo la dirección de la

Dra. Rosario Moratalla Villalba, en el Instituto Cajal, (CSIC), Madrid.

Doña Rosario Moratalla Villalba, Profesor Titular del Instituto Cajal en el CSIC de Madrid

CERTIFICA

Que Doña Isabel Espadas Villanueva ha realizado en el departamento de Neurobiología Funcional y de Sistemas, del Instituto Cajal, bajo mi dirección, el presente trabajo de investigación correspondiente a la Tesis Doctoral: “Dopamine signaling is essential in cognitive process and motor performance”.

Revisado el presente trabajo, considero que la presente memoria reúne todos los requisitos necesarios para ser sometida a juicio de la Comisión correspondiente

Y para que así conste y surta los efectos oportunos, firmo la presente en Madrid a …… de ……...de 2015.

Fdo. Rosario Moratalla Villalba

"Los científicos se esfuerzan por hacer posible lo imposible.
Los políticos, por hacer lo posible imposible"

Bertrand Russell

A mis padres y hermana

Quiero expresar mi más sincero agradecimiento a todas las personas e instituciones que, en mayor o en menor medida, han contribuido a la realización de esta Tesis Doctoral, en especial:

A mi directora de Tesis, la Dra. Rosario Moratalla Villalba, por darme la oportunidad de trabajar en su magnífico equipo, y haberme mantenido en plantilla durante todos estos años, con el gran esfuerzo que ello conlleva en momentos tan duros como los que actualmente vivimos. Agradezco especialmente la confianza que ha volcado en mi trabajo y la oportunidad de disfrutar de una serie de recursos materiales y formativos que han facilitado mi desarrollo como investigadora.

A todas las instituciones que han financiado este trabajo con los proyectos de investigación concedidos a la Dra. Moratalla: CIBERNED #CB06/05/0055, Cominidad de Madrid ref. S2010/BMD-2336 y especialmente el proyecto del Ministerio de Economía y Competitividad #BFU2010-20664 del que procede la beca FPI que he disfrutado durante estos últimos años. Deseo añadir además al Consejo Superior de Investigaciones Científicas (CSIC) y al CIBERNED, organismos con los que pude disfrutar diferentes contratos anteriores a la concesión de la beca FPI.

A la Dra. Raquel Gómez de Heras, mi tutora de la Universidad Complutense de Madrid (UCM), porque siempre ha encontrado un hueco para atenderme y prestarme su ayuda en todo lo que ha podido. Sin su orientación y la del personal de la secretaría de psicología, a los cuales estoy muy agradecida, hacía ya tiempo que habría naufragado en un mar de burocracia.

A los compañeros de AG-Ciencia y los miembros del colectivo Carta por la Ciencia y afines, por no desistir al desanimo y seguir luchando durante todo este tiempo, a pesar de la falta de recursos y personal en algunas convocatorias. Gracias a su trabajo muchos podemos seguir realizando el nuestro.

A todos los colaboradores que han hecho posible este y otros trabajos:

En primer lugar a mis maestros de microscopía electrónica, el Dr. Ricardo Martín del Instituto Cajal, quién me enseño a dar los primeros pasos en este apasionante mundo lleno de posibilidades. A la Dra. Antonia Gutiérrez y su equipo, especialmente al Dr. Jose Carlos Dávilia y Angela Gómez de la Universidad de Málaga, que me enseñaron a depurar la técnica e interpretar mejor mis resultados, además de hacerme sentir como en casa el tiempo que estuve en su laboratorio. Y finalmente, aunque no menos importante, a Martin I. Maher, técnico de microscopia electrónica del Instituto Cajal, porque ha demostrado una paciencia infinita conmigo, siempre dispuesto a realizar trabajos muchas veces nada sencillos, ayudándome a mejorar y re-elaborando protocolos, sin su ayuda este y otros estudios hubiesen sido "imposibles" de realizar.

Al Dr. Jose Maria Delgado y la Dra. Agnés Gruart de la División de Neurociencias de la Universidad Pablo Olavide de Sevilla, por su dedicación y compromiso en los estudios de electrofisiología incluidos en este trabajo.

Al Dr. Eduardo D. Martin y la Dra. Idaira Oliva del Laboratorio de Neurofisiología y Plasticidad Sináptica, del Parque Científico y Tecnológico de Albacete (PCYTA) por su ayuda con los experimentos de voltametría.

A Dr. Carlos Vicario y los miembros de su equipo, por estar siempre dispuestos a echar una mano.

Al Dr. Javier Fernández Ruiz y su equipo, especialmente a Cristina Palomo, con quien he tenido el placer de trabajar y descubrir, además de una investigadora eficaz, a una maravillosa persona.

Al Dr. Jose Luis Ortega por su consejo inestimable sobre la redacción y traducción de esta tesis.

Por supuesto, no puedo dejar de agradecer este trabajo a mis compañeros del B-01, amigos y casi familia. Gracias por vuestro apoyo y amistad en los buenos y malos momentos, dentro y fuera del laboratorio. En primer lugar, dar las gracias a nuestros técnicos que se llevan muchos de las peores cosas de este trabajo y muy pocas de las buenas. Sin su esfuerzo diario muchos trabajos no saldrían adelante. A Emy, su experiencia y sentido común son inestimables, además por cuidar siempre de nosotros como si fuésemos sus niños. A Marco, técnico como existen pocos, no se me ocurre mejor manera de decirlo, con su creatividad inagotable es capaza de convertir siempre lo imposible en posible y con su sentido del humor hacerte reír incluso en los peores momentos. A Beatriz por su eficacia y su fortaleza envidiable, siempre capaz de sacar lo mejor de si misma en las peores situaciones y dispuesta ha ayudar por mucho trabajo que tenga. Gracias también a los demás técnicos en prácticas que han pasado por el laboratorio y que tanto se han esforzado por adaptarse y atender nuestras demandas.

A Noe, por haberme mimado tanto desde el día en que llegue, enseñándome todo con suma paciencia, incluso aunque haya estado a punto de hacer saltar el laboratorio por los aires….en fin, esas cosas que pasan. No tengo forma de agradecer que haya sido mi salvavidas en tantas ocasiones. A Irene por haber sido mi guía, especialmente en mis primeros días, gracias por ayudarme a integrarme en el laboratorio y en centro, por su energía y humor, todo se vuelve demasiado triste cuando ella no esta. A Patricia, por sus inquietudes infinitas, sus ganas continuas de saber y de superarse a si misma, a su lado es imposible no aprender cada día cosas nuevas. Gracias también por dedicar su tiempo y esfuerzo en la generación de los lentivirus utilizados en este trabajo. A Sara por su carácter sereno y por se capaz de poner siempre cordura en mitad del caos. A Lula, por su increíble capacidad para es-

tar en todo. A Oscar porque aunque tenga ese "puntito canalla" en el fondo es todo corazón. A Lorena, por su tesón y su dulzura, siempre pensando en los demás antes que en si misma. A Lili, una de las mejores personas que he conocido en lo laboral y en lo personal, siempre dispuesta a ayudar y a compartir todo con los demás. A Rubén, por ser siempre el perfecto anfitrión. Y a los que se fueron hace tiempo, la Dra. Sanja Darmopil y el Dr. Oskar Ortiz, por estar siempre dispuestos a prestarme su ayuda desde la lejanía.

A los demás chicos que han pasado por el laboratorio, que han sido muchos. Especialmente a Ana por ser la niña mas dulce y con más paciencia que he conocido nunca. A Chema porque no hay lugar de Madrid donde no nos hayamos encontrado y por enseñarme a perfundir mi primer ratón sin caerme al suelo redonda. A Guille y Samu, pack-indivisible, porque son capaces de recordarme cada día las razones y la ilusión que tenía cuando empecé a trabajar en esto.

Gracias también a todo el personal del Instituto Cajal, desde el servicio de administración, pasando por las chicas de análisis de imagen, el equipo de animalario, mantenimiento y seguridad. Gracias por haberme facilitado la vida en tantas ocasiones.

A mis compañeros del Master de Psicofarmacología por ayudarme en mi adaptación a la vida madrileña. Especialmente a Aidee Berni, por haber tenido siempre abierta su casa y su corazón para acogerme. A Carmencilla que me lo perdona todo y siempre esta ahí cuando la necesito. A (Afro)-Carlos, porque con es el único con el que es posible perder tu parada de metro a ultima hora de la noche hablando de las ventajas de la resonancia de 9 Teslas. A Vic, por conseguir resolver todas mi dudas científicas, por su elegancia, su cariño y porque a su lado es imposible aburrirse.

Por supuesto es imposible olvidar la Universidad de Jaén y a quienes me enseñaron a dar mis primeros pasos en este mundo, los me dieron la motivación suficiente para seguir y llegar hasta hoy. En primer lugar dar las gracias al Dr. Gustavo Reyes y la Dra. Elisabeth Ruiz, con quienes tuve la oportunidad de acercarme a este mundo. Gracias por haberme dedicado tan atentamente su tiempo y tratarme como una más desde el primer día. Gracias por supuesto a la Dr. Carmen Torres Bares, que para mi es todo un ejemplo como científica y como persona. Gracias por enseñarme tantas cosas, por cuidarme tan bien y por no faltar nunca. Gracias por darme la oportunidad de trabajar junto a suestupendo equipo. A la Dra Marta Sabariego y a Gema cantero por ser las mejores "apañeras" del mundo, así como a la Dra Lourdes de la Torre y al resto del equipo. Nunca podré olvidar el tiempo que pase con vosotras (y aún menos la primera vez que tuve que atrapar una rata histérica).

A mi profesor de química el Dr. Carlos Marjaliza del Instituto Ojos del Guadiana de Daimiel. Por todo lo que aprendí gracias a él, aunque muchas veces mis calificaciones no fueran las mejores.

A los amigos que hice durante la carrera a los que me vuelvo a reencontrar en los sitios mas insospechados. Y por supuesto a mis amigos de toda la vida que me han visto crecer y siguen recibiéndome con los brazos abierto siempre que vuelvo.

A Ana, Sosio y Abril (mi pequeña golondrina), por estar a mi lado en todas y ser como mi familia. Existe poca gente con tan buen corazón y sensatez. Porque por mucho que la vida les quite, ellos han seguido compartiendo lo poco que tenían y no han dejado de luchar por hacer de este un mundo un lugar mejor.

A mi familia por su amor y su apoyo incondicional, especialmente en estos últimos años, tan duros para todos, en que hemos tenido que decir adiós a seres queridos que nos dejaron un vacío que nunca volverá a llenarse. Gracias por creer siempre en mi y apoyarme en todos los proyectos. Gracias a mis abuelos por cuidarme tanto, especialmente a los que ahora ya no están porque se que hubiesen disfrutado con esto. Y a mis tíos, por ser mas que tíos, también mis amigos.

Quiero dedicar especialmente esta tesis a mis padres ya que sin su ayuda todo esto hubiese sido imposible. Desde siempre me enseñaron a valorar el conocimiento, porque el saber es lo único que puede hacernos libres. Y a mi hermana a la que siento como un cachito de mi propio alma.

Finalmente y de forma especial a Pedro, por se el mejor "compañero de viaje" (#ranciofact), por no decir nunca que no a nada y sacrificar muchas cosas de su vida para hacer la mía mejor. Su empeño fue el que me animó a dar este paso.

Index

LIST OF ABREVIATIONS

6-OHDA	6-hydroxydopamine
AADC	L-amino acid decarboxylase
Ac	adenylyl ciclase
AMPA	alfa-amino-3-hydroxy-5-methyl-4-Isoxazol
ANOVA	analysis of variance
ATP	adenosine triphosphate
BAC	bacterial artificial chromosome
BG	basal ganglia
BSA	bovine serum albumin
CA	cornu ammonis
cAMP	cyclic adenosine monophosphate
CBP	CREB binding protein
cDNA	complementary deoxyribonucleic acid
COMT	catechol-O-methyltransferase
CREB	cAMP response element binding
CS	conditioned stimulus
D_1R/*Drd1a*	dopamine D1 receptor
D_2R/*Drd2*	dopamine D2 receptor
D_3R	dopamine D3 receptor
D_4R	dopamine D4 receptor
D_5R	dopamine D5 receptor
DAB	3,3´-diaminobenzidine
DABCO	1,4-diazibicyclo [2,2,2] octane
DARPP-32	cAMP-regulated phosphoprotein 32kDa
DAT	dopamine transporter
DG	dentate gyrus
DOPAC	2,4-dihydroxyphenylacetic
EDTA	ethylenediaminetetraacetic acid
EMG	electromyogram
ERK	extracellular signal-regulated protein Kinase 1 and 2
fEPSP	field excitatory postsynaptic potentials
FosB	FBJ murine osteosarcoma viral oncogene homolog B
FSCV	fast scan cyclic voltammetry
Gαi/o	inhibitory type G-protein α subunit
Gαolf	olfactory type G-protein α subunit
Gαs	stimulatory type G-protein α subunit
GABA	gamma-aminobutyric acid
GAPDH	glyceraldehyde 3-phosphate dehydrogenase
GFP	green fluorescent protein
GluR1	AMPA glutamate receptor subunit type1
GPCRs	G protein-coupled receptors
GPi	globus pallidus pars interna
GTP	guanosine triphosphate
HFS	high-frequency stimulation
HEK293	human embryonic kidney cells 293
HVA	hemovallinic acid
IEGs	immediate-early genes
ir	inmunoreactive
ITI	inter-trial interval
LB	Lewy bodies
L-DOPA	L-3,4-dyhydroxyphanyl-L-alanine
LID	L-DOPA-induced dyskinesia
LTM	long-term memory
Lv	lentiviral vector
MAO	monoamine oxidase
MCI	mild-cognitive impairment
MPTP	1-methyl-4-phenyl-1,2,3,6-Tetrahydropyridine
mRNA	messenger ribonucleic acid
MSN	medium spiny neurons
MWM	Morris water maze
Nac	nucleus accumbens
NaCL	sodium chloride
NaF	sodium fluoride
NCS-1	neuronal calcium sensor 1
NMDA	N-methyl-D-aspartate
NR1	NMDA receptor NR1 subunit
OB	olfactory bulb
ORT	object recognition test
PBS	phosphate buffer solution
PBS-Tx	triton X-100 PBS
PCR	polymerase chain reaction
PD	Parkinson´s disease
PDD	Parkinson´s disease dementia
PFA	paraformaldehyde
PFc	prefrontal crotex
PKA	protein kinase A
RT-qPCR	real time quantitative PCR
SCH23390	R-(+)-7-cloro-8-hydroxy-3-methyl-l fenyl-2,3,4,5-tetrahydro-1H-3-benzapine

SDS-PAGE	sodium dodecyl sulfate polyacrylamide gel electrophoresis
SEM	standard error of the mean
siRNA	small interferin RNA
SN	substantia nigra
SNc	substantia nigra pars compacta
SNr	substantia nigra pars reticulata
STh	subthalamic nucleus
STM	short term memory
TEM	transmission electron microscope
TH	tyrosine hydroxylase
US	unconditioned stimulus
VMAT	vesicular monoamine transporter
VTA	ventral tegmental area
WM	working memory
WT	wild type mice

Summary

Dopamine is one of the main neurotransmitters in the central nervous system involved in neuroendocrine, motivational/emotional and, especially, cognitive and motor functions. These processes are mediated by the stimulation of the principal dopamine receptors: D_1 (D_1R) and D_2 (D_2R). In this doctoral dissertation we studied the role of both receptors in learning and memory processes, as well as their regulation of striatal TH-immunoreactive (TH-ir) neurons and the involvement in motor response.

To elaborate this project we used knock-out mice for D_1 (*Drd1a*$^{-/-}$) and D_2 (*Drd2*$^{-/-}$) receptors because there are no pharmacological agents that effectively differentiate between dopamine receptors of the same family. In addition, for the striatal TH-ir neurons study, we used mice with striatal unilateral 6-OHDA lesions, chronically treated with L-DOPA, this being the most effective mechanism to induce the expression of striatal TH-ir neurons. To complete this work, we carried out behavioral tests that analyze the motor response, e.g. cylinder test, and different types of learning and memory process, e.g. Barnes maze.

The role of D_1R is essential in the learning and memory processes.

The results in behavioral test for *Drd1a*$^{-/-}$ mice showed that the dopaminergic signal mediated by D_1R is essential in learning and memory functions for spatial, associative and recognition types. Mutant animals were unable to respond correctly in these tests, showing a complete inability to spatial navigation, understand basic associations between stimuli or recognize familiar objects. All of these indicate the importance of the D_1R mediated dopaminergic response in the memories of past experiences. Therefore, our experiments indicate that the role of D_1R is essential in all described processes of learning and memory consolidation.

The D_2R absence affects learning and synaptic plasticity processes associated.

In the present work we analyzed the role of D_2R in learning and memory process as well as changes in hippocampal plasticity associated. The obtained results showed that D_2R is important but not decisive for spatial learning. However, *Drd2*$^{-/-}$ mice were unable to perform associative tasks such as the active avoidance. Afterwards, we investigated the disturbances in hippocampal synaptic plasticity process, which are the basis of the previously described alterations. For this purpose, experiments of long-term synaptic potentiation (LTP) *in vivo* were carried out. In this study, it was included a new experimental group: WT mice with the expression of the D_2R silenced through the hippocampal injection with lentiviral particles, that carries of

interference RNA (*Drd2*-siRNA). Records in *Drd2*$^{-/-}$ and *Drd2*-siRNA animals showed that high frequency stimulation in the hippocampus did not produce synaptic potentiation. Also, we use the eyeblink conditioning to relate the differences in associative learning and the effectiveness of the CA1-CA3 synapses. Control mice increased their number of conditioned responses during all sessions, but *Drd2*$^{-/-}$ and *Drd2*-siRNA mice only increased their conditioned responses during the first days. The results indicate that the learning deficits of *Drd2*$^{-/-}$ mice are due to the D_2R absence in the hippocampal region.

Striatal TH-ir neurons expression are induced by L-DOPA and mediated by D_1R and D_2R activation.

In this work we study the role of D_1R and D_2R in the expression of striatal TH-ir cells induced by chronic L-DOPA administration and its influence on motor behavior.

This study recorded an increase of TH-ir cells in hemiparkinsonian mice after L-DOPA treatment in a dose-dependent manner. Moreover, it was observed that the number of striatal TH-ir neurons descends to be virtually undetectable after the end of treatment. These experiments support the hypothesis that levels of TH-ir cells expression appears to be regulated by extrasynaptic dopamine levels, and therefore by the D_1R and D_2R action. To study this phenomenon, three different models were used: the genetic and pharmacological inactivation of D_1R and D_2R receptors in mice, and Bac-transgenic mice, which express *Drd1a*-Tomato or *Drd2*-GPF proteins. We did not observe changes respect to D_2R actions, however both genetic inactivation and pharmacological blockade of D_1R caused a significant decrease in the TH-ir neurons. However, it was found that none of the striatal TH-ir neurons expressing D_1R or D_2R, it is suggest that the TH-ir cells indirectly depend on the activation of these receptors.

Next, a series of experiments were conducted to investigate the phenotype of striatal TH-ir neurons. We observed that TH-ir neurons have morphological characteristics of striatal interneurons and were not positive for markers such as Pitx3 and Nurr1. These results indicate that the origin of TH-ir neurons is not common to the rest of mesencephalic dopaminergic neurons and could be a subpopulation of striatal interneurons.

Finally, we studied the role of the TH-ir neurons on the motor behavior using two experiments: cylinder test and voltammetry. Both tests were carried out in different phases of the experiment: basal, post-lesion and post-treatment. The results showed a spatio-temporal correlation between the presence of TH-ir neurons and the release of dopamine in the striatum, as well as an improvement on the exploratory behavior after chronic L-DOPA treatment. These neurons

would maintain the levels of dopamine in the striatum after completing the treatment, and would be involved in the maintenance of the long-term effects of L-DOPA on motor function.

In summary, this doctoral dissertation has proved the decisive performance of D_1R and D_2R in learning and memory tasks of spatial, associative and recognition types. Moreover, our findings about the role of hippocampal D_2R in synaptic plasticity processes show it is critical for *in vivo* LTP and the effectiveness evolution of CA3-CA1 synapses during a conditioning task. In addition, we proved that D_1R is involved in the regulation of the TH-ir neurons expression in the striatum of lesioned mice after L-DOPA treatment, and it is implicated in the maintenance of long-term therapeutic effects of L-DOPA on motor behavior.

Resumen

La dopamina es uno de los principales neurotransmisores del sistema nervioso central y desempeña un papel esencial en diferentes funciones: neuroendocrinas, motivacionales/ emocionales y, especialmente, motoras y cognitivas. Las funciones de la dopamina están mediadas en gran medida por la estimulación de sus principales receptores D_1 (D_1R) y D_2 (D_2R). En esta tesis hemos estudiado el papel que ambos receptores desempeñan en los procesos de aprendizaje y memoria, así como la regulación que ejercen sobre las neuronas estriatales TH-immunoreactivas (TH-ir) y su posible implicación en la respuesta motora.

Para abordar este proyecto hemos utilizado ratones knock-out para el receptor D_1 (*Drd1a*$^{-/-}$) y D_2 (*Drd2*$^{-/-}$) ya que no existen compuestos farmacológicos capaces de diferenciar eficazmente entre receptores dopaminérgicos de la misma familia. Además, para el estudio de las neuronas TH-ir realizamos lesiones con 6-OHDA a ratones que posteriormente recibieron un tratamiento crónico con L-DOPA, siendo este el mecanismo más eficaz para inducir la expresión de las neuronas TH-ir objeto de nuestro estudio. Para completar todo ello realizamos test conductuales que evalúan respuesta motora, como el test del cilindro, y diferentes tipos de aprendizaje y memoria para los cuales utilizamos test específicos. Entre estos test se encuentran: los laberintos de Barnes y Morris para memoria espacial, evitación activa/pasiva y condicionamiento del miedo para el aprendizaje asociativo, y el reconocimiento de objetos para la memoria de reconocimiento.

El papel de D_1R es esencial en los procesos de adquisición y consolidación de la memoria.

Los resultados de las pruebas conductuales para los ratones *Drd1a*$^{-/-}$ demostraron que la señal dopaminérgica mediada por D_1R es esencial en los procesos de aprendizaje y consolidación de la memoria espacial, asociativa y de reconocimiento. Los animales mutantes fueron incapaces de realizar correctamente los test conductuales evaluados, mostrando una incapacidad casi completa para orientarse espacialmente, comprender asociaciones básicas entre estímulos o reconocer un objeto conocido, lo que indica la importancia de la respuesta dopaminérgica mediada por D_1R en el recuerdo de experiencias pasadas. Por ello, podemos concluir que el papel del D_1R es esencial en los todos los procesos de aprendizaje y consolidación de la memoria descritos.

La ausencia de D_2R afecta al aprendizaje y los procesos de plasticidad sináptica asociados.

Analizamos el papel del D_2R en la función cognitiva así como los cambios en los procesos de plasticidad hipocampal asociados. Los resultados obtenidos en los ratones *Drd2*$^{-/-}$ muestran un retraso significativo en el aprendizaje espacial con respecto al grupo control. Sin embargo, es en el aprendizaje de tipo asociativo donde estos animales presentan mayores dificultades ya que son incapaces de desempeñar tareas como la evitación activa.

Además, estudiamos los procesos de plasticidad sináptica hipocampal implicados realizando experimentos de potenciación sináptica a largo plazo (LTP) *in vivo*. Para ello, además empleamos un grupo experimental nuevo formado por animales WT con el D_2R silenciado en CA1 mediante vectores lentivirales portadores de RNA interferente (*Drd2*-siRNA). Los registros mostraron que los animales *Drd2*$^{-/-}$ y *Drd2*-siRNA no tienen LTP. También utilizamos el condicionamiento palpebral para relacionar las diferencias en aprendizaje asociativo y la eficacia de la sinapsis CA1-CA3. Los ratones control aumentaron el número de respuestas condicionadas durante todas las sesiones, pero los ratones *Drd2*$^{-/-}$ y *Drd2*-siRNA solo mejoraron durante los primeros días. Los resultados indican que la respuesta conductual observada se debe a la ausencia de D_2R en el hipocampo.

Expresión de neuronas TH-ir inducida por L-DOPA y su modulación por D_1R y D_2R.

En este trabajo estudiamos la regulación que ejercen D_1R y D_2R sobre la expresión de células TH-ir estriatales inducidas por la administración crónica de L-DOPA y su influencia sobre la conducta motora. En este trabajo encontramos que el tratamiento crónico con L-DOPA produjo un incremento dosis-dependiente del número de neuronas TH-ir estriatales y finalizado el tratamiento, el número de células desciende hasta ser prácticamente indetectables a los 10 días. Estos resultados pueden indicar que la expresión de neuronas TH-ir estriatales está sujeta a los cambios en la homeostasis dopaminérgica, y probablemente mediado por la acción de D_1R y D_2R. Para analizarlo utilizamos 3 modelos: inactivación genética y farmacológica, y ratones Bac -transgénicos *Drd1a*-Tomato y *Drd2*-GFP. La inactivación de D_2R no produjo cambios, sin embargo con la inactivación de D_1R se observó un descenso del número de neuronas TH-ir estriatales. Sin embargo, en los animales BAC-transgénicos no observamos que las neuronas TH-ir colocalizaran con los marcadores rojo-tomate o verde fluorescente bajo el promotor *Drd1a* o *Drd2* respectivamente, por lo que es posible que la expresión de las neuronas TH-ir dependa de forma indirecta de la activación de estos receptores.

Finalmente, estudiamos la posible función e influencia de las neuronas TH-ir sobre la conducta motora mediante el test del cilindro y medimos la dopamina vesicular por voltametría. Ambas pruebas se llevaron a cabo en diferentes fases del experimento: basal, post-lesión y post-tratamiento. Los resultados mostraron una correlación espacio-temporal entre la presencia de neuronas TH-ir y la liberación de dopamina en el estriado, así como una mejora de la conducta exploratoria tras el tratamiento crónico con L-DOPA. Estos resultados indican que las neuronas estriatales TH-ir mantendrían los niveles de dopamina en el estriado tras haber finalizado el tratamiento y estarían implicadas en el mantenimiento de los efectos a largo plazo de la L-DOPA sobre la función motora.

En resumen, la realización de esta tesis ha demostrado el papel determinante de los receptores D_1R y D_2R en el aprendizaje y la memoria espacial, asociativa y de reconocimiento. Además destaca la importancia del papel de D_2R en los procesos de plasticidad sináptica hipocampal donde se encontró que este receptor es crítico en el establecimiento de la LTP *in vivo* y la evolución de la eficacia de las sinapsis CA3-CA1 durante una tarea de condicionamiento. Por otro lado, D_1R ha demostrado estar implicado en la regulación de la expresión de neuronas TH-ir en el estriado de ratones lesionados tras el tratamiento con L-DOPA, y que estas neuronas junto con las terminales que sobreviven a la lesión están implicadas en el mantenimiento a largo plazo de los efectos terapéuticos de la L-DOPA sobre la conducta motora.

Introduction

1. DOPAMINERGIC SYSTEM.

The dopaminergic system consists mainly of neurons that synthesize dopamine in the midbrain nuclei and project to different regions of the brain, resulting in three different pathways: nigostriatal, mesolimbic-mesocortical and tuberoinfundibular.

1.1. Dopaminergic pathways.

1.1.1. Nigrostriatal pathway.

This pathway originates from the substantia nigra (SN), a core of midbrain neurons projecting to the dorsal striatum (caudo-putamen) (Fig. 1). Their efferents provide a dense innervation to the striatum; this structure has approximately the 80% of all dopamine found in brain. SN is divided into two parts: *pars compacta* (SNc) formed by dopaminergic neurons, and *pars reticulata* (SNr) mostly formed by GABAergic neurons. This system is mainly involved in motor control and coordination, allowing the movement to take place harmoniously and conforming a particular program or pattern well established (Pavón et al., 2006; Darmopil et al., 2008).

1.1.2. Mesolimbic-Mesocortical pathways.

These pathways come from the ventral tegmental-area (VTA) in the midbrain (Fig. 1). The mesolimbic pathway innervates the ventral striatum (nucleus accumbens, NAc) and limbic structures (hippocampus, central amygdaloid nucleus, olfactory tubercle, lateral septum and stria terminalis) (Fig. 1). In addition, the mesocortical pathway projects to sensoriomotor and associative frontal cortex areas (Fig. 1). These systems mainly help to sustain attention, ideation, correct reality assessment, motivation and thought control (directionality of behavior).

1.1.3. Tubero-infundibular pathway.

The origin of this pathway is the cells from the periventricular hypothalamic nuclei and arcuate nucleus. Afferents from this pathway originate in the median eminence of hypothalamus and are projected to the pituitary. These neurons play an important role regulating the release of pituitary hormones, especially inhibiting the release of prolactin.

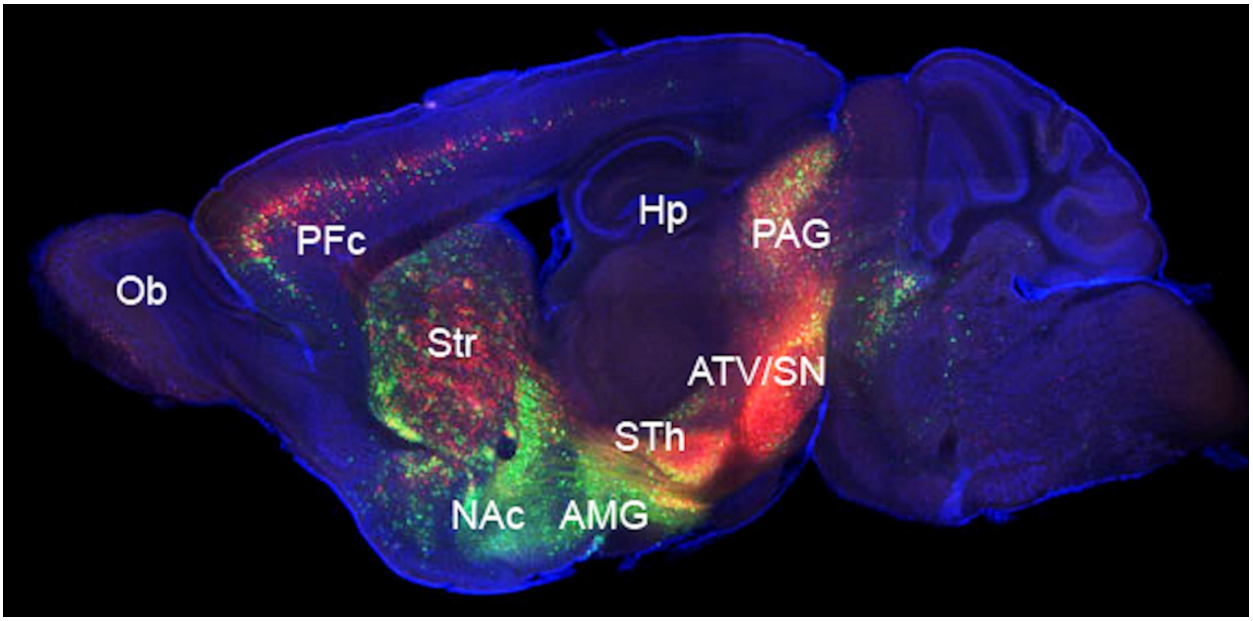

Figure 1. Principal dopaminergic inputs in the mouse brain. Visualization of monosynaptic inputs to a genetically defined population of neurons using rabies virus and cre/loxP recombination system. Direct inputs to dopamine neurons: green dots represent neurons providing inputs to dopamine neurons in the VTA, while red dots represent neurons providing inputs to SN dopamine neurons. OB: olfactory bulb. PFc: prefontal cortex. Hp: hippocampus. Str: striatum. NAc: nucleus accumbens. AMG: amigdala. STh: subthalamic nucleus. PAG: periaqueductal gray. Adapted from Mitsuko-Watabe-Uchida & Sachie Ogawa, 2012.

1.2. Brain structures of dopaminergic system involved in cognitive and motor function.

1.2.1. Basal Ganglia.

In the mid-1950s, Nauta and colleagues adopted the term Basal Ganglia (BG) to refer a group of subcortical structures that includes striatum, globus pallidus (GP), subthalamic nucleus (STh) and SN (Fig. 2). The major task of the BG is to integrate sensory, motor, associative and limbic signals to produce context-dependent behavior (Nakano, 2000). BG alterations are involved in many disorders such as Parkinson´s disease (PD), Huntington´s disease, schizophrenia, autism, depression, obsessive-compulsive disorder and other compulsive and motivational alterations (Nieullon, 2002).

Multisensory integration is considered an essential function of the BG, necessary to determine the cause of environmental changes and respond to them appropriately. This function can be carried out thanks to BG connections with other structures like cortex and thalamus.

1.2.1.1. Striatum.

The largest nucleus in BG is the striatum, which can be further divided into the caudate nucleus and putamen, undifferentiated in rodents but separated by the internal capsule in primates. The striatum has been described as an integrative center for sensory information from cerebral cortex and thalamus (Reig & Silberberg, 2014).

Heimer & Van Hoesen (1979), adopted two topographically terms for the striatum:

Ventral striatum: It delineates the most ventral aspects of the striatum and includes the NAc and portions of the olfactory tubercle. It processes mostly reward-related information.

Dorsal striatum: For more dorsal regions (caudate-putamen nucleus). It receives cortical input from neocortex and processes sensorimotor information.

Other topographical and neurochemical organization of the striatum divided this structure in striosomes and matrix (Graybiel, 1990):

Striosomes are characterized by low levels of acetylcholine and high levels of opiates and substance P. They represent approximately the 15% of the total striatal volume, and receives and processes limbic and reward-related information (White & Hiroi, 1998).

Matrix compartment is composed by cholinergic and somatostatin-containing neurons. It mainly receives associative and sensorimotor information from cortex and thalamus. This area represent the 85% of striatum (Gerfen, 1992).

In terms of neurons, the striatum distinguish two large populations:

Projection neurons, called Medium Spiny Neurons (MSNs). In rodents they represent 90-95% of total and in primates they are 75-80%. All of these neurons are GABAergic, and are divided in two subpopulations on the basis of their projection targets, that shaping two parallel and diametrically opposed pathways (Gerfen & Surmeier, 2011) (Fig. 2):

- Direct pathway or striatonigral neurons: projecting to the SNr and GP pars interna (GPi). They express substance P, dynorphin and D_1 dopamine receptor (D_1R). The activation of this pathway facilitates the movement.
- Indirect pathway or striatopallidal neurons: projecting to the SNr and GP pars interna via GP pars externa (GPe). They express enkephalin, A_2A adenosine receptors and D_2 dopamine receptor (D_2R). Conversely to the direct pathway, the activation of striatopallidal neurons inhibits the movement.

The direct and indirect pathways exert opposing effects on movements thus an imbalance in their activity is believed to lead hypokinetic (i.e., Parkinsonism) or hyperkinectic (i.e., dyskinesia) movement disorders.

Interneurons, involve only the 5-10% of the total striatal neurons in rodents and are implicated in regulation of striatal projection function. Striatal interneurons may be classified into two subpopulations: Cholinergic interneurons and GABAergic neurons, which are in turn divided into: 1) parvalbumin-containing, 2) calretinin-containing and 3) somatostatin-, neuropeptide Y- and nitric oxide synthase-containing.

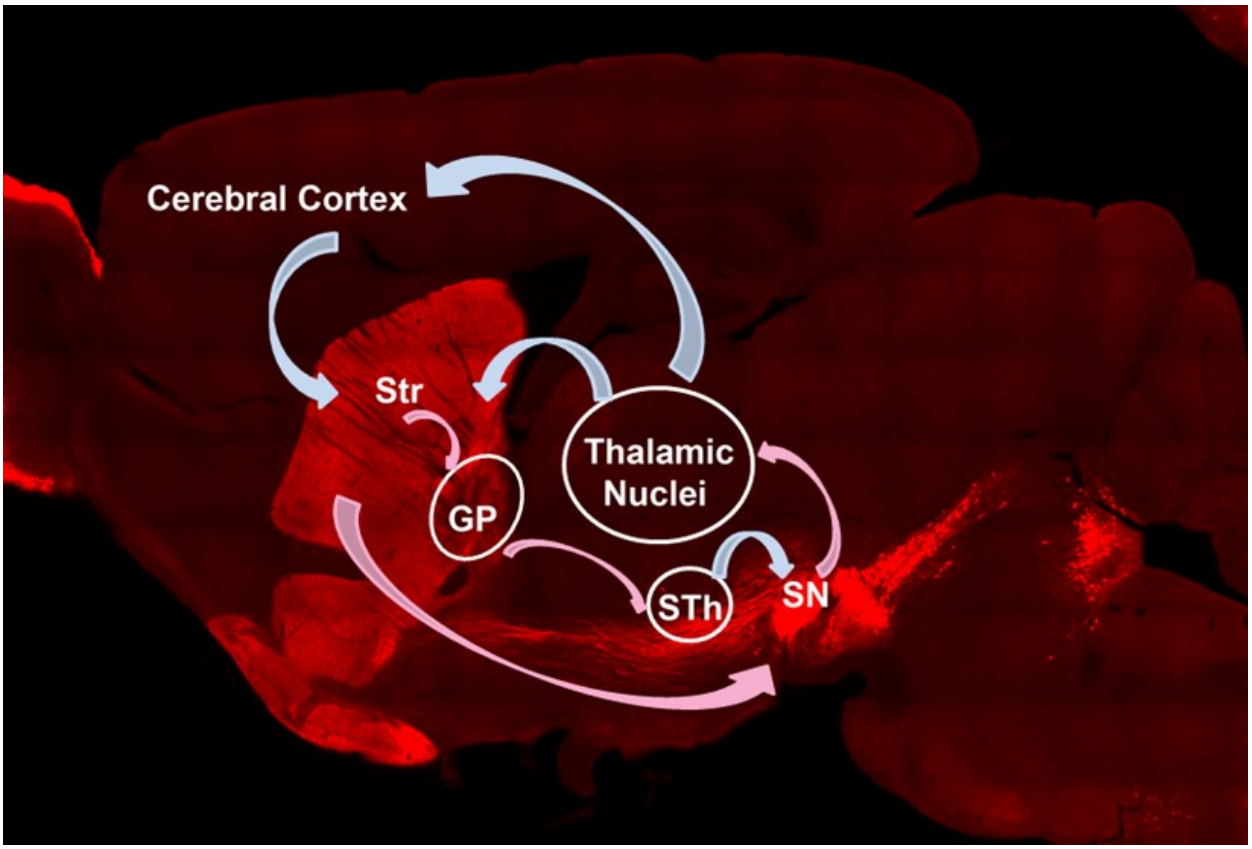

Figure 2. Schema of the basal ganglia motor circuit in the mouse brain. Sagital section of mouse brain stained with inmufluorescent tyrosine hydroxylase antibody. Blue arrows indicate glutamatergic excitatory projections and pink arrows the GABAergic inhibitory projections. Str: striatum. GP: globus pallidus. SN: substantia nigra. STh: subthalamic nucleus. Adapted from Granado et al., 2011

1.2.2. Limbic system.

Limbic system is a set of cortical, diencephalic and brainstem structures, which forms complex circuits involved in emotional aspects and cognitive functions such as learning and memory. This system includes: cingulate gyrus, hippocampus, parahippocampal gyrus, amygdala, anterior-thalamic nucleus, mammillary bodies and orbitofrontal cortex.

1.2.2.1. Hippocampus.

The hippocampus is localized in the medial temporal lobe, across and inferior to lateral ventricles. It is essential to elaborate new memories and to detect new environmental elements. Among other mechanisms, hippocampus have the ability to retrieve and compare environmental elements with others previously stored in different brain regions. Therefore, a disturbance in this structure can produce anterograde and retrograde amnesia, without compromising other types of memory as procedural. Also, hippocampus plays an important role in spatial orientation and memory, since it has "place cells" that can trigger action potentials when the animal passes through or is in a particular novel or familiar location (O´Keefe & Dostrovsky, 1971; Nadel et al., 2012; Moser et al., 2013).

Topographically, hippocampus is divided in three parts: subiculum, dentate gyrus (DG) which is consisting of fascia dentata and hilus, and cornu ammonis (CA). CA is divided into different regions: CA1, CA2 and CA3. CA3 pyramidal cells have a dendritic tree with numerous spines connected to granular cells of DG (mossy fibers system). Granular cells receives excitatory innervation and their axons innervate the CA1 pyramidal layer (Schaffer collaterals system) (Fig. 3).

From the histological point of view, CA1 has four regions:

Stratum oriens: Located in the dorsal hippocampus, containing different interneurons arborizing around basal dendrites of pyramidal neurons that release GABA. These cells receive input from the contralateral hippocampus, usually recurrent connections, especially in CA3 and CA2.

Pyramidal: Ventral to stratum oriens. This layer contains the soma of pyramidal cells. In this region starts his apical dendrite that branching the molecular layer, and several dendrites which emerge from the basal pole. The axon starts on basal pole and goes to alveus to exit from hippocampus. This layer is the main hippocampal efference.

Stratum Radiatum: Similar to oriens. Containing Schaffer collateral fibers that project from CA3 to CA1.

Stratum Moleculare: It is the most ventral one and is composed by granular cells. Here, the perforant path fibers form synapses onto distal, apical dendrites of pyramidal cells.

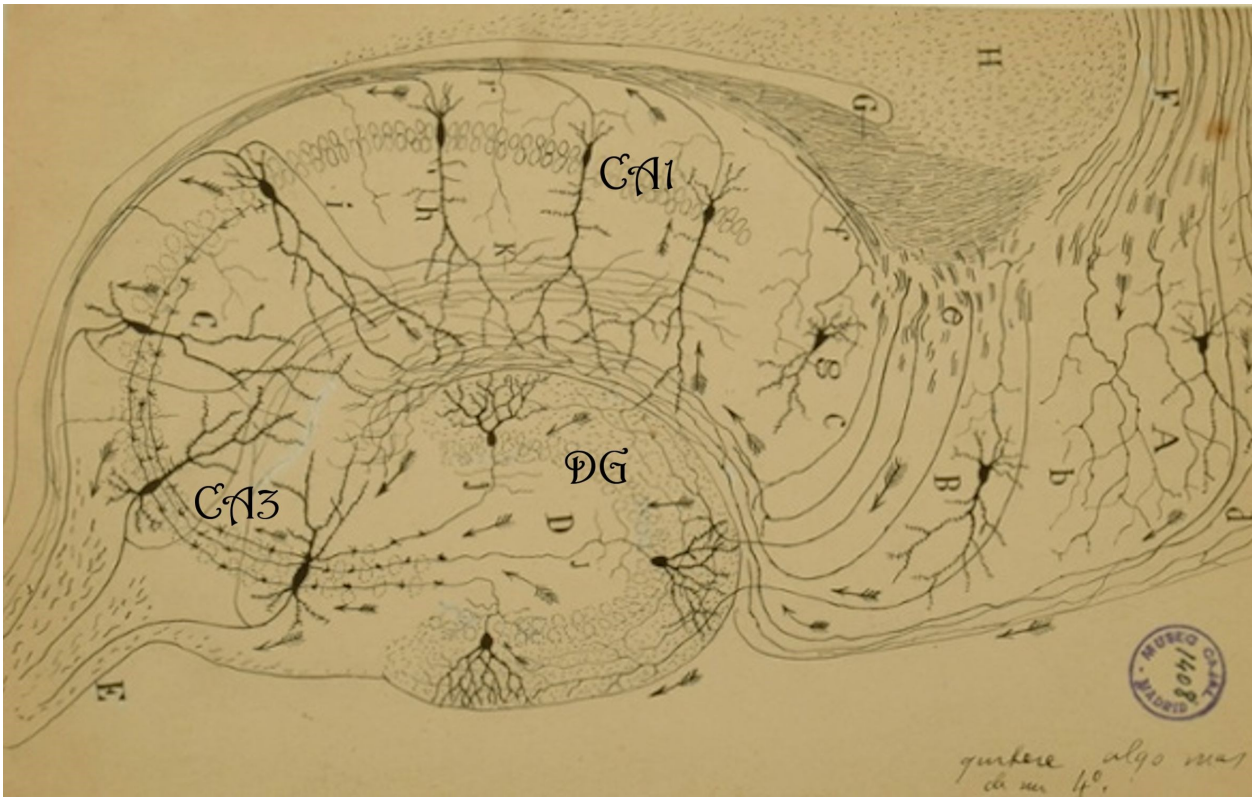

Figure 3. Hippocampus illustration of Santiago Ramón y Cajal (1901). Sketch of the structure and connnections of the Hippocampus. Ink on paper. Adapted from: Cajal Legacy, Instituto Cajal (CSIC)

Connections from hippocampal formation are mainly unidirectional and generate a closed loop that begins in the entorhinal cortex where afferent information converges from the associative cortex, orbitofrontal, insular and cingulated cortex. The hippocampus and DG also receive significant inputs from amygdala, thalamus, septum, hypothalamus and monoaminergic brainstem nuclei through the entorhinal cortex and commissural afferents from contralateral hippocampus.

Principal **afferent** pathways of the hippocampus:

Perforant pathway: The primary glutamatergic afferent of hippocampus, between the entorhinal cortex and granule DG.

Pathway from entorhinal cortex which comes from the molecular layer of subiculum, reaching apical dendrites of CA3.

Modulatory pathway: It is derived from septum, hypothalamus and brainstem through the fornix to connect with basal dendrites from pyramidal neurons of CA1 (Peterson, 1989; Dutar et al., 1995). Cholinergic neurons modulate the activity of pyramidal neurons and GABAergic interneurons. GABAergic neurons project to interneurons disinhibiting pyramidal neurons activity (Gulyas, 2003).

On the other hand, the hippocampus main **efferent** comes from pyramidal neurons to entorhinal cortex and lateral septal area, which maintain a reciprocal relationship. In addition, there are connections to other regions through the fornix and medial prefrontal and frontal cortex, septal nuclei, hypothalamus, anterior nuclei of thalamus, striatum and SN (Dutar, 1995). These large interconnections from hippocampal system synchronize the excitation and inhibition of pyramidal cells.

1.2.2.2. Amygdala.

The amygdala is a structure found in front and above of the anterior horn of the lateral ventricle, inner side of temporal lobe. Among its main functions, it is responsible for integrating explicit information from emotional processes with trends of implicit actions mediating in translation to the corresponding somatic response. It is therefore responsible for the formation and storage of associative memories especially related to emotional events (implicit memory) (LeDoux, 1999).

Topographically, the amygdala consists in different complex:

Basolateral complex: It receives inputs from sensory systems and has an important role in the acquisition of associations.

Centromedial complex: It is connected with hypothalamus, basal forebrain and brainstem (LeDoux, 1999). This nucleus is responsible for the emission of conditioned responses.

Cortical complex: It is connected to the OB and implicated in different social behaviors.

Although the amygdala is connected with almost the whole brain, this structure has several **efferences** to VTA, locus coeruleus, trigeminal nuclei and facial nerve (facial expression of fear), reticular nuclei (scape/avoidance responses, paralysis and vigilance) and from centromedial complex to hypothalamus. In adition, the amygdala receives excitatory **afferents** from cortex with emotional information, and inhibitory afferents from prefrontal and orbitofrontal cortex.

Previous studies have shown that amygdala lesion has variable effects in the acquisition processes but does not prevent learning. It is involved in fear, appetitive and place conditionings, and the consolidation of long-term memory as it is essential in the emotional aspect of the memory (McGaugh, 2015). Amygdala lesion leds to a mismatch between conscious and unconscious information processing of emotional stimuli and the inability to generate an unconscious emotional response (somatic), especially when the stimulus is emotionally charged of fear (Kandel, 2001).

In addition, emotional coordination function exerted by the amygdala is regulated by a parallel control system: the meso-limbic dopaminergic pathway (from SN and VTA). It attenuates the inhibition from the prefrontal cortex on the amygdala, releasing its sensory input, and thereby emotional perception, especially of stimuli associated with anger and fear (thus altered in cases of dopaminergic depletion and PD).

2. DOPAMINE.

Ever since the dopamine was described in 1957 by Carlsson (Carlsson et al, 1957), it has been extensively studied, demonstrating their involvement in a wide variety of processes: cardiovascular regulation, motor control and neuroendocrine functions, multidimensional brain features such as learning and memory (Grecksch & Matties, 1981), motivation (Everitt & Robbins, 2005) and emotional behaviors (Nader & LeDoux, 1999).

2.1. Synthesis, transport and storage of dopamine.

Dopamine biosynthesis occurs in the cytoplasmic region of dopaminergic terminals from the precursor aromatic amino acid tyrosine, which is generated through the amino acid phenylalanine or directly through food ingested (Levitt et al, 1965).

In neurons, two reactions transform tyrosine into dopamine (Fig. 4):

- First, the cytosolic enzyme tyrosine hydroxylase (TH) turns tyrosine to L-3,4-dihydroxyphenylalanine (L-DOPA). TH is considered the “limiting enzyme” in this pathway (Levitt et al., 1965).
- The second step is the decarboxylation of L-DOPA, catalyzed by the enzyme aromatic L-amino acid decarboxylase (AADC), that produces dopamine in the cytosol (Elsworth & Roth, 1997).

In dopaminergic neurons, dopamine is transported by the vesicle monomamine transporter (VMAT-2) from the cytosol to specialized vesicles in dendritic terminal buttons where it is stored. Besides these vesicles, dopamine may also appear stored in smooth endoplasmic reticulum (Elsworth & Roth, 1997).

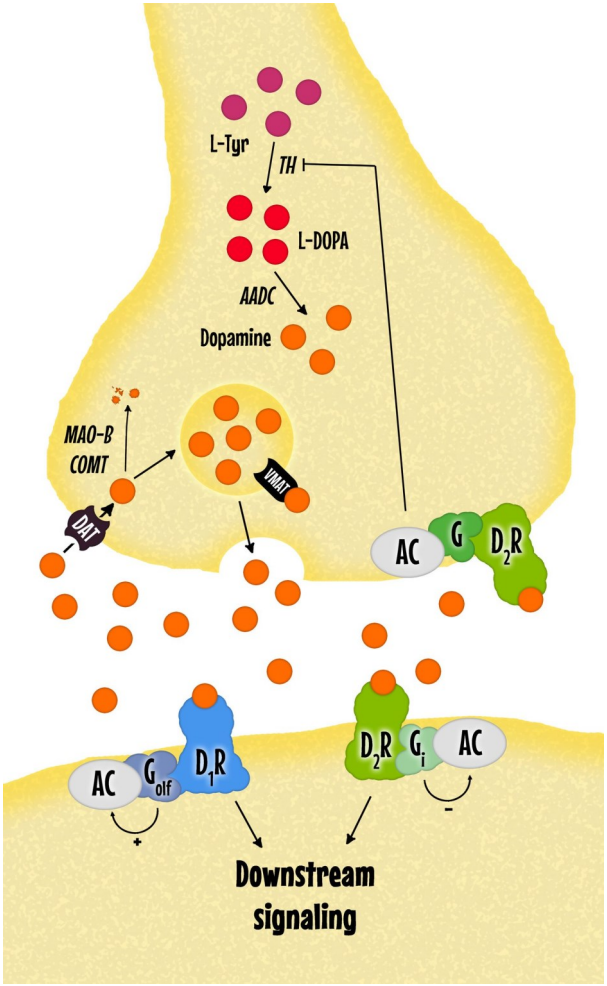

Figure 4. Dopaminergic synapse. The presynaptic terminal releases dopamine (orange circles), and regulates extracellular dopamine levels through several mechanisms: dopamine reuptake from the extracellular fluid (via DAT), dopamine transport into synaptic vesicles (via VMAT-2), dopamine synthesis (which is subjected to autoregulatory control via presynaptic D_2R), and dopamine metabolism (via MAO-B and COMT). The postsynaptic neuron responds to dopamine via two main types of receptors. The D_1R-like is coupled to G_{olf} and activates c-AMP-dependent intracellular signaling pathways. The D_2R-like is coupled to G_i and inhibits the same pathways. AADC, aromatic L-amino acid decarboxylase; AC, adenylate cyclase; COMT, catechol-O-methyltransferase; DAT, dopamine transporter; MAO-B, monoamine oxidase B; TH, tyrosine hydroxylase; VMAT-2, vesicular monoamine transporter 2. Image ®ByRibosoma.

2.2. Release, reuptake and degradation of dopamine.

Dopamine released into the synaptic cleft is carried out by the calcium input into the cell through voltage-dependent channels that activate exocytosis of dopamine transport vesicles into the synaptic cleft.

To finish neurotransmitter action and to sustain the homeostasis, dopamine is reuptaken to be metabolized or stored and released again. Reuptaking process is carried out by specific dopamine transporter (DAT) protein located in the dopaminergic terminal which can transport dopamine bidirectionally based on the concentration gradient (Amara & Kuhar, 1993). In addition, and in small amounts, glia and no-dopaminergic neurons can collect and metabolize extracellular dopamine (Elsworth & Roth, 1997).

The biodegradation of dopamine is performed by two different enzymes (Fig. 4):

1- Dopamine may experience oxidative deamination and become in 3,4-dihydroxyphenylacetic acid (DOPAC) by the action of monoamine oxidase (MAO) located in the mitochondrial external membrane. There are two isoforms, A and B: MAO-A is found in dopaminergic and adrenergic neurons and MAO-B in glial cells, astrocytes and serotonergic neurons. Overall 70% of the human brain dopamine is degraded by MAO-B.

2- Dopamine can also be converted into 3-methoxytyramine through catechol-O-methyltransferase (COMT) outside the central nervous sistem. It is important in the break-down of dopamine in the bloodstream.

The dopamine products of degradation, DOPAC and 3-methoxytyramine, have an enzymatic transformation giving rise to the homovallinic acid (HVA), an inactive metabolite (Elswoth & Roth, 1997).

2.3. Dopamine receptors.

2.3.1. Classification and activity regulation.

Dopamine exerts its action by binding to specific membrane receptors, which belong to the family of seven transmembrane domain G-protein-coupled receptors (GPCRS). Five distinct dopamine receptors have been isolated, characterized and subdivided into two subfamilies for its biochemistry and pharmacological characteristics (Vallone et al., 2000).

The *D1-like receptors subfamily* comprises D_1R and D_5R, associated with excitatory function. This subfamily is coupled to Gαs/olf, positive regulator of adenilil cyclase (AC) that transforms ATP into cyclic AMP (cAMP), resulting in the activation of the protein kinase A (PKA) (Vallone et al., 2000) (Fig. 4). In turn, activated PKA can regulate the synthesis of nuclear and cytoplasmic proteins, the membrane channels function and the sensibilization or desensitization of GPCRS. D1-family receptors are located postsynaptically and are responsible for the action of dopamine.

D2-like receptors subfamily includes D_2R, D_3R and D_4R. They are negatively coupled to AC and have inhibitory function, inhibiting PKA through Gαi/o protein, they can also inhibit calcium entry, by activating potassium channels (Fig. 4). The D_2R subtype has two splice variants coded by the same gene, the long form (D_2L) and the short form (D_2S). D2-like receptors are presynaptic and postsynaptic receptors. The presynaptic receptors, called autorreceptors, are more sensitive to dopamine action than the postsynaptic receptors (Elsworth & Roth, 1997).

These receptors regulate the synthesis and release of dopamine. When dopamine is released in extrasynaptic spaces, it stimulates somatodendritic regions and decreases the neuronal spontaneous activity, while the stimulation of nerve terminals results in an inhibition of dopamine release (Bowyer & Weiner, 1987; Tepper et al, 1984). Both processes are the result of the opening of potassium channels.

2.3.2. Localization and basic functions.

In the central nervous system D1-like receptors family predominate over D2-like receptors, and within these, D_1R is the most abundant. The highest density of D_1R is found in projection field areas of nigroestrital and mesolimbic pathways: striatum, NAc, SN, hippocampus, amygdala, olfactory tubercle, hypothalamus, thalamus and prefrontal cortex (Fremeau et al., 1991; Weiner et al., 1991; Ares-Santos et al., 2013) (Fig. 5).

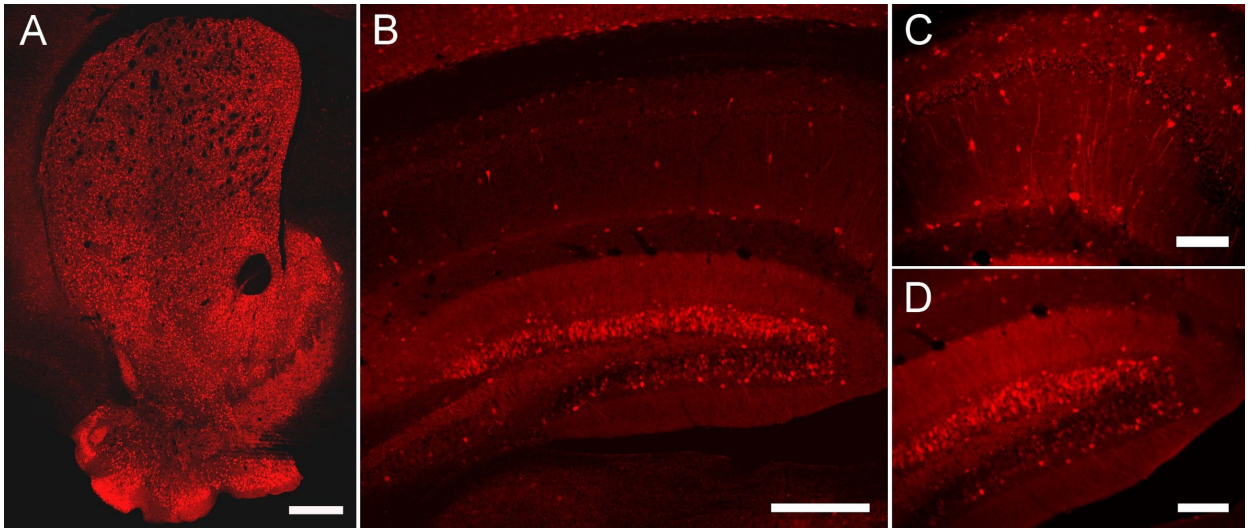

Figure 5. Expression of the D_1R in the brain. Pictures of brain sagittal sections from *Drd1a*-Tomato Bac-transgenic mouse illustrating D_1R is expressed in the striatum, NAc and olfactory tubercule **(A)** and in the hippocampal region **(B)** High magnification of CA1 region **(C)** and dentate gyrus **(D)** Scale Bars: A, B = 200 µm; C, D = 100 µm

Pharmacological experiments involve D_1R in locomotor activity (Xu et al., 1994; Moratalla et al., 1996) and in cognitive processes, including learning and memory, especially in spatial, reverse, extinction and incentive types (El-Ghundi et al., 1999; Granado et al., 2008; Ortiz et al., 2010).

D_5R have a more restricted pattern of expression and is primarily found in hippocampus, hypothalamus, lateral mammillary and thalamic nuclei, and his presence in striatum and neocortex is more limited than his presence in striatum and neocortex (Khan et al., 2000; Rivera et al., 2002; Ares Santos et al., 2013). Its main functions are learning and memory processing (Wiescholleck & Manahan-Vaughan, 2014).

D_2R expression predominates in D2-like receptors family. D_2R is mainly expressed in striatopallidal indirect pathway and cortex (Le Moine et al., 1990; Xu et al., 1994; Rivera et al., 2002). It is also abundant in other regions rich in dopamine as olfactory tubercle, NAc, cortex and VTA (Ares-Santos et al., 2013) (Fig. 6). Also, previous experiments demonstrated the presence of D_2R in hippocampal regions, DG and CA1-stratum radiatum of mice (Higuera-Matas et al., 2010; Gangarosa et al., 2012) and humans (Camps et al., 1989). D_2R is involved in prolactin secretion, certain aspects of behavior and in the regulation of motor function. Stimulation of D_2R results in the inhibition of striatopallidal pathway activity (Selemon et al., 1990; Gerfen, 2000).

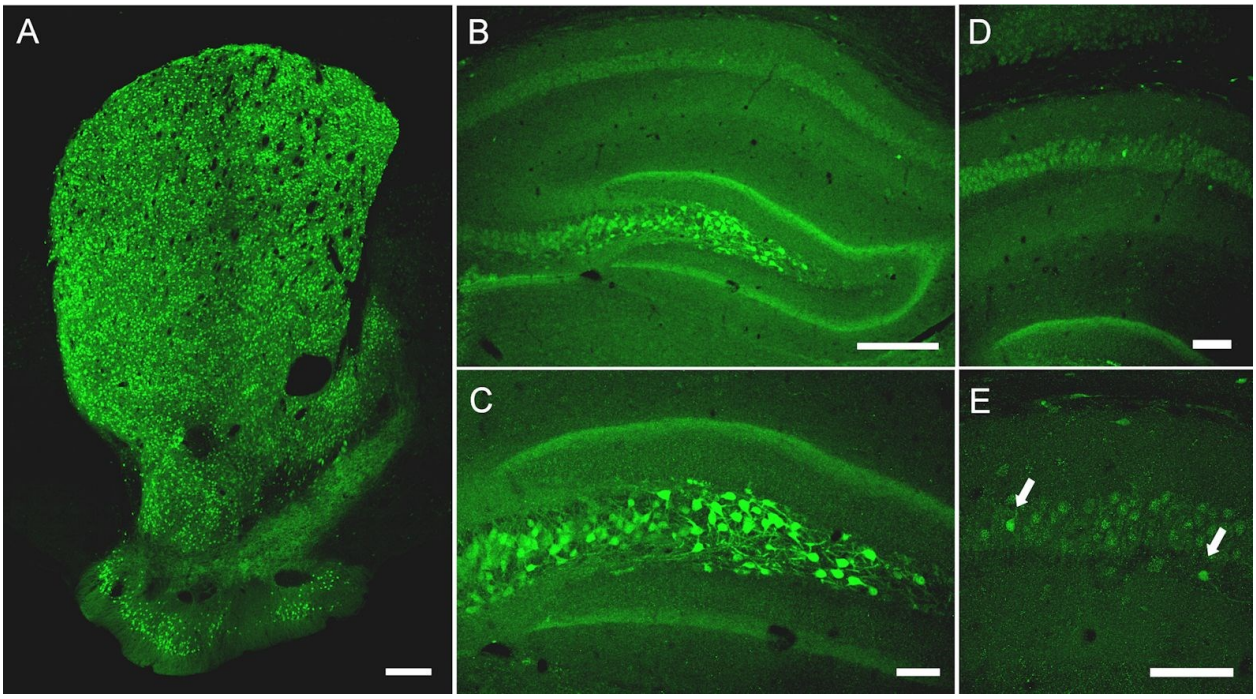

Figure 6. Expression of D_2R in the brain. Pictures of brain sagittal sections from D_2R-GFP Bac-transgenic mouse illustrating D_2R is expressed in striatum, NAc and olfactory tubercule **(A)** and in the hippocampal region **(B).** High magnification of mossy neurons in hilus, **(C)** CA1 region and **(D)** the GFP positive neurons in pyramidal cell layer (white arrows) **(E).** Scale Bars: A, B = 200 µm; C, D, E = 100 µm.

Distribution of D_3R and D_4R is predominantly found in limbic areas. The D_3R is mainly located in NAc, olfactory tubercle, putamen, cerebral cortex and islands of Calleja (Diaz et al., 2000; Ares-Santos et al., 2013). This receptor would be involved in regulation of motor function and behaviors associated with drug-abuse (Collins & Woods, 2007; John et al., 2015). The D_4R is primarily expressed in frontal cortex, amygdala, hippocampus, hypothalamus and midbrain, and practically does not exist in the striatum (Rivera et al., 2002; Ares-Santos et al., 2013). D_4R is usually implicated in attentional process, memory, emotional response and novel ty seeking (Floresco & Magyar, 2006; Wells et al., 2013; Xie et al., 2015; Thanos et al., 2015).

3. ROLE OF D_1R AND D_2R IN COGNITIVE FUNCTION.

3.1. Definition and basic concepts.

3.1.1. Learning and memory.

We understand *Learning* as a set of processes that produce changes in the central nervous system, modifying the behavior of an organism as a result of environmental experience and stimulate the adaptation to the environment.

Associated to this concept, we found the functions of retention, storage and retrieval of information that we describe as *Memory*. Memory is not a unitary process; it consists in several processes that depend on different brain areas and conform a complex system (Squire et al., 1995).

For these reasons, memory can be classified into different forms:

Immediate memory or sensory memory: It is responsible for defining the ability to remember all no-attending information for a short time. Its storage capacity is very large and can concentrate multitude of different information and even different sensory modalities.

Short term memory (STM)/ Working memory (WM): Its main function is to establish connections with incoming and existing information to facilitate recognition and reviewing processes for their subsequent consolidation in long term memory. Its capacity is limited and, if information is not reinforced, it is lost in minutes.

Long term memory (LTM): Here is stored and consolidated information of interest to the STM, can stay from days to months or even for the rest of life.

Other memory classification depending of conscious/unconscious processes:

Declarative or explicit: The neural basis is in the hippocampal system. The hippocampus is the main mediator of relational learning. It is based on information stored about the environment or personal experience that can be evoked deliberately and consciously. It allows to do comparisons and generalizations to similar situations.

Implicit or procedural: When a continuous and repetitive learning occurs, declarative memory can turn into non-declarative or implicit, this second type is "unconsciously". Therefore, it relates to the basic forms of learning as may be habituation, sensitization, perceptual learning, classical conditioning and motor learning. It is dependent on regions of the neocortex and subcortical nuclei which receive significant input from the brainstem, thalamus and cortex.

3.2.1. Synaptic plasticity and LTP

The learning and memory processess described above would not be possible to carry out without several changes that occur in our brain, falling under the concept of "*Synaptic plasticity*" (Morris, 2006). There are changes in the strength of synaptic connections induced by experience (Bliss & Collingridge, 1993) and involving behavioral changes that may be or not be beneficial to the individual (Malenka & Bear, 2004).

Long-term change in synaptic potentiation (LTP) has been frequently regarded as an elementary model to study the mechanisms of neuronal plasticity. LTP is an artificial modification of induced synaptic transmission, consisting of a lasting increase of a postsynaptic response for presynaptic stimulus. This change of basal condition to enhance condition is usually induced by the application of a high frequency stimulus (tetanizationg). Other studies have shown that this phenomenon may occur in almost all neuronal inputs in the hippocampus and may last for several weeks or through life. Hippocampus LTP is considered the base of memory processes.

In mammals, the explicit memory is related to hippocampal LTP. LTP, as memory storage, has two phases: an early transitory effect (E-LTP) and a late phase of consolidation (L-LTP). E-LTP lasts at most 3-4 h. This is not long enough for a hippocampal memory trace to guide systems-level consolidation. However, protein synthesis-dependent L-LTP lasts longer. This phase can last 24 h and uses transmission routes of cAMP-dependent signals, PKA-CREB pathway and the MAP kinases to transform the STM in LTM (Kelleher et al., 2004).

Although the glutamatergic system has been the main object of study in learning processes and memory consolidation, now we have more evidences of the importance of the dopaminergic system in these processess. It is known that integration of glutamate- and dopamine-mediated signals is necessary to induce effective LTP in different brain areas, including cerebral cortex (Gurden et al., 1999; Granado et al., 2008; Ortiz et al., 2010; Xu et al., 2010), striatum (Calabresi et al., 1992; Kim et al., 2013) and especially the hippocampus (Huang & Kandel, 1995; O´Carroll & Morris, 2004; Gangarossa et al., 2014). Hippocampus receives important afferents of dopaminergic neurons in the SN (A8,9) and VTA (A10) (Scatton et al., 1980; Gasbarri et al., 1997; Lisman & Grace, 2005) necessaries to induce changes in synaptic plasticity. Interestingly, the exposure to a novel environment provokes an increase in dopamine, that facilitates LTP (Li et al., 2003), linking dopamine signaling with enhances LTP and with the new information acquisition and storage (Lisman & Grace, 2005).

3.2. Role of dopamine in cognitive process.

Dopamine is involved in the elaboration, control and acquisition of new information. Neuro-computational models described its role as a neuromodulator of major cognitive functions (Dreher & Burnod, 2002; Goto et al., 2007). Dopaminergic fibers innervate different structures related with emotional, motivational, learning and memory processes as hippocampus, prefrontal cortex, striatum and amygdala, and it is related with associated synaptic plasticity processes. For example, it is known that the activation of striatal dopaminergic input serves as entry door for function information on the working memory (O'Reilly, 2006).

Dopaminergic dysfunction significantly alters spatial learning and short and long-term memory in rodents and in non-human primates (Wishaw & Dunnett, 1985; Williams & Goldman-Rakic, 1995). An elegant series of studies have definitively implicated the dopamine in learning, using dopamine-deficient mutant mice (DD), which lack TH in dopaminergic neurons (Zhou & Palmiter, 1995). The DD mice are impaired in spatial, procedural and associative learning (Fadok et al., 2009; Darvas & Palmiter, 2009, 2010; Darvas et al., 2011). Therefore, these results evidenced that dopamine is crucial for associative learning, instrumental learning, and for spatial and working memory tasks.

Additionally, similar results were found in PD patients and in animal models of PD, where dopamine depletion causes cognitive deficits (Dubois & Pillon, 1997; Levin & Katzen, 2005). For example: MPTP-treated monkeys fail in operant task performances of visual discrimination (Scheneider & Roeltgen, 1993) and other studies indicated that hemiparkinsonian rats show an impairment in the Morris water maze, the two way active avoidance task (Da Cunha et al., 2002) and spatial discrimination (De Leonibus et al., 2007).

In humans over age and in the course of certain psychiatric and neurological diseases such as PD, Hungtinton disease, schizophrenia or depression, where there is an alteration of dopaminergic signal, cognitive ability decreases (Brown & Marsden, 1990; Okubo et al, 1997; Bäckman & Farde, 2001). In addition, fluctuations in execution and information processing have been strongly and linearly associated with a decline of dopaminergic activity, especially in relation to the age of subjects (Volkow et al., 1998; Ma et al., 1999; Kaasinen et al., 2000a; Reeves et al., 2002; Bäckman et al., 2010; Nevalainen et al., 2014) (Fig. 7).

3.3. Previous studies about the role of D_1R and D_2R in learning and memory process.

Since dopamine is directly involved in cognitive processes as previously reviewed, the study of D_1R and D_2R is of paramount importance. Their function play an essential role in dopamine response and maintenance within optimal levels for the development of cognitive performance, without necessarily having opposite consequences.

D_1R has been implicated in mediating dopamine effects especially in spatial and associative learning and memory processes, as well as in synaptic plasticity and in the associated gene expression (Müller et al., 1998; El-Ghundi et al., 1999; O'Carrol & Morris, 2004; Granado et al., 2008; Ortiz et al., 2010). It has been shown that exposure to a new situation, a phenomenon closely related to dopamine (Ljungberg et al., 1992), facilitates the induction of LTP dopamine-dependent through D_1R family (Li et al., 2003).

Previous studies with D_1R knock-out mice (*Drd1a*$^{-/-}$) showed impaired spatial learning and memory. In these mice, genetic deletion of D_1R induced a decrease in the different phases of LTP, E-LTP and L-LTP, and altering the transition from onte to other. Previous works form our laboratory and others have shown that D_1R is required for the maintenance of L-LTP throught the early genes ARC and Ziff 268 expression in CA1 region (Matthies et al., 1997; Smith et al., 1998; El-Ghundi et al., 1999; Granado et al., 2008; Ortiz et al., 2010).

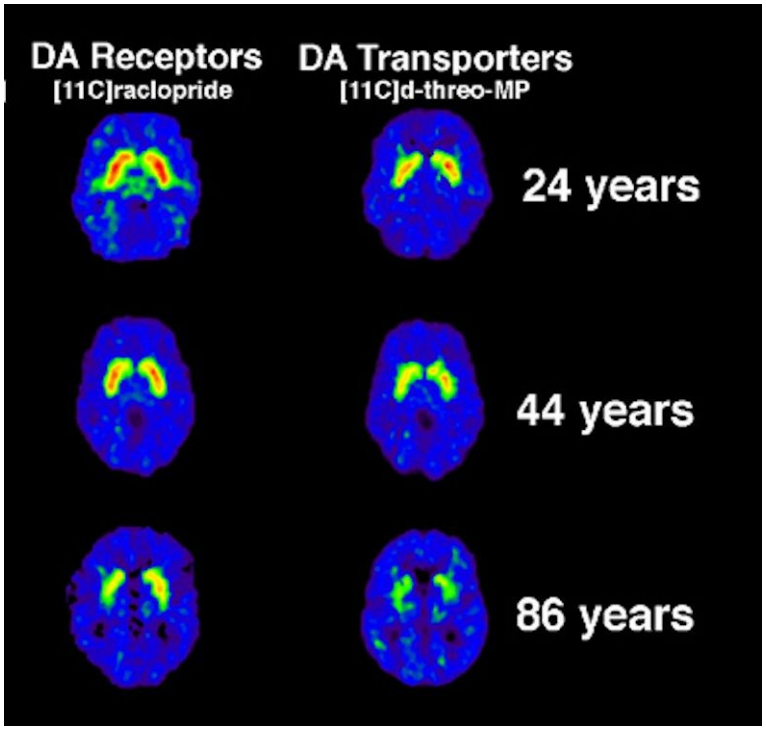

Figure 7. DAT and D_2R decrease with age. A comparison of PET scans from three subjects showing the concentration of D_2R and dopamine transporters in the brain. Red indicates highest concentrations, purple indicates lowest. Adapted from Volkow ND, 1998.

In line with these results, *in vivo* and *postmortem* studies in human and rodent found a decline in cognitive functions associated with a decrease in D_1R density (Cortés et al., 1989; Rinne et al., 1990; Sunahara et al., 1991; Wang et al., 1998) and further in D_2R. Moreover, D_2R shows an exponential age-related path which is exacerbated after reaching middle age and a decline rate estimated at 10% per decade (Rinne et al., 1990; Nordström et al. 1992; Volkow et al., 1998; Ichise et al., 1998; Bäckman et al., 2000) (Fig. 7). PET studies found a clear D_2R loss in prefrontal, temporal, parietal, anterior cingulate and occipital cortex, as well as in hippocampus, amygdala and thalamus, which appears to be part of normal aging decline. This D_2R decrease is associated with changes in executive function, episodic memory and speed of response (Inoue et al., 2001; Kaasinen et al., 2000a, 2002). In addition, studies that eliminate the age factor found a correlation between D_2R binding and glucose consumption, in the execution of certain tasks, especially in episodic memory (Bäckman et al., 2000; Volkow et al., 2000). These results indicate that the cognitive deficits are directly related with the D_2R decrement and it is not due exclusively to the aging.

Further, D_2R density decreases in several brain areas, included hippocampus, correlates with cognitive dysfunctions in neurodegenerative diseases such as PD, Alzheimer and Lewy bodies dementia (Joyce et al., 1993, 1998; Kemppainen et al., 2003; Tanaka et al., 2003; Piggott, 1999, 2007; Christopher et al., 2014, 2015). In addition, some studies reported that the use of major tranquilizers, in particular D_2R antagonists, deteriorates cognitive function in patients with dementia (McShane et al., 1997).

Despite of the evidence provided for these studies about the role of D_2R in cognitive performance, results obtained in genetic and pharmacological models are contradictory, since show both, dysfunctions (Glickstein et al., 2002; Fadok et al., 2009) and improvement(Setlow & McGaugh, 2000) of cognitive performance. For these reasons, in this work we present data and discuss the role of the main dopamine receptors in cognitive functions.

4. PARKINSON´S DISEASE.

In 1817 James Parkinson published an essay about a disease that defined as *"shaking palsy",* a clinical syndrome that presents: "involuntary tremulous motion, propensity to bend the trunk forward and senses and intellects uninjured". Seventy years later, Charcot defined this illness as "Parkinson´s disease". Nowadays, we know that the cause of this disorder is a progressive neurodegenerative loss of nigrostriatal dopaminergic neurons in the SNc particularly. Also new studies show that PD may cause non-motor signs and symptoms such as cognitive, psychiatric,

autonomic and sensory disturbances.

4.1. Epidemiology and etiology.

PD is the second most common age-related neurodegenerative disorder after Alzheimer´s disease, affecting more than 4 million people worldwide and it is estimated to affect 9 million people by 2030 (Dorsey et al., 2007).

About 90% of idiopathic PD cases are sporadic with unknown etiology and the 10% have a genetic origin. Genetic influences would be greater in the early-onset (≤50 years) compared with late-onset PD (>50 years) (Marder et al., 2003). The etiology of sporadic PD still remains uncertain but points to multifactorial causes, combining genetic and environmental factors.

Previous works indicated that free cytosolic dopamine auto-oxidizes spontaneously and forms different toxic products and reactive oxygen species (Muñoz et al., 2012; Goldstein et al., 2014) which may induce the loss of dopaminergic neurons together with increases in oxidative stress and neuroinflammation processes caused by environmental toxins, infections…. In addition, alterations in cell function caused by genetic mutations as those in which mitochondrial action is compromised (Schapira, 2008), associated to the aggregation of α-synuclein (Dauer & Przedborski, 2003) or related with this, as in the case of glucocerebrosidase enzyme action (Murphy & Halliday, 2014). All these factors lead to an alteration of the cell homeostasis and the autophagy processes leading to the degeneration of dopaminergic neurons. It is possible that the SNc neurons, that have a extreme bioenergetics demand of maintain the massive number of synapses and the immense axonal field, are more vulnerable to these effects than other regions (Bolam & Pissadaki, 2012).

4.2. Neuropathological features.

In connection with the loss of dopaminergic neurons in SNpc, PD is neuropathologically characterized by the presence of Lewy Bodies (LBs) and Lewy neurites in vulnerable neuron populations. LBs are intracytoplasmic insoluble protein inclusions, whose principal component is α-synuclein (Braak et al., 2002; Bellucci et al., 2012).

The neurodegeneration in PD is not limited to dopaminergic neurons, but it also occurs in other brain regions, which may account for both motor and non-motor symptoms of the disease. The presence of LBs can also appear in other areas such as amygdala, dorsal motor nucleus of vagus nerve, locus coeruleus, hippocampus, OB and neocortex. In addition, the degeneration also affects noradrenergic, serotonergic and cholinergic systems.

Besides, when a loss of dopaminergic fibers in the striatum takes place, a variety of compensatory adjustments occur and consist of: sprouting of surviving dopaminergic axons (Song & Haber, 2000), increased firing of spared dopaminergic terminals (Grace, 2008), decreased activity of the DAT (Sossi et al., 2008), increased dopamine synthesis via TH (Bezard et al., 2000), up regulation of D_2R receptors in striatopallidal neurons (Kaasinen et al., 2000b; Cai et al., 2002) and increased excitability of the target striatal MSNs (Azdad et al., 2009). All this results in a profound imbalance between the two main striatal pathways as we can see in the following scheme (Fig. 8):

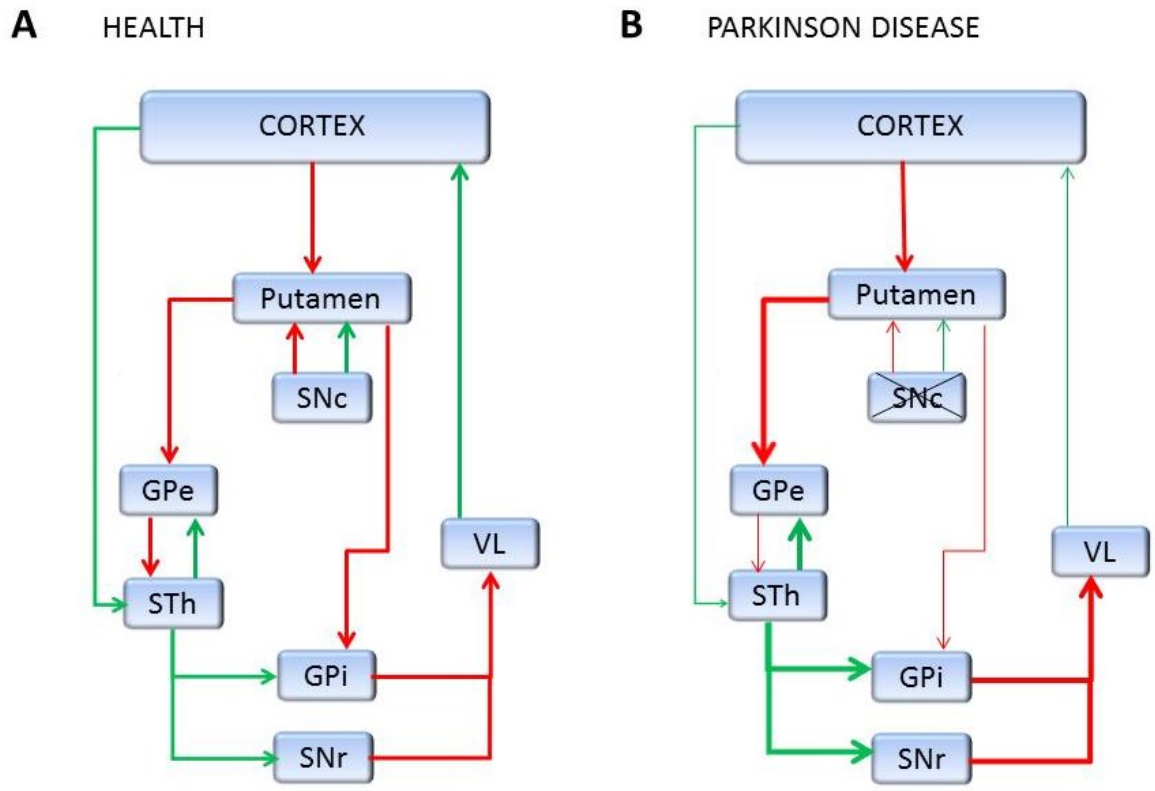

Figure 8. The schemes represent models of the basal ganglia motor circuit in healthy (A), and parkinsonian (B) states. Cortical motor areas project glutamatergic axons to the putamen, which sends GABAergic projections to the GPi and the SNr by two pathways: the monosynaptic GABAergic "direct circuit" (putamen-GPi) and the "indirect circuit" (putamen-GPe-STh-GPi/SNr). Dopamine from the SNc facilitates putaminal neurons in the direct pathway and inhibits those in the indirect pathway. Activation of the direct pathway leads to reduced neuronal firing in the GPi/SNr and movement facilitation, while activation of the indirect pathway suppresses movements. The STh is also activated by an excitatory projection from the cortex, a connection that was not included in the original model. In PD **(B)**, dopamine deficit leads to increased activity in the indirect circuit, in which STh hyperactivity is a key characteristic, and hypoactivity in the direct circuit. Together, these actions result in increased GPi/SNr output inhibition of the VL nucleus of the thalamus and reduced activation of cortical and brainstem motor regions. Green arrows indicate excitatory activity and red arrows indicate inhibitory activity. GPe=globus pallidus pars externa. GPi=globus pallidus pars interna. SNc=substantia nigra pars compacta. SNr=substantia nigra pars reticulata. STh=subthalamic nucleus. VL=ventrolateral nucleus. Adapted from: Rodriguez-Oroz et al., 2009.

4.3. Clinical features.

Both, the course of the disease and the symptomatology as well as their qualitative and quantitative aspects, show great variability between patients. PD clinical manifestations begin when dopamine concentrations fall below 60-70% in striatum (Rodriguez-Oroz et al., 2009). If PD is untreated, approximately 80% of patients with subsequently diagnosed with PD become severely disabled or die 10-14 years after onset of disease.

4.3.1. Motor features.

The accepted criteria for a clinical diagnosis of PD includes the presence of two of the three classical motor features (rest tremor, rigidity and bradykinesia), unilateral onset, a strong clinical response to L-DOPA and the absence of features suggestive of any other motor disorders.

The more frequently motor features are:

Bradykinesia is considered the cardinal feature of PD. This symptom appears as a generalized movement slowness, especially in the initiation of movement, which critically cannot be explained by an intrinsic limitation in execution, but rather is a problem of scaling speed to movement distance. The severity of bradykinesia has a positive correlation with the dopaminergic depletion which in extreme induces *Akinesia* or inability to initiate movement.

Rest tremor is the most common type of tremor in PD, resulting from alternant contractions of agonist and antagonist muscles. It often starts asymmetrically and affects one side of the body more than other.

Rigidity, beside to bradikynesia and tremor, is included in the classic triad of motor symptoms in PD. Rigidity emerges as an increase in muscle tone at rest and augmented resistance to passive displacement. In many cases it is associated with pain.

Postural instability appears in advanced PD due to the loss of postural reflexes. Over time it often becomes resistant to therapy and it is the most common cause of falls.

Other motor symptoms: re-emergence of primitive reflexes for a breakdown of the frontal lobe inhibitory mechanisms, bulbar dysfunction (dysarthria, hipophonia, etc.), respiratory disturbances and neuro-ophthalmological abnormalities.

4.3.2. Non-motor features.

Non-motor symptoms are unresponsive to dopamine replacement therapy and they can become very exacerbated (Weintraub et al., 2008). The most common include: depression and anxiety, sleep REM disturbance, olfactory dysfunction, behavioral and cognitive impairment and autonomic dysfunction, such as urinary difficulties, constipation, sexual disturbances and cardiovascular changes.

Neuropsychiatric symptoms affect quality of life for patients and caregivers. They may precede motor symptoms and are common in PD. Hospitalization for delirium, depression, psychosis and anxiety is sometimes necessary. Prevalence levels in psychiatric symptoms may oscillate depending on methodology: depression (40-56%), apathy (38.8-60%) and anxiety (16.7-43%) (Borek et al., 2006; McKinlay et al., 2008; Leentjens et al., 2011). Other symptoms are derived from the use of dopamine agonists, as the impulse control disorders (ICDs) (Weintraub, 2009; Ceravolo et al., 2010) and psychotic symptoms (Borek et al., 2006).

Cognitive deficits has been associated with hypodopaminergic states, even before the appearance of the first motor symptoms, in domains such as executive dysfunction, decreased mental flexibility (Floresco & Magyar, 2006), processing information (Zalla et al., 1998), and serious difficulties of associative learning and working memory (Sprengelmeyer et al., 1995; Dubois & Pillon, 1997, Sarazin et al., 2002), particularly habit learning requiring a high number of associations (Knowlton et al., 1996).

Mild-cognitive impairment (MCI) appear in approximately 20-50% of individuals with PD in early stages of the disease. Symptomatology, in many cases can go unnoticed and it represents a degree of cognitive impairment that is not normal for age. These patients exhibit non amnesic deficits in cognitive domains such as executive function, psychomotor speed, language, attention and visuospatial function. However, the cognitive phenotype of PD-MCI is heterogeneous because some patients demonstrate grater amnestic deficits. MCI has been increasingly recognized as a distinct entity and a potential prodromal state as well as a risk factor for developing PD dementia (PDD) in a 80% of prevalence, particularly those with posterior cortical profiles (Borek et al., 2006; Monastero et al., 2012). Knowledge of MCI in early-stages of PD is essential in understanding and predicting PDD process (Goldman & Litvan, 2011).

PDD typically reflects a “subcortical dementia” syndrome with greater impairment in non-amnestic cognitive domains (executive and visuospatial functions) and less impairment in declarative memory, language and praxis. Epidemiological studies suggest that the point prevalence rate of dementia in PD is about 40% (Aarsland et al., 2005).

4.4. L-DOPA treatment.

The treatment options for patients with PD include non-pharmacological measures, pharmacotherapy and surgical therapy. Nevertheless, there is no treatment to solve or delay the curse of the disease. Treatment is usually palliative and includes:

Pharmacologic agents: L-DOPA, dopamine agonists, dopamine metabolism inhibitors (in conjunction with L-DOPA), Amantadine (the only antidyskinetic agent), anticholinergic agents and genetic therapies.

Surgical treatments: Ablation for stereotaxic surgery, deep brain stimulation and intrastriatal transplants of fetal mesencephalic tissue.

However only L-DOPA, a precursor of dopamine, remains the single most effective agent in the treatment of PD. This drug is usually administered with carbidopa or benserazide, a peripheral decarboxylase inhibitor which blocks peripheral conversion of L-DOPA to dopamine thus allowing dose reduction and also minimizing peripheral adverse effects (nausea, hypotension, etc.). L-DOPA can cross the blood-brain barrier to the brain where is decarboxylated and stored in synaptic vesicles for subsequent release in dopaminergic terminals or in other catecholaminergic cells when the last terminals disappear.

In spite of the advantage of L-DOPA therapy, its chronic administration and the pulsatile stimulation that dopamine produces in the last terminals provoke the appearance of side effects after 6 years. The complications include a decrement in the effect called “wearing off” period, when the PD symptoms returns for decrease of L-DOPA plasma levels and abnormal stereotypic movements, “dyskinesias”, specially in the peak-dose of drug (Pavón et al., 2006; Cenci, 2007; Kakkar et al., 2015).

4.5. Animal models of PD.

The neuroanatomical characteristics of human and the unknown specific mechanism implicated in origin of PD make that any animal model for PD research, directly replicate all the features of human disease. Normally, the election of a specific PD model depends on the aspect to the disease studied. Animal models generally include: pharmacologically-induced models (e.g. reserpine), neurotoxicant-induced models (e.g. MPTP and 6-OHDA), genetic models ($Pitx3^{-/-}$) and viral models (e.g. viral particles with mutant α-synuclein). The 6-OHDA model and Aphakia mice ($Pitx3^{-/-}$) were used for this study:

4.5.1. Model of 6-hydroxydopamine (6-OHDA).

This model consists in stereotaxic injections of 6-OHDA in the nigrostriatal pathway, median forebrain bundle or striatum, because 6-OHDA cannot cross the blood-brain barrier. When the 6-OHDA is injected into the striatum, it is taken up by dopaminergic and noradrenergic transporters into monoaminergic neurons and retrogradly transported to the dopaminergic cell bodies of the SN, where is accumulated in the cytosol. There, it autooxided generating reactive oxygen species and producing mitochondrial dysfunction. This causes a partial and slow degeneration of dopaminergic nigrostriatal neurons lasting 1-3 weeks.

4.5.2. Aphakia Model.

In some circumstances, genetic models provide a more reliable approach to human disease (Dauer & Przedborski, 2003). Pitx3-deficient aphakia mouse is usually used as a model of PD to study the principal motor disturbances. Pitx3 is a homeodomain transcription factor expressed in dopaminergic neurons in the brain and is essential for the normal development of the midbrain dopaminergic system (Jacobs et al., 2009). Inactivation of Pitx3 induces selective loss of dopaminergic neurons in the SNc and, as a consequence, major dopamine depletion in the striatum, providing a genetic model of PD (Nunes et al., 2003; Hwang et al., 2003, 2005; Ding et al., 2007).

4.6. Tyrosine hydroxylase-immunoreactive (TH-ir) neurons in the denervated striatum.

The presence of TH-ir straital neurons was described for the first time in 1987 by Dubach and colleagues (Dubach et al., 1987). In this pioneer paper the authors described these cells in the primate brain but subsequent works demonstrated that these neurons also exist in the striatum of rodents and humans (Betarbet et al., 1997; Cossette et al., 2005; Hout & Parent, 2007; Busceti et al., 2008). The number of these neurons increases significantly in PD patients (Porritt et al., 2000; Hout et al., 2007) and in animal models of PD (Mura et al., 1995, 2000; Betarbet et al., 1997; Lopez-Real et al., 2003; Jollivet et al., 2004; Darmopil et al., 2008), but their origin and function are poorly understood.

4.6.1. Phenotype of TH-ir neurons.

Striatal TH-ir neurons were identified based on TH expression. Convincing evidence with BrdU experiments demonstrated that the striatal TH-ir neurons that appear in rodents and monkeys following dopaminergic denervation result from a phenotypic shift in which pre-existent GABAergic interneurons begin to express TH, rather than from the birth of new neurons (Mao et al., 2001; Darmopil et al., 2008; Tande et al., 2006).

These neurons express GAD-67 in rodents in a 99% (Betarbet et al., 1997; Tande et al., 2006; San Sebastián et al., 2007; Busceti et al., 2012) and GAD-65 in human brains (Cossette et al., 2005). Other studies show that only 1% is positive for calbindine, a marker for striatal projection neurons, or parvoalbumin, nNOS, neuropeptide Y and less than 10% express calretinine, for striatal interneurons (Betarbet et al., 1997; Mazloom & Smith 2006; Tande et al., 2006; Darmopil et al., 2008).

In addition, 26% of the TH-ir neurons in primates express the NMDA glutamate receptor subunit NR1, while 75% express the GluR1 subunit of AMPA glutamate receptors. Virtually none of the TH-ir cells express the GluR2/3 subunits of the AMPA receptor or the mGluR1/5 subunits of the metabotropic glutamate receptor (Betarbet & Greenamyre, 1999).

The first study demonstrating that these neurons are functionally active, comes from the group of Rosario Moratalla (Darmopil et al., 2008). They showed that L-DOPA treatment in parkinsonian animals induced FosB expression in these TH-ir striatal neurons. Other groups showed that TH-ir neurons in the intact striatum exhibit electrical activity profiles characteristic of GABAergic neurons (Ibáñez-Sandoval et al., 2010; Masuda et al., 2011). Also, some of these striatal TH-ir neurons express AADC, the enzyme required for dopamine production. This feature makes these neurons a potential striatal stores for exogenously administered L-DOPA where it may be converted into dopamine (Tashiro et al., 1989; Mura et al., 1995; Lopez-Real et al., 2003; Darmopil et al., 2008; Busceti et al., 2012).

In addition, VMAT-1 has been detected in EGFP-TH-BAC-transgenic mice (Ibáñez-Sandoval et al., 2010), and VMAT-2 in 50% of TH-ir neurons in monkey striatum (San Sebastián et al., 2007), indicating that these neurons can produce and store dopamine. Furthermore, in PD patients (Porritt et al., 2000), MPTP-treated monkeys (Tandé et al., 2006) and neonate mice lesioned with 6-OHDA (Busceti et al., 2012) these neurons also express DAT. However, in other study co-localization of these markers was not found (Weihe et al., 2006; Darmopil et al., 2008), suggesting that TH-ir can release dopamine in non-vesicular manner.

4.6.2. Morphology of TH-ir neurons.

Striatal TH-ir neurons are more abundant in primates than in rodents and display a more varied morphology, although there are also conflicting data about the morphology of TH-ir neurons between both species.

In monkeys, many TH-ir neurons are small (6-16 μm), bipolar, oval or round perykarion with small and aspiny dendrites (Dubach et al., 1987, Bertabet et al., 1997; Levesque et al., 2003; Cossette et al., 2004, 2005) and only few (<1%) are large (15-25 μm), multipolar with spiny dendrites (Bertabet et al., 1997) (Fig. 9). These dendrites sometimes have TH-ir spines and inputs to dendritic shafts are either symmetrical or asymmetrical, while inputs onto the perikaryon mainly form symmetrical synapses (Meredith et al., 1999). Besides, these studies in monkey found a deeply invaginated membrane surrounding their large nucleus (6-10 μm), typical of striatal interneurons.

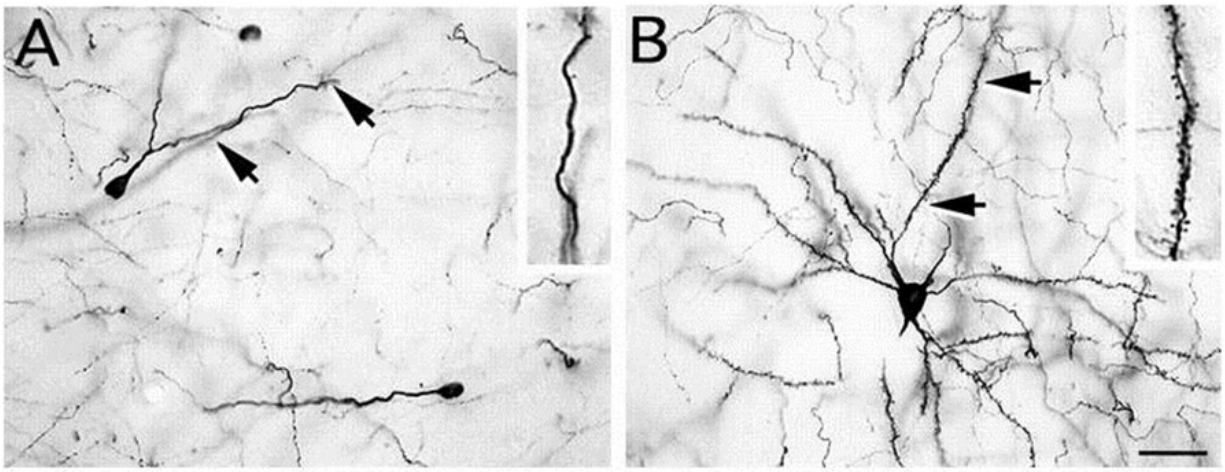

Figure 9. Aspiny and spiny TH-ir neurons in the striatum of MPTP-treated monkeys. A. Photomicrograph of an aspiny oval-shaped neuron with smooth dendrite. These TH-ir neurons were observed much more frequently than the spiny neurons after MPTP treatment. **B.** Photomicrograph of a spiny TH-ir neuron with a number of primary dendrites that are densely covered with spines. The insets in A and B show a magnified image of a portion of the dendrite denoted by the arrows. Scale bar: 30 μm. Adapted from Betarbet et al., 1997.

In rodents lesioned with 6-OHDA, most TH-ir neurons have a smaller diameter (6–12 μm), oval perikaryon with a few varicose aspiny dendrites (Tashiro et al., 1989; Meredith et al., 1999; Lopez-Real et al., 2003; Jollivet et al., 2004), although some of them have spines (Darmopil et al., 2008). A small number of larger (10–15 μm), multipolar TH-ir neurons with spiny dendrites have also been reported in the 6-OHDA-lesioned rat striatum (Lopez-Real et al., 2003; Jollivet et al., 2004).

4.6.3. Regulation of TH-ir neurons expression in lesioned striatum.

The effect of L-DOPA on striatal TH-ir neurons in humans is somewhat controversial. In one study, PD patients treated with L-DOPA showed a marked increase in the number of striatal TH -ir neurons compared to controls (Porritt et al., 2000), in accordance with findings in animal models of PD (Tashiro et al., 1989; Betarbet et al., 1997; Meredith et al., 1999; Mao et al., 2001; Nakahara et al., 2001; Palfi et al., 2002; Lopez-Real et al., 2003; Jollivet et al., 2004; Mazloom & Smith, 2006; Tandé et al., 2006; Darmopil et al., 2008). In contrast, another study reported a reduction in the number of TH-ir neurons in the striatum of MPTP-lesioned monkeys and PD patients treated with L-DOPA (Hout et al., 2007, 2008).

However, it is clear that TH-ir neurons are markedly increased in rodent striatum after rapid dopamine fluctuation, as it has been observed after 6-OHDA lesion (Meredith et al., 1999; Lopez-Real et al., 2003; Mura et al., 2000; Depboylu et al., 2014) or MPTP (Nakahara et al., 2001; Bubak et al., 2015) and methamphetamine treatment (Meredith et al., 1999). Also, studies in the new born striatum of mice reported an increase of TH-ir neurons in early postnatal development of the dopaminergic striatal innervation, and found that the number of these cells decrease when dopamine axons develop a full pattern of striatal innervation (Baker et al., 2003; Busceti et al., 2008; 2012). This further supports the concept that the expression of TH-ir neurons in the striatum is determined by the fluctuations of local dopamine levels.

Hypotheses & Objectives

Hypotheses:

1. Dopaminergic signaling through D_1R and D_2R activation in the hippocampus regulate learning and memory processess.

2. Dopaminergic signaling through D_1R and D_2R activation in the striatum regulates the phenotypic shift of a small population of striatal neurons to express TH.

Principal objectives:

1. To analyze the role of D_1R in spatial, associative and recognition processes of learning and memory mediated by the hippocampus.

2. To analyze the role of D_2R in spatial and associative learning and memory process, and its effects in the underlying synaptic plasticity in the hippocampus.

3. To study the dopaminergic regulation, mediated by D_1R and D_2R in the appearance of striatal TH-ir neurons, and its possible influence in motor response.

Sub-objectives:

1.1. To determine the role of the D_1R in spatial learning and memory function.

1.2. To study the role of the D_1R in associative learning and memory function.

1.3. To analyze the role of the D_1R in recognition memory process.

14. To study potential motor, emotional, motivational and pain sensitivity alterations in *Drd1a*$^{-/-}$ mice.

2.1. To study the consequences of the D_2R absence in spatial learning and memory function.

2.2. To determine the D_2R functions in associative learning and memory consolidation.

2.3. To study potential motor, emotional, motivational and pain sensitivity alterations in *Drd2*$^{-/-}$ mice which will influence in test response.

2.4. To analyze the role of the D_2R in eyeblink conditioning mediated by hippocampus.

2.5. To study the role of dopamine D_2R in CA3-CA1 synaptic plasticity changes induced by LTP in *Drd2*$^{-/-}$ mice and mice with intrahippocampal injections of *Drd2*-siRNA.

3.1. To study the influence of L-DOPA treatment on TH-expression in striatal neurons.

3.2. To study the role of D_1R and D_2R on the expression of TH-ir striatal neurons.

3.3. To study the phenotype and morphology of TH-ir neurons in the striatum.

3.4. To study the possible role of TH-ir striatal neurons in motor behavior.

Materials & Methods

1. ANIMALS.

This study was carried out in adult male mice C57/BL6, and in mice lacking D_1R (*Drd1a*$^{-/-}$); (Moratalla et al., 1996; Centonze et al., 2003; Granado et al., 2014) or D_2R (*Drd2*$^{-/-}$); (Kelly et al., 1997; Granado et al., 2011) and Pitx3 deficient *aphakia* mice (Pitx3$^{-/-}$) (Smidt et al., 2004; Beeler et al., 2010; Espadas et al., 2012; Cremer et al., 2015). Wild-type (WT) and homozygous *Drd1a* $^{-/-}$ or *Drd2*$^{-/-}$ and Pitx3$^{-/-}$ mice used in this study were derived from the mating of heterozygous mice and their genotype was determined by PCR analysis. Another group is composed by bacterial artificial chromosome (BAC)-transgenic mice used to show the co-localization study for striatal TH-ir neurons: *Drd1a*-Tomato or *Drd2*-enhanced green fluorescent protein [eGFP] (Suárez et al., 2014).

Adult mice weighting 24-30 g (3-6 months old at the start of the experiment) were housed in standard Plexiglas cages with maximum of 6 animals per cage. Environmental conditions were strictly controlled; light/dark cycle of 12 h, temperature (22 ± 1°C) and humidity (55 ± 9%). Food and water were available *ad libitum*. For all behavioural test were used a 26 lux intensity of illumination. Animal maintenance and all experimental procedures were performed in accordance with the guidelines of the European Union (2010/63/UE) and Spanish regulations (Real Decreto 53/2013). All efforts were made to minimize the number of animals used in this study and their suffering. The experimental protocols involving animals were approved by the CSIC Bioethical Committee.

2. LEARNING AND MEMORY MODELS.

2.1. Behavioral test.

2.1.1. Spatial learning

Barnes Maze. In this test, *Drd1a*$^{-/-}$, *Drd2*$^{-/-}$ and their corresponding WT animals (n= 10 for each group) received reinforcement to escape from the open platform surface to a small dark recessed chamber located under the platform called "escape box" (Ortiz et al., 2010). The paradigm consists of a circular platform (92 cm diameter) with 20 holes (hole diameter: 5 cm) along the perimeter (Fig. 10). Spatial cues were placed in the walls of the room during the experiment. The experiment was divided in three different phases. During the first 11-14 days, mice were trained to enter into the escape box; in the second part, mice rested for 3 days and were tested for long-term spatial memory. In the last phase, animals were trained again in the Barnes maze for 3 days, but the escape box was placed in a new position 180º from the original position. The

task conditions during all phases were identical; each animal was placed in the middle of the maze in a black cylindrical start. After 10 s elapsed, the cylinder was lifted, and the mouse was free to explore the maze. The trial ended when the mouse entered the escape box or after 2 min had elapsed; in this case, mice was guided to the escape box. In all cases, mice were allowed to stay 30 s in the escape box. All animals were given four training trials per day, and trials were separated by 20 min. After each trial, the maze was cleaned with 70% alcohol to eliminate the use of intramaze cues. The parameters recorded were: latency time to scape box, immobility time and number of holes exploring (to study motivational and emotional aspects).

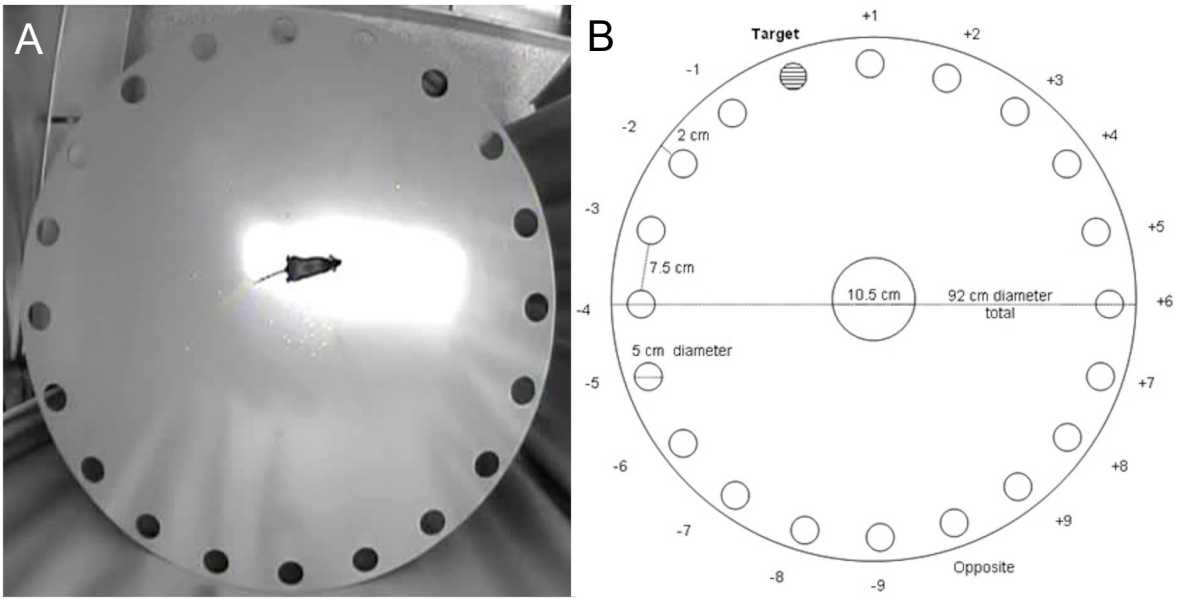

Figure 10. Barnes Maze. The picture illustrates a photograph **(A)** and scheme **(B)** of the Barnes maze used for spatial learning. Sizes and distances are described in the scheme. The position of the target and opposite holes is indicated.

Morris Water maze (MWM). Previous studies describe that *Drd2*$^{-/-}$ mice have motor coordination problems and explore poorly the environment (Baik et al., 1995). To discard the influence of these motor problems we use caffeine (an A_2A receptor antagonist) to facilitate motor execution of these mice. Previously to the training (day 0), each mouse received a trial of 1 min into the MWM, with free exploration. 2 h after de habituation, each animal received 15 mg/kg of caffeine intraperitoneal; 5 min after the injection mice explored the maze free 1 min. During the training, spatial learning and memory were assessed in *Drd2*$^{-/-}$ mice (n=9) and WT (n=10) littermates using the MWM as described previously (Granado et al., 2008), without caffeine. The maze consisted of a circular tank (100 cm of diameter) filled with 21 ºC water located in a room with visible external cues. During the acquisition trials (days 1 to 12), mice were trained to

escape from water by swimming from variable starting points around the tank to the hidden platform and allowed to remain there for 15 s. Mice that failed to find the platform within 60 s were guided to the platform and placed on it for 15 s. After each trial, mice were dried and returned to their home cages. All sessions were recorded by a video camera located above the tank. Mice received 4 trials per day, for 12 consecutive days, with an inter-trial interval of 5-7 min, and their escape latency was recorded for each trial. In the probe trials (no platform), conducted on the first day (day 0), 48h (with caffeine) and 72h (without caffeine) after the last acquisition trial (day 15), mice were allowed to swim for 60 s (Fig. 11). Spatial learning was measured by latency to platform, distance, duration of time spent in the target quadrant and the number of platform crosses.

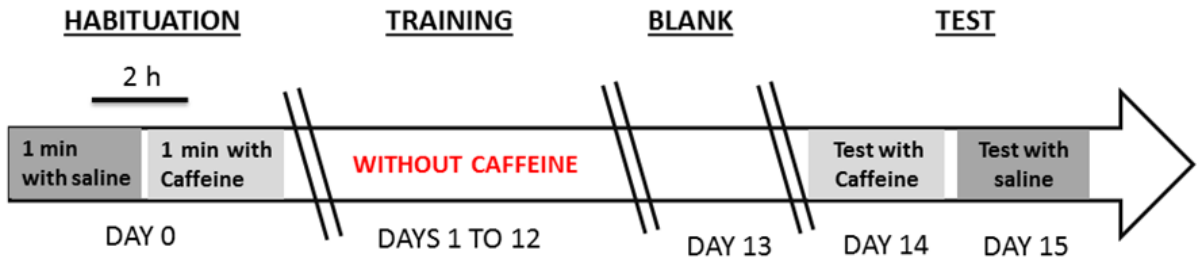

Figure 11. Experimental design. The arrow represents the time-course of Morris water maze experiment. In the first phase of experiment (habitation, day 0), mice freely explored the maze, 1 minute after saline administration and then 2 h later with caffeine (15 mg/kg). All mice performed the training phase without caffeine (days 1 to 12). After a 24 h break (day 13), mice were tested in two different moments: at day 14 after caffeine administration and at day 15 with saline. Caffeine was given to increase motor ability, impaired in *Drd2*$^{-/-}$ mice.

2.1.2. Associative Learning.

Active avoidance. For this test, we used a two-way shuttle-box (AccuScan Instruments, Inc. Columbus, Ohio) with acrylic walls and stainless steel bars in the floor controlled by a programming/recording unit with a shock generator (AccuScan Instruments, Inc.) (Ortiz et al., 2010). *Drd1a*$^{-/-}$, *Drd2*$^{-/-}$ and their corresponding WT mice (n= 10 for each group) were given one training session each day for 8 consecutive days. Each training session consisted of an adaptation period of 3 min, in which animals were allowed to move freely from one compartment to the other, followed by 20 trials separated by an inter-trial interval (ITI) of 20 s (± 5 to counteract any time associations). In each trial, a red light and a tone (100 GHz, 100 dB) were presented simultaneously for 10 s in the compartment where the animal stayed and were used as conditioned stimulus (CS). After 5 s of the CS, mice received a 0.2 mA electric foot-shock as unconditioned stimulus (US) for a maximal duration of 10 s. An avoidance response was defined as when the animal crossed to the opposite compartment of the box after the CS started but before the US was delivered. Crossings while the shock was being delivered were considered escape

responses. Response latencies were counted as the time (in seconds) from the onset of the CS until the animal crossed into the opposite compartment. The number of crosses during the ITI was determined as a measure of general activity. The test session was performed three days after the end of the training phase. The apparatus was cleaned after each animal trial.

Passive Avoidance. This test was performed as previously described (Pittenger et al., 2006; Ortiz et al., 2010). *Drd1a* $^{-/-}$ (n=10) and WT (n= 10) mice were placed into the passive avoidance box (Ugo Basile) with two different compartments, one dark and the other illuminated and white. On the first test day, we measured the time that each mouse spent in the white compartment. As soon as the animal crossed to the black compartment, the automatic door was closed, and animal received an electrical foot-shock (0.4 mA or 0.8 mA, 1s). The test was repeated 1 and 24 h after the first trial with foot-shock in the same conditions.

Fear Conditioning-Extinction. To assess contextual fear conditioning in *Drd2*$^{-/-}$ and their corresponding WT mice (n= 10 per group), we used a fear conditioning task as previously described (Alarcón et al., 2004; Ortiz et al., 2010). On training day, mice were placed in the conditioning chamber for 2 min before onset of the CS (a 30 s tone). During the last 2 s, the US, an electrical shock of 0.7 mA, was presented paired with the CS. Animals were maintained in the chamber for an additional 30 s before returning to home cage. Conditioning was tested 24 h later by measuring the freezing behaviour with a tracking video system (Panlab, Barcelona, Spain). To check hippocampal-dependent conditioning, each mouse was placed into the same context where trained (5 min) and any tone were presented. Mice were re-placed into the conditioning chamber, and the freezing time was measuring for 5 min without the tone to assess contextual conditioning. Animals were returned to home cages for 3 h and placed into a novel chamber to test cued fear conditioning. After 1 min in the novel context, the tone was presented for 30 s, and freezing time was measured for 2 min.

To study fear extinction, the US was modified because mice of different genotypes acquired different levels of freezing behaviour with the original paradigm. The new US consisted of 3 consecutive electrical shocks (0.7 mA for 2 s, with 2 min inter-shocks intervals) delivered in the conditioning chamber followed by a 2 min measurement of freezing time before returning animals to home cages, which resulted in similar freezing times for all mice. Extinction was studied for 6 consecutive days, by placing animals for 5 min in the same context used for conditioning.

2.1.3. Recognition Memory.

Object recognition test. Object recognition testing (ORT) was performed in *Drd1a*$^{-/-}$ (n=10) and WT mice (n= 10), as previously described (Puzzo et al., 2013). One day before training, mice were allowed to familiarize with the apparatus (a plastic box 40 cm long, 30 cm wide and 30 cm high) for 15 min. The ORT consisted in a trial of 10 min. This protracted exposure has been shown to allow the animals to learn the task. On the first day, two identical objects were placed in the central part of the box, equally distant from the perimeter. Each mouse was placed in the apparatus and allowed to explore them. Exploration was defined as the mouse pointing its nose toward the object from a distance of no more than 2 cm. Then, each animal was then returned to its cage. The trial test was performed 24 h later to test memory retention. Mice were presented with two objects, a "familiar" and a "novel" object. To avoid olfactory cues, the objects and the apparatus were cleaned with 70% ethanol after each trial. The following parameters were evaluated: time of exploration of each object and total time of exploration of the two objects expressed as percentage of exploration of novel and familiar object.

2.1.4. Emotional response.

Elevated-plus maze (P-maze). To measure anxiety-related behaviour, an P-maze was used for *Drd1a*$^{-/-}$, *Drd2*$^{-/-}$ and their corresponding WT mice (n= 10 for each group). The maze was elevated 40 cm above the floor level and consisted of two open and two closed arms of the same size (30 x 5 cm); closed arms were surrounded by walls of 15 cm high. The arms were constructed of grey Plexiglas slabs radiating from a central platform (5 x 5 cm) to form a plus sign

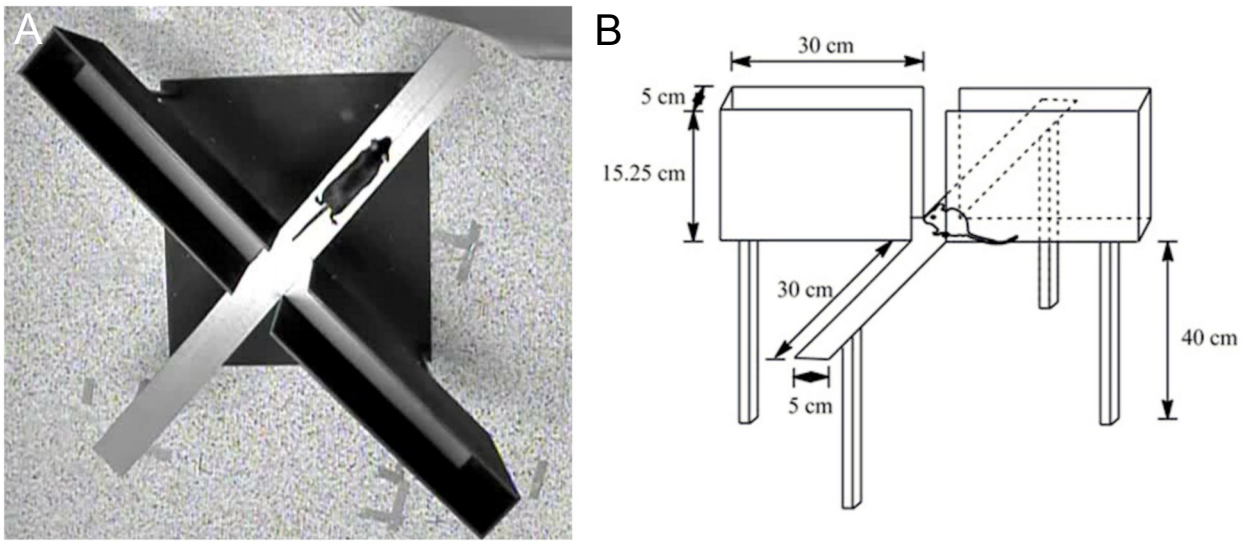

Figure 12. Elevated-plus maze. The picture illustrates a photograph **(A)** and scheme **(B)** of the elevated-plus maze used for measure anxiety-related behaviour. Sizes an distances are described in the scheme. The initial position of mice in the maze is indicated.

(Fig. 12). All arms were illuminated equally. Mice were placed in the central platform, between open and closed arms, and were free to explore freely for 5 min. We measured: time spent in the open sections and the number of crossings between open and closed arms.

Porsolt test. This test was performed as previously described by Porsolt et al., 1978. *Drd1a*$^{-/-}$, *Drd2*$^{-/-}$ and WT mice (n= 10 for each group) were given in a single trial in which they were forced to swim inside narrow Plexiglas cylinders (height, 25 cm; diameter, 10 cm) containing 10 cm water, maintained at 24-25ºC, an left there for 6 min. The total immobility time was measured during the last 4 min of the trial .

2.1.5. Sensorimotor test

Sensitivity to electric shock. This test was performed as described by El-Ghundi et al., 2001. Briefly, mice were subjected to a series of mild foot-shocks with gradually increasing amperage (0.02, 0.04, 0.06, 0.08, 0.1, 0.15, 0.2, 0.25, 0.3, 0.4, 0.5, 0.6 mA). Duration of foot-shock was 1 s with 20 s inter-shock intervals. For each group (n=10) of mice *(Drd1a*$^{-/-}$, *Drd2*$^{-/-}$ and WT mice), we determined the shock intensity that produced each of the following initial sensation responses: sniffing and staring at the floor bars, licking and biting the floor bars, alternate stand on the paws, startle response, jumping and vocalization (Ortiz et al., 2010).

Nociceptive thresholds. We used three different acute nociceptive test: hot plate, plantar test and tail immersion test. In all test cut-off time of 20 s was used to prevent tissue damage in the absence of response. We used the *plantar test* apparatus (Ugo Basile) to measure peripheral pain responses with paw withdrawal latencies in response to radiant heat (55ºC). Mean paw withdrawal latencies were determined from the average of three separate trials, taken at 5 min intervals in each group of mice. The *hot plate* test was used to investigate central supraspinal nociception. This test was performed with a hot plate apparatus (Ugo Basile) at 52ºC. We measured the time (in seconds) to paw licking or paw withdrawal in response to heat. For *tail immersion* test, about 3 cm of the distal part of the tail was immersed into a temperature-controlled water bath (52 ± 0.5ºC). Latency was the time from tail immersion until it was removed or vigorously pulled away. This test was used to assess the nociception at central spinal level.

Cylinder test. Spontaneous forelimb use was evaluated in the cylinder test in WT and WT-6OHDA-lesioned mice (n=11) (Espadas et al., 2012; Ruiz-DeDiego et al., 2015). Each animal was placed in a 10 cm diameter glass cylinder and videotaped for 3 min. The number of ipsi- and contra-lateral forepaw touches to the cylinder was counted by an observed blind to the

experimental conditions of the animals (Fig. 13). Data are expressed as percentage of contralateral touches. Mice were tested 3 weeks after the 6-OHDA lesion, and 1, 4, 7 and 10 days after chronic L-DOPA treatment (25 mg/kg, i.p., daily for 21 days).

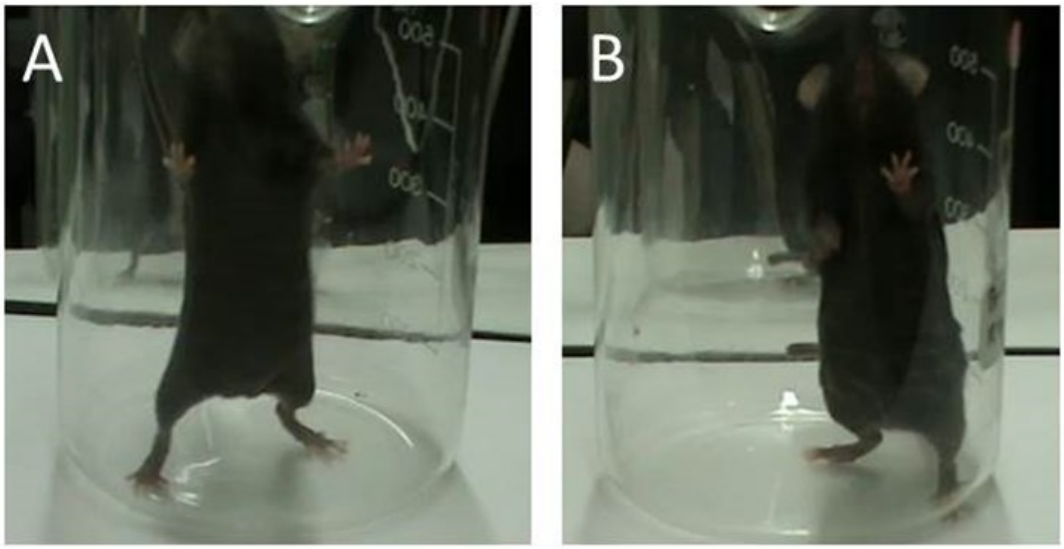

Figure 13. Cylinder test. Photographs of a beaker with a naïve mouse **(A)** that typically use both paws to explore the wall of cylinder and a lesioned mouse **(B)** that mainly use the ipsilateral paw of the lesion to explores the wall of cylinder.

2.2. Electrophysiology.

2.2.1. Lentivirus

Lentivirus constructuion. To silence the mouse *Drd2* (GenID: 13489) *in vivo,* three different sequences were designed and cloned into BamHI and XhoI sites of pRNAT-U6.2 by GenScript Corporation USA. The 3 siRNA used were: 5'GAT CCC GCG TAG CAG CCG AGC TTT CTT CAA GAG AGA AAG CTC GGC TGC TAC GCT TTT TTC CAA CTC GAG 3' (D_2RNAi01), 5' GGA TCC CGC GCC GAG TTA CTG TCA TGT TCA AGA GAC ATG ACA GTA ACT CGG CGC TTT TTT CCA ACT CGA G 3' (D_2RNAi02), 5' GGA TCC CGC TAC CTG ATA GTC AGC CTC TTC AAG AGA GAG GCT GAC TAT CAG GTA GTT TTT TCC AAC TCG AG 3' (D2RNAi03). As control, we used a mock siRNA with no target in mouse: 5' GGA TCC CGA CGT CCA GGC TGC TTC GAT TGA TAT CCG TCG AAG CAG CCT GGA CGT CTT TTT TCC AAC TCG AG 3' (Control RNAi).

Lentivirus production. Each lentiviral vector plasmids (pRNAT-U6.2-D2RNAi01,-D2RNAi02, -D2RNAi03; Genscript, USA), together with the packaging plasmid psPAX2 and the envelope plasmid pMD2G were co-transfected into human embryonic kidney (HEK) 293T

cells to produce viral particles. High-titer stocks [1×10^7 transduction units (TU) per microliter] were obtained by ultracentrifugation and resuspension of the viral pellet in TNE buffer (in mM: 50 Tris-HCl, pH 7.5, 130 NaCl, and 1 EDTA). Viral stocks were stored at −80°C.

Determination of lentivirus silencing efficiency in vitro. The efficiency of the lentiviruses at silencing was tested *in vitro* in ST*Hdh*$^+$/*Hdh*$^+$ cells because this cell line expressed D_2R (Kiyomi et al., 2006). Cells were obtained from the Coriell Institute, New Jersey, USA (CH00097). Cells were grown at 33°C in Dulbecco's modified Eagle's medium supplemented with 10% fetal bovine serum, 1% non-essential amino acids, 2 m*M L* -glutamine, 1% penicillin-streptomycin, 0.8 mg/ml Geneticin, and 40g/ml puromycin (Invitrogen). The cells remain proliferative under these conditions (Cattaneo & Conti, 1998; Trettel et al., 2000). A total of 1×10^5 ST*Hdh*$^+$/*Hdh*$^+$ cells were plated per well in six-well plates. The next day, lentivirus (Lv) stocks were mixed with 10 µg/ml Polybrene (Sigma), incubated for 30 min at room temperature, added to the cells, and incubated at 37°C. After 48 h, the medium was replaced with normal growth medium, and cells were left for an additional 48 h. Cells were solubilized in lysis buffer for Western blot (see below). For *in vitro* silencing of *Drd2* cells were infected with 4 µl of Lv preparation, either 4 µl of Lv-Mock-GFP used as control or 4 µl of one of the three Lenti-*Drd2*-siRNA or 4 µl of all three Lenti-*Drd2*siRNAs together.

Quantitative real-time PCR. Primer sets for rat and mouse *Drd2*, and Gapdh were designed to amplify 100 to 200 bp products. The following specific primer pairs were used: *Drd2*, 5′-CATTGTCTGGGTCCTGTTCCT-3′ and 5′-GACCAGCAGAGTGACGATGA-3′; Gapdh, 5′-ATGACTCTACCCACGGCAAG-3′ and 5′-CATACTCAGCACCAGCATCAC-3′. Gapdh was used as an endogenous control for normalization. Total RNA was extracted from the ST*Hdh*$^+$/*Hdh*$^+$ cells (for *in vitro* quantification) or from the brains of treated animals (for *in vivo* quantification) using *Illustra RNAspin kit* (GE Healthcare). First-strand cDNA was generated from 1 µg of total RNA with iScript™ cDNA Synthesis kit (Bio-rad) in a total volume of 20 µl. For Real-Time PCR analysis, the reaction was performed in 25 µL using the fluorescent dye Power SYBER Green PCR Master Mix (Applied Biosystem, Foster City, CA) and a mixture of 5 pmol of reverse and forward primers. Quantification was performed on a StepOne detection system (Applied Biosystem, Foster City, CA). PCR cycles proceeded as follows: 3 min at 95°C (initial denaturation); 20°C/s temperature transition up to 95°C for 45 s, 45 s at 62°C, repeated for 40 cycles (amplification).

The melting-curve analysis showed the specificity of the amplications. Threshold cycle,

which inversely correlates with the target mRNA level, was measured as the cycle number at which the reporter fluorescent emission appears above the background threshold. To ensure that equal amounts of cDNA were added to the PCR, the Gapdh housekeeping gene was amplified. Data analysis is based on the ΔΔCt method with normalization of the raw data to housekeeping genes as described in the manusfacturer's manual (Applied Biosystem, Foster City, CA). All PCRs were performed in triplicates.

Western blotting. To check silencing efficiency following striatum injection of lentivirus, striatum was dissected, homogenized in lysis buffer (50 mM Tris, 300 mM NaCl, 1% Triton X-100, 25 mM NaF, 1 mM sodium orthovanadate, 4 mM sodium pyrophosphate, 1 mM EDTA, and 1 tablet of Complete protease inhibitor; Roche). The samples were centrifuged at 10.000g at 4ºC for 15 min. Supernatants were placed into new tubes and protein concentration was quantified by BCA (Sigma) method. Solubilized extracts were resolved in sodium dodecyl sulphate-polyacrylamide gel electrophoresis (SDS-PAGE). Membranes were blocked with 5% BSA in Tris-Buffered Saline, 0.2% Tween-20 for 1 h at room temperature and incubated over night at 4ºC with primary antibody against D_2R (1:1000, Millipore, Temecula, California, USA). Membranes were washed and incubated for 1 h at room temperature with peroxidise-conjugated secondary anti-rabbit antibody (1: 20000, Vector, Burlingame, California, USA). Proteins were visualized using Super Signal West Pico Chemiluminescent Substrate (Pierce). Then, membranes were stripped in 0.5 M Tris-HCl buffer, pH 6.8; containing 10% SDS, 100 mM β-mercaptoethanol for 20 min at room temperature, washed with TBS-tween and incubated with anti-Actin antiserum (1:1000, Sigma Aldrich, St. Louis, Missouri, USA) as a control for protein loading. Signals were detected with films that were exposed and digitized and quantified with Quantity One software (Bio-Rad Laboratories).

2.2.2. Surgery.

To carried out input/output curves, paired-pulse facilitation, LTP and classical eyeblink conditioning were used a set of four groups of animals: WT, *Drd2*$^{-/-}$, WT-GFP and *Drd2-siRNA (*n = 10 animals per group). Mice were anesthetized with 0.8-1.5% isoflurane, supplied from a calibrated Fluotec 5 (Fluotec-Ohmeda, Tewksbury, MA, USA) vaporizer, at a flow rate of 1–2 min oxygen (AstraZeneca, Madrid, Spain) and delivered by a mouse anaesthesia mask (David Kopf Instruments, Tujunga, CA). In the first surgical step, animals from groups WT-GFP and *Drd2-siRNA* received a unilaterally stereotaxic injection of 2µl of Lv-Mock-GFP or a mix of Lv

-*Drd2*-siRNAs of concentrated lentiviral stocks (0.2µg/µl) into the hippocampus. The injection was carried out with a Hamilton syringe and performed unilaterally at the following coordinates, calculated from Bregma and skull surface: anterior -2.4; lateral +1.5 (right side); ventral -2.0 (Paxinos & Franklin, 2004).

3 Weeks later, as illustrated in Figure 14, all animals included in the groups mentioned above were implanted with bipolar stimulating electrodes in the right Schaffer collateral-commissural pathway of the dorsal hippocampus (2 mm lateral and 1.5 mm posterior to Bregma; depth from the brain surface, 1.0-1.5 mm) (Paxinos & Franklin, 2004) and with a recording electrode in the ipsilateral stratum radiatum underneath the CA1 area (1.2 mm lateral and 2.2 mm posterior to Bregma; depth from the brain surface, 1.0-1.5 mm). These electrodes were made of 50-µm, Teflon-coated tungsten wire (Advent Research Materials, Eynsham, UK). The final position of hippocampal electrodes was determined as described previously (Gruart et al., 2006; Ortiz et al., 2010). The recording electrode was implanted in the CA1 area using as a guide the field potential depth profile evoked by paired (40-ms interval) pulses presented to the ipsilateral Schaffer collateral pathway. The recording electrode was fixed at the site where a reliable monosynaptic (≤ 5 ms) fEPSP was recorded (Gruart et al., 2006). Evoked fEPSPs presented a large negative wave when the recording electrode was located at the stratum radiatum or a positive shape when recorded near the pyramidal cell layer (Schwartzkroin, 1986; Gruart et al., 2006; Ortiz et al., 2010).

Animals selected for the classical eyeblink conditioning were also implanted with stimulating electrodes on the left supraorbital nerve and with recording electrodes in the ipsilateral orbicularis oculi muscle (Fig. 14). Electrodes were made of 50-µm, Teflon-coated, annealed stainless steel wire (A-M Systems, Carlsborg, WA, USA) bared at the tips for ~0.5 mm. The tips were bent into a hook to facilitate stable insertion in the upper eyelid.

A 0.1-mm bare silver wire was affixed to the skull as a ground. All the wires were connected to two four-pin sockets (RS-Amidata, Madrid, Spain). The sockets were fixed to the skull with the help of two small screws and dental cement. The implantation procedures used in this chronic preparation have been described in detail (Gruart et al., 2006). Experimental sessions started one week after surgery.

To verify location of stimulating and recording electrodes after completion of experiments, mice were deeply re-anesthetized (sodium pentobarbital, 50 mg/kg), and perfused/fixed transcardially with saline and 4% phosphate-buffered paraformaldehyde (PFA). Selected brain sections (50-µm thick) including the dorsal hippocampus were obtained in a microtome (Leica, Wetzlar, Germany), mounted on gelatinized glass slides, and Nissl stained with 0.1% toluidine.

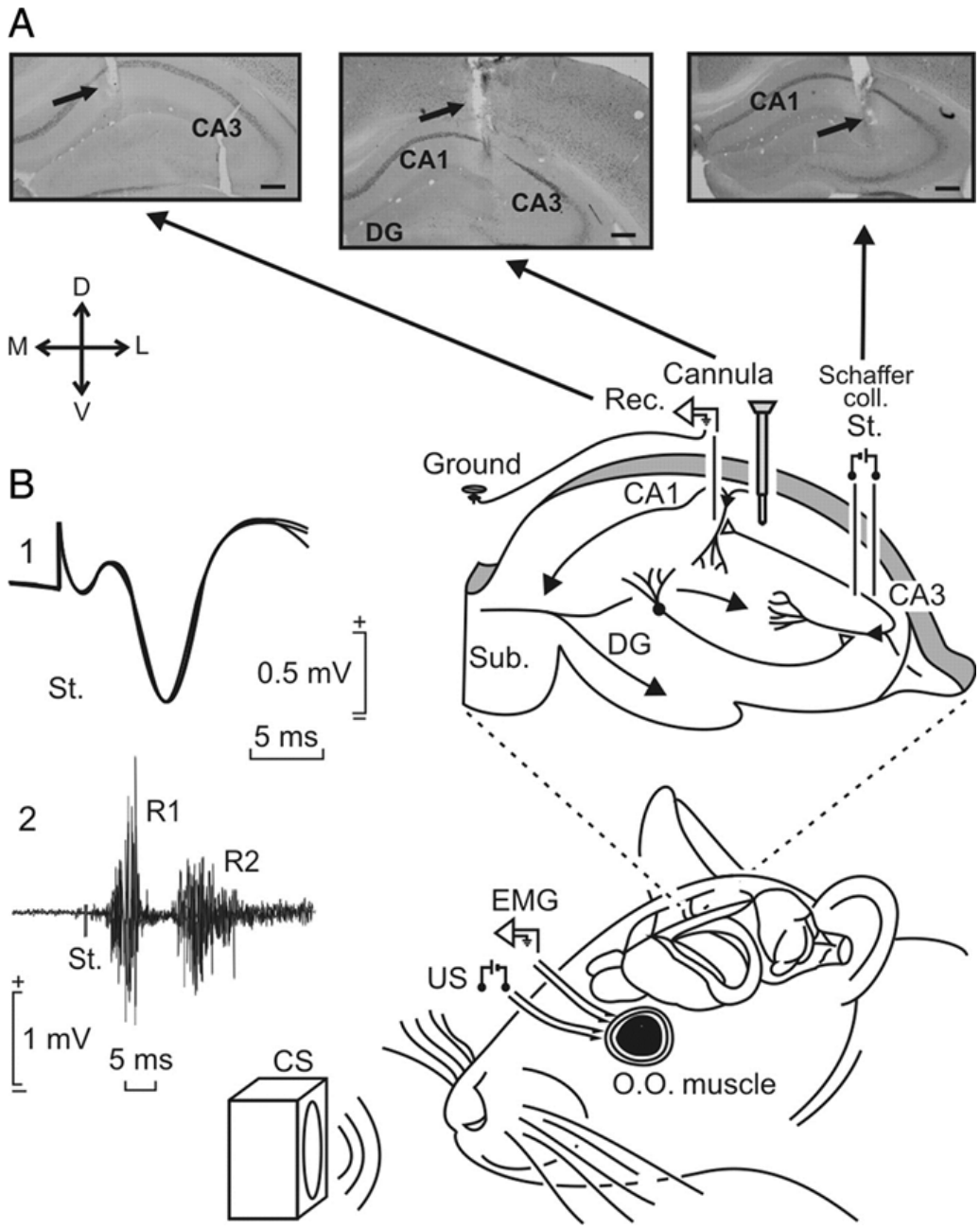

Figure 14. Experimental design for classical conditioning and LTP. Classical eyelid conditioning was achieved with a trace paradigm, using a tone as a CS. The loudspeaker was located 30 cm from the animal's head. Animals were implanted with bipolar stimulating electrodes on the left supraorbital nerve for US presentations. Eyelid conditioned responses were recorded with EMG electrodes implanted in the ipsilateral orbicularis oculi (O.O.) muscle. The top diagram illustrates that animals were also implanted with stimulating (St.) and recording (Rec.) electrodes to activate Schaffer collaterals and to record fEPSPs evoked at the pyramidal CA1 area of the right hippocampus and indicates the injection point for *Drd2*-siRNA or Lv-Mock. **A.** Photomicrographs illustrating the location of stimulating and recording electrodes and lentivirus injection site. Scale bars: 200 µm. DG= dentate gyrus; Sub= subiculum; D, L, M, V= dorsal, lateral, medial, and ventral. **B.** The two sets of traces on the left illustrate: 1, a fEPSP evoked at the CA3-CA1 synapse; and, 2, an EMG recording evoked at the O.O. muscle by a single suprathreshold pulse presented to the supraorbital nerve. Both traces were collected during a conditioning session of a control animal. Calibrations as indicated. Adapted from Ortiz et al., 2010.

***Note:* Electrofisiological studies were performed in collaboration with Dr. José María Delgado and Dra. Agnés Gruart in his laboratory (División de Neurociencias, Univ. Pablo de Olavide, Sevilla)**

2.2.3. Electrophysiology study.

Recordings were made using six differential amplifiers with a bandwidth of 0.1 Hz to 10 kHz (P511, Grass-Telefactor, West Warwick, RI, USA; Fig. 14B). Hippocampal recordings were made with a high impedance probe (2 × 1012 W, 10 pF; Fig. 14B).

For input-output curves, the stimulus intensity was raised to 0.4 mA in steps of 20 mA. The selected inter-stimulus interval was 40 ms, because it results in maximum facilitation of the CA3-CA1 synapse (Madroñal et al., 2007). For paired-pulse facilitation, pulse intensity (50-400 μA) was set at 30-40% of the amount necessary to evoke a maximum fEPSP response, and the following inter-stimulus intervals were used: 10, 20, 40, 100, 200, and 500 ms (Gureviciene et al., 2004). In order to avoid unwanted interactions between successive pairs of stimuli, the inter -pulse delay was always ≥ 20 s.

For evoking LTP, we used a high-frequency stimulation (HFS) train consisting of five 200-Hz, 100-ms trains of pulses at a rate of 1 per second (1/s). This protocol was presented six times, at intervals of 1 min. As indicated above for paired-pulse facilitation, pulse intensity was set at 30-40% of the amount necessary to evoke a maximum fEPSP response for baseline recordings and after the HFS train. In order to avoid evoking a population spike and/or unwanted hippocampal seizures, the stimulus intensity during the HFS train was set at the same intensity used for generating baseline records. Before presenting the animals with the HFS train, we collected baseline records for 15 min, by presenting using single pulses (a 100-μs, square, negative -positive pulse) at a rate of 1 per 2 s (1/20 s). Following the HFS train, we presented the same set of pulses for 30 min. An additional recording session lasting for 15 min was carried out 24 h after the HFS session.

2.2.4. Classical eyeblink conditioning.

Trace eyeblink conditioning, a form of associative learning, was shown to induce a progressive increase in strength at the hippocampal CA3-CA1 synapse in awake mice (Gruart et al., 2006; Madroñal et al., 2009) that correlates with the progressive increase in conditioned responses. LTP is well-established as a form of synaptic memory, but is usually studied under non-physiological conditions. Here, we simultaneously assess trace eyeblink conditioning and synaptic efficiency by measuring changes in evoked extracellular field excitatory postsynaptic potentials (fEPSPs) at the CA3-CA1 synapse in behaving animals during conditioning.

For classical conditioning, using a trace paradigm, a total of three animals at a time were placed in separate small (5 × 5 × 10 cm) plastic chambers located inside a larger (30 × 30 × 20 cm) Faraday box. Classical conditioning was achieved using a trace paradigm consisting of a tone (20 ms, 2.4 kHz, 85 dB) presented as a CS. The US consisted of a cathodal, square pulse applied to the supraorbital nerve (500 μs, 3 times the threshold) 500 ms after the end of the CS. A total of two habituation and 10 conditioning sessions were carried out for each animal. A conditioning session consisted of 60 CS-US presentations, and lasted ~30 min. For proper observation of CR profiles, the CS was presented alone in 10% of the cases. CS-US presentations were separated at random by 30 ± 5 s. For habituation sessions, only the CS was presented, at the same frequency of 30 ± 5 s. As a criterion for "CR" we consider the presence, during the CS -US interval, of EMG activity lasting > 10 ms and initiated > 50 ms after CS onset. In addition, the integrated EMG activity recorded during the CS-US interval had to be at least 2.5 times greater than the averaged activity recorded immediately before CS presentation (Porras-García et al., 2005). The total number of CRs per session was computed and expressed as a percentage of the maximum (60 CRs per session = 100%).

Synaptic field potentials in the CA1 area were evoked during habituation and conditioning sessions by a single 100-μs square, biphasic (negative-positive) pulse applied to the ipsilateral Schaffer collaterals 300 ms after CS presentation. Stimulus intensities ranged from 50 to 250 mA. For each animal, the stimulus intensity was selected according to data collected from the input-output curves, usually at ~30% of the intensity necessary for evoking a maximum fEPSP response (Gureviciene et al., 2004). An additional criterion for selecting stimulus intensity was that a second stimulus, presented 40 ms after a conditioning pulse, evoked a larger (> 20%) synaptic field potential (Bliss & Gardner-Medwin, 1973).

3. PARKINSON MODELS.

3.1. Striatal unilateral 6-OHDA lesion and L-DOPA treatment.

Mice were anesthetized with 0.8-1.5% isoflurane, supplied from a calibrated Fluotec 5 (Fluotec-Ohmeda) vaporizer, at a flow rate of 1–2 L/min oxygen (AstraZeneca) and delivered by a mouse anaesthesia mask (David Kopf Instruments). Vaseline was used to protect the eyes during surgery. Thirty minutes before lesion, the mice received an intraperitoneal injection of 20 mg/kg of the noradrenaline reuptake inhibitor desipramine hydrochloride (Sigma-Aldrich) to protect the noradrenergic neurons from 6-OHDA neurotoxicity (Breese & Traylor, 1971).

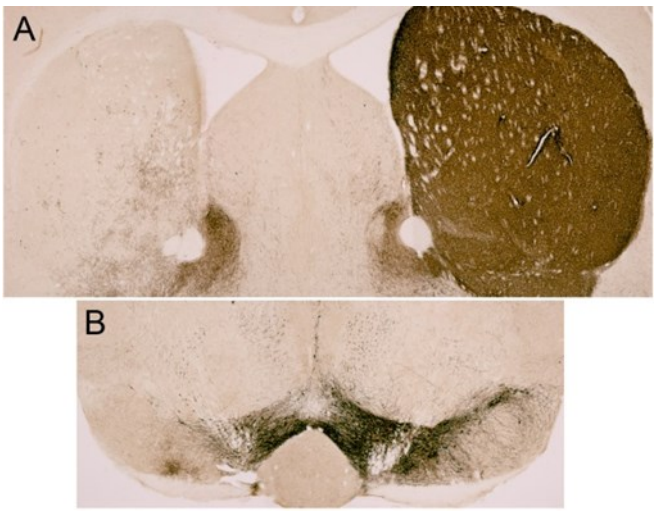

Figure 15. Denervation after unilateral lesion. Photomicrographs of coronal brain sections from a 6-OHDA lesioned animal immunostained with tyrosine hydroxylase, illustrating the TH loss in the striatum **(A)** and the substantia nigra **(B)**. Images from: Darmopil et al., 2008.

Using a Hamilton syringe (Hamilton, Bonaduz, Switzerland), 4 µl of 6-OHDA-HBr solution (5 mM) in 0.1 % ascorbic acid (Sigma-Aldrich) was injected in the left striatum in two different deposits (DV_1 = -4 mm and DV_2 = -3 mm) 2µl each though a single needle penetration at the following stereotaxic coordinates relative to bregma and dural surface; AP = 0.65; L = 2.0 (Paxinos & Franklin, 2004) (Fig. 15). After the injection, the skin was sutured and the animals were removed from the stereotaxic instrument and placed on a heating pad for 30 min. During the first week after surgery animals received injections of saline solution to prevent dehydration, as well as supplementary food.

Mice were left 3 weeks for recovery after the lesion and then submitted to L-DOPA methyl ester (Sigma-Aldrich) treatment for 3 weeks. 6-OHDA or sham operated *Drd1a*$^{-/-}$ and *Drd2*$^{-/-}$ mice and their WT littermates, along the Pitx3$^{-/-}$ mice received daily intraperitoneal injections of 25 mg/kg of L-DOPA, with an injection of 10 mg/kg Benserazide hydrochloride (Sigma-Aldrich), a peripheral blocker of L-DOPA decarboxylase, 20 min prior to L-DOPA injection. The D_1R and D_2R antagonist SCH23390, (3 mg/kg) or Raclopride (2 mg/kg), and simvastatine (20 mg/kg) were administered in a group of 6-OHDA-lesioned mice, 30 min before L-DOPA treatment.

3.2. Histological studies.

3.2.1.Tissue preparation

Adult animals were sacrificed by an overdose of pentobarbital (Laboratorios Normon, Madrid, Spain) and they were injected intracardially with 0.5 ml of 1% heparin (Rovi, Madrid,

Spain), which was followed by the perfusion of 10 ml of saline and 60 ml of 4 % paraformaldehyde pH 7.4. Animals that received L-DOPA were sacrificed 1 h after the last L-DOPA injection. The animal's brains were post-fixed for 24 h and they were then transferred to a solution of 0.1 M PB containing 0.02% sodium azide for storage at 4 °C. To obtain regular blocks, brains were further immersed in 3% agarose and cut at a thickness of 30 μm using a vibratome (Leica, Microsystems).

3.2.2. Immunohistochemistry

Immunostaining was carried out in free-floating sections using a standard avidin–biotin immunocytochemical protocol (Rivera et al., 2002; Grande et al., 2004). Endogenous peroxidase activity was quenched by incubation for 10 min in 0.1 M PBS containing 0.2% Triton X-100 (PBS-TX) with 3% hydrogen peroxide. Non-specific binding sites were blocked for 60-90 min with 5%-10% of the appropriate serum in PBS-TX. Sections were incubated overnight with specific primary antibodies.

Table 1. Primary antibodies for immunohistochemistry

Host	Source	Made	Dilutions
TH	Rabbit polyclonal	Millipore, Temecula, CA, USA	1:1000
TH	Mouse Monoclonal	Millipore	1:250
Nurr1	Rabbit polyclonal	Millipore	1:1000
Pitx3	Rabbit polyclonal	Invitrogen, Paisley, UK	1:500
Tomato (Ds-Red)	Rabbit polyclonal	Invitrogen	1:1000
GFP	Rat monoclonal	Nacalai, Tesque, Kyoto, Japan	1:1000

All primary antibodies were diluted in 0.1 M PBS-TX and 1% serum of the animal in which the secondary antibody was produced. For immunohistochemistry with monoclonal antibodies, we used a mouse on mouse kit (Vector Laboratories, Inc. Burlingame, CA, USA) to block mouse IgGs in the tissue according to the manufacturer's instructions. After incubation with the primary antibody (usually overnight), the sections were washed and incubated with the appropriate biotinylated secondary antibody 1:500 (all from Vector Laboratories) for 1-2 h at room temperature. After washing, the sections were incubated with streptavidin-peroxidase complex (1:5000, Zymed, San Francisco, CA, USA) for 1 h. Peroxidase reactions were developed in 0.05% 3,3´ - diaminobenzidine (DAB) (Sigma-Aldrich) and 0.002% H_2O_2. After developing the reaction, stained sections were mounted, dried, dehydrated and coverslipped with Permount mounting medium (Fisher Chemicals, Fair Lawn, NJ; USA) and examined using a light micros-

cope (Leica, Heidelberg, Germany).

Double-labeling fluorescent immunohistochemistry was performed as before (Granado et al., 2011). Sections were incubated for 2 h at room temperature with the appropriate Alexa-conjugated (1:500, all from Molecular Probes, Invitrogen, Eugene, OR, USA). Sections were mounted in fluorescent mounting medium (DABCO, Fluka, Buchs, Switzerland), coverslipped, kept in the dark at 4 °C until they were examined by laser confocal microscopy (Leica). The specific immunofluorescence of the Alexa 488 (green) or Alexa 594 (red) fluorophores was visualized by excitation at 488 nm or 594 nm, respectively.

3.2.3. Transmission Electron Microscopy

Striatal TH-ir neurons were ultrastructural described by TEM following the immunohistochemistry protocol. We lesioned 5 C57BL6 mice with 6-OHDA and treated with L-DOPA during 25 days, after were perfused with PFA 4% and Glutaraldehide 2.5%. We cryoprotected the tissue in sacarose solution (2%) 24 h and before the brains were frozen with liquid nitrogen and thawed in cold 0,1M PB. Sections (30 μm thick) were cut with a vibratome (Leica Microsystems) and immunostained for TH (polyclonal primary antibody 1:1000). After DAB reaction, sections were washed with PBS, post fixed in 1% osmium tetroxide in 0,1M PB, dehydrated in graded ethanol's (1% uranyl acetate was included at the 70% ethanol), the last ethanol (100º) was mixed with 50% of Durcupan, and finally mounted on Durcupan ACM resin (Fluka) slides under a plastic coverslip, and cured for 48 h at 57ºC. Selected areas with TH-ir neurons of the striatum were dissected out, re-embedded in Durcupan, and cut in ultrathin sections (70 nm) with ultramicrotme Leica EM UC6 (Leica Microsystems). Finally, the sections were mounted on Formvar-coated 200 mesh grids stabilized with evaporated carbon film (Ted Pella Inc., CA, USA), stained with lead citrate, and examined in a Jeol JEM1200 EX-II electron microscope (Fig. 16).

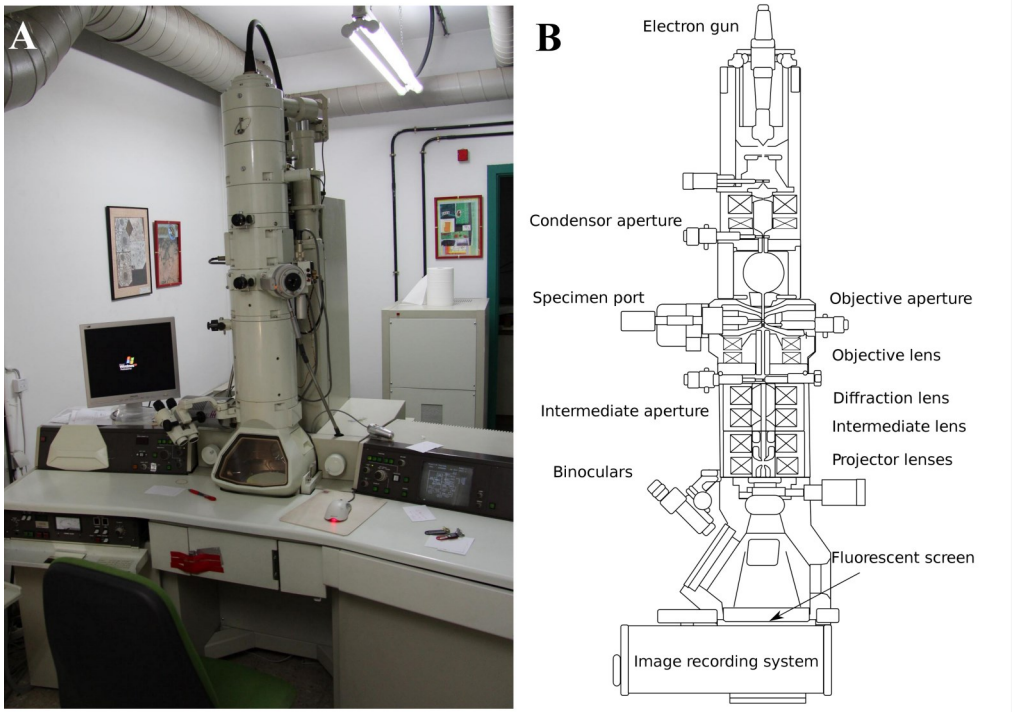

Figure 16. Transmission electron microscope. The picture illustrated a photograph of a Transmision electron microscope model Jeol JEM1200 EX-II **(A)** and an scheme illustrating the internal composition of a standard transmission electron microscope with his different parts **(B).**

3.2.4. Image analysis

Stereological quantification of TH-ir neuronal density in the 6-OHDA-lesioned mice striatum. TH-ir neurons in the striatum were quantified in coronal sections through the striatum of mice using the optical fractionator, Stereo investigator program (Microbrightfield, Colchester, VT, USA) as described before (Ares-Santos et al., 2012). All stereological analyses were carried out in a Nikon Eclipse 80i microscope, with the aid of an interactive computer system comprising a high-precision motorized microscope stage, a 0.5 μm resolution microadaptor (Heidenhain VZR401), a solid-state Microbrightfield CX9000 videocamera and a high resolution video monitor. TH-ir neurons were counted in the lesioned area, on every 10^{th} section throughout the striatum, yielding 6-8 sections per animal. Each brain section was viewed at low power (2x objective) in which the striatum and the lesioned area of the striatum outlined. Then, starting at a random microscope visual field, the number of TH-ir cells was counted at higher power (10x). The nucleus´s equatorial plane was used as counting unit. The data were then exported to Neuroexplorer (Microbrightfield) and Convex Hull Analysis was performed to determine the cross-sectional area of the striatum and the relative density of TH-ir neurons. Data were expressed as the number of TH-ir neurons per mm^3 of striatum (Fig. 17). We analyzed 6-8 animals per group, except for the aphakia mice, for which we analysed 3 animals per group.

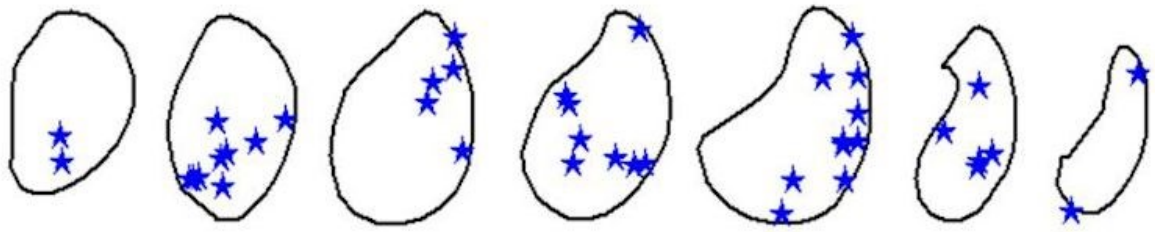

Figure 17. Example of stereological quantification for TH-ir neurons in the lesioned striatum. Image illustrating the profiles of different rostro-caudal sections from a lesioned striatum. Marks show the position of TH-ir neurons with a blue star symbol.

Fluorescence doble-inmunolabeling colocalization analysis. Co-localization analysis in doble-immunolabeling of TH-ir neurons were carried out in a complete reconstruction of the lesioned striatum with a series of 20x photomicrograph with Laser confocal microscopy (Leica), each image consisted in a stack of different channels in different planes of Z axis. Image processing and analysis were performed with ImageJ, image analysis software (Solís et al, 2014). Each channel was separated and the images were transform to grayscale, detected in merge the points of co-localization that appear in white.

3.3. Fast scan cyclic voltammetry (FSCV) quantification of striatal dopamine release in brain slices.

For measurements of dopamine release, brain slices were prepared from mice after 6-OHDA lesion, and 1, 4, 7 and 10 days after chronic L-DOPA treatment (25 mg/kg, i.p., daily for 21 days). Three mice were used for each experimental condition.

Transverse brain slices (450 μm thickness) were prepared from mice using conventional methods (Martín & Buño, 2005), and incubated for > 1 h at room temperature (21–24 °C) in artificial cerebrospinal fluid (aCSF). The aCSF contained: NaCl 124 mM, KCl 2.69 mM, KH_2PO_4 1.25 mM, $MgSO_4$ 2 mM, $NaHCO_3$ 26 mM, $CaCl_2$ 2 mM and glucose 10 mM, and was gassed with 95% O_2 and 5% CO_2. Slices were transferred to an immersion recording chamber and superfused (2.5 ml/min) with gassed aCSF warmed to 32-34 ºC. Following 1 h of equilibration, a bipolar tungsten stimulating electrode with a tip separation of 200 μM (A-M Systems, Inc., Carlsborg, WA, USA) was placed in the dorsolateral striatum as we indicated previously (Granado et al., 2011; Ares-Santos et al., 2012) (Fig. 18). A carbon fibre electrode (CFE; 10 μm diameter; 50 μm exposed length) was placed 100-200 μm from stimulating electrode. FSCV at the CFE was used to detect changes in extracellular concentrations of dopamine following electrical stimulation of the brain slice. Stimuli were single biphasic pulses (20 V, 500 μs) delivered

via a 2100 isolated pulse stimulator (A-M Systems). Stimulus intervals between pulses were not less than 5 min. FSCV was carried out using a three electrode voltage-clamp amplifier (VAMP-1, Registim LLC, Coral Gables, FL, USA). The working electrode was connected to active CFE, an Ag/AgCl was used as reference electrode, and a platinum wire was used as auxiliary electrode. Using the common reference and auxiliary electrodes, a brief sawtooth voltage waveform with a voltage scan rate of 400 V/s was applied consecutively every 200 ms to working CFE electrode. The sawtooth had four phases: 0 to -1 V, to +1.4 V, to -1 V to 0 V. Changes in extracellular dopamine were determined by monitoring the current at the peak oxidation potential for dopamine. Subtracting the current obtained before stimulation from the current obtained in the presence of dopamine created background-subtracted cyclic voltammograms. Current was digitized at 10 kHz using PowerLab 4/25 T (AD Instruments, Bella Vista, Australia) acquisition system. Data were acquired and analysed with Scope software (AD Instruments). Electrodes were calibrated with dopamine standards of known concentration in the recording chamber before and after each use. The average of the pre- and post-calibration measurements was used as the calibration factor.

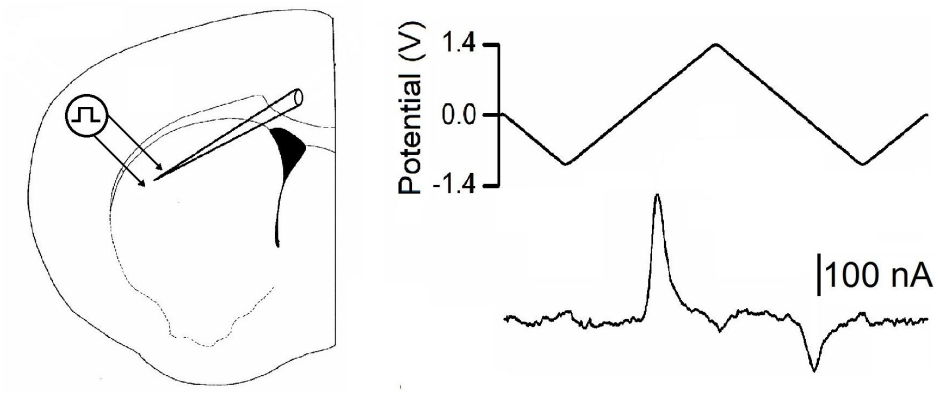

Figure 18. FSCV quantification of striatal dopamine release in brain slices. Left, schematic diagram illustrating the placement of the carbon recording electrode and the bipolar stimulating electrode in the dorsolateral striatum. Right, fast-scan cyclic voltammetry voltage waveform at 400V/s scan rate (upper trace), and subtracted voltammograms for 1µM of dopamine (lower trace). Adapted from Granado et al., 2011.

***Note:* FSCV were performed in collaboration with Dr. Eduardo D. Martín and Dra. Idaira Oliva in his laboratory (Labortory of Neurophysiology and Synaptic Plasticity, PC y TA, IDINE, UCLM, Albacete).**

4. STATISTICAL ANALYSIS.

Behavioural values: Data are presented as mean ± SEM.

Learning experiments: To assess genotype and trial differences in the Barnes maze, Morris water maze, active or passive avoidance, and fear conditioning, test were performed using repeated-measures, two-way ANOVA where genotype (WT and *Drd1a*$^{-/-}$ or *Drd2*$^{-/-}$) and time (day of trials for passive avoidance or freezing test) were entered as independent variables. Relevant differences were analysed pair-wise by post-hoc comparisons with Tukeys's test.

Recognition memory, sensorimotor and emotional test: one way ANOVA followed by 2 -tailed Student´s t-test.

Western blotting and immunohistochemical studies: Data are presented as mean ± SEM. The results was analysed using Student's t test.

Electrophysiology: EMG and hippocampal activity, and 1V rectangular pulses corresponding to CS and US presentations, were stored digitally on a computer through an analog/digital converter (1410 Plus; CED), at a sampling frequency of 11-22 Hz and an amplitude resolution of 12 bits. Commercial computer programs (Spike 2 and SIGAVG; CED) were modified to represent EMG and fEPSP recordings. Data were analysed off-line for quantification of CRs and fEPSP slope using custom representation programs (Porras-García et al., 2005; Gruart et al., 2006). Data are represented as mean ± SEM. Acquire data were analysed using a two-way ANOVA, with group, session, or time as the repeated measure. Contrast analysis was added to further study significant differences. Regression analysis was used to study the relationship between the fEPSP slopes and the percentage of CRs.

Stereological quantification: All data are expressed as mean ± S.E.M. The results was analysed by Student-Newman test.

Voltammetry: All data are expressed as mean ± SEM. Statistical analysis for quantification data analysis was performed using one way ANOVA or t-test Differences in evoked dopamine release in treatment groups were stablished using the 2-tailed Student´s t-test.

For all statistical studies, the threshold for statistical significance was set at $p < 0.05$. SigmaPlot 12 software was used for graphing and statistical studies.

Results

1. DOPAMINERGIC SIGNALING BY D_1R IN HIPPOCAMPUS REGULATES LEARNING AND MEMORY PROCESS

1.1. *Drd1a*$^{-/-}$ mice exhibit impaired spatial learning in the Barnes maze.

To confirm the role of D_1R in spatial learning, we used the Barnes maze because it is less aversive and stressful than the water maze (Barnes, 1979; Harrison et al., 2009). In the Barnes maze, WT mice quickly learned to escape the open field and reach the black escape box, as shown by the rapid decline in escape latency (Fig. 19). By day 7 of training, escape latency has reached a minimum that was maintained throughout the training phase (11 day) and during the probe trial, 3 days later (Fig. 21). In contrast, there was no reduction in escape latency for *Drd1a*$^{-/-}$ mice, even after an 11 days training period (Fig. 19).

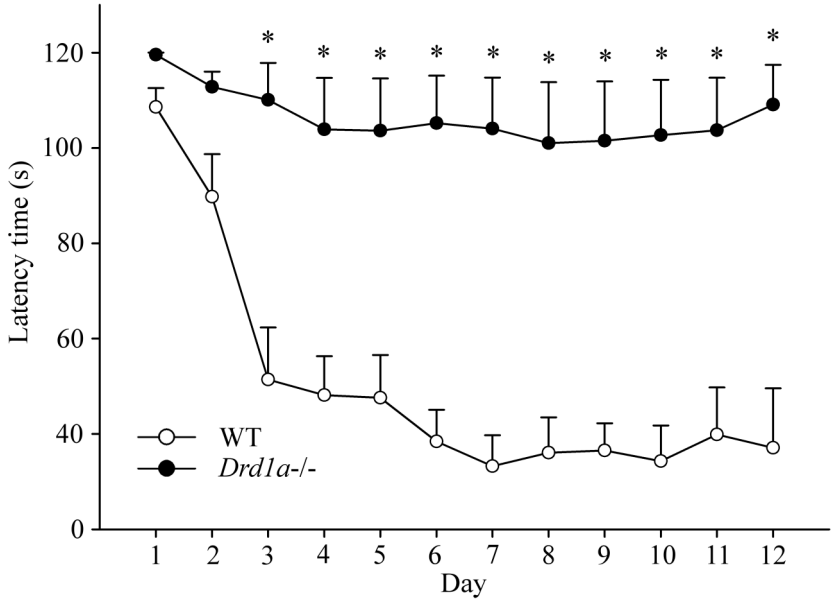

Figure 19. Progression of escape latency during the training phase in the Barnes maze. *Drd1a*$^{-/-}$ mice did not reduce escape latency at any time during the experiment (*$p < 0.005$). Data shows the mean values ± SEM. Statistics were determined with repeated-measures two-way ANOVA followed by Tukey's test for post-hoc analysis.

To rule out the possibility that inactivation of *Drd1a* increases anxiety levels in these mice, masking their capacity to respond in the Barnes maze, we evaluated the immmovility time during the first day of training in the Barnes maze, as an indirect measure of anxiety. We chose the first day of training because on this day, the two groups showed similar latency times for crossing to the black escape box. WT and *Drd1a*$^{-/-}$ mice spend similar amounts of time immobile during the first day of training (Fig. 20A). In addition, recent work has shown that pharmacological blockade or genetic inactivation of D_1R is implicated in motor hyperactivity and com-

pulsive disorders (Ferland et al., 2014; Nakamura et al., 2014), therefore, ruled out that in our model such alterations influence the exploratory behavior and the correct acquisition the escape response with the immobility time test and nose pokes response. There are similarities between Barnes maze and hole board test (specially designed to measure novelty seeking), we quantified the total number of holes that mice explored in a novel situation (day 1 of training) as an indirect measure of motivation through exploratory behavior. Contrary to expectations, we found no significant differences between holes explored by *Drd1a*$^{-/-}$ and their WT littermates (Fig. 20B). These data supports our hypothesis that deficits in the Barnes maze are mainly due to a disability in the spatial learning and memory process.

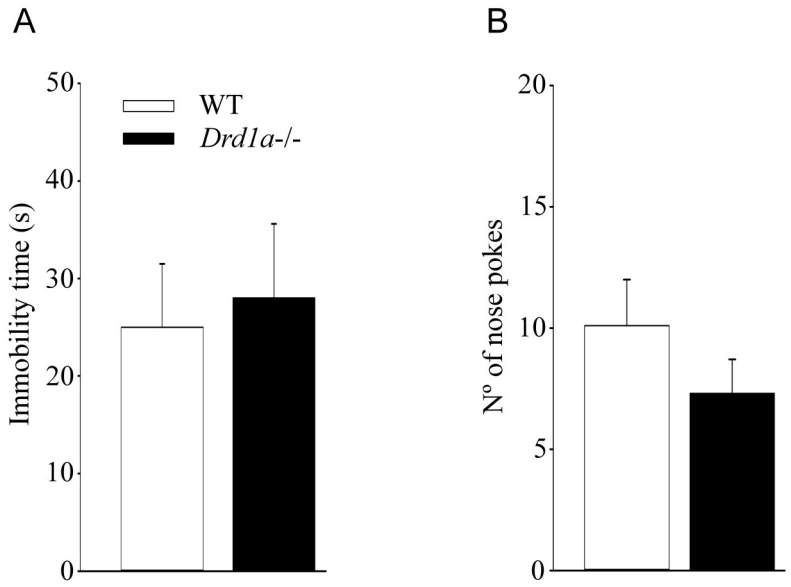

Figure 20. Anxiety levels and exploratory behavior are normal in dopamine *Drd1a*$^{-/-}$ mice at day 1 of training. A. Immobility during the first day of training in Barnes maze. WT and *Drd1a*$^{-/-}$ mice showed similar levels of immobility. **B.** Nº of holes explored during the first day of training in Barnes maze. Nose pokes were similar in WT and *Drd1a*$^{-/-}$ mice. Data shows the mean values ± SEM.

In addition, *Drd1a*$^{-/-}$ mice showed no reduction in escape latency in a probe trial performed 3 days after training, to evaluate memory consolidation (Fig. 21A), or during the relearning trials, when the escape hole was moved to the opposite side of the training arena (Fig. 21B). With the previous study in the MWM (Granado et al., 2008) these data indicate that the D_1R is required for spatial learning in more than one paradigm. Our demonstration that loss of D_1R does not increase indicators of anxiety supports the notion that our results are attributable to an important role of D_1R in spatial learning.

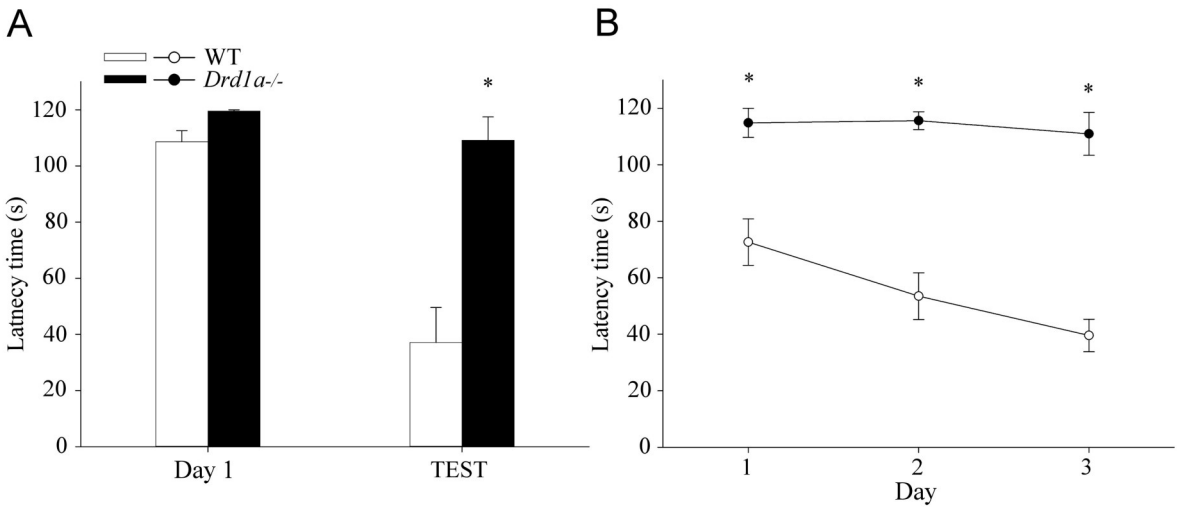

Figure 21. Hippocampus-dependent learning is impaired in dopamine *Drd1a*$^{-/-}$ mice. A. Probe trial performed three days after the training phase. Histograms represent the time spent searching for the escape hole. *Drd1a*$^{-/-}$ mice did not reduce searching time during the probe trial (*p<0.005). **B.** Escape latency during the relearning phase. For this test, the escape hole was located opposite to its position in the training phase (*p < 0.001). Statistics were determined with with Student's t test (**A**) and repeated-measures two-way ANOVA followed by Tukey's test for post -hoc analysis. Data shows the mean values ± SEM

1.2. Associative learning is impaired in *Drd1a*$^{-/-}$ mice

Previous studies show that D_1R antagonist increased sensitivity to pain (Burkey et al., 1999). Therefore, as we used an electric shock as aversive stimulus for associative test, we carry out a battery of nociceptive test in our mice. Three nociceptive thermal tests were used that impact in different degree peripheral or central processing of painful stimuli and measured the latency of withdrawal response. We found significantive differences in all three assays, the pain threshold was actually lower for *Drd1a*$^{-/-}$ than WT mice (Fig. 22), indicating that *Drd1a*$^{-/-}$ mice are more

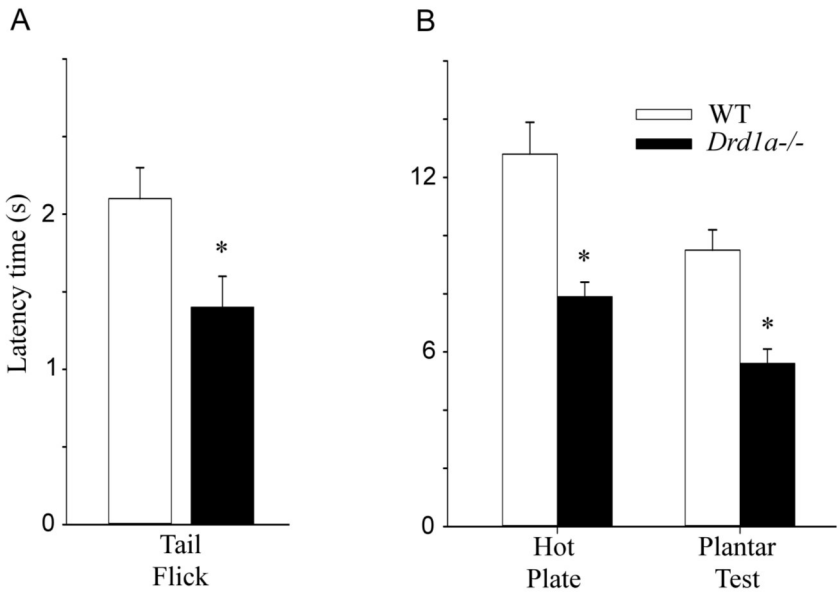

Figure 22. Pain sensitivity in *Drd1a*$^{-/-}$ mice. Pain sensitivity thresholds (in seconds, mean ± SEM) of mice in the tail-flick test **(A)**, hot plate and plantar test **(B)**. *Drd1a*$^{-/-}$ mice exhibit lower pain thresholds than WT mice in all three test, indicating higher pain sensitivity. Statistics were determined with with Student's *t* test . *p<0.05 vs. WT mice.

sensitive than WT mice. In the tail-flick test *Drd1a*$^{-/-}$ mice showed a latency of 1.4 ± 0.2 and their WT mice 2.1 ±0.2; in the plantar test *Drd1a*$^{-/-}$ mice showed 5.6 ± 0.5 vs. WT mice 7.9 ± 0.5; and in the hot plate test *Drd1a*$^{-/-}$ mice showed 9.5 ± 0.7 vs. 12.9 ± 1.14, for WT mice.

Passive avoidance. Passive avoidance learning depends on multiple cortical and subcortical structures, including both dorsal a ventral striatum as well as hippocampus and amygdala (Pittinger et al., 2006). In this test, avoidance response or entry latency increases with foot-shock intensity (Crawley et al., 2007). First we determined the sensitivity to foot-shock for both genotypes by gradually increasing foot-shock intensity (0.01-0.6 mA) and monitoring the onset of behavioural indicators of pain. WT and *Drd1a*$^{-/-}$ mice showed similar sensitivity thresholds to foot-shock (Fig. 23A), responding with a sudden stare at floor bars, startle response, and jumping and vocalization at the same foot-shock intensities in both genotypes. Jumping and vocalization responses, indicative of pain threshold, were elicited with 0.12 mA in both groups of mice.

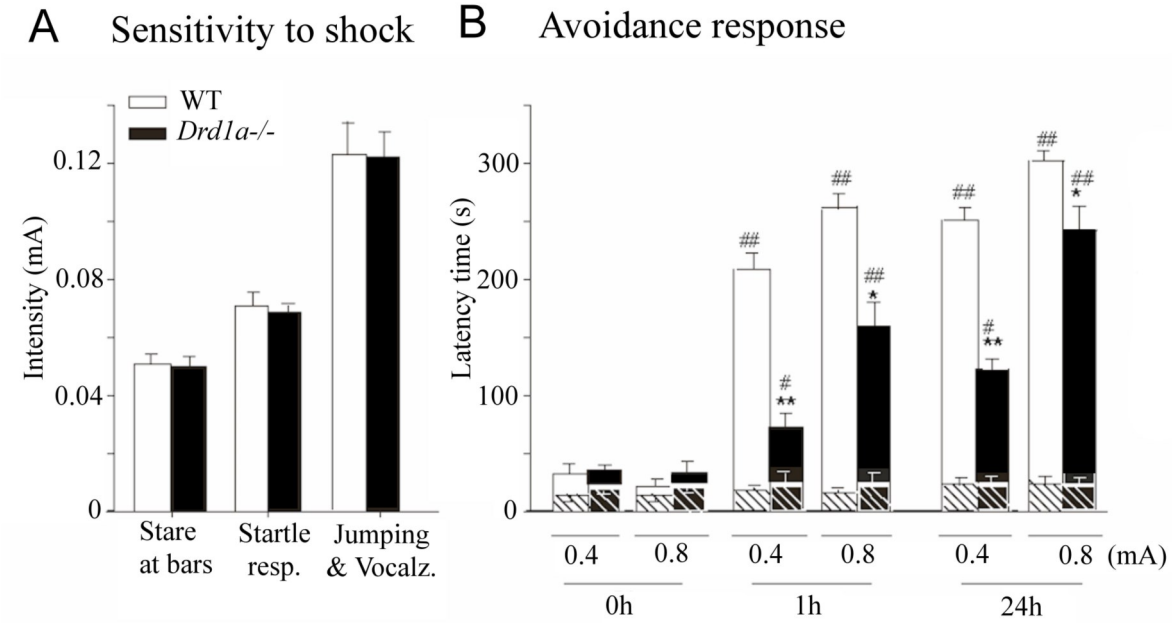

Figure 23. Performance in the passive avoidance test is impaired in *Drd1a*$^{-/-}$ mice. **A.** Thresholds for foot shock responses. Increasing intensity foot-shocks were delivered to WT and *Drd1a*$^{-/-}$ mice, and the threshold for each listed behaviour was determined. Thresholds for all three response behaviours were similar in the two genotypes. **B.** Avoidance response. Latency refers to the time spent in the light compartment before mice enter the dark compartment which was paired with foot-shock in a single training trial. *Drd1a*$^{-/-}$ mice show partial impairment of passive avoidance at both 0.4 and 0.8 mA. *$p < 0.01$ and **$p < 0.001$ vs. WT; $^{\#}p < 0.01$ and $^{\#\#}p < 0.001$ vs. Pre-shock (0 h). Data show mean ± SEM. Statistics were determined by repeated-measures two-way ANOVA followed by *post-hoc* analysis with Tukey's test.

Passive avoidance experiments were performed with a moderate (0.4 mA) and a strong (0.8 mA) electric stimulus (Viosca et al., 2009), both well above the pain threshold (Fig. 23B). Baseline entry latency times in the passive avoidance test were similar in all experimental groups. However, after the training with either 0.4 or 0.8 mA foot-shocks, *Drd1a*$^{-/-}$ mice exhibited a shorter latency than WT mice (Fig. 23B), indicative of reduced memory strength. When animals were tested 24 h after 0.4 mA foot-shock, WT mice showed a latency time of 250 s compared with 123 s in *Drd1a*$^{-/-}$ mice ($p< 0.001$). With a 0.8 mA shock, this difference was smaller but still statistically significant ($p< 0.01$) (Fig. 23B).

Two-Way Active avoidance. Dopamine depletion impairs the acquisition and maintenance of conditioned avoidance responses (Shannon et al., 1999), suggesting that dopamine receptors are involved in this behavior. To determine whether the dopamine D_1R plays a role in this associative learning task, we used the two-way active avoidance paradigm. In his paradigm, WT mice learned the avoidance response within the first 2 days of training, while *Drd1a*$^{-/-}$ mice were unable to learn it, even with an extensive period of training (Fig. 24). Differences between *Drd1a*$^{-/-}$ and WT mice were first evident on the second day of training (*$p < 0.001$) and persisted throughout of avoidance learning in *Drd1a*$^{-/-}$ mice (Fig. 24).

The crossing latency reflects how rapidly an animal crosses to the safe compartment after the onset of the CS to avoid the foot-shock (Smith et al., 2002). WT animals progressively reduced their crossing latency, whereas *Drd1a*$^{-/-}$ mice did not, again indicating that *Drd1a*$^{-/-}$ mice were unable to learn that the foot-shock would follow the CS (Fig. 24). Differences in latency between WT and *Drd1a*$^{-/-}$ mice were first observed on the second day of the training phase ($p< 0.001$).

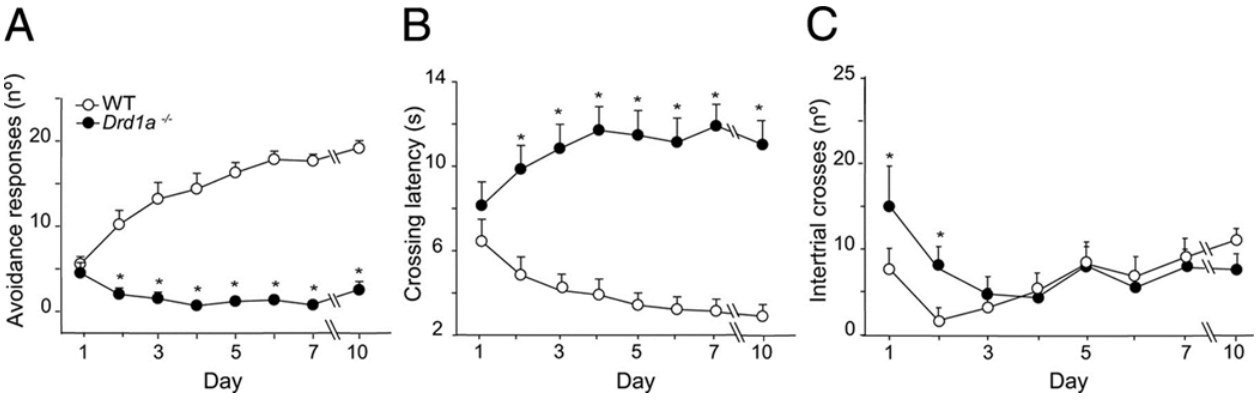

Figure 24. Active avoidance performance is impaired in dopamine *Drd1a*$^{-/-}$ mice. A. Progression of active avoidance responses during the training phase. *Drd1a*$^{-/-}$ mice did not increase the number of avoidance responses during the training phase (*$p < 0.001$). **B**. Time-course of crossing latencies for WT and *Drd1a*$^{-/-}$ mice during the training phase. *Drd1a*$^{-/-}$ mice did not decrease escape latency at any point during training (*$p < 0.001$). **C**. Number of inter-trial crosses. From day 3 on, there was no significant difference between WT and *Drd1a*$^{-/-}$ mice in the number of inter-trial crosses. Data shown are mean values ± SEM. Statistics performed with repeated measures two-way ANOVA, followed by post-hoc analysis with Tukey's test.

Except for the first 2 days, we found no difference between WT and *Drd1a*$^{-/-}$ mice in baseline crossing behavior, determined by counting crossings during the ITIs in the training phase or on the test day (Fig. 24). Thus, the poor performance of the *Drd1a*$^{-/-}$ mice in this paradigm suggests impaired associative learning rather than changes in locomotor behavior.

We found during the first days of training an increase in crossing latency for *Drd1a*$^{-/-}$ mice (Fig. 24B). In fact, most of the mice stop their avoidance responses, close to zero in the last days of training (Fig. 24A). If we analyze the response pattern shown in curves (Fig. 24A,B), we observed that is similar to that obtained in paradigms of "learned helplessness". In this paradigm the animals did not found escape from their position and, in consequence, cease to emit escape or avoidance responses, being able to develop a depressive features. In order to show that this pattern of response is due an important deficit in associative learning and not because of previous emotional disturbances in *Drd1a*$^{-/-}$ mice phenotype, we performed two basic emotional test: The P- Maze, detecting changes in anxiety levels, and the Porsolt test, to detecting depressive symptoms in these mice at basal level (Fig. 25).

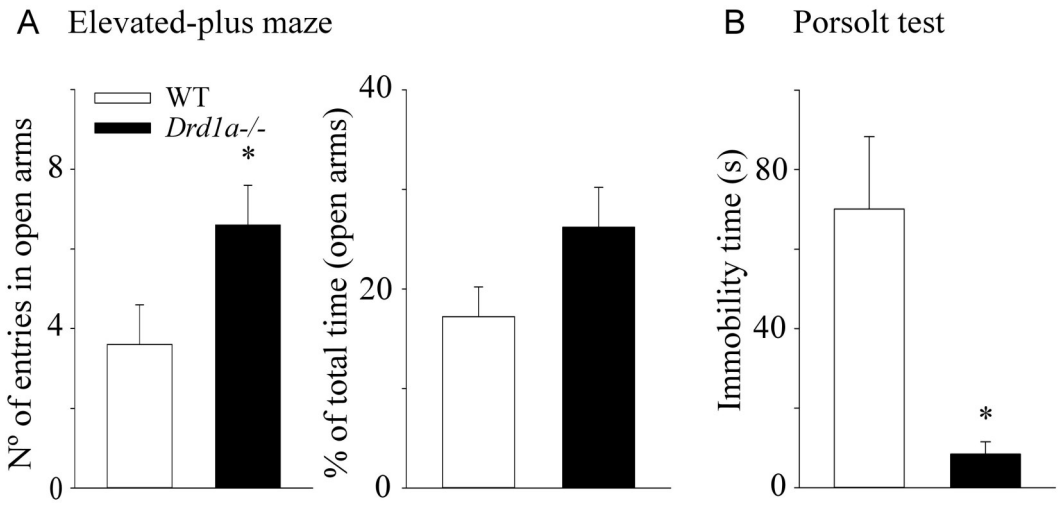

Figure 25. Emotional response in *Drd1a*$^{-/-}$ mice. **A**. Anxiety-like behaviour of *Drd1a*$^{-/-}$ and WT mice illustrated by the number of entries and percentage of total time spent in the open arms of the elevated plus maze test. *Drd1a*$^{-/-}$ mice make more entries in open arms and spend more time but this late one is not statistically significant. These results indicate lower anxiety levels than the WT mice (*$p < 0.05$). **B**. Porsolt test shows that *Drd1a*$^{-/-}$ mice spend less time immobile than WT mice (*$p < 0.05$). Data is expressed in seconds, mean ± SEM. Statistics were determined with Student´s *t* test.

Results obtained in the P-maze test showed a greater number of entries in open arms of the maze by *Drd1a*$^{-/-}$ mice compared to WT (p <0.05) along with a tendency to further exploration of these, which indicates the probability that the basal levels of anxiety in these mice are less

than their WT littermates (Fig. 25A). Similarly, the immobility time in the Posolt test was significantly lower in *Drd1a*$^{-/-}$ mice than in their WT littermates (Fig. 25B; $p < 0.05$; WT: 70 ± 18; *Drd1a*$^{-/-}$: 8.4 ± 3.1), ruling out the possibility of depressive behavior.

1.3. Recognition memory is impaired in *Drd1a*$^{-/-}$ mice.

Object Recognition. We studied recognition memory in a task based on the natural tendency of rodent to explore unfamiliar objects, which depends in part on hippocampal integrity (Broadbent et al., 2010; Barker & Warbuton, 2011). On the first day, mice were allowed to explore two identical objects; after 24 h mice were kept in the arena containing the same object as in the day 1 and a new object. We measured the exploration time for the familiar and the novel object. *Drd1a*$^{-/-}$ mice displayed an impairment of memory, as they spent almost the same time exploring the familiar and the novel object (12.7 ± 3.4 vs 12.1 ± 1.5, respectively). WT mice showed a good recognition memory since they spent less time in exploring the familiar than the novel object (11.2 ± 3.6 vs. 28.4 ± 5.9, respectfully) (Fig. 26).

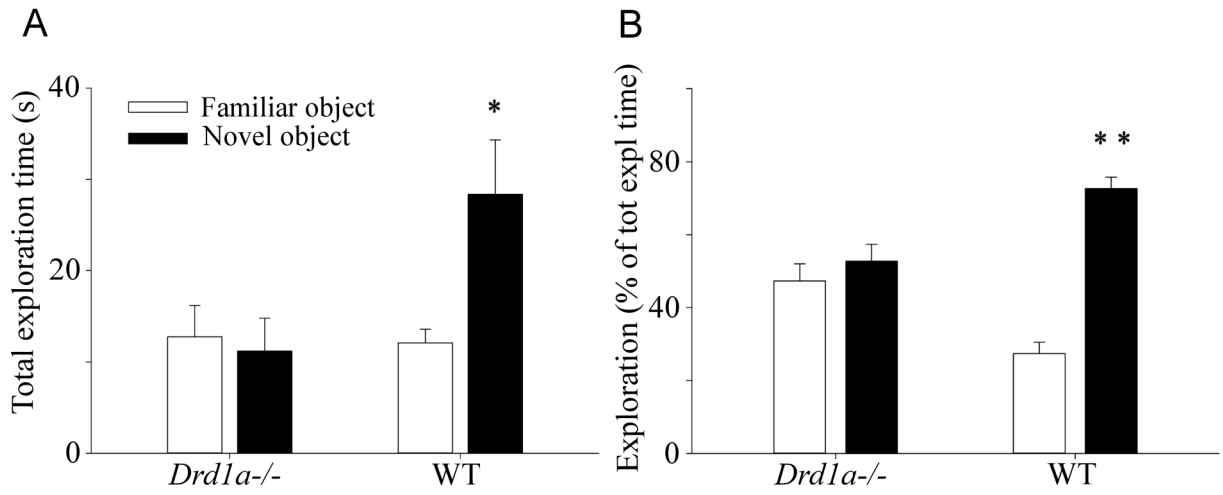

Figure 26. Object recognition test is impaired in *Drd1a*$^{-/-}$ mice. A. Total exploration time in the test day. **B.** Percentage of exploration time spent exploring familiar and the novel object in the test day (24 h retention interval). Data show the mean ± SEM. Statistical significance: *$p < 0.05$; **$p < 0.001$ vs. familiar object. Statistics were determined with Student´s *t* test.

2. DOPAMINERGIC SIGNALING BY D_2R IN HIPPOCAMPUS REGULATE ASSOCIATIVE LEARNING AND CHANGES IN SYNAPTIC PLASTICITY.

2.1. The D_2R is important for acquisition and consolidation of spatial memory.

We used the Barnes maze with a similar protocol of D_1R experiments to assess the role of dopamine D_2R in spatial learning and memory. WT mice learned to escape the open field and reached the black scape box, as shown the rapid decline in escape latency (Fig. 27A). By day 9 of training, escape latency has reached a minimum that was maintained throughout the training phase (14 day) and during the probe trial, 3 days later. But the *Drd2*$^{-/-}$ mice had a slower reduction in escape latency than WT mice (Fig. 27A).

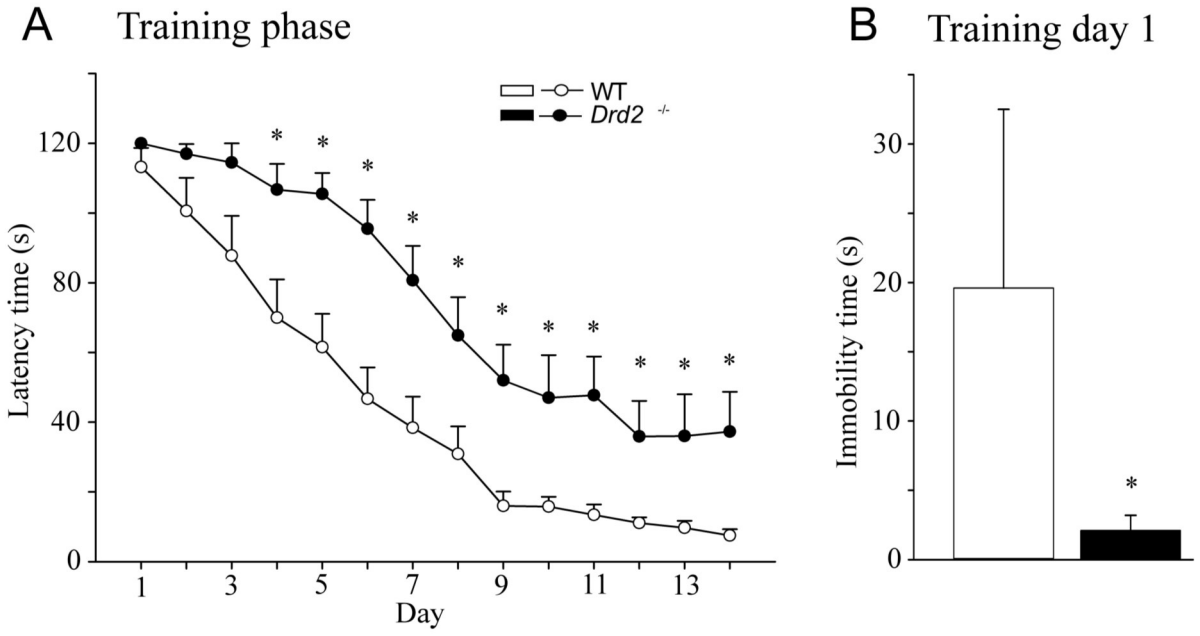

Figure 27. Inactivation of D_2R impaired hippocampus–dependent learning. A. Progression of escape latency during the training phase in the Barnes maze *Drd2*$^{-/-}$ mice reduce less than WT the escape latency during the experiment (**p*< 0.001). **B.** Immobility during the first day of training. *Drd2*$^{-/-}$ mice showed a significantly reduced immobility time (**p*<0.001). Data show the mean values ± SEM. Statistics were determined with repeated-measures two-way ANOVA followed by Tukey´s test for *post hoc* analysis (A).

The inactivation of *Drd2* is possible that modify the anxiety basal response in these mice, preventing a better execution in the maze. The immobility time during the first trial was evaluated on the first day of training in the Barnes maze, as an indirect measure of anxiety. *Drd2*$^{-/-}$ mice spent less time immobile than WT (Fig. 27B).

In addition, *Drd2*$^{-/-}$ mice showed less reduction in escape latency in a probe trial performed 3 days after training to evaluate memory consolidation (Fig. 28A). During the relearning trials, when the escape hole was moved to the opposite side of the training arena, *Drd2*$^{-/-}$ mice once more show similar deficits to the training phase (Fig. 28B). These data indicate that the D_2R is required for spatial learning.

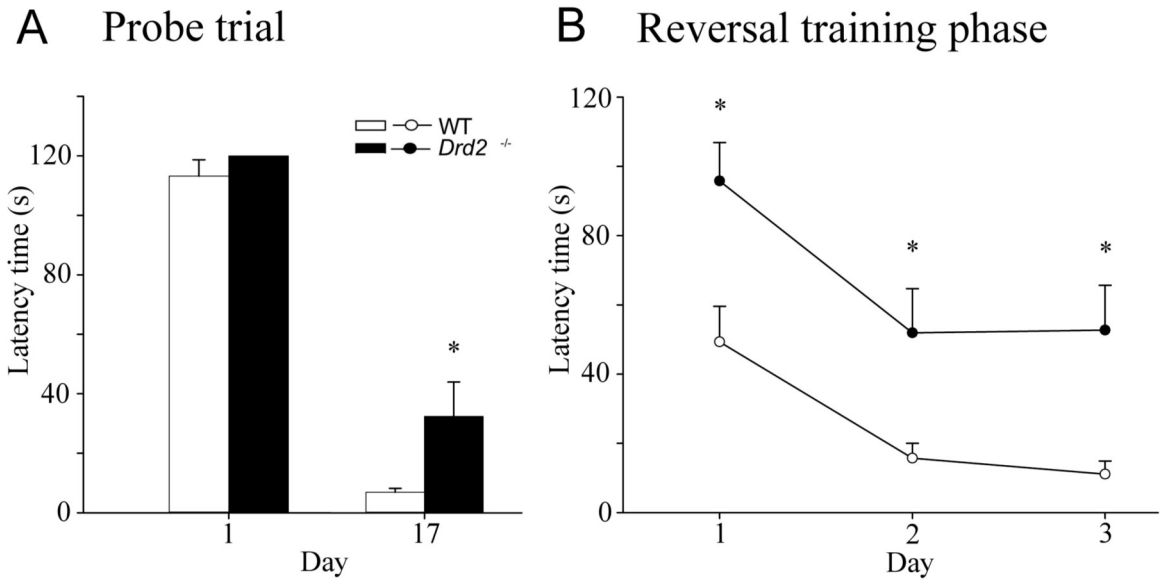

Figure 28. Inactivation of *Drd2* impaired spatial learning. A. Probe trial performed 3 days after the training phase. Histograms represent the time spent searching for the escape hole. The *Drd2*$^{-/-}$ mice reduce searching time during the probe trial, but the latency of WT mice is significantly reduced (*p<0.01). **B.** Escape latency during the relearning phase. For this test, the escape hole was located opposite to its position in the training phase (*p<0.01). Data show the mean values ± SEM. Statistics were determined with Student's t test (A) and repeated-measures two -way ANOVA followed by Tukey´s test for *post hoc* analysis (B)

Although, it has been shown that *Drd2*$^{-/-}$ mice have no severe motor impairment (Kelly et al., 1998) recent studies have found hypoactivity in this mice (Nakamura et al., 2014) which may lead to reduced exploratory response. Therefore, it was necessary to exclude that the slow acquiring of minimum escape response in the Barnes maze compared to their WT were not due to less exploratory response.

First, we measured the number of holes explored by *Drd2*$^{-/-}$ mice (Fig. 29A), quantifying the holes explored in the Barnes maze the first day of training. We found that *Drd2*$^{-/-}$ mice explored less holes (8.2 ± 1) than WT mice (11.8 ± 1.4) (Fig. 29A) until day 4 of training in which the number of holes explored are similar in both genotypes and are maintained for the rest of training (Fig. 29B). For these reason, we can not reject that the delay acquisition of *Drd2*$^{-/-}$ mice is due to a lower exploratory response.

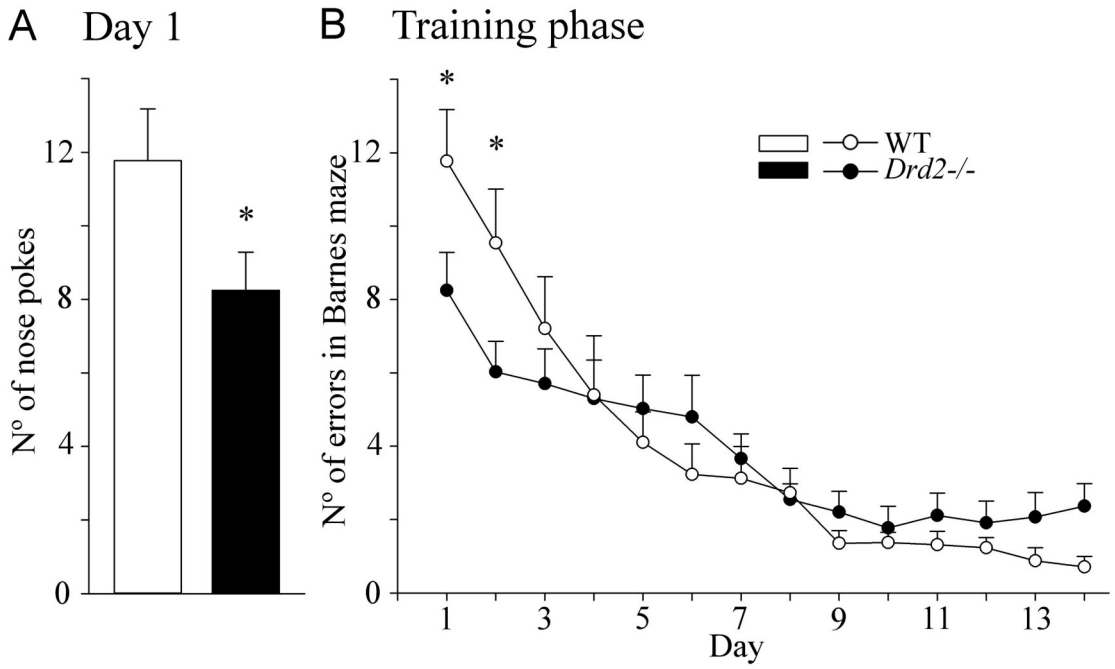

Figure 29. Exploratory behavior in *Drd2*$^{-/-}$ mice. A. Number of holes explored during the first day of training. *Drd2*$^{-/-}$ mice showed a significantly reduced exploratory behavior (*p<0.05). **B.** Modification of errors during the training phase in the Barnes maze. Except for the first two days, *Drd2*$^{-/-}$ mice show similar number of errors than WT during the training phase (*p<0.001). Data show the mean values ± SEM. Statistics were determined with Student's *t* test

2.2. A_2A receptor antagonist does not improve spatial learning in *Drd2*$^{-/-}$ mice.

In the previous experiments we could not possible ruled out the possibility that a poor environmental exploration could cause the slower execution of *Drd2*$^{-/-}$ mice on the Barnes maze. Therefore, to discharge this influence another spatial maze was performed, the MWM. This test requires hippocampal function and suitable motor coordination (Martin & Morris, 2002; Granado et al., 2008). In addition mice were administered caffeine (an A_2A receptor antagonist) that improves exploratory and motor behavior in these mice even in the absence of D_2R (Chen et al., 2001). After habituation to the water maze with caffeine, mice were given 4 training trials per day for 12 consecutive days without caffeine. WT mice quickly learned to reach the platform, reaching the minimum escape latency by day 7, with no further significant change in escape latency between days 7 and 12 (Fig. 30A). In contrast, the reduction in escape latency over the course of training occurred more slowly in *Drd2*$^{-/-}$ mice than in their WT mice and did not reach the lowest latency level of the WT mice (Fig. 30A).

Furthermore, Fig. 30B represents the distance traveled per day the two groups. Both, *Drd2*$^{-/-}$ and WT mice, decreased over training phase as mice were learning the task.

However, *Drd2*$^{-/-}$ mice from the beginning of the experiment, traveled greater distances to search for the platform than WT, further supporting that this deficit is not due to a less environmental exploration and supports an impairment in spatial learning in *Drd2*$^{-/-}$ mice. These results indicate that inactivation of *Drd2* does not completely inhibit learning, but impairs it significantly, in a way that training is required for *Drd2*$^{-/-}$ mice to reach the same level of learning that their WT.

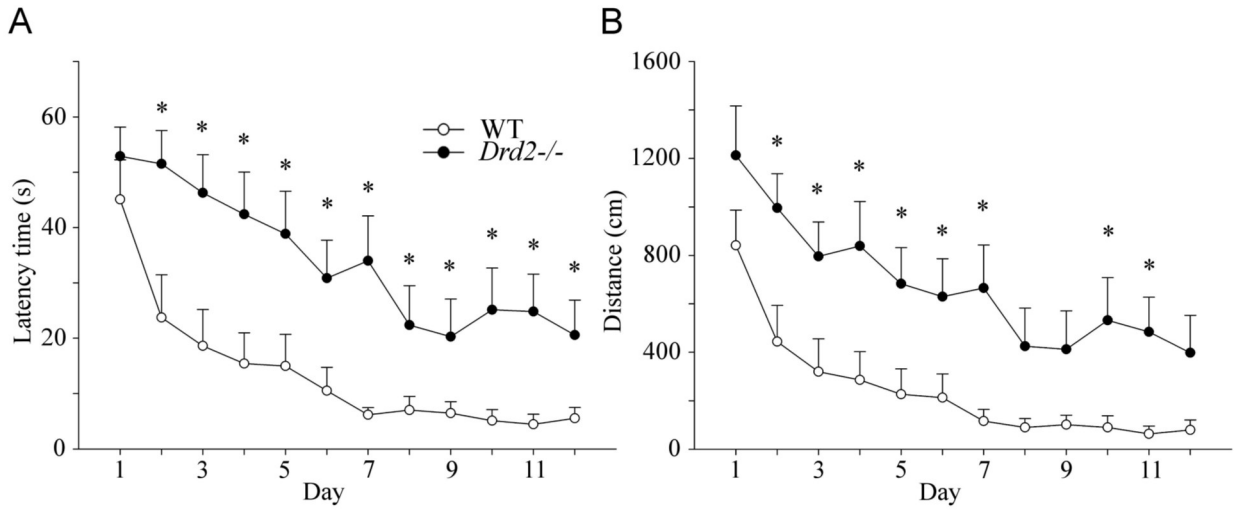

Figure 30. *Drd2*$^{-/-}$ mice shows slow spatial learning even after pre-exposition to MWM with caffeine. A. Progression of escape latency during the training phase in the MWM. *Drd2*$^{-/-}$ mice reduce less than WT the escape latency during the experiment (**p*<0.001). **B**. Distance trail during the training phase decrease through the days, but is much higher in *Drd2*$^{-/-}$ mice than in WT mice (**p*< 0.05). Data show the mean values ± SEM. Statistics were determined with repeated-measures two-way ANOVA followed by Tukey´s test for *post hoc* analysis.

Retention was tested at 48 h (Test 1-with caffeine) and 74 h (Test 2-without caffeine) after the training period by removing the submerged platform. We measured the percentage of time that mice spent in each quadrant of the pool and the number of crosses through the platform location site. WT mice spent selectively more time in the target quadrant in Test 1 with caffeine (66.3 ± 3.2 %) and in Test 2 without caffeine (50 ± 3.7 %) during retention test than on the first day of training (26.3 ±.1.9 %) (Fig. 31B). Although *Drd2*$^{-/-}$ mice slightly increased their time in the target quadrant compared to the first day of training, (25.6 ± 2.5%), in Test1 (56.1 ± 4.3 %) and in Test 2 (34.5 ± 3.3%) this increase was significantly lower than that of WT animals (Fig. 31*B*, Test 1: $p < 0.001$, test 2: $p < 0.001$).

Similarly, in the two test probes, *Drd2*$^{-/-}$ mice made significantly fewer crosses through the platform location site than WT mice, in Test 1 with caffeine (8 ± 0.7 vs. 10.2 ± 0.5; p=0.019) and in Test 2 without caffeine (6.7 ± 0.5 vs. 9.7 ± 0.7; p=0.002) (Fig. 31A).

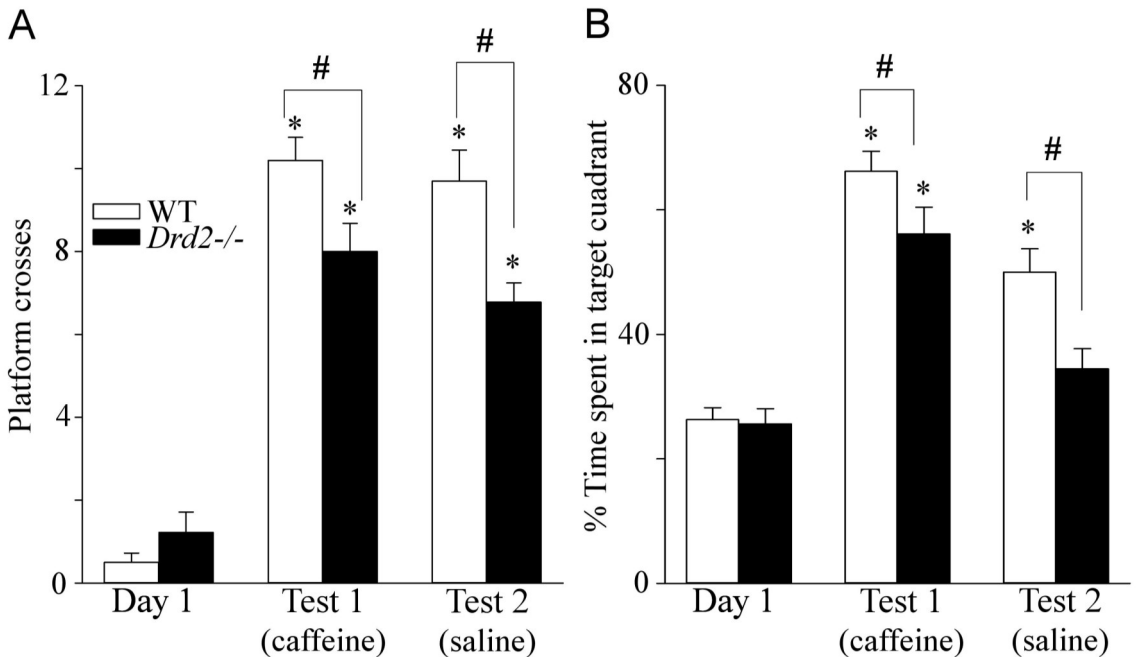

Figure 31. *Drd2*$^{-/-}$ mice shows spatial retention deficits. Probe trial performed after the training phase: 48h later with caffeine (15mg/kg) and 74 h without caffeine (saline). **A.** Histograms represent the number of platform crosses both type of mice increase platform crosses during the Tests 1 and 2(*p< 0.001), but the number of crosses of WT mice is significantly higher in the two conditions ($^{\#}p$<0.05). **B.** Histograms represent the percentage of time spent in target quadrant. The WT and *Drd2*$^{-/-}$ mice increase searching time during the tests (*p<0.001), but the values of WT mice are significantly higher in the two tests ($^{\#}p$<0.05). Data show the mean values ± SEM. Statistics were determined with repeated-measures two-way ANOVA followed by and with Student's *t* test.

Both groups decreased the time spent in the target quadrant and the number of platform crosses between Test 1 and Test 2. However, in both conditions, the differences between the two groups were maintained, ruling out the possibility of a motor impairment influence. Finally, these results are similar to the results obtained using the Barnes maze, and suggest that *Drd2* $^{-/-}$ mice are unable to consolidate the navigation strategies.

2.3. Nociceptive threshold of *Drd2*$^{-/-}$ mice.

Similar to D_1R experiments, as we were going to use an electric shock as aversive stimulus for associative test, we carry out a battery of nociceptive test in *Drd2*$^{-/-}$ and WT mice. Two nociceptive thermal test were used, that impact in different degree peripheral or central processing of painful stimuli. It was measure the latency of withdrawal response, we did not find significantly differences between *Drd2*$^{-/-}$ and WT mice in the tail-flick test and the plantar test (Fig. 32A).

In addition, before the associative learning task, we first determined the sensitivity to foot-shock for both genotypes by gradually increasing foot-shock intensity (0.01-0.6 mA) and monitoring the onset of behavioural indicators of sensation or pain. WT and *Drd2*$^{-/-}$ mice showed similar thresholds to foot-shock for all 3 behavioural signs (Fig. 32B): approximately 0.025 for

staring at bars, 0.1 mA for the startle response, and 0.17 mA for jumping.

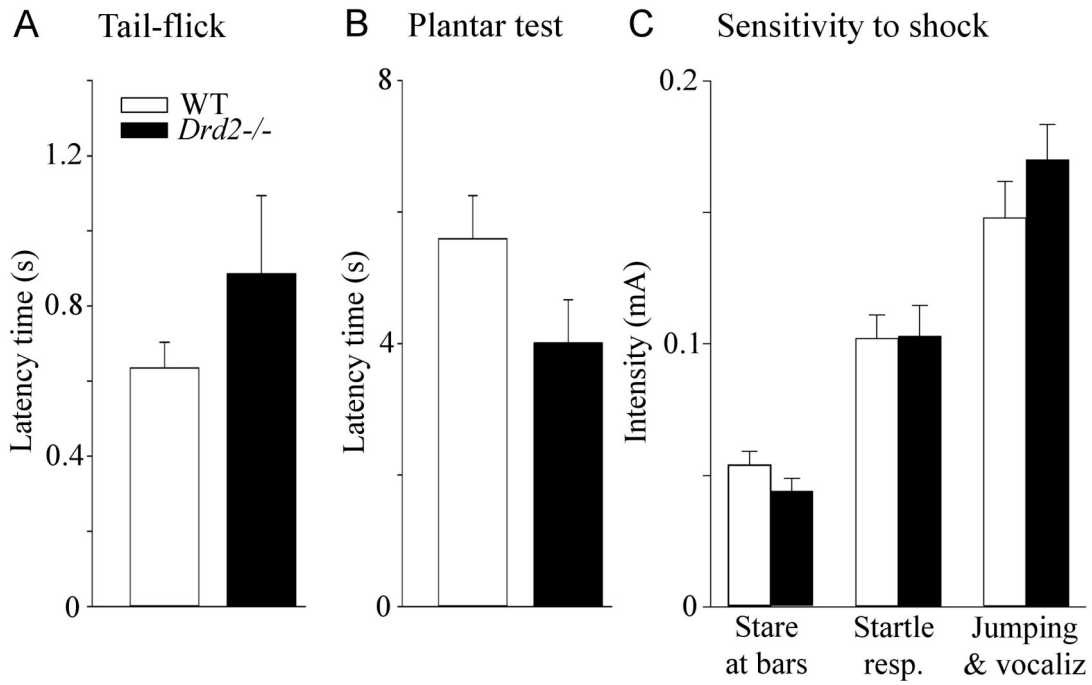

Figure 32. Pain sensitivity in *Drd2*$^{-/-}$ mice. Pain sensitivity thresholds (in seconds, mean ± SEM) of mice in the tail-flick test **(A)**, plantar test **(B)** and sensitivity to shock **(C)**. Thresholds for foot-shock responses. Thresholds for all three nociceptive test were similar in both genotypes.

2.4. Associative learning is impaired in *Drd2*$^{-/-}$ mice

Two-way Active avoidance. Drd2$^{-/-}$ mice were completely unable to learn in the two way active avoidance task, in agreement with similar previous results (Fetsko et al., 2005). While WT mice learned the task during the first two days, there was no change in the response of the *Drd2*$^{-/-}$ mice throughout the entire 11-day training phase, indicating that these mice did not learn to associate the CS with the foot-shock (Fig. 33A). In fact, *Drd2*$^{-/-}$ mice crossed to the other compartment only when the shock was delivered, within 5 s of starting the trial, (Fig. 33B). Differences in crossing latency between WT and *Drd2*$^{-/-}$ mice were first observed on the second day of training ($p < 0.001$) and continued over the entire test. ITI crosses were higher, but not significantly, in *Drd2*$^{-/-}$ than in WT mice for the first three days (Fig. 33C), supporting the conclusion that the poor performance of the *Drd2*$^{-/-}$ mice in this paradigm is due to impaired associative learning and not to locomotor activity.

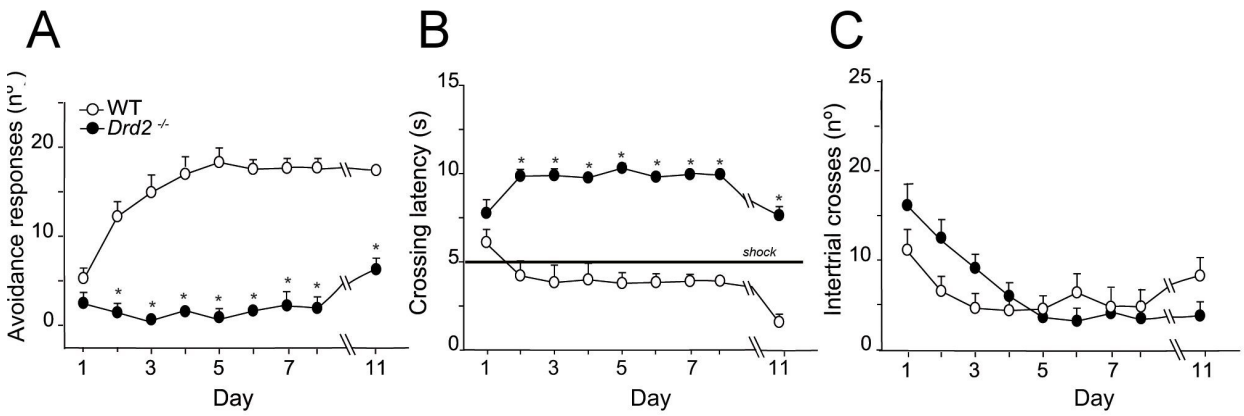

Figure 33. **Active avoidance performance is impaired in dopamine *Drd2*$^{-/-}$ mice. A.** Progression of active avoidance responses during the training phase. *Drd2*$^{-/-}$ mice did not increase the number of avoidance responses during the training phase (**p*<0.001). **B.** Time-course of crossing latencies for WT and *Drd2*$^{-/-}$ mice during the training phase. *Drd2*$^{-/-}$ mice did not decrease escape latency at any point during training (**p*<0.001). **C.** Number of inter-trial crosses, IT. The number of IT crosses was similar in both genotypes, indicating that *Drd2*$^{-/-}$ mice have the same crossing ability than WT. Data shown are mean ± SEM. Statistics were performed with repeated-measures two-way ANOVA, followed by post hoc analysis with Tukey´s test.

Fear conditioning learning. We studied the role of D_2R in a fear conditioning task that measures the ability to associate an aversive stimulus, in this case an electric foot-shock (US), with a neutral environmental context (CS). This memory depends on hippocampal and amygdalar function. In this test, learning is evaluated by the percentage of time that animals freeze when re-exposed to the CS. In our experiments, baseline levels of freezing were similar in the two genotypes before the shock (Fig. 34A).

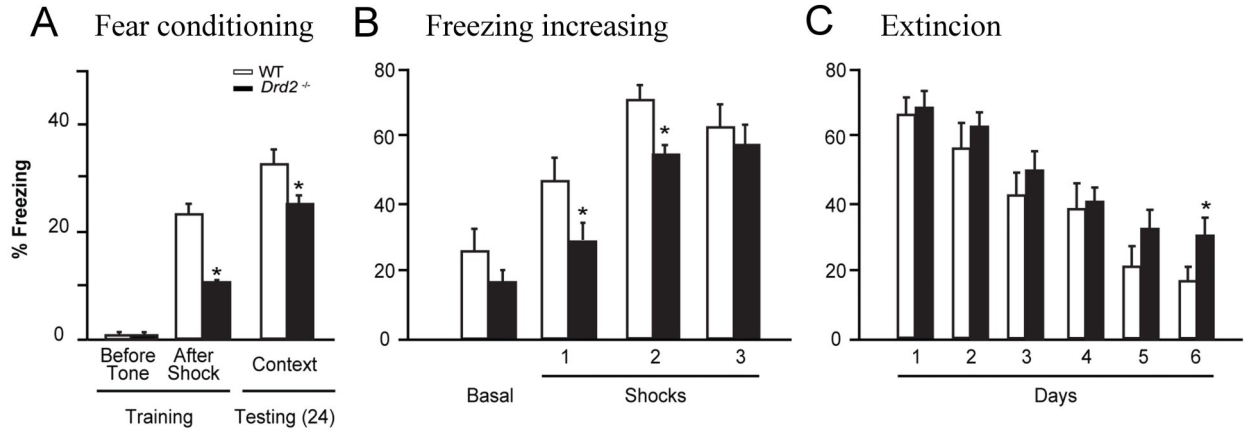

Figure 34. Performance in the fear conditioning is reduced in *Drd2*$^{-/-}$ mice. A. After the shock, *Drd2*$^{-/-}$ mice spent significant (**p*<0.01) less time freezing than their WT littermates, and 24 h after shock, freezing times were still significantly lower in *Drd2*$^{-/-}$ mice, although the magnitude of the difference was reduced (**p*< 0.01). **B.** Freezing time after 3 foot-shocks separated by 2 min to stabilish similar freezing times in both genotypes. **C.** Daily freezing time in the context without foot-shock. The extinction curve was similar for both groups of mice, except the last day, in which *Drd2*$^{-/-}$ mice have higher values indicating lower extinction. Data shown are mean ± SEM. Statistics were performed with repeated-measures two-way ANOVA, followed by post hoc analysis with Tukey´s test.

However, immediately after the shock, *Drd2*$^{-/-}$ mice spent significant ($p< 0.01$) less time freezing than their WT littermates, and 24 h after shock, freezing times were still significantly lower in *Drd2*$^{-/-}$ mice, although the magnitude of the difference was reduced (Fig. 34A).

We study fear extinction, 48 h after fear conditioning, delivered three consecutive foot-shocks separated by 2 min to establish similar freezing times in both genotypes (Fig. 34B), as described previously (Ortiz et al., 2010). Subsequently, mice were tested for freezing in the US context daily for six consecutive days without foot-shock. The extinction curve was similar for both groups of mice, with *Drd2*$^{-/-}$ mice presenting slightly higher values every day. However, this difference was only significant on the last day of the experiment, day 6 (Fig. 34C). These results indicate that the *Drd2*$^{-/-}$ is necessary for normal fear extinction.

2.5. Emotional response of *Drd2*$^{-/-}$ mice.

As we know, dopamine is involved in motivational and emotional aspects, for this reason it was necessary evaluate the emotional behavior of *Drd2*$^{-/-}$ mice. In addition, we find similar results to *Drd1a*$^{-/-}$ mice in active avoidance for *Drd2*$^{-/-}$ mice: an increase in crossing latency and a decrease in avoidance responses during the first days of training resulting in most of these stop their avoidance responses in last days of training (Fig. 33A,B).Therefore, we performed two emotional tests: P-Maze, and Porsolt (Fig. 35).

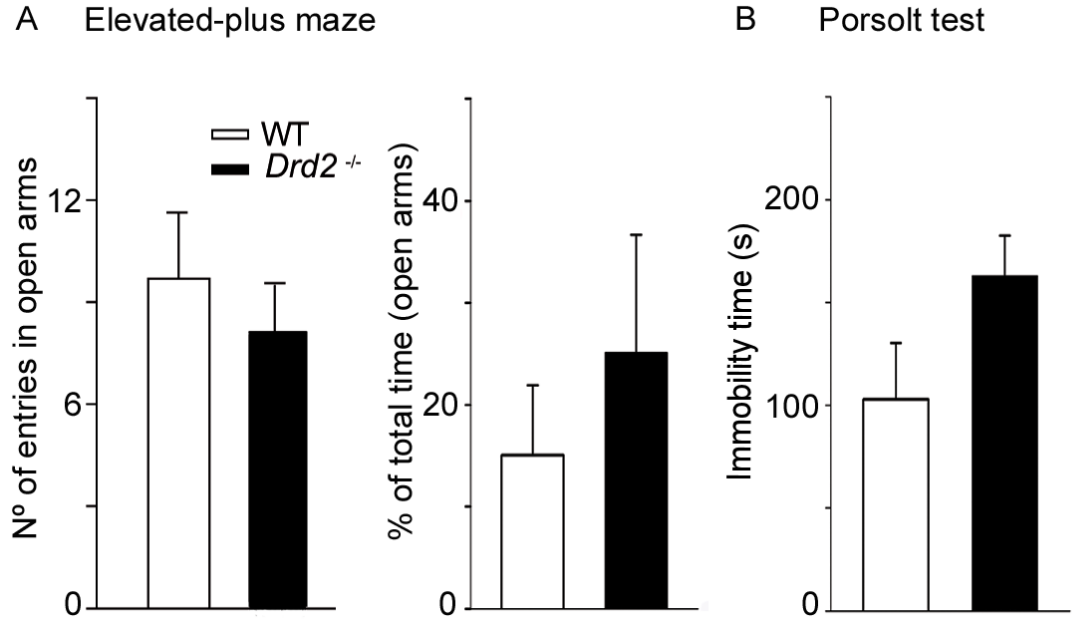

Figure 35. *Drd2*$^{-/-}$ mice show not affect emotional response. A. P-maze: anxiety-like behavior of *Drd2*$^{-/-}$ and WT mice illustrated by the number of entries and percentage of total time spent in the open arms of the elevated plus maze. *Drd2*$^{-/-}$ mice showed similar number of entries and time spent in the open arms. **B.** Porsolt test: WT and *Drd2*$^{-/-}$ mice showed similar time immobile. Data shows are mean ± SEM.

The results obtained in the number of entries and time spent in the open arms of P-maze were not significantly different between *Drd2*$^{-/-}$ and WT mice (Fig. 35A). In addition, WT and *Drd2*$^{-/-}$ mice showed similar immobility times in Porsolt test (Fig. 35B). These results indicate that emotional response was similar in both genotypes. We consider that the pattern of response in active avoidance is exclusively due to an importan deficit in associative learning and not to anxious or depressive signs in *Drd2*$^{-/-}$ mice phenotype.

2.6. *In vitro* and *in vivo* siRNA-mediated knock-down of dopamine D_2R

We used Lv-based RNA interference to knock-down D_2R expression in adult animals to rule out developmental compensatory effects in the absence of the D_2R in *Drd2*$^{-/-}$ mice. We designed three siRNAs sequences targeted against different regions of the *Drd2* mRNA. These sequences were inserted into the transfer plasmid of the Lv system, and their efficiency at silencing *Drd2* was assessed in ST*Hdh*$^{+}$/*Hdh*$^{+}$ cells (Fig. 36A). Then, 4 days after infection, there was a dramatic decreased in D_2R protein expression in these cells with Lv-*Drd2*-siRNA mix compared with de cells given Lv-GFP alone. Western blotting revealed a 90.3% decrease in D_2R protein in ST*Hdh*$^{+}$/*Hdh*$^{+}$ cells.

To assess whether Lv-*Drd2*-siRNAs can deplete D_2R expression *in vivo*, we stereotaxically injected the striatum and hipocampus with the mix of Lv-*Drd2*-siRNAs (2µl) mix or with Lv-Mock-GFP as a control. One week after the injection, there were dramatic decreases in D_2R protein or mRNA (*Drd2*$^{-/-}$) levels in these regions in *Drd2*-siRNA injected mice compared with animals given injections of Lv-GFP. We include the striatum in this experiment because the expression of D_2R in this region is higher than in the hippocampus, and this allows us to better assessed the capacity of our vectors to silence *Drd2*. Quantitative RT-PCR revealed an 55% decrease in *Drd2* mRNA expression in the striatum (Fig. 36B), and western blotting revealed a 58% decline in D_2R protein in Lv-*Drd2*-siRNAs injected mice and 66% in *Drd2*$^{-/-}$ mice (Fig. 36C). Both decreases were statistically significant compared to Lv-GFP injected mice. We determined the spread of the virus within the hippocampus in the Lv-GFP-injected mice using immunohistochemistry and found that particles infected ~2mm^2 along the rostrocaudal axis, infecting most of the dorsal hippocampus, including the pyramidal cell layer and dentate gyrus (Fig. 36D, E).

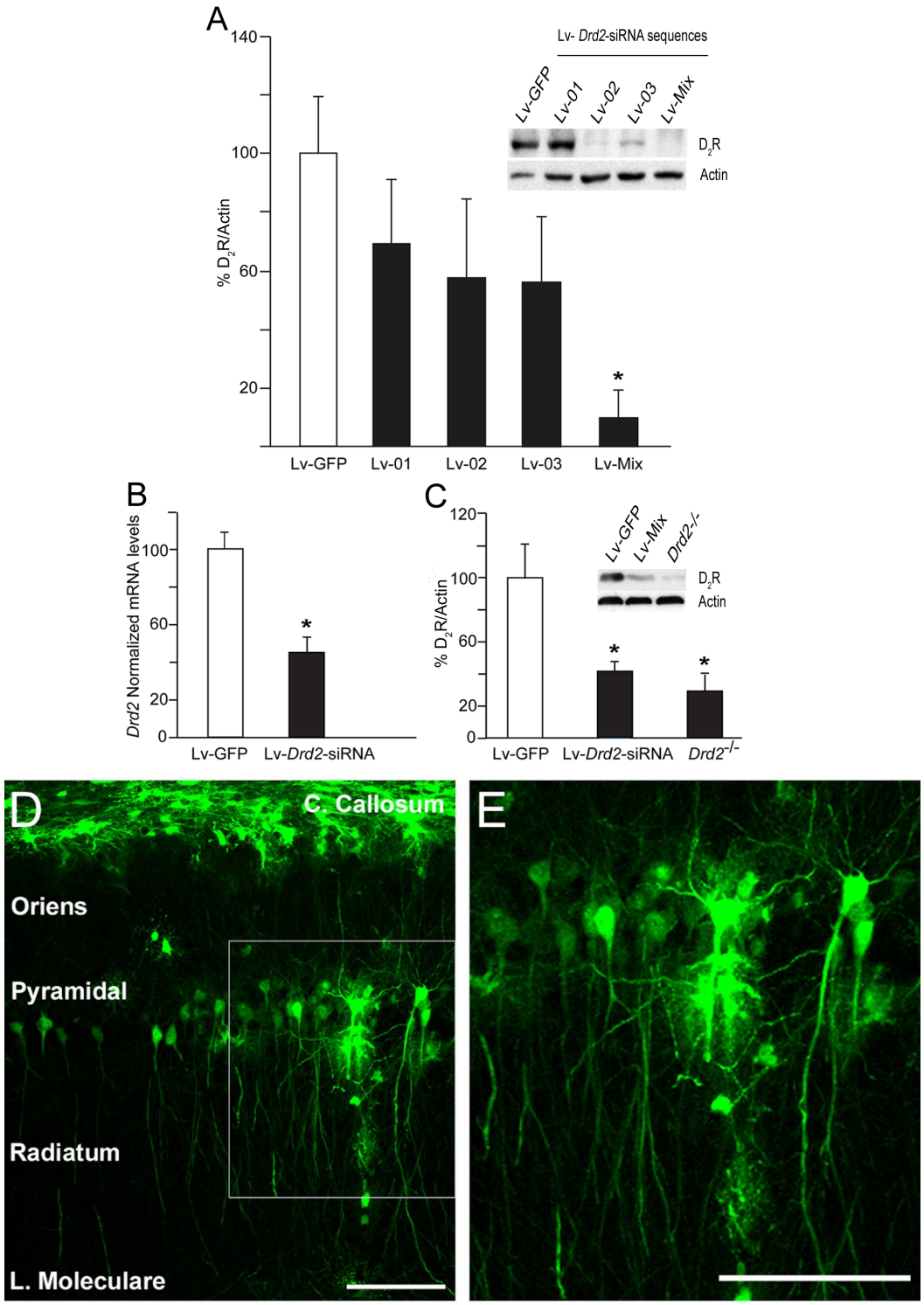

Figure 36. siRNA-mediated *Drd2* silencing in vitro and in vivo. A. Drastic reduction of *Drd2* protein expression cells *in vitro* after infection with *Drd2*-siRNA constructs, **p*= 0.014. **B.** *Drd2* mRNA levels in striatum 48 h after injection of *Drd2*-siRNAs mixture determined by RT-PCR and expressed as a percentage of Drd2 mRNA expression in Lv-GFP-injected animals. Injection of *Drd2*-siRNAs specifically decreased *Drd2* mRNA expression. **C.** D_2R protein levels were decreased 48 h after injection of siRNAs. D_2R protein levels were decreased after injection of siRNAs, **p* = 0.0049, and levels in *Drd2*$^{-/-}$ mice were significantly lower **p* = 0.021. **D.** Photomicrograph of a coronal brain section illustrating the spread of lentiviral infection in the CA1 layer of the hippocampus of WT mice injected with Lv-GFP particles. **E.** High-magnification image of infected pyramidal cells illustrated in **D, E.** Statistics were performed by Student's *t* test. Scale bar = 100 μm.

2.7. Input/output curves and paired-pulse facilitation in the CA3-CA1 synapse were normal in *Drd2*$^{-/-}$ and in *Drd2*-siRNA mice.

In order to determine the basal synaptic transmission in the four groups of animals included in this study, we measured fEPSPs evoked at the CA3-CA1 synapse by the electrical stimulation of Schaffer collaterals at increasing intensities (0.02 mA to 0.4 mA, in 0.02 mA steps) in the following groups of alert behaving mice: WT, *Drd2*$^{-/-}$, WT mice injected with Lv-*Drd2*$^{-/-}$-siRNA (*Drd2*-siRNA), and WT-Sham. Input-output curves revealed no significant differences in basal synaptic transmission between the four groups (Fig. 37A). Interestingly, input-output curves collected from the four groups of mouse were best adjusted by sigmoid curves ($r \geq 0.984$; $p < 0.001$), with no significant differences ($p = 0.067$) between the four groups.

Using the double-pulse test with inter-pulse intervals ranging from 10 to 500 ms, we found a significant ($p < 0.05$) increase in slope of fEPSPs evoked by the 2nd pulse at short time intervals (10-100 ms). There were no significant differences between WT, *Drd2*$^{-/-}$, WT-Sham, and *Drd2*-siRNA mice ($p = 0.181$, Fig. 37B).

The stimulus intensities used in the remainder of this study (for the LTP study and for CA3-CA1 activation during classical eyeblink conditioning) were selected from within a range of 30-40% of the saturating intensity (i.e., the asymptotic values), but still able of evoking facilitation of the second pulse.

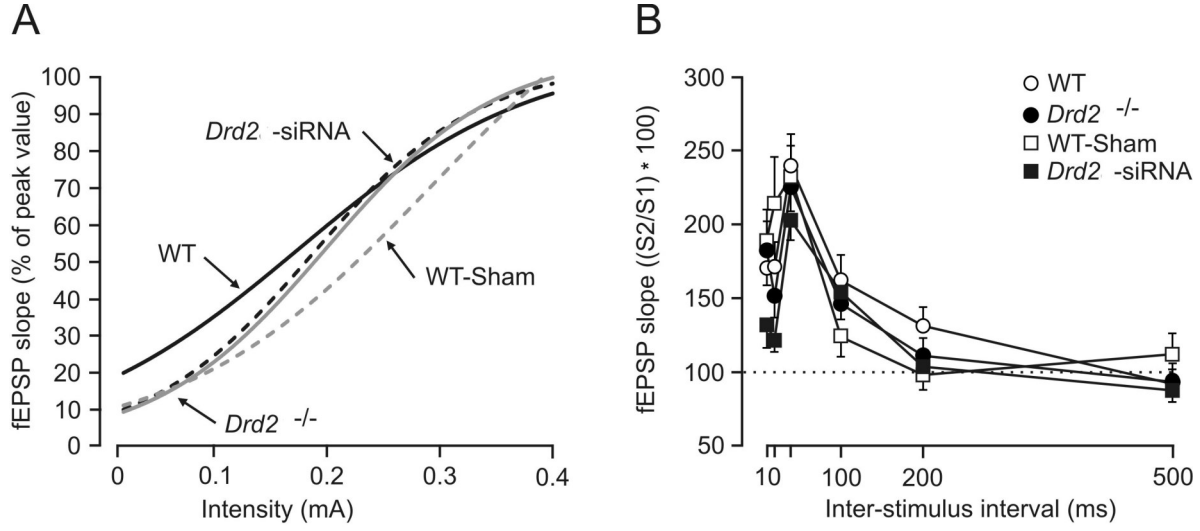

Figure 37. Input-output curves and paired-pulse facilitation in the CA3-CA1 synapse in WT, *Drd2*$^{-/-}$, WT-Sham and *Drd2*-siRNA mice. A. Input-output curves collected from the four experimental groups. Stimulus consisted of single pulses presented at increasing intensities in 20 mA steps. Collected data was best adjusted by sigmoid curves ($r \geq 0.984$; $p < 0.001$; n = 3 animals per group), with no significant ($p = 0.067$) differences between groups. **B**. Paired-pulse facilitation of fEPSPs recorded in the CA1 area following stimulation of Schaffer collaterals. The data shown are mean ± SEM slopes of the second fEPSP expressed as a percentage of the first for the six (10, 20, 40, 100, 200, and 500 ms) inter-pulse intervals. The four groups of mouse presented a significant ($p < 0.05$) paired-pulse facilitation at short (10-40 ms) inter-pulse intervals, but no significant differences ($p = 0.181$) between groups.

2.8. LTP evoked at the CA3-CA1 synapse is significantly reduced in behaving *Drd2*$^{-/-}$ and in *Drd2*-siRNA mice.

To explore the role of the D_2R in hippocampal LTP, we compared CA3-CA1 fEPSPs following HFS of Schaffer collaterals in WT, *Drd2*$^{-/-}$, WT-Sham, and *Drd2*-siRNA mice (Fig. 38A, B). To determine baseline responses, Schaffer collaterals were stimulated every 20 s for 15 min. The stimulus consisted of a 100-µs, square, negative-positive pulse. After HFS, the same single stimulus was presented every 20 s for 30 min and repeated 24 h later, for 15 min. We found LTP in WT and WT-Sham mice for the two recording sessions (Fig. 38A, B). As already reported for the hippocampal CA3-CA1 synapse (Gruart et al., 2006; Madroñal et al., 2007; Ortiz et al., 2010), 15 min after HFS, the response to the single stimulus in both WT and WT-Sham groups was > 150% of baseline values ($p < 0.001$; white circles, Fig. 38A, B).

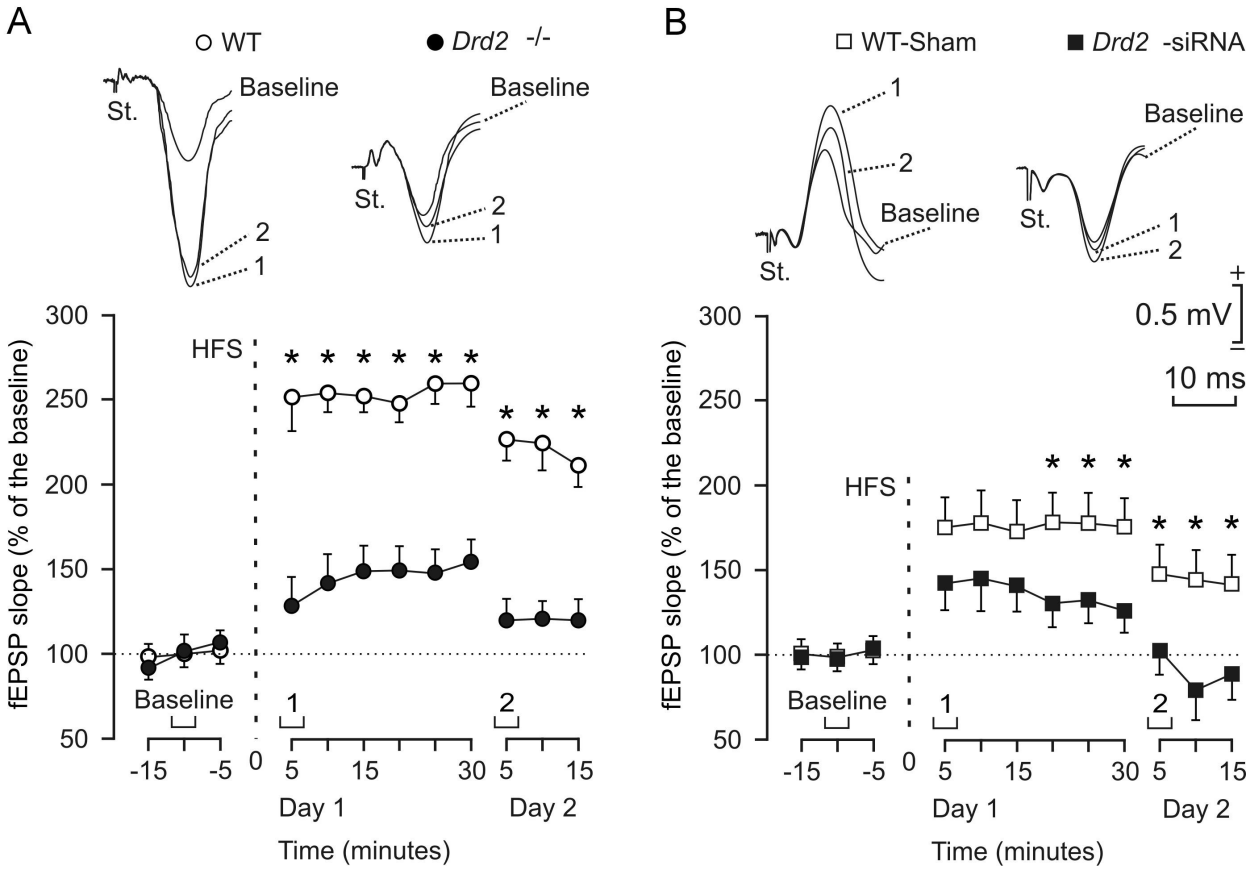

Figure 38. LTP induction in the CA3-CA1 synapse in WT, *Drd2*$^{-/-}$, WT-Sham and *Drd2*-siRNA mice. A. Representative fEPSPs recorded from WT and *Drd2*$^{-/-}$ animals before (baseline), and 5 min (1) and 24 h (2) after HFS. Graphs illustrate the time-course of changes in fEPSPs (mean ± SEM) following HFS stimulation of the Schaffer collaterals. The HFS train was presented after 15 min of baseline recordings, at the time marked by the dashed line. fEPSPs are given as a percentage of the baseline (100%) slope. WT mice presented a significantly larger LTP than *Drd2*$^{-/-}$ animals (*$p < 0.001$). **B.** Same analysis as in *A* for WT-Sham and *Drd2*-siRNA groups. Here again, the control group presented a significantly larger LTP than *Drd2*-siRNA mice (*$p < 0.05$).

Significant LTP persisted at 24 h post-HFS ($p < 0.001$; Fig. 38A, B). Although *Drd2*$^{-/-}$ mice showed a small (< 150%) LTP at the CA3-CA1 synapse after HFS (Fig. 38A, black circles), the collected fEPSP slopes were significantly smaller ($p < 0.001$) than values collected from WT animals for the two post-HFS sessions. Slopes of fEPSP collected from *Drd2*-siRNA mice after the HFS (Fig. 38B, black squares) were significantly ($p < 0.05$) smaller than those collected from WT-Sham only during the second post-HFS session. Thus, both *Drd2*$^{-/-}$and *Drd2*-siRNA mice presented a reduced LTP in the hippocampal CA3-CA1 when compared with their litter-mate controls.

2.9. Classical trace eyeblink conditioning is significantly reduced in *Drd2*$^{-/-}$ and *Drd2*-siRNA mice.

As illustrated in Fig. 39A,B, the neural premotor circuits involved in the generation of reflex eyelid responses function normally in the four groups of animals used in this study (WT, *Drd2*$^{-/-}$, WT-Sham, and *Drd2*-siRNA). Indeed, reflex eyeblinks evoked by the electrical stimulation of the supraorbital nerve were similar to previous descriptions in WT mice (Gruart et al., 2006). There were no significant differences between the four groups of mice in the latency and amplitude of reflexively evoked blinks (not illustrated; $p \leq 0.362$).

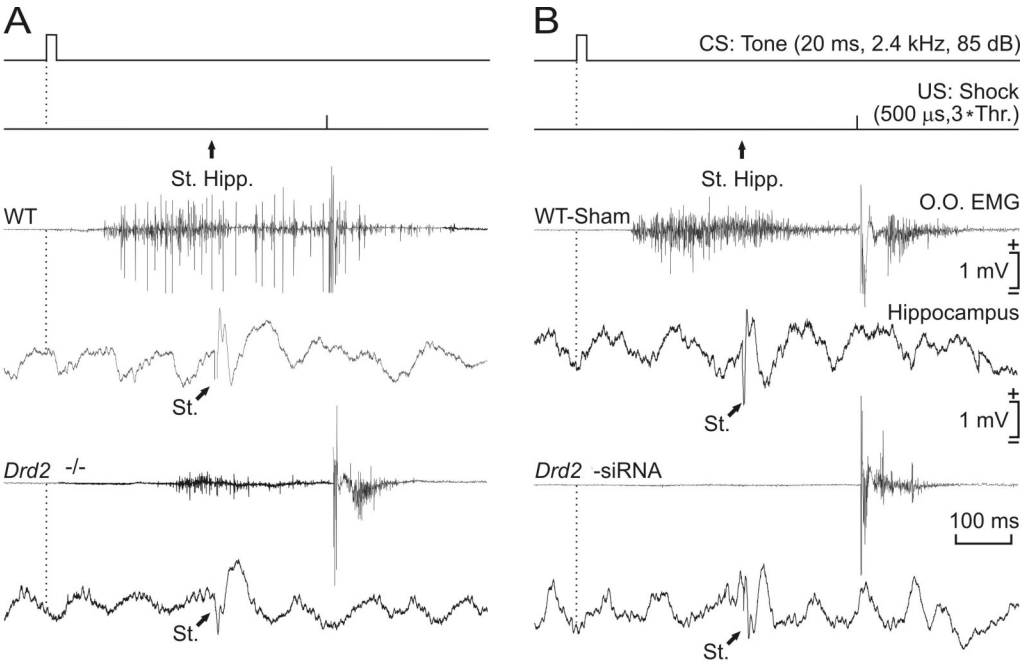

Figure 39. Evolution of CA3-CA1 synaptic field potentials in WT, *Drd2*$^{-/-}$, WT-Sham and *Drd2*-siRNA mice. A, B, From top to bottom are illustrated the conditioning paradigm, representative EMG and hippocampal recordings collected during paired CS-US presentations for WT and *Drd2*$^{-/-}$ mice (**A**) and for WT-Sham and *Drd2*-siRNA mice (**B**). The moment of stimulus presentation at Schaffer collaterals (St.) is indicated, as is the time of delivery of CS (dashed line). Data shown were collected during the 9th conditioning session.

In order to investigate the behavioral consequences of the deficit in synaptic plasticity at the CA3-CA1 synapse observed in *Drd2*$^{-/-}$ and *Drd2*-siRNA mice, we evaluated classical conditioning of eyeblink responses in the four groups of experimental animals using a trace paradigm (CS, tone; US, shock) with a 500-ms interval between the end of the CS and the beginning of the US (Fig. 39A, B).

As illustrated in Fig. 40A, WT mice increased the percentage of CRs across the successive conditioning sessions, being significantly different from habitation values from the 3rd to the 10th conditioning sessions ($p < 0.001$; Fig. 40A).

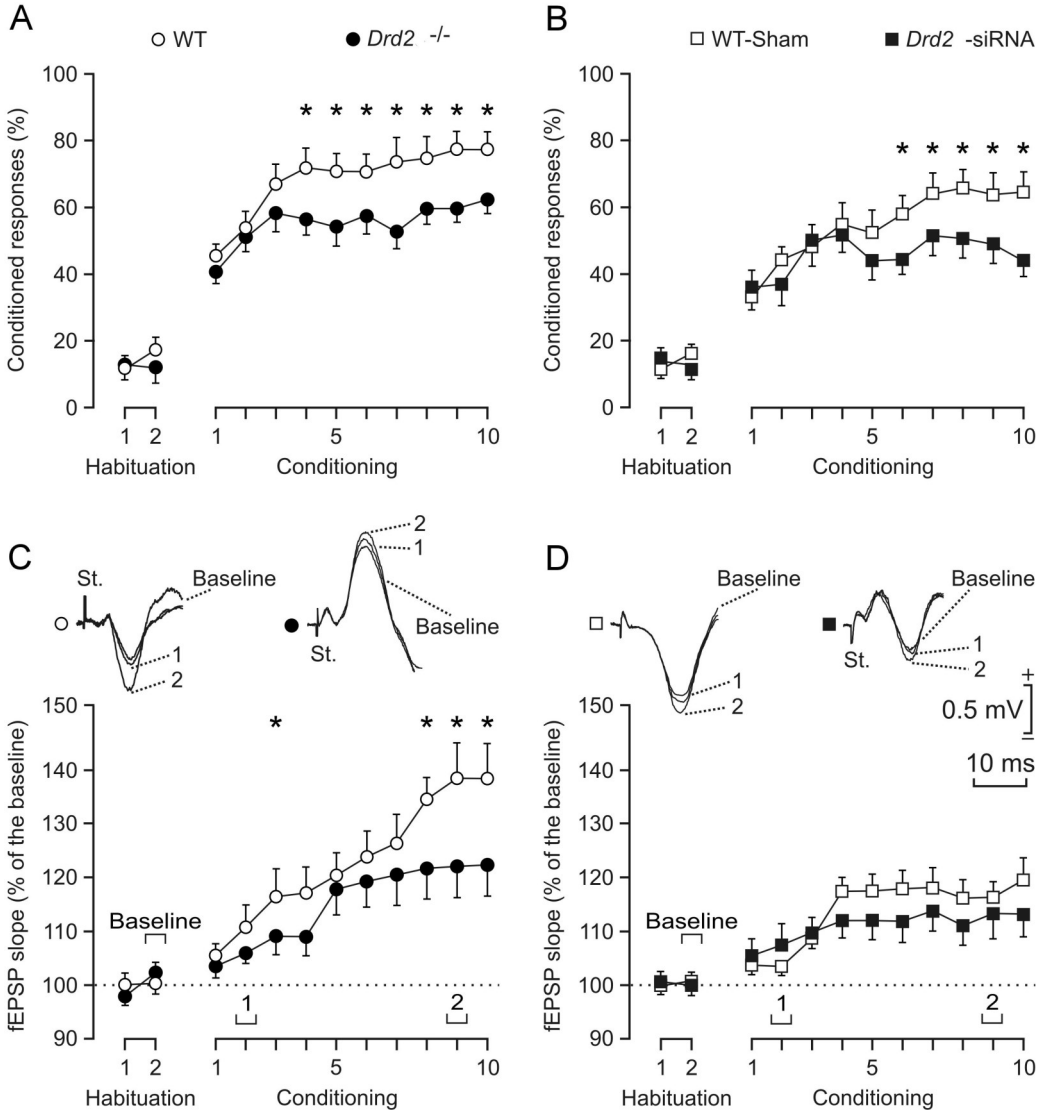

Figure 40. Evolution of learning curves in WT, *Drd2*$^{-/-}$, WT-Sham and *Drd2*-siRNA mice. A.B. Percentage of eyelid CRs reached by the four experimental groups. The acquisition curve presented by the WT group was significantly larger than values reached by the *Drd2*$^{-/-}$ group (*A*; $*p < 0.05$). The acquisition curve of the WT-Sham group was also significantly larger than that presented by *Drd2*-siRNA animals (*B*; $*p < 0.05$). **C, D.** Evolution of fEPSPs evoked at the CA3-CA1 synapse across conditioning for WT and *Drd2*$^{-/-}$ mice (**C**) and for WT-Sham and *Drd2*-siRNA animals (**D**). fEPSP slopes are expressed as the percentage of fEPSP slope values collected during habituation sessions for each group. Differences in fEPSP slopes between WT and *Drd2*$^{-/-}$ groups were statistically significant at the indicated sessions (*C*; $*p < 0.05$), indicating that activity-dependent synaptic plasticity was severely impaired in both *Drd2*$^{-/-}$ mice. No significant differences were found between the WT-Sham and *Drd2*-siRNA groups ($p = 0.154$).

This learning curve presented a profile similar to that reported previously in WT mice (Takatsuki et al., 2003; Gruart et al., 2006; Ortiz et al., 2010). In contrast, the percentage of CRs in the *Drd2*$^{-/-}$ group increased in a more slowly way, reaching lower asymptotic values than their littermate controls (Fig. 40A). Thus, the percentage of CRs presented by the WT group was significantly different from that of the *Drd2*$^{-/-}$ group from the 4th to the 10th conditioning sessions (Fig. 40A; $p < 0.05$). Similarly, WT-Sham animals presented learning curves similar to those seen in WT mice, while CRs in *Drd2*-siRNA mice presented a significantly lower percentage of CRs from the 6th to the 10th conditioning sessions (Fig. 40B; $p < 0.05$).

2.1. Learning-dependent changes in CA3-CA1 synaptic strength were reduced in *Drd2*$^{-/-}$ and *Drd2*-siRNA mice.

As shown recently in behaving mice, trace eyeblink conditioning is associated with an increase in synaptic strength at the hippocampal CA3-CA1 synapse (Gruart et al., 2006; Madroñal et al., 2007). We evaluated here the effect of D_2R loss on fEPSPs evoked at the CA3-CA1 synapse. Electrical stimulation of Schaffer collaterals 300 ms after CS presentation evoked a fEPSP in the CA1 area in all four experimental groups (Fig. 39A,B). Although the stimuli presented to Schaffer collaterals disrupted the regular theta rhythm recorded in the CA1 area, the rhythm reappeared in phase about 200 ms afterwards. The slope of the evoked fEPSPs increased in the four experimental groups over the course of conditioning when Schaffer collateral stimulation took place during the CS-US interval (Fig. 40C,D).

Nevertheless, there were clear differences between the two controls (WT and WT-Sham) and the two experimental (*Drd2*$^{-/-}$ and *Drd2*-siRNA) groups. In agreement with previous studies (Gruart et al., 2006; Madroñal et al., 2007; Ortiz et al., 2010), and as illustrated in Fig. 40*C, D,* fEPSP slopes recorded in WT (140%) and WT-Sham (120%) mice were significantly elevated over baseline values ($p < 0.05$) by the 10th conditioning session. In contrast, although the slopes of evoked fEPSPs in *Drd2*$^{-/-}$ (120%) and *Drd2*-siRNA (110%) mice were elevated over baseline, they were smaller than in corresponding control animals (Fig. 40C,D). Collected fEPSP slopes were significantly (Fig. 40C; $p < 0.05$) different between WT and *Drd2*$^{-/-}$ mice, but not ($p = 0.154$) between WT-Sham and *Drd2*-siRNA animals. In summary, the decreased performance in associative learning tasks noticed in *Drd2*$^{-/-}$ and *Drd2*-siRNA mice compared with their respective controls was paralleled by a decline in activity-dependent increases in synaptic strength at the CA3-CA1 synapse during classical conditioning of eyelid responses.

3. DOPAMINERGIC SIGNALING BY D_1R AND D_2R IN STRIATUM REGULTES THE PHENOTYPIC SHIFT OF A POPULATION OF STRIATAL NEURONS AND MOTOR BEHAVIOR.

3.1. L-DOPA treatment dose-dependently increased the number of TH-ir neurons in the denervated mouse striatum.

In a previous study we demonstrated that TH-ir neurons appear in the lesioned striatum soon after denervation and that L-DOPA treatment significantly increased the number of TH-ir cells (Darmopil et al., 2008).

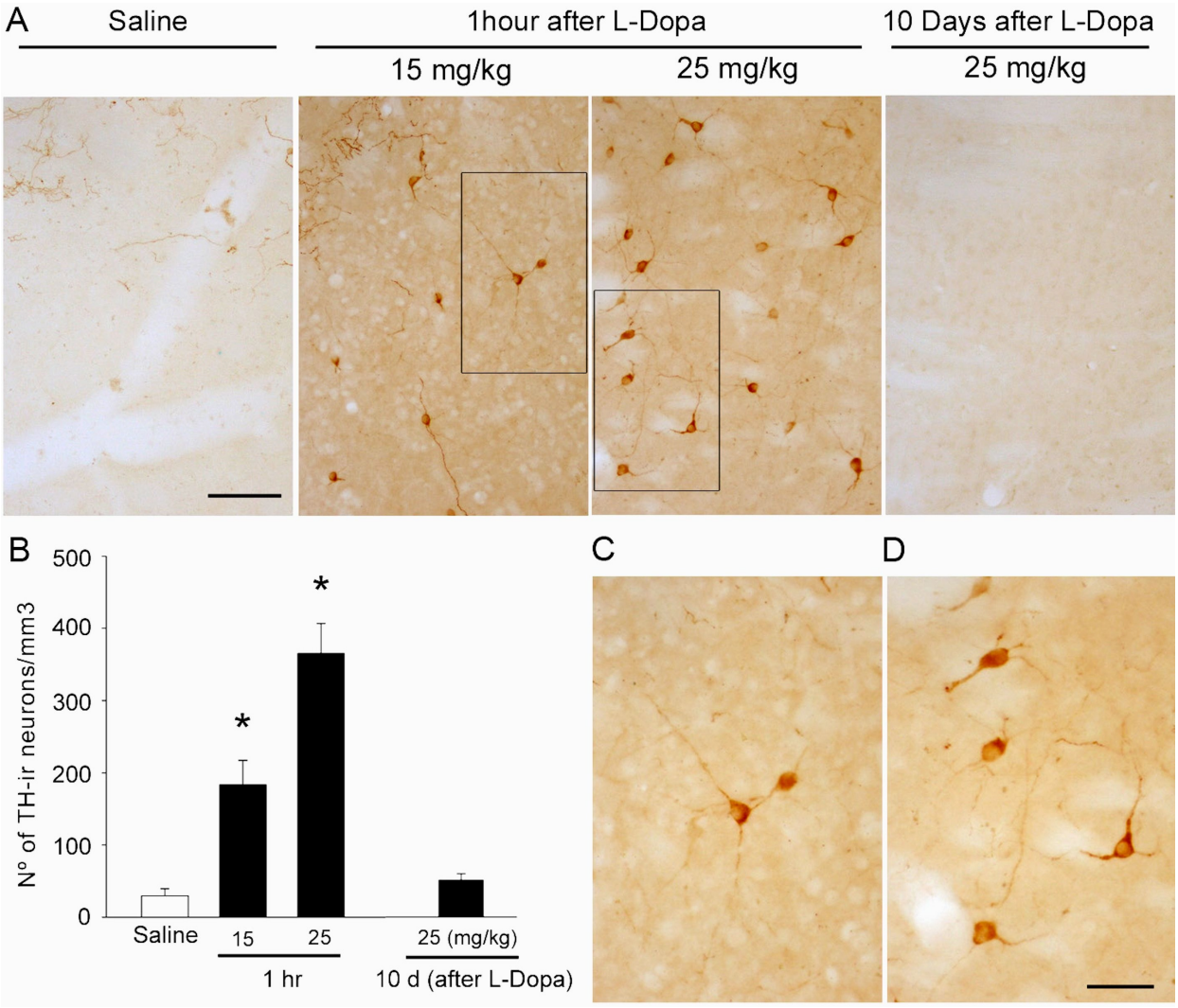

Figure 41. L-DOPA treatment dose-dependently increased the number of striatal TH-ir neurons in the 6-OHDA-lesioned striatum. A. Photomicrographs of TH-ir neurons in the lesioned striatum of mice treated for 2 weeks with saline, 15 mg/kg L-DOPA or 25 mg/kg L-DOPA. Mice were killed 1 h or 10 days after the last L-DOPA treatment as indicated. Note the increase in the intensity of TH-ir staining and the number of TH-ir neurons induced by increasing the L-DOPA dosage. **B**. Histogram showing the density of TH-ir neurons (mean ± SEM) in the 6-OHDA-lesioned striatum of mice treated with L-DOPA or saline. *p<0.001 vs. saline or vs. 15mg/kg L-DOPA (n = 6), one way ANOVA followed by Student-Newman test. C and D are high magnification images of the areas marked in the upper panels. Scale bar = 100 µm for A and 50 µm for C and D.

To see if this effect of L-DOPA is dose-dependent, we examined changes in the density of striatal TH-ir neurons after 3 weeks of daily treatment with either 15 mg/kg or 25 mg/kg L-DOPA. While there was no discernible difference between the two doses in cell body morphology of the TH-ir neurons, we observed generally more intense and complete TH-ir of the dendritic tree in striatum of mice treated with 25 mg/kg L-DOPA (Fig. 41A): more and longer dendrites were apparent in these animals. In addition, daily L-DOPA treatment significantly increased the density of TH-ir neurons in the lesioned striatum in a dose-dependent manner (Fig. 41A,B). Stereological counting confirmed the dose-dependence of the L-DOPA effect: following a 3-week treatment with 15 mg/kg L-DOPA, there were 183±33 TH-ir neurons/mm^3 in the striatum; the number of TH-ir neurons nearly was doubled when the dose was increased to 25 mg/kg (365±41, Fig. 41B). However, 10 days following L-DOPA withdrawal, the number of TH-ir neurons in the striatum decreased significantly, (50±9 TH-ir neurons/mm^3 $p< 0.001$) returning nearly to the basal levels observed in lesioned mice treated with saline, 29±10 TH-ir neurons/mm^3.

3.2. The D_1R, but not D_2R, is important for induction of TH-ir neurons in the denervated striatum after L-DOPA.

To establish the role of D_1R and D_2R in the L-DOPA-induced increase in TH-ir neurons in denervated animals, we performed unilateral striatal lesions with 6-OHDA in *Drd1a*$^{-/-}$ or *Drd2*$^{-/-}$ mice and their WT littermates (Fig. 42). After 3 weeks of daily saline or L-DOPA (25 mg/kg) administration, we estimated the number of TH-ir neurons in the lesioned striatum. Unbiased, stereological counting revealed 493±30 TH-ir neurons/mm^3 in lesioned striatum of L-DOPA-treated WT control littermates for *Drd1a*$^{-/-}$ mice, and 676±127 neurons/mm^3 in the WT control littermates for *Drd2*$^{-/-}$ mice (Fig. 42). This difference did not reach significance, but indicated some variability between groups of animals with different genetic backgrounds. Genetic disruption of D_1R decreased the number of TH-ir neurons (202±33) in the lesioned striatum of L-DOPA-treated hemiparkinsonian mice by 59% compared with WT littermates (Fig. 42A, C). In addition, the intensity of striatal TH-ir staining was much weaker in *Drd1a*$^{-/-}$ than WT animals and was localized to the cell soma: there was little or no labelling of dendrites in the striatum of *Drd1a*$^{-/-}$ mice (Fig. 42A). In contrast, there was no statistical difference in the number of TH-ir neurons (505±106) in the lesioned striatum of L-DOPA-treated *Drd2*$^{-/-}$ hemiparkinsonian mice compared to their WT littermates (Fig. 42B,C). Moreover, the intensity of TH staining in cell soma and neuropil was also similar in *Drd2*$^{-/-}$ mice and their WT (Fig. 42B).

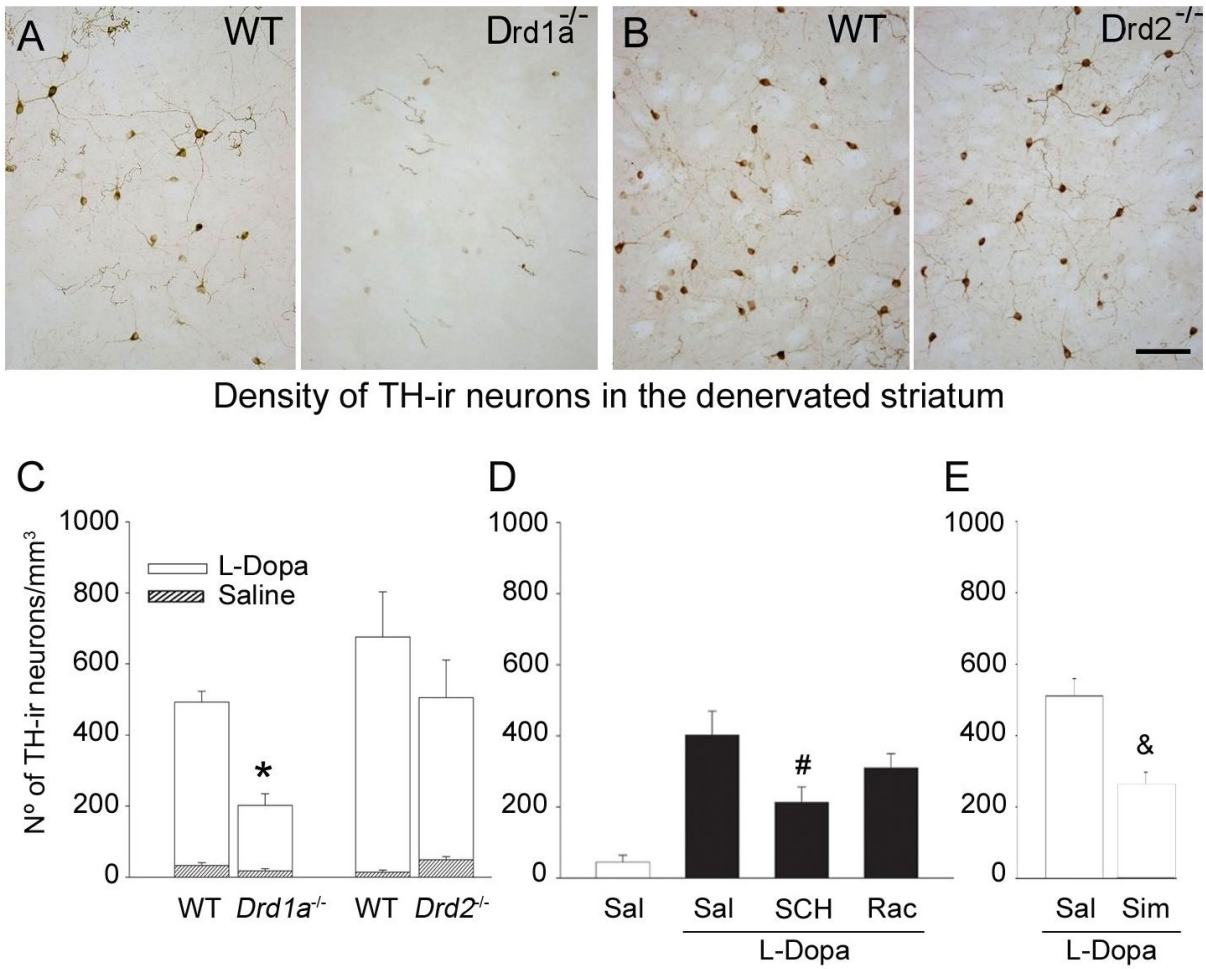

Figure 42. Role of D_1R and D_2R in the L-DOPA-induced increase in striatal TH-ir neurons in the lesioned striatum. **A, B.** High magnification photomicrographs of TH-ir in coronal sections through the lesioned striatum of L-DOPA treated *Drd1a*$^{-/-}$ (**A**), or *Drd2*$^{-/-}$ (**B**) mice and their corresponding WT hemiparkinsonian littermates. **C,D, E** Histograms show stereological quantification of TH-ir neuron density in coronal sections of lesioned striatum in *Drd1a*$^{-/-}$ and *Drd2*$^{-/-}$ mice treated with L-DOPA or saline (**C**) and in WT lesioned mice treated with saline or 0.3 mg/kg of SCH23390 or 2 mg/kg of raclopride 30 min before L-DOPA (**D**) or pretreated with 15 mg/kg of simvastatin 3 h before L-DOPA, an inhibitor of ERK activation (**E**). Data are expressed as mean ± SEM. *p<0.001 vs. WT and *Drd2*$^{-/-}$ mice, $^{\&}p$<0.05; $^{\#}p$<0.005 vs L-DOPA alone, one way ANOVA followed by Student-Newman test in C and D and by Student *t* test in E (n = 5-7). Scale bar = 100 µm.

To demonstrate that the effects we see in the *Drd1a*$^{-/-}$ and *Drd2*$^{-/-}$ mice are due exclusively to the absence of the receptors rather than to compensatory mechanisms secondary to global D_1R and D_2R deletion, we carried out a similar experiment in 6-OHDA-lesioned WT animals using pharmacological blockade of dopamine D_1R or D_2R families (Fig. 42D). We found that administration of the D_1R antagonist SCH23390 (0.3 mg/kg) 30 min before each L-DOPA dose (25 mg/kg) significantly reduced (p< 0.005) the number of TH-ir neurons in the lesioned striatum (213 ± 43 neurons/mm^3) compared to animals treated with L-DOPA alone (402±66). In contrast, pre-treatment with raclopride (2 mg/kg), a preferential D_2R antagonist, had no significant effect on the number of TH-ir neurons in the lesioned striatum of L-DOPA-treated WT mice (309 ± 40 neurons/mm^3), see Fig. 42D. Thus, either genetic inactivation or pharmacological blockade of D1R decreased the number of TH-ir neurons induced by L-DOPA in the dopamine-

depleted striatum while genetic inactivation or pharmacological blockade of D_2R had no effect.

Because L-DOPA activates the ERK signalling pathway, through D_1R activation, in denervated striatal neurons (Pavón et al., 2006; Schuster et al., 2008), we investigated whether ERK is important for the induction of TH-ir neurons by L-DOPA, using simvastatin, an inhibitor of ERK activation. We administered 15 mg/kg simvastatin daily for 3 days before starting L-DOPA treatment and then 3 h before each dose of L-DOPA for 15 days. Following this paradigm, the number of striatal TH-ir neurons decreased by half compared to animals treated with L-DOPA alone (Fig. 42).

3.3. TH-ir neurons induced by L-DOPA do not express D_1R or D_2R.

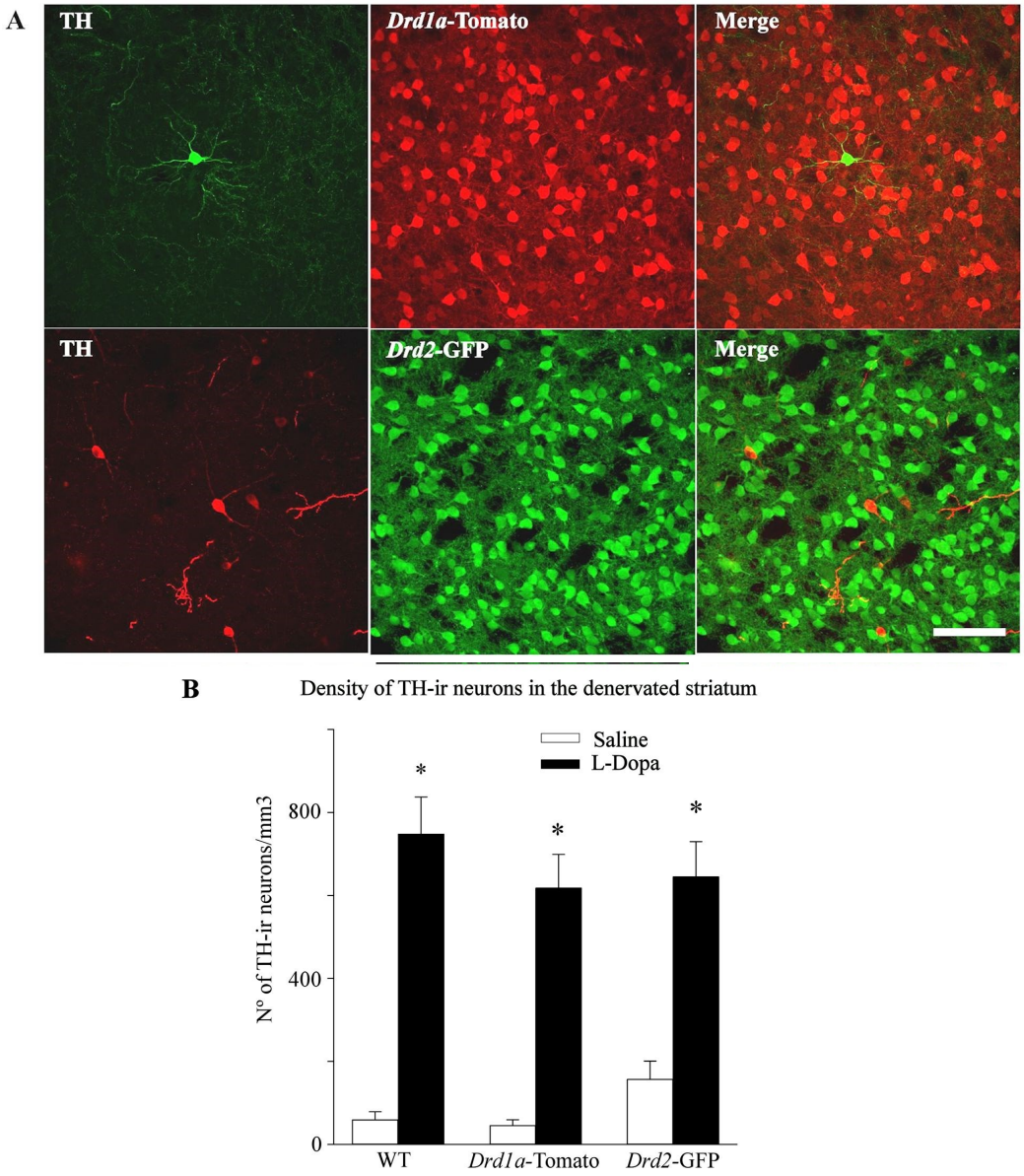

Figure 43. TH-ir neurons do not colocalize with D_1R- or D_2R-containing neurons. A. Confocal photomicrographs shows that TH-ir neurons do not colocalize with *Drd1a*-Tomato or *Drd2*-GFP neurons in the lesioned striatum. **B.** Quantification of TH-ir neurons demonstrating that the number of these neurons increases similarly in WT and BAC-transgenic mice after L-DOPA treatment, (*$p < 0.001$). Data are expressed as mean ± SEM. one way ANOVA followed by Student *t* test was used. Scale bar = 50 µm

Although it has been shown that dopamine D_1R plays an important role in TH-ir striatal neurons expression, we found that these neurons do not contain D_1R or D_2R. These studies were carried out using *Drd1a*-Tomato and *Drd2*-GFP hemilesioned with 6-OHDA. TH-immunoreactivity did not colocalized with any of the fluorescence probes (tomato red in D_1R-containing neurons, or GFP in D_2R-containing neurons) (Fig. 43A), so the response of these neurons to D_1R activation could be due to an indirect mechanism. We also check the number of TH-ir neurons in lesioned striatum of the BAC-transgenic mice to verify that there were no differences between the two strains and WT mice lesioned and treated with L-DOPA. We found no differences between the three strains (Fig. 43B).

3.4. Ultrastructure of TH-ir neurons.

Previous studies with electron microscopic analysis of TH-ir neurons showed the ultrastructural features and synaptology of these neurons in monkeys (Mazloom & Smith, 2006) and rats (Meredith et al., 1999), but there are not studies in mice. To test if these neurons are similar between species, we performed ultrastructural studies with a transmission electron microscope (TEM) of TH-ir striatal neurons of lesioned mice.

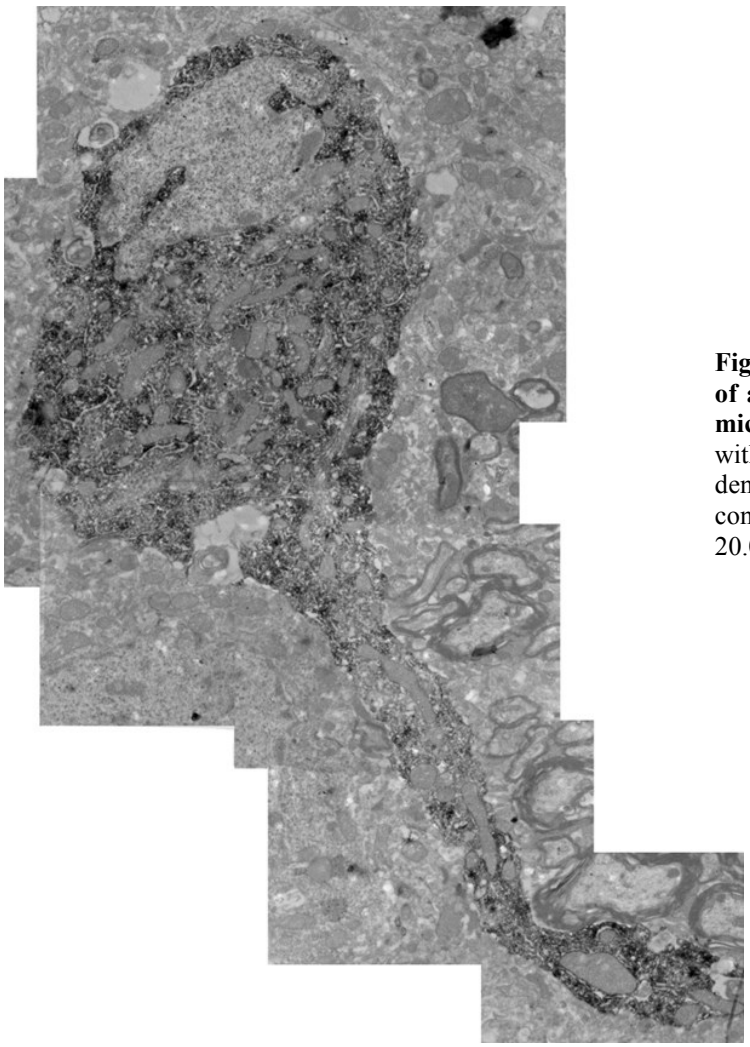

Figure 44. Panoramic reconstruction of a striatal TH-ir neuron in lesioned mice. Micrographs show a TH-ir soma with the nucleus, cytoplasm and one dendrite. The images that form the reconstruction were taken from a TEM at 20.000x.

At the electron microscopic level TH-ir cell bodies and dendrites showed strong immunostaining (Fig. 44, 45). The DAB deposit was intense and homogeneously distributed throughout the cytoplasm, but the nucleus was devoid of immunoreactivity (Fig. 45). In line with other studies, cell bodies were small, and the shape was typically round or oval (Fig. 45). In all neurons examined, the nuclear membrane was deeply invaginated, a typical ultrastructural characteristic of striatal interneurons (Difiglia et al., 1980) (Fig. 44, 45). Also, these neurons have a high number of mitochondria, both features are indicative of a high activity.

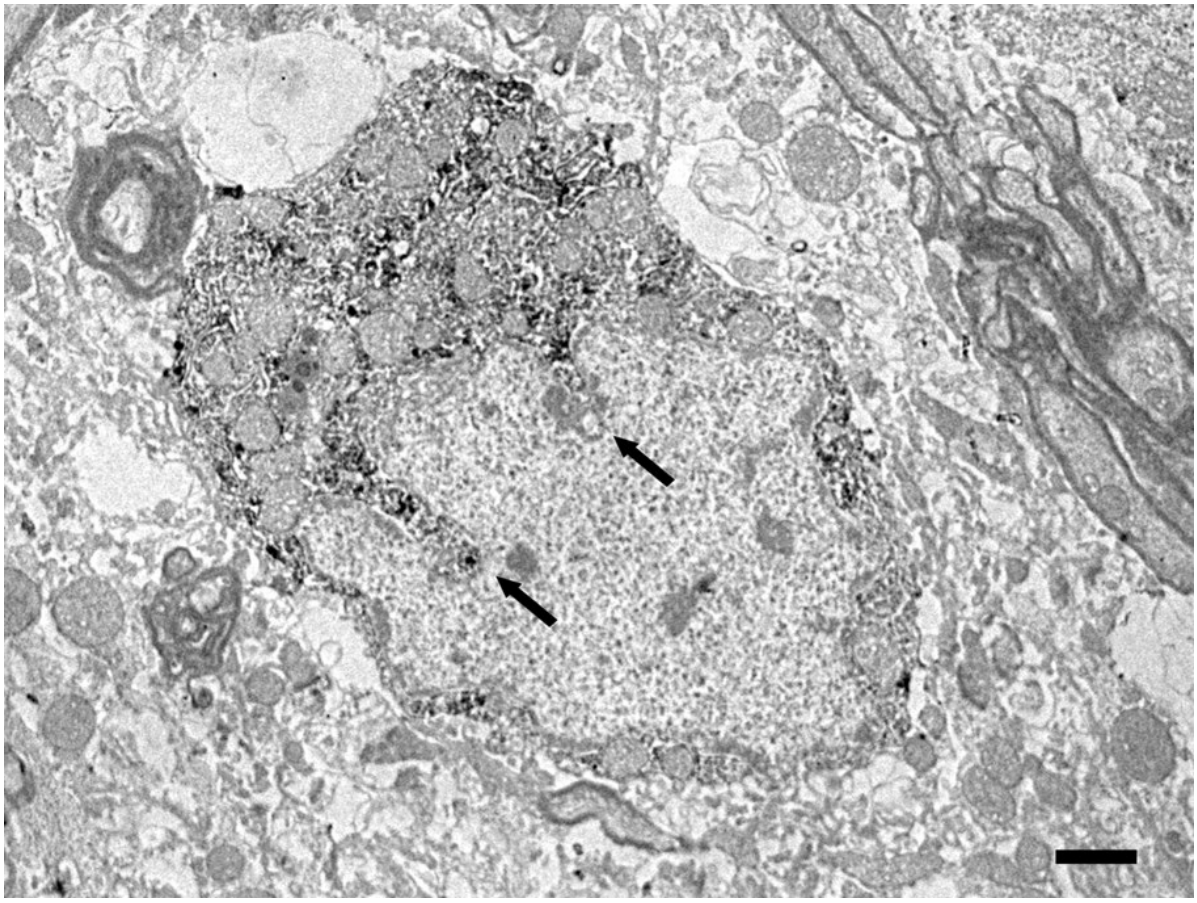

Figure 45. Micrograph of TH-ir perikaryon. Note the intense peroxidase labeling of the cytoplasm. The arrows indicate the nuclear invagination, a common ultrastructural feature of striatal interneurons. Scale bar = 2 μm

The TH-ir striatal neurons are able to establish a high number of functional synapses of asymmetric type (excitatory) (Fig. 46, 47). In addition, the synaptic elements found labelled with DAB were mainly postsynaptic (Fig. 47). This may be because identifying presynaptic terminals is particularly difficult for two reasons: a) the DAB signal mask the content of the terminal and no vesicles are displayed or b) low DAB signal difficult to identify the terminal (Fig. 46). However, detection of postsynaptic elements is easier since postsynaptic membranes, in active synapses, have more electrodense appearance.

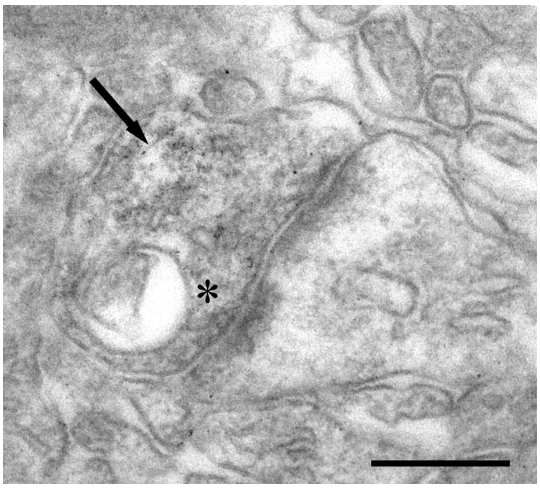

Figure 46. TH-immunostained axon-terminal. The picture illustrates an axon-terminal immunostained with TH (arrow) in the striatum of 6-OHDA lesioned mice. Note the presence of numerous vesicles in the presynaptic terminal (asterisk), and the electrodense membrane in the postsynaptic element. Scale Bar = 0.25 μm.

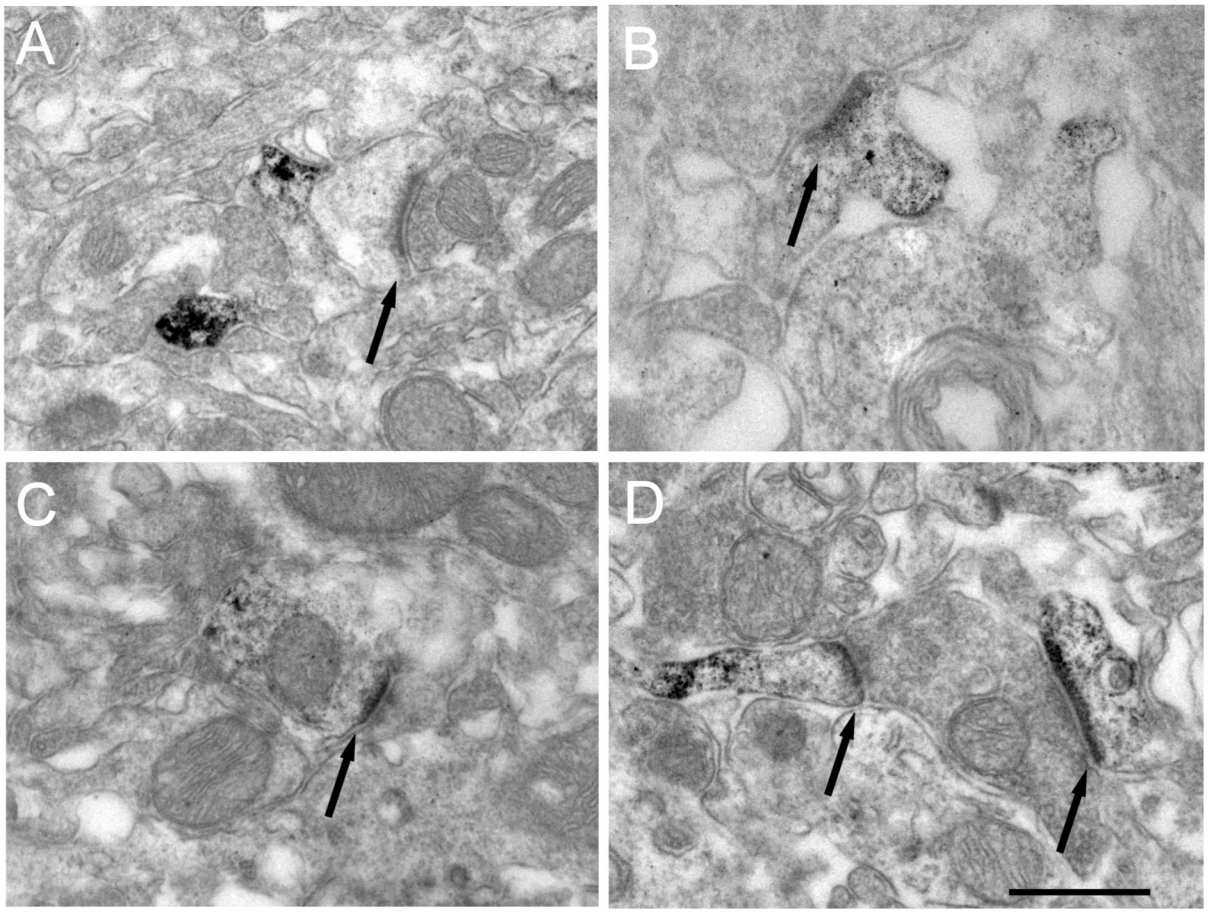

Figure 47. Synaptic connectivity of TH-ir neurons. Images illustrate postsynaptic elements of asymmetric synapses **A.** A spine immnulabeled with TH indicated by the arrow. **B, C, D.** Show various examples of TH-immunoreactives postsynaptic elements. Scale Bar = 0.5 μm.

These results indicate that TH-ir neurons have similar morphological characteristics to those found in monkeys (Mazloom & Smith, 2006). For his shape and size, we can infer that may be GABAergic interneurons, however a minority of these cells are spiny neurons. In this case we found very few axon-terminals, this could be because the proportion of dendrites is much higher than the axon-terminals. In addition the high number of mitochondria and asymmetric synapses indicates that these neurons are functionality and very active as have been shown before (Darmopil et al., 2008).

3.5. L-DOPA-induced TH-ir neurons in the lesioned striatum with distinct phenotype that midbrain dopaminergic neurons.

Pitx3 is a homeodomain transcription factor expressed in dopaminergic neurons in the brain and is essential for the normal development of the midbrain dopaminergic system (Jacobs et al., 2007, 2009). Inactivation of Pitx3 induces selective loss of dopaminergic neurons in the SNc and, as a consequence, major dopamine depletion in the striatum, providing a genetic model of PD (Hwang et al., 2003; Ding et al., 2007, 2011). Based on these results, we investigated whether the L-DOPA-induced appearance of TH-ir neurons in the dopamine-depleted striatum requires Pitx3. We treated Pitx3-deficient aphakia mice with L-DOPA (25 mg/kg) or saline daily for 21 days.

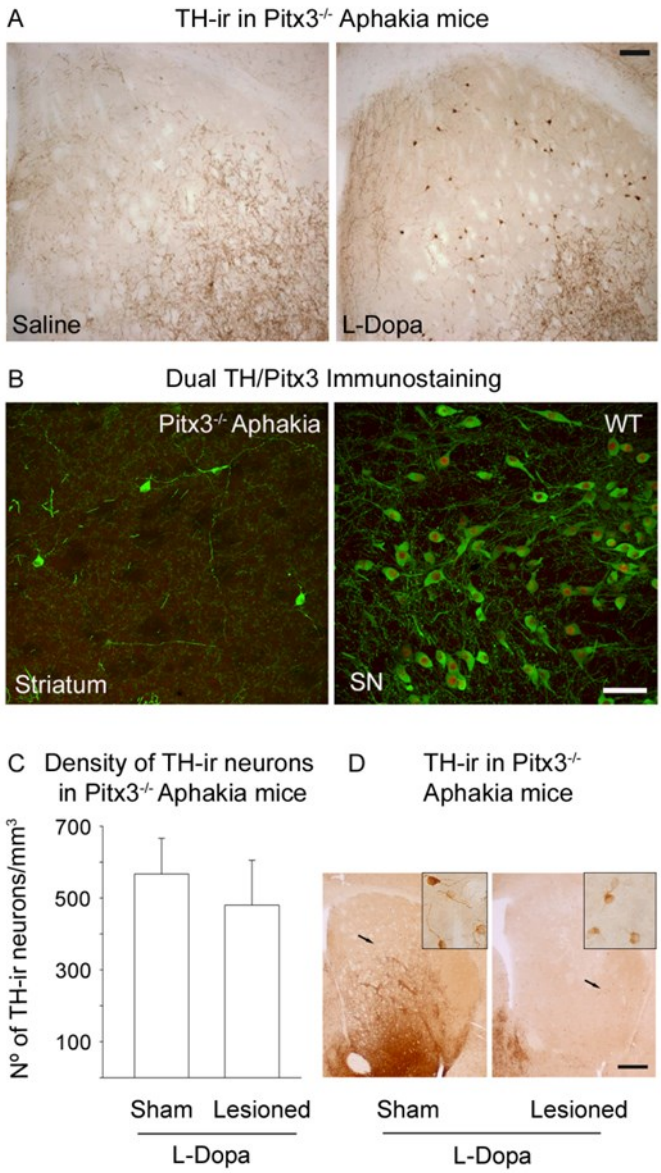

Figure 48. The transcription factor Pitx3 is not necessary for L-DOPA-induced TH expression in striatal TH-ir neurons. **A.** Photomicrographs of coronal sections through dorsal striatum of Pitx3$^{-/-}$ mice treated with saline or L-DOPA. No TH-ir neurons are visible in the striatum of Pitx3$^{-/-}$ mice treated with saline but TH-ir striatal neurons are clearly present after 3 weeks of daily treatment with 25 mg/kg L-DOPA. **B.** Double-inmmunostaining for TH (green) and Pitx3 (red) in coronal sections of Pitx3$^{-/-}$ mice striatum and WT mice SN. Note that striatal TH-ir neurons do not express Pitx3 in contrast to SN TH-ir neurons from WT mice. **C.** Histograms show stereological quantification of TH-ir neurons density in coronal sections of lesioned and sham-operated-striatum of aphakia mice treated with L-DOPA. **D.** Photomicrographs of coronal sections through the 6-OHDA and Sham lesioned striatum of aphakia treated with L-DOPA. Note that the lack of Pitx3 does not alter the number of TH-ir neurons per mm^3 in the lesioned-compared with the sham-operated striatum in the aphakia mice.Scale bar = 200 µm in A, 25 µm in B and 400 µm in D.

We observed a large increase in striatal TH-ir neurons after L-DOPA administration while no TH-ir neurons were observed in striatum of saline-treated animals (Fig. 48A). Dual immunocytochemistry studies, conducted in parallel with SN coronal sections from a WT animal, confirmed that these TH-ir neurons do not express Pitx3 in the aphakia mice, while a strong signal was evident in the WT mice (Fig. 48B).

To rule out the possibility that Pitx3 plays a role in the appearance of TH-ir neurons after striatal injury, we quantified TH-ir neurons in 6-OHDA-lesioned or sham-operated aphakia mice treated with L-DOPA. We found no significant differences (Fig. 48, $p = 0.2$) in the density of TH-ir neurons in lesioned and sham-operated aphakia mice. Indeed, in these mice, the lesion increased the absolute number of TH-ir neurons in the striatum an also increased the lesioned area (Fig. 48) therefore the number of striatal TH-ir neurons per mm^3 was not altered compared to sham-operated aphakia mice. These results indicate that Pitx3 is not necessary for induction of TH-ir neurons in the lesioned striatum by L-DOPA.

Another transcription factor that is a critical determinant of midbrain dopaminergic neurons during development is Nurr1. It is a member of the orphan nuclear receptor family of transcription factors required for the differentiation of mesencephalic dopaminergic neurons. This factor induces the expression of dopaminergic genes such as *Th* (Vergaño-Vera et al., 2014). Similar to Pitx3 results, dual immunohistochemistry studies for Nurr1 and TH confirmed that these TH-ir neurons do not express this transcription factor of midbrain dopaminergic neurons (Fig. 49)

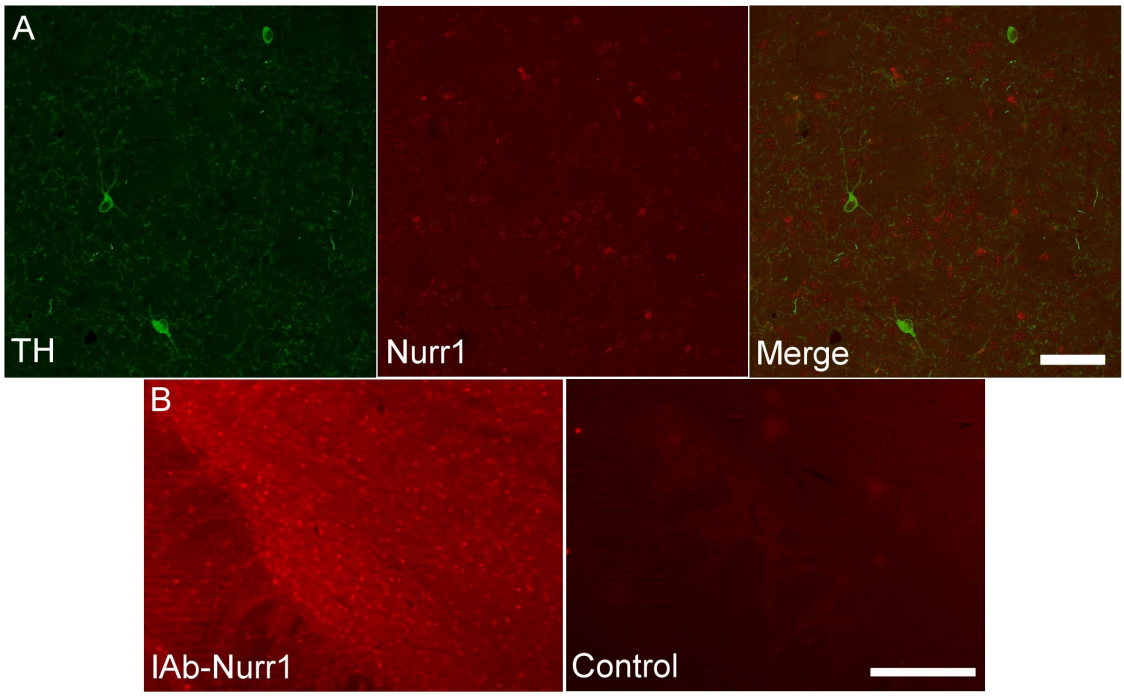

Figure 49. TH-ir neurons do not express the transcription factor Nurr1. A. Photomicrographs of coronal striatal sections of lesioned mice treated with L-DOPA stained with TH (green) and Nurr1 (red). Note that TH-ir neurons do not express Nurr1. **B.** Shows the specificity of Nurr1 signal in SN with primary antibody (left panel) and without (right panel). Scale bar = 200 μm

3.6. Long-duration effects of chronic L-DOPA treatment on forelimb use in hemiparkinsonian mice.

To evaluate whether TH-ir neurons in the striatum could be involved in the long-term efficacy of chronic L-DOPA treatment, we studied spontaneous forelimb use in the cylinder test at various time points before and after lesion and before and after chronic L-DOPA treatment (Fig. 50). Forelimb use asymmetry has been used to assess the efficacy of the 6-OHDA lesion in mice (Lundblad et al., 2004; Pavón et al., 2006; Darmopil et al., 2009) as well as the motor effect of L-DOPA administration (Lundblad et al., 2004). Before lesion, animals use both forelimbs equally to support their body weight: the ratio of forelimb use or wall contact for the right and left forelimbs was 51.5%. In unilaterally 6-OHDA-lesioned animals, the ratio for use of the forelimb contralateral to the lesion decreased to 33.7% (p<0.001 vs. unlesioned animals) illustrating the degree of asymmetry in limb use due to the dopamine deficiency in the lesioned striatum. Chronic L-DOPA treatment induced a significant long-term motor improvement in the contralateral forelimb, 1 day after the three-week L-DOPA treatment, the ratio of forelimb use was similar to that observed in unlesioned animals (50.5%, Fig. 50), indicating a complete recovery in this particular motor function (p<0.001 vs. lesioned animals). Although the forelimb efficacy eventually decreased again with time, the improvement persisted for at least 4 days after the end of the L-DOPA treatment (46.7%; p<0.001).

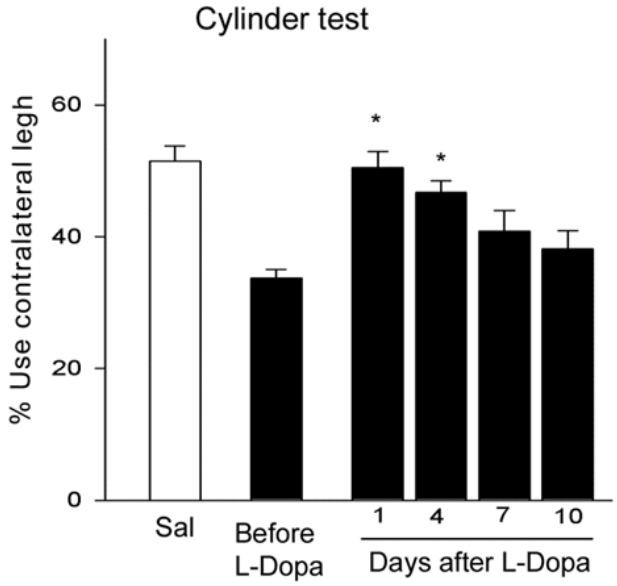

Figure 50. Chronic L-DOPA treatment reverses forelimb use asymmetry induced by striatal 6-OHDA lesion. Forelimb use asymmetry was measured by the cylinder test in mice before and 3 weeks after unilateral 6-OHDA lesion. Mice were then treated for 3 weeks with daily administration of L-DOPA (25 mg/kg) and reassessed with the cylinder test at 1, 4, 7 and 10 days after L-DOPA withdrawal. Data are expressed as percent ± SEM of wall contact performed with the contralateral limb, *p<0.01 vs. lesioned mice treated with saline, n=11, one way ANOVA followed by Student-newman test.

Later on, after 7 days, we still observed a mild recovery (40.8% p=0.08) but that is not significantly different from the values obtained in lesioned mice (33.7%). The positive motor effect of L-DOPA was no longer detectable 10 days after the L-DOPA treatment: the ratio of contralateral to ipsilateral forelimb use decreased to 38.2%, similar to that observed in lesioned animals without L-DOPA treatment (Fig. 50).

3.7. Effect of L-DOPA administration on striatal dopamine overflow in hemiparkinsonian mice.

Electrical stimulation of striatal slice preparations induces extrasynaptic dopamine release, termed "synaptic overflow", due to the synchronized firing of numerous dopamine terminals (Garris et al., 1994). Therefore, we next examined whether L-DOPA treatment (25 mg/kg) in hemiparkinsonian animals modifies extrasynaptic dopamine overflow in the lesioned and unlesioned striatum by determining dopamine overflow in striatal slices at 1, 4 and 10 days after chronic administration of L-DOPA. In sham lesioned mice, single biphasic electrical stimuli (0.5 ms, 20 V) elicited reliable dopamine release reaching a peak of 0.30 ± 0.02 μM in contralateral (Fig. 51 A; n = 4) and 0.34 ± 0.02 μM in ipsilateral (Fig. 51A; open circles; n = 5) striatal slices. Peak overflow was reached within 0.4 s and returned to baseline within 1.4 s (Fig. 51A). We next examined dopamine release in the striatum after nigro-striatal denervation. 6-OHDA lesioned mice showed an abolition of dopamine overflow in ipsilateral striatum (Fig. 51B; open circles; n = 5), accompanied by a significant increase (0.49 ± 0.07 μM) in dopamine overflow in contralateral striatum (Fig. 51B; filled circle; n = 5) compared to sham lesioned animals (Fig. 51A,F). These results suggest that there is compensatory adaptation in the intact side of the striatum in lesioned animals. Interestingly, these changes in both hemispheres were counteracted by L-DOPA administration. Thus, 1 day after chronic L-DOPA treatment, dopamine overflow was similar in sham-operated and lesioned animals (Fig. 51C,F). This effect of L-DOPA declined significantly by 4 day (Fig. 51D) after the end of L-DOPA treatment and by 10 day, the peak of dopamine release was similar to that seen in slices from lesioned animals without L-DOPA treatment (Fig. 51C,F,G). These results suggest that L-DOPA treatment temporarily restores dopamine overflow in ipsilateral and contralateral striatum after nigrostriatal denervation.

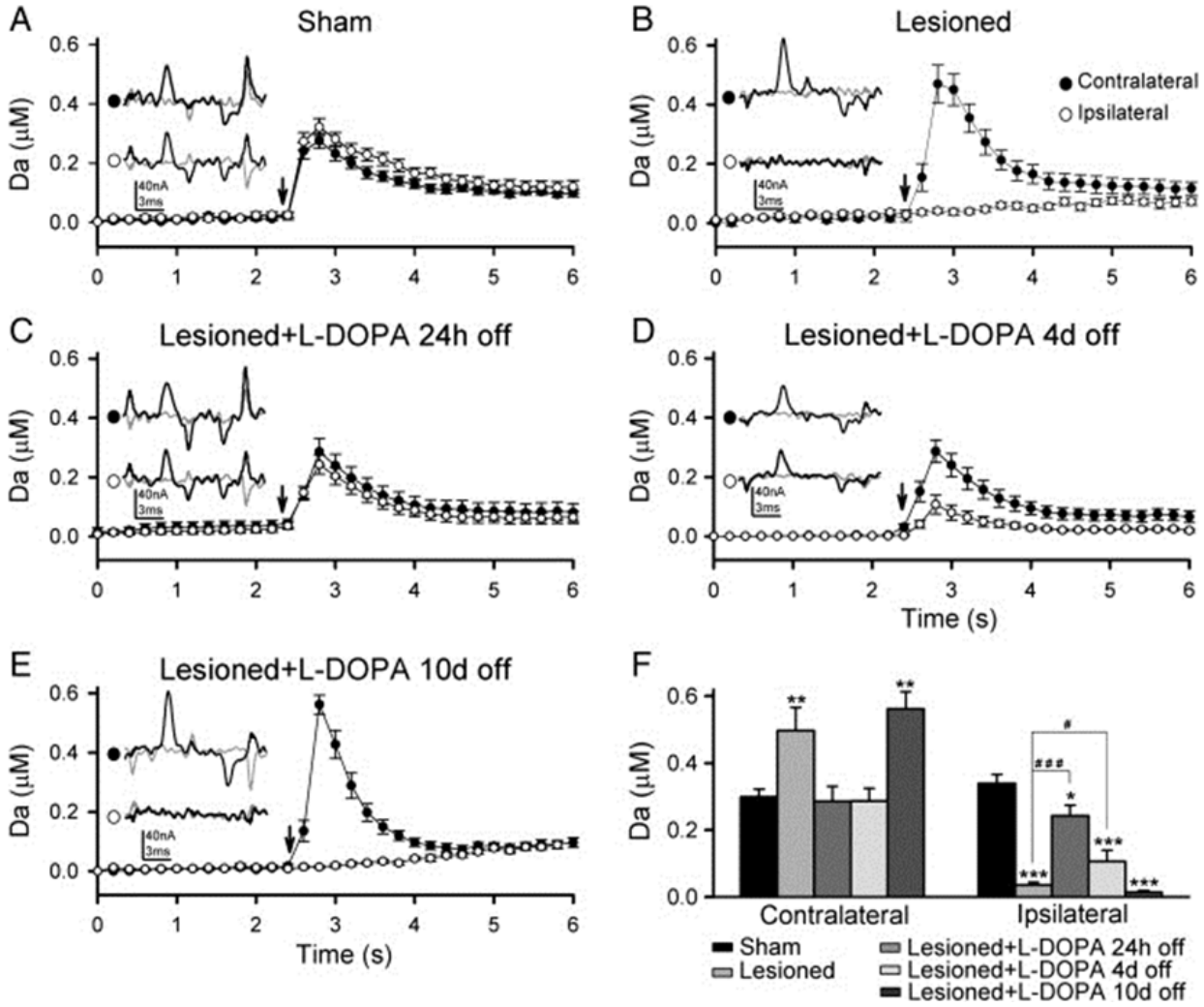

Figure 51. **Long-term effect of L-DOPA on electrically stimulated striatal dopamine overflow in the lesioned and unlesioned striatum. A.** Time-course of dopamine overflow evoked by a single intrastriatal stimulus (arrow; 20 V, 0.5 ms) in contralateral (n = 4) and ipsilateral (n = 5) striatal slices from sham lesioned animals. Inset shows voltammogram response for dopamine release before (gray trace) and after (black trace) electrical stimulation. **B**: Same as A but in 6-OHDA lesioned mice. Note the abolition of dopamine overflow in the ipsilateral striatum (n = 5) and the increase in dopamine overflow in the contralateral striatum (n = 5). **C-E**: Same as A but in 6-OHDA lesioned mice 24 hours (**C:** contralateral, n = 7; ipsilateral, n = 11), 4 days (**D:** contralateral, n = 12; ipsilateral, n = 10) and 10 days (**E:** contralateral, n = 6; ipsilateral, n = 8) after stopping L-DOPA treatment. **F**: Bar graph illustrates peak dopamine release in different experimental conditions. Significant differences with respect to sham lesioned mice are indicated by (*p< 0.05), (**p< 0.01) and (***p< 0.001). Significant differences with respect to ispilateral 6-OHDA lesioned animals are indicated by ($^{\#}p$ < 0.05) and ($^{\#\#\#}p$< 0.001), one way ANOVA followed by 2-tailed Student´s *t* test.

Discussion

The specificity dopamine distribution in brain structures related with motor response, reward/ motivation, learning and memory processes reflects the relevance of dopaminergic system in these functions and in the changes of synaptic plasticity associated. These processes could not be carried out without a proper functioning that involves primarily the action of D_1R and D_2R as key elements modulating dopaminergic transmission.

1. DOPAMINERGIC SIGNALING BY D_1R IN HIPPOCAMPUS REGULATES LEARNING AND MEMORY PROCESS.

The D_1R is expressed in the main brain areas implicated in learning and memory process. Our findings in different tests indicate that spatial, associative and recognition memory are abolished or dramatically reduced in *Drd1a*$^{-/-}$ mice, but these deficits are not due to motor or emotional and motivational disturbances.

1.1. Dopamine D_1R is critical for acquisition and consolidation of spatial memory.

It has been suggested that the Barnes maze discriminates spatial learning more clearly than the MWM for mice (Barnes, 1979; Harrison et al., 2009; Patil et al., 2009). *Drd1a*$^{-/-}$ mice were tested in the Barnes maze to consolidate the previous findings that D_1R is necessary for spatial learning in the MWM. Our results in Barnes maze test are in agreement with previous results from our laboratory (Granado et al., 2008) and others (Smith et al., 1998; Xing et al., 2010). Unlike a previous water maze study in which *Drd1a*$^{-/-}$ mice did learn after extended training (El -Ghundi et al., 1999), we saw no decrease in the escape latency for *Drd1a*$^{-/-}$ mice in the Barnes maze even after extended training. In addition, two indicators of anxiety level, immobility during the first day of training in the Barnes maze, and performance in the P-Maze, revealed no increase in anxiety in the knockout animals, so it is unlikely that the impaired performance of *Drd1a*$^{-/-}$ mice in the Barnes maze is attributable to an effect of the knockout on anxiety. In addition, the number of holes explored at day 1 of training was similar to their WT, indicating that these animals have similar exploratory behavior. Our results confirm the crucial role of D_1R in spatial learning.

1.2. The D_1R is critical for acquisition and consolidation of fear memories.

While spatial memory is hippocampus-dependent, other forms of associative learning also depend on the amygdala. To further assess the role of D_1R in associative learning, we used two

paradigms that evaluate fear memory. In the active avoidance test, *Drd1a*$^{-/-}$ mice did not decrease their escape latency at any point during the training trials. Similar random crossing scores for WT and *Drd1a*$^{-/-}$ mice indicate that this finding is not caused by decreased locomotor activity. Furthermore, *Drd1a*$^{-/-}$ mice stop responding to the conditioned stimulus throughout the days of training, exhibiting a pattern of response similar to the "learned helplessnesses" phenomenon (Seligman et al., 1975). However the results in Porsolt test, that assess depressive symptom, do not indicate a depressive tendency for these mutant mice at basal level.

The results of passive avoidance trials further confirm that this impairment learning was not caused by locomotor deficits or freezing. In passive avoidance, *Drd1a*$^{-/-}$ mice showed some learning at 0.4 and in 0.8 mA, but were significantly impaired compared with WT mice 1 and 24 h after the training. Thus, the avoidance impairment associated with D_1R inactivation is likely attributable to abnormal acquisition of learning or to abnormal short term memory retrieval, but not to deficits in memory consolidation. These mice showed similar avoidance responses at 1 and 24 h after the shock, indicating that they are able to retrieve what they have learned. Together, these studies suggest that with moderate intensity stimuli, D_1R are important for fear conditioning, but at higher intensities, D_1R-independent mechanisms predominate. Similar results were obtained with Egr1 mutant mice, which exhibit deficits in spatial memory that can be rescued by extensive training (Jones et al., 2001).

In addition, previous studies show that D_1R antagonists increase sensitivity to pain (Burkey et al., 1999), a decrease in dopamine levels can sensitize to pain and reduce the avoidance response. Therefore, we performed three different test to assess pain sensitivity in basal conditions for *Drd1a*$^{-/-}$ and WT mice. In all test (tail-flick, hot-plate and plantar test) *Drd1a*$^{-/-}$ mice exhibited a lower threshold of response than WT mice. Thus, we carry out the test "sensitivity to foot-shock". We found that *Drd1a*$^{-/-}$ and WT mice have similar pain sensitivity threshold indicating that sensitivity to electric shock could not affect associative tests performance.

1.3. Dopamine D_1R is critical for recognition memory.

Drd1a$^{-/-}$ mice exhibit similar time in ORT exploring the novel object than the familiar one on test day, it is possible that they not recognize any of the objects. The ORT exploits the tendency of rodents to spend more time exploring a novel object than a familiar one, suggesting that they recognize objects at different locations. This action involves different processes in different brain structures, including the hippocampal region. The hippocampus is essential for encoding spatial and episodic memories (Ryan et al., 2010), and for novelty detection include ORT, specially in long-term memory test of the object recognition (Hamond et al., 2004). The role of

hippocampus is important in novelty detection for his multiple connections with other brain structures because this type of memory involves the comparison of an existing memory with new sensory information. CA1 hippocampal region recives dopaminergic proyections from the VTA (a part of functional loops detectin novelty, Lisman & Grace, 2005) and from SN (Gasbarri et al., 1997). In addition, this kind of memory is impaired in animal models of PD and restored by the action of L-DOPA vía D_1R (Costa et al., 2012).

1.4. Dopamine D_1R is involved in learning and in the related changes in synaptic strength at the hippocampal CA3-CA1 synapse.

The behavioral disturbances found in *Drd1a*$^{-/-}$ mice are in agreement with previous findings in our laboratory. The three processes: associative learning, activity-dependent synaptic plasticity and LTP, seem to be functionally related (Gruart et al., 2006; Madroñal et al., 2007). Our previous work shows that D_1R does not affect normal transmission, but contributes to synaptic plasticity during the acquisition and storage of new information (Ortiz et al., 2010). D_1R are also necessary for evoking LTP of the CA3-CA1 synapse after HFS of afferent Schaffer collaterals (Granado et al., 2008; Ortiz et al., 2010). In addition, acquisition of classically conditioned eyelid responses and the increase in CA3-CA1 synaptic strength across training are severely impaired in *Drd1a*$^{-/-}$ and mice injected with lentiviral particles silencing the D_1R *(Drd1a* -siRNA), suggesting the D_1R plays an important role in hippocampal mechanisms related to learning and memory (Ortiz et al., 2010).

1.5. Possible molecular mechanisms of D_1R-mediated learning and memory process.

The mechanism by which D_1R mediates associative learning are not known. One possibility is that D_1R-triggered cAMP signaling phosphorylates CREB (cAMP response element-binding protein) which activates the histone acetyl transferase enzyme CBP-binding protein (Mayr et al., 2001; Alarcón et al., 2004), inducing expression of immediate-early genes, including Egr1 and Arc, which play a crucial role in reference memory (Guzowsky et al., 2000; Jones et al., 2001). Alternatively, D_1R could directly phosphorylate NMDA receptors or the Protein kinase C ζ isoform in hippocampus and amygdala, potentiating and maintaining synaptic strength (Gardner et al., 2001; Impey et al., 2002; Kelleher et al., 2004; Sacktor, 2008) by increasing the influx of calcium induced by NMDA receptor activation, as occurs in prefrontal cortex neurons (Kruse et al., 2009). Direct interaction between D_1R and NMDA receptors within the plasma membrane of pyramidal neurons may also occur, since D_1R can physically interact with NR1

and NR2A subunits, modulating receptor trafficking (Lee et al., 2002; Pei et al., 2004; Fiorentini et al., 2006). Co-activation of both receptors increases the presence of GluR1 receptors and facilitates their incorporation into synapses in hippocampal neurons (Smith et al., 2005; Gao et al., 2006; Sacktor, 2008). It is also possible that D_1R is selectively activated by burst firing NMDAR-dependent of dopamine neurons, mainly during the presentation of salient events (Zweifel et al., 2009). In addition, recent studies demonstrated that D1-like receptor agonists promoted the survival of newborn cells in the adult hippocampus (Takamura et al., 2014).

These results demonstrate that dopamine D_1R has a critical role in learning and memory process, and in the subsequent synaptic plasticity changes. However, the D_1R activation is principally attributable to temporally increases of dopamine (Goto & Grace, 2005; Wall et al., 2011), and the D_2R are may be implicated in mediating the tonic dopamine release (Goto et al., 2007; Wall et al., 2011). For this reason it is possible that D_2R inactivation affects cognitive functions and synaptic plasticity associated process similar to D_1R.

2. DOPAMINERGIC SIGNALING BY D_2R IN HIPPOCAMPUS REGULATE ASSOCIATIVE LEARNING AND CHANGES IN SYNAPTIC PLASTICITY.

Dopamine receptors D_1R and D_2R are expressed in dopaminergic fibers that inervate hippocampal region (Goldsmith & Joyce 1994; Missale et al., 1998; Nguyen et al., 2014). When D_2R are completely abolished (*Drd2*$^{-/-}$ mice) or partially inactivated in hippocampal region CA1 with LV-*Drd2*-siRNA, associative learning was significantly impaired. Also exists a disturbance in synaptic plasticity process in hippocampus leading a blockade in acquisition of CRs and prevents LTP induction in CA3-CA1 synapse.

2.1. Drd2$^{-/-}$ mice exhibit slower spatial learning not due to motor impairment.

Previous studies, with MWM, found that D_2R antagonists could improve the performance in this spatial test (Setlow & McGaugh, 1999 & 2000). In these studies D_2R antagonists was administrated to mice after the training affecting consolidation memory process, but not the acquisition. However, in this work the genetic inactivation of D_2R in mice elicits differences in acquisition process during the training.

Interestingly, we found that *Drd2*$^{-/-}$ mice despite of exhibit impairment in learning, they were able to learn after extended training. *Drd2*$^{-/-}$ mice showed greater latency of response than WT mice in the three phases of Barnes maze experiment (training, test and reversal), that involves a delay acquisition in scape response and less spatial learning. On the other hand, we ruled out

the possibility that this was due to an emotional, motivational or motor disturbance in *Drd2*$^{-/-}$ mice because the results in P-maze and Porsolt were similar in both genotypes. Only the exploratory behavior, immobility time and the number of holes exploring at day 1 of training in Barnes maze, exhibit less exploratory activity in *Drd2*$^{-/-}$ mice, in according with previous studies in hole board (Hranilovic et al., 2008). So we could not discard with this test, motivational and motor disturbances to the full extent.

Therefore, we performed other spatial test, the MWM. In this test, mice were administrated with caffeine at the day of habituation (day 0) and in Test 1 (48 h), to facilitate the motor response and to increase the exploratory behavior (Chen et al., 2001). Nonetheless, *Drd2*$^{-/-}$ mice showed similar learning pattern than in the Barnes maze, but run more distances than the WT mice in all training days, ruling out the influence of less exploratory behavior and the hypolocomotion in these mice. Also, *Drd2*$^{-/-}$ mice showed similar results in Test 1 (48 h after the training) with caffeine, and Test 2 (74 h after the training) without caffeine, the difference between the groups were increased. Based on these results we conclude that the delay in the escape response is mainly for a deficit in spatial navigation.

In addition, a recent work Nguyen et al., 2014, showed important changes in hippocampal place cell responses of *Drd2*$^{-/-}$ mice during manipulations of spatial and familiar environmental cues. The place-cell representation of space is essential because is thought to underlie certain forms of spatial learning. This group found that *Drd2*$^{-/-}$ mice, in a familiar environment, have reduced number of hippocampal place cell activation and affected the intra-field firing rate, spatial tuning and spatial coherencia in the hippocampus.

2.2. Dopamine D_2R is critical for acquisition and consolidation of associative memories.

To further assess the role of D_2R in associative learning, we used two paradigms to evaluate fear memories.

In active avoidance test, *Drd2*$^{-/-}$ mice, similar to *Drd1a*$^{-/-}$ mice, did not decrease their escape latency at any time point during the training trials. Similar random crossing scores for WT and *Drd2*$^{-/-}$ mice indicate that this finding is not caused by decreased locomotor activity. In this experiment *Drd2*$^{-/-}$ mice did not reduce their scape latency during the training trials, displaying a response pattern similar to models of learned helplessness (Seligman et al., 1975). However *Drd2*$^{-/-}$ mice showed similar results to WT mice on P-maze and Porsolt test, which indicates that this pattern of response cannot be explained by previous emotional disturbances. Also, according with other studies, if learning does not occur in early trials the animal can asses the si-

tuation as *"uncontrollable",* in which case there is a decline in dopamine release that hinder the establishment of new memories (Anisman, 1977; Cabib & Puglisi-Allegra, 1994).

We use the fear conditioning test to discriminate between hippocampus and amygdala dependent associative learning. *Drd2*$^{-/-}$ mice showed longer freezing time in contextual (hippocampus-dependent) fear conditionings; this result is supported by similar work (Fadok et al., 2009). We found no differences between WT and *Drd2*$^{-/-}$ mice in extinction of fear conditioning in the first five days, only in the final day.

The D_2R activation is critical for flexibility and reward learning. Similar to these results, other studies have linked the D_2R functions in striatum, amygdala and NAc to aversive conditioned learning responses (Nakanishi et al., 2014; Slagter et al., 2015; Brandão et al., 2015).

In addition, as we have demonstrated, the response in associative tests was not due to differences in nociception in agreement with other studies (Mansikka et al., 2005).

2.3. Dopamine D_2R is involved in associative learning and in the related changes in synaptic strength at the hippocampal CA3-CA1 synapse.

It is widely accepted that hippocampal circuits are involved in the acquisition of classically conditioned eyelid responses (Berger et al., 1983; Moyer et al., 1990; Gruart et al., 2006; Ortiz et al., 2010). Using unitary *in vivo* recordings, hippocampal pyramidal cell firing in response to CS presentations increases across conditioning sessions (McEchron & Disterhoft, 1997; Múnera et al., 2001; McEchron et al., 2003). Eyeblink conditioning, a form of associative learning, was recently show to induce a progressive increase in strength at the hippocampal CA3-CA1 synapse in awake mice (Gruart et al., 2006; Madroñal et al., 2009) that correlates with the progressive increase in conditioned responses.

To directly demonstrate the relationship between LTP and associative learning, we studied the role of D_2R in associative learning and synaptic plasticity in mice. LTP is well-established as a form of synaptic memory, but is usually studied under non-physiological conditions. We found that D_2R are also necessary for evoking and maintenance of LTP at the CA3-CA1 synapse after HFS of afferent schaffer collaterals. Since input-output curves and paired-pulse potentiation were normal in both *Drd2*$^{-/-}$ and *Drd2*-siRNA mice. We conclude that the D_2R does not affect normal transmission but contributes to synaptic plasticity during the acquisition and storage of new information.

LTP *in vivo* results are related with previous classical *in vitro* studies. Classical studies used a pharmacological block of D_2R with the antagonist Domperidone. They does not found differences in LTP-induction, but the LTP-maintenance was abolished (Dunnwiddie et al., 1982; Frey et al., 1989, 1990). These authors suggest that an additional stimulation of presynaptic afferents is required for the maintenance of LTP. The L-LTP which depend on dopamine-mediated signals also requires the induction of an increased protein synthesis. In addition, recent works *in vitro* shows that the genetic deletion or pharmacologic blockade of D_2R inhibit the LTP expression in temporal CA1 region (Rocchetti et al., 2014).

Further, our approach here is unique in that we simultaneously assess classical eyeblink conditioning and synaptic efficiency by measuring changes in evoked extracellular fEPSPs at the CA3-CA1 synapse in awake animals during conditioning. We compared WT mice to *Drd2*$^{-/-}$ mice. In addition, we used siRNA technology to silence D_2R in hippocampal adult mice *in vivo*. Our data reveal a functional relationship between acquisition of associative learning and the increase in synaptic strength at the CA3-CA1 synapse, by revealing that all two are dramatically impaired when D_2R is eliminated or reduced.

2.4. Possible molecular mechanisms of D_2R-mediated learning and memory process.

The possible molecular mechanism of D_2R mediated the hippocampal synaptic transmission is not yet clear. It is possible that genetic deletion and pharmacologic blockade of D_2R severely impairs NMDA-dependent LTP in CA1, corresponding with remodelling of mesohippocampal dopamine fibers and decreases learning and memory task performance. Also, the loss of presynaptic control on dopamine levels for the absence of D_2R, may produce an overactivation of postsynaptic D_1R and a decrease in DAT action (Ares-Santos et al., 2013; Rocchetti et al., 2014).

In addition, previous studies indicate the presence of a synergistic effect between D_1R and D_2R dopamine receptors (Ichihara et al., 1992) that may results in the activation of a third intracellular signaling pathway by the activation of Gq protein, that increasing intracellular calcium levels (Lee et al., 2004). Although is not yet proved the existence of these heterodimers in hippocampal neurons.

Dopamine receptors also participate in multiple non-Gα protein signaling mechanisms. Dopamine receptors mediated effects can involve Gβ/Gγ proteins as well as other receptors (Missale et al., 1998; Beaulie & Gainetdinov, 2011). For example, D_2Rs form heterodimers with A_2A receptors (Canals et al., 2003) and Sigma-1 receptors (Navarro et al., 2013) and recruit protein

Kinase A/glycogen synthase kinase 3 (AKT/GSK3) signaling pathways via a slower cAMP-independent signaling mechanism (Beaulieu et al., 2005, 2007). G-protein-coupled receptor kinases and arrestins, normally associated with receptor desensitization, form a scaffold for D_2R receptor interactions with protein phosphatase 2A and AKT (Lovestone et al., 2007; Money & Stanwood, 2013).

Besides, NCS-1 (neural calcium sensor 1) regulates D_2R phosphorylation through an interaction with G protein-coupled receptor kinase 2 (GRK2). NCS-1 and D_2R are associated *in vitro* and co-localize in monkey and rat striatum (Kabbani et al., 2002), also co-immunoprecipite in mouse hippocampal lysates of CA1, CA3 and DG regions (Saab et al., 2009). Previous studies show that this interaction between NCS-1 and D_2R is critical for LTP facilitation in DG, and may also underlie the promotion of specifics forms of exploration and enhancements in spatial memory acquisition (Kabbani et al., 2002).

Even if basal synaptic transmission is normal in *Drd2*$^{-/-}$ and *Drd2*-siRNA mice, previous studies found a decrease in the number of spines and synapsis in PFc and hippocampus of *Drd2*$^{-/-}$ mice and in mice treated with D_2R antagonists (Sugahara & Shiraishi, 1998; Critchlow et al., 2006; Wang et al., 2009). D_2R has been linked to neuronal development during adulthood in both dendritic trees and spine density, while D_1R is involved in neurogenesis and neuronal maturation process.

Finally, several experiments in rodents demonstrated a critical interaction between D_2R and hippocampal cholinergic signalling. Mice injected with raclopride in ventral hippocampal region present a decreased cholinergic activity and a poor performance in passive avoidance test (Fujishiro et al., 2005). The chronic treatment with no-specific D_2R antagonist, haloperidol, leads to a decreased of acetyl-cholinergic fibbers in hippocampus and an impairment in spatial memory tasks, like MWM in rats (Terry et al., 2003; Parikh et al., 2004).

2.5. D_1R and D_2R are essential in cognitive dopamine dependent process.

Neurocomputational models propose the role of dopamine as a principal neuromodulator of the central nervous system, responsible of the "adaptive navigation" process. These models involve very complex strategies of response to determine the questions: *"Where we are?", "Where do we go?"* and *"How can we go?"*. For these functions, dopamine coordinates the action of different neurotransmission systems and brain structures, specially PFc, BG and hippocampus (Mizumori et al., 2009).

Some of these models propose as central hypothesis a dual response of dopaminergic system that determine cognitive functions (Deher & Burnod, 2002). Dopamine would response to a

particular input: a) first, a sharp increase for seconds (*phasic response*), and b) later, a sustained response above the basal level for minutes (*tonic response*). The phasic response directly depend on the firing of dopaminergic neurons, and the tonic phase is independent of this (Schultz, 2007; Brischoux et al., 2009).

The different dopamine levels, which would reach the dopaminergic curve of response, are moving into a particular range, out of which functions would not be carried out correctly. This effect indicates the possibility of a U-inverted shape dopamine-execution pattern of response. Therefore, both high and low levels of dopamine in response to different inputs, may cause a less efficient neuromodulation of neuronal noise in information processing, causing a less distinctive neuronal representations and a poor cognitive performace (Li & Sikström, 2002). Through this mechanism, dopamine would be able to focus attention on the strong cortical signals, promoting an increase in the firing rate of innervated neurons, substracting the neuronal signal relative to the background noise and, in consequence, facilitating the adjust of responses (Nicola et al., 2000; Bamford et al., 2004). Human studies that relate aging and cognitive function, suggest that reduction in dopaminergic activity could cause an increment in the neuronal noise and decline cognitive functions (Li et al., 2001). In addition, studies in healthy subjects, suggest that dopaminergic neuromodulation is critically involved in the synchronization of the oscillatory activity that facilitates the access and review the working memory (Breakspear et al., 2003; Seamans & Yang, 2004; Li et al., 2005).

For these reasons, some authors propose that dopaminergic tone could be involved in basic processes of consciousness (Palmiter, 2011) as executive functions, implementation of plans, directing attention and working memory, all related to the prefrontal cortex and thalamus but not rely exclusively on them. Dopaminergic deficit can keep the reflexes intact but provokes difficulty managing and adapt the behavior to the environment (Palmiter, 2011), because includes motivational and arousal aspects. RD Palmiter propose that dopaminergic neurons could act modulating glutamatergic inputs of thalamus and cortex; sustaining the dopaminergic tone through the actions of D_1R and D_2R (Palmiter, 2011).

D_1R and D_2R receptors, promote the release of dopamine and maintain the optimum levels for the development of dopaminergic response within an optimal range. The D_1R would only be activated by temporary increases in dopamine (Goto & Grace, 2005; Grace et al., 2007; Wall et al., 2011). However, D_2R has more affinity for dopamine and would be implicated mediating the effects of dopamine tonic release (Goto et al., 2007; Wall et al., 2011). D_2R activation may serve as a phasic gating signal indicating when new information should be encoded and maintained in working memory or when an updating of current representations is needed (Glickstein, 2002).

3. DOPAMINERGIC SIGNALING BY D_1R AND D_2R IN STRIATUM REGULATES THE PHENOTYPIC SHIFT OF A POPULATION OF STRIATAL NEURONS AND MOTOR BEHAVIOR.

As described above, the action of D_1R and D_2R are necessary to maintain a suitable dopaminergic balance and, therefore, an effective function of the dopaminergic system processes.

Previous studies from our laboratory and others have shown that TH-ir neurons are induced following unilateral lesion of the striatum and the number and staining intensity of TH-ir neurons is further increased by L-DOPA treatment. However, the mechanisms leading to TH protein expression after dopaminergic denervation and L-DOPA treatment remain unclear. In the present study we have explored the mechanisms of their regulation of TH expression and the functional implications of increased TH expression in this cell population. Our results demonstrated that the induction of TH-ir neurons by L-DOPA is dose-dependent and requires D_1R function. We further demonstrated a tight spatio-temporal correlation between the presence of these striatal TH-ir neurons, the recovery of dopamine overflow and forelimb use induced by L-DOPA treatment.

3.1. The number of TH-ir neurons in the denervated striatum are increased by L-DOPA treatment in a dose-dependent manner.

Although some studies have identified a small number of TH-ir neurons in the caudoputamen of normal animals, including monkeys, rats and mice (Dubach et al., 1987), their number increased in parkinsonian human brains (Porritt et al., 2000), and in brains of non-human primates and rodents following dopamine depletion (Betarbet et al., 1997; Jollivet et al., 2004; Tande et al., 2006). L-DOPA treatment further increases the number of TH-ir neurons in hemiparkinsonian rats (Mura et al., 1995; Lopez-Real et al., 2003; Jollivet et al., 2004) and mice (Darmopil et al., 2008). Similar results have been reported in the caudate nucleus and putamen of parkinsonian patients treated with L-DOPA (Porritt et al., 2000).

In the current study, we demonstrate that the L-DOPA-induced TH-ir neurons increase is dose-dependent: 25 mg/kg L-DOPA induced nearly twice as many TH-ir neurons as 15 mg/kg L-DOPA. Although is tempting to propose that the number of TH-ir neurons correlates with the severity of dyskinesias as has been reported (Francardo et al., 2011), several of our findings do not support it. While L-DOPA-induced TH-ir neurons are evident for more than 4 days, L-DOPA-induced dyskinesias do not last for more than 3 h (Westin et al., 2007; Darmopil et al.,

2009). While causing only a 47 to 59% reduction in the number of TH-ir neurons. It is also possible that dopamine produced by striatal TH-ir neurons reduce sensitization of dopamine receptors; in which case, their chronic stimulation by L-DOPA might produce less dyskinesia.

We further found that the increase in TH-ir neurons was dependent on continue L-DOPA treatment: by 10 days after the final L-DOPA injection, the number of striatal TH-ir neurons had returned to baseline and TH-ir neurons were detected only in the ventral striatum or close to the remaining dopaminergic fibres, in agreement with previous studies from our laboratory (Darmopil et al., 2008). These results indicate that the L-DOPA-induced increase in TH-ir neurons in the dopamine-depleted striatum is a specific and regulated process.

As in previous studies in humans, monkeys and rodents (Porritt et al., 2000; Palfi et al., 2002; Lopez-Real et al., 2003; Darmopil et al., 2008) the TH-ir neurons that appeared following dopamine depletion in our study were most frequently found close to spared dopaminergic terminals, further supporting their dopamine dependency, as these terminals are the most likely site of conversion of L-DOPA to dopamine and have higher dopamine turnover. These findings suggest that TH expression in striatal neurons is regulated by L-DOPA and by the local concentration of dopamine within a very narrow concentration range, because they are undetectable in the normal or in completely denervated striatum, but are dose-dependently induced by L-DOPA in the partially denervated striatum.

3.2. Induction of TH-ir neurons in lesioned striatum by L-DOPA requires the D_1R, but not the D_2R.

The effect of L-DOPA on the induction of TH phenotype in striatal neurons was markedly diminished in hemi-parkinsonian *Drd1a*$^{-/-}$ mice: both the increase in number of TH-ir neurons and the increase in intensity of staining were blocked. In contrast, neither the number nor the staining intensity of striatal TH-ir neurons in L-DOPA-treated hemi-parkinsonian *Drd2*$^{-/-}$ mice was significantly different from their WT littermates. These results are corroborated by our studies using pharmacological blockade of the D_1R or D_2R receptor families and reveal a critical and specific role for the D_1R in the L-DOPA mediated induction of TH phenotype in striatal neurons. Results with D_1R antagonist are in according with recent studies that demonstrate a decrease in the number of TH-ir striatal neurons during the development of striatal innervation (Busceti et al., 2012). We showed previously that D_1R inactivation completely abolished L-DOPA-induced ERK activation (Darmopil et al., 2009), thus ERK signalling may play a role in induction of TH-ir neurons by L-DOPA. Our finding that simvastatin reduced the number of L-DOPA-induced TH-ir neurons in the depleted striatum by 50% supports this effect.

Interestingly, following L-DOPA treatment striatal TH-ir cells also express FosB (Darmopil et al., 2008) and this induction of FosB is also mediated by D_1R stimulation (Darmopil et al., 2009). Thus, L-DOPA induction of the TH phenotype may be partially mediated by increased FosB expression in these neurons, a possibility further suggested by the presence of a FosB binding domain (AP-1 site) in the regulatory part of the TH gene (Lewis-Tuffin et al., 2004). In addition, some studies shown a positive correlation with an increase in the number of TH-ir striatal neurons, FosB expression and the level of LID in mice models of PD (Francardo et al., 2011; Smith et al., 2012; Keber et al., 2015). However, previous studies in our laboratory demonstrate that LIDs normally disappear 2 h after the L-DOPA injection (Solís et al., 2015; Ruiz-DeDiego et al., 2015) but the long-lasting therapeutics effects of L-DOPA associated with TH-ir cells founds in these work can last 1 week after the chronic treatment.

In addition, it is clearly that D_1R is implicate in the expression of striatal TH-ir neurons, but our results with *Drd1a*-Tomato and *Drd2*-GFP mice, demonstrated that TH-ir neurons not express D_1R or D_2R. However, recent studies suggest two possible regulation pathways of TH-ir neurons mediated by dopamine: a) A pathway directly related with the fluctuations in dopamine levels and b) An indirect pathway related the action of D_1R by enhancing the release of acetylcholine (Busceti et al., 2012). In this way, a recent study demonstrate that TH-ir neurons express nicotinic cholinergic receptors, and spikes to brief application of nicotinic agonist (Ibáñez-Sandoval et al., 2015). Nicotinic receptors are largely restricted to striatal interneurons where they exert excitatory effects on GABAergic interneurons firing (English et al., 2011; Koós and Tepper, 2002), and are also present on dopaminergic terminals, where it has been proposed that they may elicit dopamine release independent of dopaminergic neuronal activity (Cachope et al., 2012; Threlfell et al., 2012).

3.3. Ultrastrcuture of striatal TH-ir neurons in mice.

There are only two studies to date that analyse the ultrastructure of TH-ir neurons. The present study is the first in the mouse. Our results are similar in some aspects to those found MPTP treated monkeys (Mazloom & Smith, 2006), but not in rat (Meredith et al., 1999).

Striatal TH-ir neurons in the rat study have a dark nucleus and smooth nuclear envelopes (autophagic vesicles). The elevated number of autophagic vesicles and the rupture of mitochondria visible in this TH-ir neurons indicated that the brain tissue dissected for the analysis was an infarcted area, unsuitable for the ultrastructure study. However, we are in agreement with the presence of TH-immnunostained spines, not found in the monkey study. Inputs to dendritic

shafts were found that can make asymmetrical (excitatory) synaptic contacts.

On the other hand, results in the monkey study were similar to those found in this study. They found that TH-ir neurons have light nuclei with the nuclear membrane deeply invaginated, with shape round or oval and small cell bodies. These results demonstrate that the vast majority of intrastriatal TH-ir neurons display the ultrastructural features of interneurons (Mazloom & Smith, 2006; San Sebastián, 2007).

3.4. Pitx3 and Nurr1 are not required for L-DOPA-induced TH-ir neurons in the striatum.

The TH gene also contains a Pitx3 binding site (Cazorla et al., 2000; Messmer et al., 2007). However, we found that Pitx3 is not necessary for L-DOPA regulation of TH transcription in these neurons, as evidenced by our finding that L-DOPA increased the number of striatal TH-ir neurons in Pitx3 deficient aphakia mice to a similar degree as in WT mice. Our results in 6-OHDA-lesioned aphakia mice also rule out the possibility that Pitx3 is required for the increase in TH-ir neurons induced by striatal injury. Pitx3 is an important transcription factor in the development, maturation and migration of the dopaminergic system in the midbrain (Nunes et al., 2003; Smidth et al., 2004). However, our results demonstrate that Pitx3 is not necessary for denervation- or L-DOPA-induced TH expression in striatal neurons in adult mice. This may be because these striatal TH-ir neurons are not generated from the same progenitors as SNc dopaminergic neurons, and they could be derived from other striatal neuronal populations that undergo a phenotypic shift after denervation (Tande et al., 2006; Darmopil et al., 2008; Unal et al., 2011).

Supporting the concept that these TH-ir neurons have a distinct phenotype, we also found that these neurons do not express Nurr1, a determinant transcription factor of midbrain dopaminergic neurons, in contrast with human studies (Cossette et al., 2004). Nurr1 is required for the differentiation of mesencephalic dopaminergic neurons, induces the expression of dopaminergic genes such as *Th, Vmat 2* and *Dat* (Vergaño-Vera et al., 2014). In support of this possibility, 95% of TH-ir neurons also expressed GABA (Unal et al., 2011), which is expressed in all types of striatal neurons except cholinergic interneurons. Our results further show that in the denervated striatum, L-DOPA is able to trigger and maintain this phenotypic shift by stimulating and increasing the transcriptional/translational activity of the *Th* gene.

3.5. Identity of L -DOPA-induced TH-ir neurons in the striatum.

There is some controversy about the identity of striatal TH-ir neurons. Previous studies indicated that these neurons may be MSNs based on the expression of Darpp32, dynorphin, enkephalin or calbindin markers (Betarbet et al., 1997; Darmopil et al., 2008; Masuda et al., 2011). In addition, these same studies and others shown that most of these neurons also express striatal interneurons markers such as PV, nNOS, NPY and especially, GAD-67 (99%) in rodents (Betarbet et al., 1997; Mazloom & Smith, 2006; Tande et al., 2006; San Sebastián et al., 2007; Darmopil et al., 2008; Busceti et al., 2012).

Recent studies that using eGFP-TH BAC transgenic mice identified a much larger population of TH-expressing striatal neurons in naïve striatum (Ibañez-Sandoval et al., 2010, 2015; Depbuoylu et al., 2014). Whole-cell recordings in striatal slices demonstrated that eGFP-TH neurons comprise four electrophysiologically distinct neurons types whose properties have not been reported previously in striatum. Further, based on retrograde labelling, lack of expression of interneuronal markers, and GABAergic properties, they concluded that these neurons represent a previously unidentified subpopulation of TH-expressing interneurons. However, no all eGFP-TH neurons are detected at basal conditions. After the 6-OHDA lesion eGFP-TH BAC transgenic mice had shown an increase in the number of eGFP-TH neurons in the lesioned striatum (Depbuoylu et al., 2014). As we say previously, the phenotypic shift of TH-ir neurons in the striatum is mainly determined by the fluctuations of local dopamine levels.

In addition, previous studies demonstrated that striatal gene expression is altered by chronic L -DOPA treatment (Pavón et al., 2006). Perhaps L-DOPA itself plays some intracellular signaling role in the TH-ir neurons (Ugrumov, 2009). The function of L-DOPA in TH-ir neurons remains unknown, but one possibility is that it is supplied to monoenzymatic AADC cells of the striatum or the terminals of nigrostriatal dopaminergic neurons via the aminoacid transporters (Ugrumov, 2009) and thereby contributes to dopamine release in a compromised striatum.

Nowadays the controversy remains unclear. More experiments are needed to clearly stablish the identity of TH-ir neurons in the dopamine depleted striatum. Regardless of their identity, our data suggest that these TH-ir neurons may have a beneficial effect in PD, therefore understanding the regulation of these neurons in dopamine-depleted striatum is important and is the goal of this work.

3.6. Time-course of striatal dopamine overflow and improvement in motor function after chronic L-DOPA treatment in lesioned mice.

Although the function of striatal TH-ir neurons in the dopamine-depleted striatum is unknown, it has been demonstrated that they produce L-DOPA that can be released by a non-exocitotoxic mechanism (Weihe et al., 2006), and those TH-ir neurons that express the AADC enzyme can also produce dopamine. L-DOPA released by these cells may also be converted to dopamine in the nearby remaining dopaminergic terminals. Our voltammetry experiments demonstrate a significant decrease in electrically stimulated dopamine release in slices from lesioned striatum compared to striatal slices from naïve animals. There was a strong increase, almost two-fold, in dopamine release in the contralateral unlesioned striatum of unilaterally lesioned animals, indicating that the unilateral lesion affects both hemispheres. Thus, the unlesioned striatum increases the synthesis of dopamine in an attempt to compensate for the lack of dopamine in the lesioned striatum as indicated previously (Bjorklund & Dunnett, 2007). Interestingly, our data show that chronic L-DOPA treatment transiently restores electrically stimulated dopamine overflow in the striatum, so that dopamine overflow in both sides is equal and similar to that obtained in the striatum of sham lesioned mice. Stimulated dopamine overflow levels remain normal in the contralateral unlesioned striatum even 4 days following L-DOPA withdrawal, but there is a significant decrease in dopamine overflow on the lesioned side, although it remains greater than in lesioned striatum of mice without L-DOPA treatment. 10 days after L-DOPA withdrawal, dopamine overflow levels in both hemispheres reverted to the levels obtained in lesioned animals treated with saline. Remarkably, stimulated dopamine overflow in the lesioned striatum after L-DOPA correlates with the presence of striatal TH-ir neurons: it is highest with L-DOPA treatment and decreases progressively to baseline over the first 10 days after the end of L-DOPA treatment. Therefore it is possible that these striatal TH-ir neurons contribute to the normalization of stimulated dopamine overflow in the lesioned striatum during chronic L-DOPA treatment and for a short period after the treatment ends.

The time-course of the effect of L-DOPA on stimulated dopamine overflow and TH-ir neurons also coincides with the time-course of motor improvement that we observed in lesioned animals chronically treated with L-DOPA. We found that this treatment temporarily reversed the forelimb asymmetry induced by the 6-OHDA lesion, supporting normal motor function in the forelimbs for 4 days after L-DOPA withdrawal; however, this effect wore off by 7 to 10 days after L-DOPA withdrawal. Thus, the period of improvement in motor function overlaps with the period of greatest local dopamine overflow in the lesioned striatum and with the pre-

sence of the highest number of striatal TH-ir neurons.

Interestingly, similar temporal motor improvement was observed in Pitx3$^{-/-}$ after cessation of L-DOPA treatment (Beeler et al., 2010) in which we observed similar increase of striatal TH-ir neurons. The reversal of forelimb use asymmetry observed during the first 4 days after L-DOPA treatment suggests that the small amount of dopamine available after chronic L-DOPA treatment is sufficient to normalize forelimb asymmetry in mice, whether this dopamine comes from the remaining dopamine fibres or from the local TH-ir neurons. It is therefore possible that the induction of striatal TH-ir neurons following L-DOPA treatment in denervated mice is responsible for the temporal improvement in parkinsonian symptoms that we observed after the chronic L-DOPA treatment. It has been shown previously that very small numbers of dopamine -producing cells can reduce parkinsonian symptoms in denervated rats and monkeys following carotid body grafts into the striatum (Espejo et al., 1998; San Sebastian et al., 2007). In addition our observations are in line with the motor recovery after intrastriatal viral vector injections confining TH, and AADC in monkeys (Muramatsu et al., 2002). Altogether our results demonstrate a tight spatio-temporal correlation between the time-course of striatal dopamine overflow, the improvement in motor function and the presence of striatal TH-ir neurons after chronic L-DOPA treatment in lesioned mice.

The results presented here suggest that induction of striatal TH-ir neurons might underlie the long-term beneficial effect of L-DOPA therapy observed in parkinsonian patients: while the anti-parkinsonian effect of L-DOPA eventually disappears after cessation of treatment, patients report beneficial effects for some time following L-DOPA withdrawal (Nutt et al., 1995; Fahn, 2006). Understanding the functional implications and the molecular mechanisms of this phenotypic change could contribute to the development of new therapies for Parkinson's disease with the goal of providing a more persistent therapeutic effect than that offered by current drugs.

4. FUTURE PERSPECTIVES.

Most diseases that involving the dopaminergic system elicit changes in the expression and function of the main dopamine receptors: D_1R and D_2R, whose study is necessary to know what happens in motor and cognitive functions under physiological and pathophysiological conditions.

During aging and in the course of certain neurodegenerative diseases, such as Parkinson or Alzheimer, there is a decreased in dopamine levels and a down-regulation of D_1R and D_2R. This phenomenon is normally accompanied with a pathological decline in cognitive and motor

functions, that could completely impair patients ability.

For these reasons is necessary to continue our research to understand the possible molecular mechanisms implicated in the origin of these diseases and the development new therapeutic targets that improve the quality of life of patients and aging subjects.

Conclusions

1. Dopamine D_1R is critical for acquisition and consolidation of spatial memory.
2. Dopamine D_1R is critical for acquisition of associative learning.
3. Dopamine D_1R is critical for recognition memory process.
4. Dopamine D_2R influences in acquisition and consolidation of spatial memory.
5. Dopamine D_2R is critical for acquisition of fear memories.
6. Dopamine D_2R is involved in associative learning and in the related changes in synaptic strength at hippocampus.
7. TH-ir neurons are increased by L-DOPA treatment in a dose-dependent manner.
8. TH-ir neurons do not express D_1R and D_2R receptors, but D_1R receptors are implicated in the expression of these neurons.
9. TH-ir cells have ultrastructural characteristics of GABAergic striatal interneurons.
10. TH-ir striatal neurons do not expression Pitx3 and Nurr1, indicating that these neurons have different origin that midbrain dopaminergic neurons.
11. The time-course of the effect of L-DOPA on stimulated dopamine overflow and TH-ir neurons similar with the time-course of motor improvement.

Bibliography

Aarsland D, Zaccai J, Brayne C (2005). A systematic review of prevalence studies of dementia in Parikinson´s disease. *Mov Disord*. **20**: 1255-1263.

Alarcón JM, Malleret G, Touzani K, Vronskaya S et al., (2004) Chromatin acetylation, memory, and LTP are impaired in CBP+/- mice: a model for the cognitive deficit in Rubinstein-Taybi syndrome and its amelioration. *Neuron.* **6**: 947-959.

Amara SG, Kuhar MJ (1993). Neurotransmitter transporters: Recent progress. Annu *Rev Neurosci*. **16**: 73-93.

Anisman H (1977). Time-dependent changes in activity, reactivity, and responsivity during shock: effects of cholinergic and catecholaminergic manipulations. *Behav Biol*. **21**: 1-31.

Ares-Santos S, Granado N, Oliva I, O´Shea E et al., (2012). Dopamine D_1 receptor deletion strongly reduces neurotoxic effects of methamphetamie. *Neurobiol Dis*. **45**: 810-820.

Ares-Santos S, Granado N, Moratalla R (2013). The role of dopamine receptors in the neurotoxicity of methamphetamine. *J Intern Med*. 273: 437-453.

Azdad K, Chávez M, Don Bischop P, Wetzelaer P et al., (2009). Homeostatic plasticity of striatal neurons intrinsic excitability following dopamine depletion. *Plos One*. **4**: e6908.

Bäckman L, Ginovart N, Dixon RA, Wahlin TB et al., (2000). Age-related cognitive deficits mediated by changes in the striatal dopamine system. *Am J Psychiatry*. **157**: 635-637

Bäckman L, Farde L (2001). Dopamine and cognitive functioning: brain imaging findings in Huntington´s disease and normal aging. *Scand J Psychol*. **42**: 287-296.

Bäckman L, Lindenberg U, Li SC, Nyberg L (2010). Linking cognitive aging to alterations in dopamine neurotransmitter functioning: recent data and future avenues. *Neurosci Biobehav Rev*. **34:** 670-677.

Baik JH, Picetti R, Sajardi A, Thiriet G et al., (1995). Parkinsonian-like locomotor impairment in mice lacking dopamine D2 receptors. *Nature*. **377**: 424-428.

Baker H, Kobayashi K, Okano H, Saino-Saito S (2003). Cortical and striatal expression of tyrosine hydroxylase mRNA in neonatal and adult mice. *Cell Mol Neurobiol*. **23**: 507-518.

Bamford NS, Robinson S, Palmiter RD, Joyce JA et al., (2004). Dopamine modulates release from corticostriatal terminals. *J Neurosci*. **24**: 9541-9552.

Barnes CA (1979). Memory deficits associated with senescence: a neurophysiological and behavioral study in the rat. *J Comp Physiol Psychol.* **93**: 74-104.

Barker GR, Warburton EC (2011). When is the hippocampus involved in recognition memory? *J Neurosci*. **31**: 10721-1073.

Beaulieu JM, Sotnikova TD, Marlon S, Lefkowitz RJ et al., (2005). An Akt/β-Arrestin 2/PP2A signaling complex mediates dopaminergic neurotransmission and behavior. *Cell*. **122**: 261-273.

Beaulieu JM, Tirotta E, Sotnikova TD, Masri B et al., (2007). Regulation of Akt signaling by D2 and D3 dopamine receptors in vivo. *J Neurosci*. **27**: 881-885.

Beaulie JM, Gainetdinov RR (2011). The physiology, signaling and pharmacology of dopamine receptors. *Pharmacol Rev*. **63**: 182-217.

Beeler JA, Cao ZFH, Kheirbek MA, Ding Y et al., (2010). Dopamine-dependent motor learning insight into levodopa´s long-duration response. *Ann Neurol.* **67**: 639-647.

Belluci A, Zaltieri M, Navarria L, Grigoletto J et al.,(2012). From α-synuclein to synaptic dysfunctions: new insights into the pathophysiology of Parkinson´s disease. *Brain Res*. **1476**: 183-202.

Berger TW, Rinaldi P, Weisz DJ, Thompson RF (1983). Single-unit analysis of different hippocampal cell types during classical conditioning of rabbit nictitating membrane response. *J Neurophysiol.* **50**:1197-1219.

Bertabet R, Turner R, Chockkan V, Delong MR et al., (1997). Dopaminergic neurons intrinsic to the primate striatum. *J Neurosci.* **17**: 6761-6768.

Bertabet R & Greenamyre JT (1999). Differential expression of glutamate receptors by the dopaminergic neurons of the primate striatum. *Exp Neurol.* **159**: 401-408.

Bezard E, Jaber M, Gonon F, Boireau A et al., (2000). Adaptative changes in the nigrostriatal pathway in response to increased 1-methyl -4-phenyl-1,2,3,6-tetrahydropyridine-induced neurodegeneration in the mouse. *Eur J Neurosci*. **12**: 2892-2900.

Bjorklund & Dunnet (2007). Dopamine neuron systems in the brain: an update. *Trends Neurosci*. **30**: 194-202.

Bliss TVP, Gardner-Medwin AR (1973). Long-lasting potentiation of synaptic transmission in the dentate area of the unaneesthetized rabbit following stimulation of the perforant path. *J Physiol (Lond).* **232**: 357-374.

Bliss TV, Collingridge GL (1993). A synaptic model of memory: long-term potentiation in the hippocampus. *Nature.* **361**:31-9

Bolam JP, Pissadaki EK (2012). Living on the edge with too many mouths to feed: why dopamine neurons die. *Mov Disord*. **27**: 1478-1483.

Borek LL, Amick MM, Friedman JH (2006). Non -motor aspects of Parkinson´s disease. *CNS Spectr*. **11**: 541-554.

Bowyer JF, Weiner N (1987). Modulation of the Ca^{+2}-evoked release of (3H)-dopamine from striatal synaptosomes by dopamine D2 agonists and antanoginist. *J Pharmacol Exp Ther.* **241**: 27-33.

Braak H, Del Tredici K, Bratzke H, Hamm-Clement J et al., (2002). Staging of the intracerebral inclusion body pathology associated with idiopathic Parkinson´s disease (preclinical and clinical stages). *J Neurol*. **249**: 1-5.

Brandão ML, de Oliveira AR, Muthuraju S, Colombo AC, Saito VM, Talbot (2015). Dual role of dopamine D2-like receptors in the mediation of conditioned and unconditioned fear. *FEBS Lett*. doi: 10.1016/j.febslet.2015.02.036.

Breakspear M, Terry JR, Friston KJ, Harris AWF et al., (2003). A disturbance of nonlinear interdependence in scalp EEG of subjects with first episode schizophrenia. *NeuroImage*. **20**: 466-478.

Breese GR & Taylor TD (1971). Depletion of brain noradrenaline a dopamine by 6-hydroxydopamine. *Br J Pharmacol*. **42**: 88-89.

Brischoux F, Chakraborty S, Brierly D, Ungless MA (2009). Phasic excitation of dopamine neurons in ventral VTA by noxious stimuli. *Proc. Natl. Acad. Sci. USA*. **106**: 4894-4899.

Broadbent NJ, Gaskin S, squire LR, Clark RE (2010). Object recognition memory and the rodent hippocampus. *Learn Mem*. **17**: 5-11

Brown RG, Marsden CD (1990). Cognitive function in Parkinson´s disease: from description to theory. *TINS*. 13: 21-29.

Bubak AN, Redmond DE, Elsworth JD, Roth RH et al., (2015). A potential compensatory role for endogenous striatal tyrosine hydroxylase-positive neurons in a nonhuman primate model of Parkinson´s disease. *Cell Transplant.* **24:** 673-80

Burkey AR, Carstens E, Jasmin L (1999). Dopamine reuptake inhibition in the rostral agranular insular cortex produces antinociception. *J Neurosci*. **19**: 4169-4179.

Busceti CL, Biagioni F, Mastroiavoco F, Bucci D et al., (2008). High number of striatal dopaminergic neurons during early postnatal development: correlation analysis with dopaminergic fibers. *J Neural Transm.* **115**: 1375-1383.

Busceti CL, Bucci D, Molinaro G, Di Pietro P et al., (2012). Lack or inhibition of dopaminergic stimulation induces a development increase of striatal tyrosine hydroxylase-positive interneurons. *Plos One*. **7.** doi: 10.1371/journal.pone.0044025

Cabib S and Puglisis-allegra S (1994). Opposite responses of mesolimbic dopamine system to controllable and uncontrollable aversive experiences. *J Neurosci*. **14**: 33-40.

Cachope R, Mateo Y, Mathur BN, Irving J et al., (2012). Selective activation of cholinergic interneurons enhances accumbal phasic dopamine release: setting the tone for reward processing. *Cell Rep*. **2:** 33-41.

Cai G, Wang HY, Friedman E (2002). Increased dopamine receptor signalling and dopamine receptor-G protein coupling in denervated striatum. *JPET*. **302**: 1105-1112.

Calabresi P, Pisani A, Mercuri NB, Bernardi G (1992). Long-term potentiation in the striatum is unmasked by removing the voltage-dependent magnesium block of NMDA receptor channels. *Eur J Neurosci.* **4**: 929-935.

Camps M, Cortés R, Gueye B, Probst A, Palacios JM (1989). Dopamine receptors in human brain: autoradiographic distribution of D2 sites. *Neuroscience*. **28**: 275-290.

Canals M, Marcellino D, Fanelli F, Ciruela F et al., (2003). Adenosise A_{2a}-dopamine D_2 receptor-receptor heteromerizacion. *J Bio Chem*. **278**: 46741-46749.

Carlsson A, Lindqvist M, Magnusson T (1957). 3,4 -Dihydroxyphenylalanine and 5-hydroxytryptophan as reserpine antagonist. *Nature*. **180**: 1200

Cattaneo E, Conti L (1998). Generation and characterization of embryonic striatal conditionally immortalizaed ST14A cells. *J Neurosci Res*. **53**: 223-34.

Cazorla P, Smidt MP, O´Malley KL, Burbach JP (2000). A response element for the homeodomain transcription factor Pitx3 in the tyrosine hydroxylase gene promoter. *J. Neurochem.* **74**: 1829-1837.

Cenci MA, Lee CS, Björklund A (1998). L-DOPA-induced dyskinesia in the rat is associated with striatal overexpression of prodynorphin- and glutamic acid decarboxylase mRNA. *Eur J Neurosci*. **10**: 2694-2706.

Cenci MA (2007). L-DOPA-induced dyskinesia: cellular mechanisms and approaches to treatment. *Parkisonism Relat Disord*. **13**: S263-7.

Cenci MA (2014). Presynaptic mechanisms of L-DOPA-induced dyskinesia: The findings, the debate, ant the therapeutic implications. *Front Neurol*. **5**: 242.

Centonze D, Grande C, Saulle E, Martín AB et al., (2003). Distinct roles of D_1 and D_5 dopamine receptors in motor activity and striatal synaptic plasticity. *J Neurosci*. **23**: 8506-8512.

Ceravolo R, Frosini D, Rossi C, Bonuccelli U (2010). Spectrum of addictions in Parkinson´s disease: from dopamine dysregulation syndrome to impulse control disorders. *J Neurol.* **257**: S276-S283.

Chen JF, Moratalla R, Impagnatiello F, Grandy DK et al., (2001). The role of the D_2 dopamine receptor (D_2R) in A_{2a} adenosine receptor ($A_{2a}R$)-mediated behavioural and cellular responses as revealed by A_{2a} and D_2 receptor knockout mice. *Proc. Natl. Acad. Sci. USA*. **98**: 1970-1975.

Christopher L, Marras C, Duff-Canning S, Koshimori Y et al., (2014). Combined insular and striatal dopamine dysfunction are associated with executive defictis in Parkinson´s disease with mild cognitive impairment. *Brain*. **137**: 565-75.

Christopher L, Duff-Canning S, Koshimori Y, Segura B et al., (2015). Salience network and parahippocampal dopamine dysfunction in memory-impaired Parkinson disease. *Ann Neurol*. **77:** 269-80.

Collins GT, Woods JH (2007). Drug and refinforcement history as determinants of the response-maintaining effects of quinpirole in the rat. *J Pharmacol Exp Ther*. **323**: 599-605.

Cortés R, Gueye B, Pazos A, Probst A, Palacios JM (1989). Dopamine receptors in human brain: autoradiographic distribution of D1 sites. *Neuroscience*. **28**: 263-73.

Cossette M, Parent A, Lévesque D (2004). Tyrosine hydroxylase-positive neurons intrinsic to the human striatum express the transciption factor Nurr1. *Eur J Neurosci*. **20**: 2089-2095.

Cossette M, Lévesque D, Parent A. (2005). Neurochemical characterization of dopaminergic neurons in human striatum. *Parkinsonims Relat Disord*. **11**: 277-286.

Costa C, Sgobio C, Siliguini S, Tozzi A et al., (2012). Mechanisms underlying the impairment of hippocampal long-term potentiation and memory in experimental Parkinson´s disease. *Brain*. **135**: 1884-99

Crawley JN (2007). What's wrong with my mouse?: Behavioral phenotyping of transgenic and knock out mice. Hoboken, NJ, Wiley.

Cremer JN, Amunts K, Graw J, Piel M et al., (2015). Neurotransmitter receptor density changes in *Pitx3*^{AK} mice- a model relevant to Parkinon´s disease. *Neuroscience*. **285**: 11-23.

Critchlow HM, Maycox PR, Skepper JN, Krylova O (2006). Clozapine and haloperidol differentially regulate dendritic spine formation and synaptogenesis in rat hippocampal neurons. *Mol Cell Neurosci*. **32**: 356-365.

Da Cunha C, Mendes Angelucci ME, Canteras, NS, Wonnacott S, Takahashi RN (2002). The lesion of the rat substantia nigra pars com-

pacta dopaminergic neurons as a model for Parkinson´s disease memory disabilities. *Cellular and Molecular Neurobiology*. **22**: 227-237.

Darmopil S, Muneton-Gomez VC, de Ceballos ML, Bernson M & Moratalla R (2008). Tyrosine hydrosylase cells appearing in the mouse striatum after dopamine denervation are likely to be projection neurones regulated by L-DOPA. *Eur J Neurosci*. **27**: 580-592.

Darmopil S, Martín AB, De Diego IR, Ares S, Moratalla R (2009). Genetic inactivation of dopamine D_1 but not D_2 receptors inhibits L-DOPA-induced dyskinesia and histone activation. *Biol Psychiatry*. **6**: 603-613.

Darvas M, Palmiter RD (2009). Restriction of dopamine signaling to the dorsolateral striatum is sufficient for many cognitive behaviors. *Proc. Natl. Acad. Sci. USA*. **106**: 14664-14669.

Darvas M, Palmiter RD (2010). Restricting dopaminergic signaling to either dorsolateral or medial striatum facilitates cognition. *J Neurosci*. **30**: 58-65

Darvas M, Fadok Jp, Palmiter RD (2011). Requirement of dopamine signalling in the amygdale and striatum for learning and maintenance of a conditioned avoidance response. *Learn Mem.* **18**: 136-143.

Dauer W, Przedborski S (2003). Parkinson´s disease: Mechanisms and models. *Neuron*. **39**: 889-909.

De Leonibus E, Pascucci T, Lopez S, Oliverio A, Amalric M, Mele A (2007). Spatial deficits in a mouse model of Parkinson disease. *Psychopharmacology*. **194**: 517-525.

Delfino M, Kalisch R, Czisch M, Larramendy C et al., (2007). Mapping the effects of three dopamine agonists with different dyskinetogenic potential and receptor selectivity using pharmacological functional magnetic resonance imaging. *Neuropsychopharmacology*. **32**: 1911-1921.

Depbuoylu C, Klietz M, Maurer L, Oertel WH et al., (2014). Transcriptional and structural plasticity of tyrosine hydroxylase expressing neurons in both striatum and nucleus acccumbens following dopaminergic denervation. *J Chem Neuroanat*. **61-62**: 169-75.

Diaz J, Pilon C, Le Foll B, Gros C, Triller A, Schwartz JC, Sokoloff P (2000). Dopamine D3 receptors expressed by all mesencephalic dopamine neurons. *J Neurosci*. **20**: 8677-8684.

Difiglia M, Pasik T, Pasik P (1980). Ultrastructure of Golgi-impregnated and gold-toned spiny and aspiny neurons in the monkey neostriatum. *J Neurocytol*. **9**: 471-492.

Ding Y, Restrepo J, Won L, Hwang DY et al., (2007). Chronic 3,4-dihdroxypyhenylalanine treatment induces dyskinesia in aphakia mice, a novel genetic model of Parkinson´s disease. *Nerobiol Dis*. **27**: 11-23.

Ding Y, Won L, Britt JP, Lim AS et al., (2011). Enhanced striatal cholinergic neuronal activity mediates L-DOPA-induced dyskinesia in parkinsonian mice. *Proc. Natl. Acad. Sci. USA*. **108**: 840-845.

Dorsey ER, Constantinescu R, Thompson JP, Biglan KM et al., (2007). Projected number of people with Parkinson disease in the most populous nations, 2005 through 20130. *Neurology*. **68**: 384-386.

Dreher JC, Burnod Y (2002). An integrative theory of the phasic and tonic modes of dopamine modulation in the prefrontal cortex. *Neural Netw*. **15**: 583-602.

Dubach B, Schmidt R, Kundel D, Bowden DM et al., (1987). Primate neostriatal neurons containing tyrosine hydroxylase: immunohistochemical evidence. *Neurosci Lett*. **75**: 205-210.

Dubois B, Pillon B (1997). Cognitive deficits in Parkinson's disease. *J Neurol*. **244**: 2-8.

Dunwiddie TV, Roberson NL, Worth T (1982). Modulation of long-term potentiation: effects of adrenergic and neuroleptic drugs. *Pharmacol Biochem Behav*. **17**: 1257-1264.

Dutar P, Bassant MH, Senut MC, Lamour Y (1995). The septohippocampal pathway: structure and function of a central cholinergic system. *Physiol Rev*. **75**: 393-427.

El-Ghundi M, Fletcher PJ, Drago J, Sibley DR et al., (1999). Spatial learning deficit in dopamine D1 receptor knockout mice. *Eur J Pharmacol*. **383**: 95-106.

El-Ghundi M, O'Dowd BF, George SR (2001). Prolonged fear responses in mice lacking dopamine D_1 receptor. *Brain Res*. **892**: 86-93.

Elsworth JD, Roth RH (1997). Dopamine synthesis, uptake, metabolism and receptors: relevance to gene therapy of Parkinson´s disease. *Exp Neurol*. **144**: 4-9.

English DF, Ibañez-Sandoval O, Stark E, Tecuapetla F et al., (2011). GABAergic circuits mediate the reinforcement-related signals of striatal cholinergic interneurons. *Nat Neurosci*. **15**: 123-30.

Espadas I, Darmopil S, Vergaño-Vera E, Ortiz O, Oliva I, Vicario-Abejón C, Martín ED, Moratalla R (2012). L-DOPA-induced increase in TH-immunoreactive striatal neurons in parkinsonian mice: insights into regulation and function. *Neurobiol dis*. **48***: 271-81.*

Espejo M, Ambrosio S, Llorens J, Cutillas B (1998). Intrastriatal grafts of fetal mesencephalic cell suspensions in MPP^+-lesioned rats: a microdialysis study *in vivo*. *Neurochem Res.* **23**: 1217-1223.

Everitt BJ, Robbins TW (2005). Neural systems of reinforcement for drug addiction: from actions to habits to compulsion. *Nat Neurosci*. **8**: 1481-1490.

Fabrini G, Brotchie JM, Grandas F, Nomoto M, Goetz CG (2007). Levodopa-induce dyskinesias. *Mov Disord*. **22**: 1379-1389.

Fadok JP, Dickerson TM, Palmiter RD (2009). Dopamine is necessary for cue-dependent fear conditioning. *J Neurosci.* **29**: 11089-11097.

Fahn S (2006). Levodopa in the treatment of Parkinson´s disease. *J Neural Transm Suppl*. **71**: 1-15.

Ferland JMN, Zeeb FD, Yu K, Kaur S et al., (2014). Greater sensitivity to novelty in rats is associated with increased motor impulsivity following repeated exposure to a stimulating environment: Implications for the etiology of impulse control deficits. *Eur J Neurosci*. **40**: 3746-3756.

Fetsko LA, Xu R, Wang Y (2005). Effects of age and dopamine D2L receptor-deficiency on motor and learning functions. *Neurobiol Aging.* **26**: 521-30.

Fiorentini C, Rizzetti MC, Busi C, Bontempi S et al., (2006). Loss of synaptic D1 dopamine/N-

methyl-D-aspartate glutamate receptor complexes in L-DOPA-induced dyskinesia in the rat. *Mol Pharmacol.* **69**: 805-812.

Floresco SB, Magyar O (2006). Mesocortical dopamine modulation of executive functions: Beyond working memory. *Psychopaharmacology*. **188**: 567-85.

Francardo V, Recchia A, Popovic N, Andersson D et al., (2011). Impact of the lesion procedure on the profiles of motor impairment and molecular responsiveness to L-DOPA in the 6 -hydroxydopamine mouse model of Parkinson´s disease. *Neurobiol Dis*. **42**: 327-340.

Fremeau RT, Duncan GE, Fornaretto MG, Dearry A et al., (1991). Localization of D1 dopamine receptor mRNA in brain supports a role in cognitive, affective and neuroendocrine aspects of dopaminergic neurotransmission. *Proc. Natl. Acad. Sci. USA*. **88**: 3772-3776.

Frey U, Hartmann S, Mathies H (1989). Domperidone, an inhibitor of the D2-receptor blocks a late phase of an electrically induced long-term potentiation in the CA1-region in rats. *Biomed Biochem.* **7**: 473-476.

Frey U, Schroeder H, Matthies H (1990). Dopaminergic antagonists prevent long-term maintenance of posttentanic LTP in the CA1 region of rat hippocampal slices. *Brain Res*. **522**: 69-75.

Fujishiro H, Umegaki H, Suzuki Y, Oohara-Kurotani S et al., (2005). Dopamine D_2 receptor plays a role in memory function: implications of dopamine-acetylcholine interaction in the ventral hippocampus. *Psychopharmacology*. **182**: 253-61.

Gangarossa G, Longueville S, De Bundel D, Perroy J et al., (2012). Characterization of dopamine D_1 and D_2 receptor-expressing neurons in the mouse hippocampus. *Hippocampus*. **22**: 2199-2207.

Gangarossa G, Ceolin L, Paucard A, Lerner-Natoli M et al., (2014). Repeated stimulation of dopamine D1-like receptor and hyperactivation of mTOR signaling lead to generalized seizures, altered dentate gyrus plasticity and memory deficits. *Hippocampus*. **24**: 1466-1481.

Gao C, Sun X, Wolf ME (2006). Activation of D1 dopamine receptors increases surface expression of AMPA receptors and facilitates their synaptic incorporation in cultured hippocampal neurons. *J Neurochem*. **5**: 1664-1677.

Gardner B, Liu ZF, Jiang D, Sibley DR (2001). The role of phosphorylation/ dephosphorylation in agonist-induced desensitization of D1 dopamine receptor function: evidence for a novel pathway for receptor dephosphorylation. *Mol Pharmacol*. **59**: 310-321.

Garris PA, Ciolkowski EL, Pastore P, Wightman RM (1994). Efflux of dopamine from the synaptic cleft in the nucleus accumbens of the rat brain. *J Neurosci.* **14**: 6084-6093.

Gasbarri A, Sulli A, Packard M (1997). The dopaminergic mesencephalic projections to the hippocampal formation in the rat. *Prog NeuroPsychopharmacol Biol Psychiatry*. **21**: 1-22.

Gerfen CR (1992). The neostriatal mosaic: multiple levels of compartmental organization. *TINS.* **15**: 133-139.

Gerfen CR (2000). Molecular effects of dopamine on striatal-projection pathways. *Trends Neurosci*. **23**: S64-70.Gerfen CR, Surmeier DJ (2011).

Gerfen CR, Surmeier DJ (2011). Modulation of striatal projection systems by dopamine. Annu *Rev Neurosci*. **34**: 441-66.

Glickstein SB, Hof PR, Schmauss C (2002). Mice lacking dopamine D2 and D3 receptors have spatial working memory deficits. *J Neurosci*. **22**: 5619-5629.

Goldman JG, Litvan I (2011). Mild cognitive impairment in Parkinson´s disease. *Minerva Med*. **102**: 441-459.

Goldsmith SK, Joyce JN (1994). Dopamine D2 receptor expression in hippocampus and parahippocampal cortex of rat, cat and human in relation to tyroxine hydroxylase-immunoreactive fibers. *Hippocampus.* **4**: 354-73

Goldstein DS, Kopin IJ, Sharabi Y (2014). Catecholamine autotoxicity. Implications for pharmacology and therapeutics of Parkinson disease and related disorders. *Pharmacol Ther*. **144**: 268-282.

Goto Y, Grace AA (2005). Dopaminergic modulation of limbic and cortical drive of nucleus accumbens in goal-directed behavior. *Nat Neurosci*. **8**: 805-12.

Goto Y, Otani S, Grace AA (2007). The ying and yang of dopamine release: a new perspective. *Neuropharmacology*. **53**: 83-87.

Grace AA, Floresco SB, Goto Y, Lodge DJ (2007). Regulation of firing of dopaminergic neurons and control of goal-directed behaviors. *Trends Neurosci*. **30**: 220-7.

Grace AA (2008). Physiology of the normal and dopamine-depleted basal ganglia: insights into levodopa pharmacotherapy. *Mov Disord*. **23**. doi: 10.1002/mds.22020

Granado N, Ortiz O, Suárez LM, Martín ED, Ceña V, Solís JM, Moratalla R (2008). D1 but not D5 dopamine receptors are critical for LTP, spatial learning, and LTP-Induced arc and zif268 expression in the hippocampus. *Cereb Cortex*. **18**:1-12.

Granado N, Ares-Santos S, Oliva I, O´Shea E, Martin ED, Colado MI, Moratalla R (2011). Dopamine D2-receptor knockout mice are protected against dopaminergic neurotoxicity induced by methamphetamine or MDMA. *Neurobiol Dis*. **42**: 391-403.

Granado N, Ares-Santos S, Moratalla R (2014). D1 but not D4 dopamine receptors are critical for MDMA-induced neurotoxicity in mice. *Neurotox Res*. **25**: 100-109.

Grande C, Zhu H, Martín AB, Lee M, Ortiz O, Hiroi N, Moratalla R (2004). Chronic treatment with atypical neuroleptics induces striosomal FosB/DeltaFosB expression in rats. *Biol Psychiatry.* **55**: 457-463.

Graybiel AM, Ohta K, Roffler-Tarloy S (1990). Patterns of cell and fiber vulnerability in the mesostriatal system of the mutant mouse weaver. I. Gradients and compartments. *J Neurosci*. **10**: 720-33.

Grecksch G, Matties H (1981). The role of dopaminergic mechanisms in the rat hippocampus for the consolidation in a brightness discrimination. *Psychopharmacology (Berl).* **75**: 165-168.

Gruart A, Muñoz MD, Delgado-García JM (2006). Involvement of the CA3-CA1 synapse in the acquisition of associative learning in behaving mice. *J Neurosci.* **26**: 1077-1087.

Gurden H, Tassin JP, Jay TM (1999). Integrity of the mesocortical dopaminergic system is necessary for complete expression of in vivo hippocampal-prefrontal cortex long-term potentiation. *Neuroscience*. **94**: 1019-1027.

Gulyás AI, Hájos N, Katona I, Freund TF (2003). Interneurons are the local targets of hippocampal inhibitory cells which project to the medial septum. *Eur J Neurosci*. **17**: 1861-1872.

Gureviciene I, Ikonen S, Gurevicius K, Sarkaki A et al., (2004). Normal induction but accelerated decay of LTP in APP + PS1 transgenic mice. *Neurobiol Dis*. **15**:188-195.

Guridi J, González-Redondo R, Obeso JA (2012). Clinical features, pathophysiology and treatment of levodopa-induced dyskinesias in Parkinson´s disease. *Parkinsons Dis*. ID: 943159.

Guzowski JF, Lyford GL, Stevenson GD, Houston FP et al., (2000). Inhibition of activity-dependent arc protein expression in the rat hippocampus impairs the maintenance of long -term potentiation and the consolidation of long-term memory. *J Neurosci*. **20**: 3993-4001.

Hammond RS, Tull LE, Stackman RW (2004). On the delay-dependent involvement of the hippocampus in object recognition memory. *Neurobiol Learn Mem*. **82**: 26-34.

Harrison FE, Hosseini AH, McDonald MP (2009). Endogenous anxiety and stress responses in water maze and Barnes maze spatial memory tasks. *Behav Brain Res*. **198**: 247-251.

Heimer L, Van Hoesen G (1979). Ventral striatum. The Neuostriatum. *Ed 1. RGE Oberg*, 147-158. New York: Pergamon.

Higuera-Matas A, Botreau F, Del Olmo N, Miguéns M et al., (2010). Periadolescent exposure to cannabinoids alters the striatal and hippocampal dopaminergic system in the adult rat brain. *European Neurophychofarmacology*. **20**: 895-906.

Hout P, Levesque M, Parent A (2007). The fate of striatal dopaminergic neurons in Parkinson´s disease and Huntington´s chorea. *Brain*. **130**: 222-232.

Hout P, Parent A (2007). Dopaminergic neurons intrinsic to the striatum. *J Neurochem*. **101**: 1441-1447.

Hout P, Levesque M, Morissette M, Calon F et al., (2008). L-Dopa treatment abolishes the numerical increase in striatal dopaminergic neurons in parkinsonian monkeys. *J Chem Neuroanat*. **35**: 77-84.

Hranilovic D, Bucan M, Wang Y (2008). Emotional response in dopamine D2L receptor-deficient mice. *Behav Brain Res*. **195**: 246-250.

Huang YY, Kandel ER (1995). D1/D5 receptor agonists induce a protein synthesis-dependent late potentiation in the CA1 region of the hippocampus. *Proc. Natl. Acad. Sci. USA*. **92**: 2446-2450.

Hwang DY, Ardayfio P, Kang UJ, Semina EV, Kim KS (2003). Selective loss of dopaminergic neurons in the substantia nigra of Pitx3-deficient aphakia mice. *Brain Res Mol Brain Res*. **114**: 123-131.

Hwang DY, Fleming SM, Ardayfio P, Moran-Gates T et al., (2005). 3,4-dihydroxyphenylalanine reverses the motor deficits in Pitx3-deficient aphakia mice: behavioural characterization of a novel genetic model

of Parkinson´s disease. *J Neurosci*. **23**: 2132-7

Ibañez-Sandoval O, Tecuapetla F, Unal B, Shah F et al., (2010). Electrophysiological and morphological characteristics and synaptic connectivity of tyrosine hydroxylase-expressing neurons in adult mouse striatum. *J Neurosci*. **30**: 6999-7016.

Ibañez–Sandoval O, Xenías HS, Tepper JM, Koós T (2015). Dopaminergic and cholinergic modulation of striatal tyrosine hydroxylase interneurons. *Neuropharmacology.* **95**: 468-76.

Ichihara K, Nabeshima T, Kameyama T (1992). Effects of dopamine receptor agonists on passive avoidance learning in mice: interaction of dopamine D_1 and D_2 receptors. *Eur J Phar*. **213**: 243-249.

Ichise M, Ballinger JR, Tanaka F, Moscovitch M et al., (1998). Age-related changes in D_2 receptor binding with Iodine-123-Iodobenzofuran SPECT. *J Nucl Med*. **39**: 1511-1518.

Impey S, Fong AL, Wang Y, Cardinaux JR et al., (2002). Phosphorylation of CBP mediates transcriptional activation by neural activity and CaM kinase IV. *Neuron.* **34**: 235-244.

Inoue M, Suhara T, Sudo Y, Okubo Y et al., (2001). Age-related reduction of extrastriatal dopamine D_2 receptor measured by PET. *Life sciences*. **69**: 1079-1084.

Jacobs FMJ, Smits SM, Noorlander CW, Von Oerthel L et al., (2007). Retinoic acide couteracts developmental defects in the substantia nigra caused by Pitx3 deficiency. *Development*. **134**: 25673-2684.

Jacobs FMJ, van Erp S, van der Linden AJA, von Oerthel L et al., (2009). Pitx3 potentiates Nurr-1 in dopamine neurons terminal differentiation through release of SMRT-mediated repression. *Development*. **136**: 531-540.

Jankovic J (2005). Motor fluctuations and dyskinesias in Parkinson´s disease: clinical manifestations. *Mov Dirsord.* **20**: S11-S16.

John WS, Newman AH, Nader MA (2015). Differential effects for the dopamine D3 receptor antagonist PG01037 on cocaine and methamphetamine self-administration in rhesus monkeys. *Neuropharmacology*. **92**: 34-43.

Jollivet C, Montero-Menei CN, Venier-Julienne MC, Sapin A et al., (2004). Striatal tyrosine hydroxylase immunoreactive neurons are induced by L-dihydroxyphenylalanine and nerve growth factor treatment in 6-hydroxydopamine lesioned rats. *Neurosci Lett.* **362**: 79-82.

Jones MW, Errington ML, French PJ, Fine A et al., (2001). A requirement for the immediate early gene Zif268 in the expression of late LTP and long-term memories. *Nat Neurosci*. **4**: 289-296.

Joyce JN, Kaeger C, Ryoo H, Goldsmith S (1993). Dopamine D2 receptors in the hippocampus and amygdala in Alzheimer´s disease. *Neurosci Lett*. **154**: 171-4.

Joyce JN, Myers AJ, Gurevich E (1998). Dopamine D2 receptor bands in normal human temporal cortex are absent in Alzheimer´s disease. *Brain Res.* **784**: 7-17.

Kaasinen V, Vilkman H, Hietala J, Nagren K et al., (2000a). Age-related dopamine D2/D3 receptor loss in extrastriatal regions of the human brain. *Neurobiol Aging*. **21**: 683-688.

Kaasinen V, Ruottinen hM, Nagren K, Lehikoinen P et al., (2000b). Upregulation of putaminal dopamine D2 receptos in early Parkinson´s disease: a comparative PET study with (^{11}C)Raclopride and (^{11}C)*N*-Methylspiperone. *J Nucl Med*. **41**: 65-70.

Kaasinen V, Kemppainen N, Nagren K, Helenius H et al., (2002). Age-related loss of extrastriatal dopamine D2-like receptors in women. *J Neurochem*. **81**: 1005-1010.

Kabbani N, Negyessy L, Lin R, Goldman-Rakic P, Levenson R (2002). Interaction with neuronal calcium sensor NCS-1 mediates desensitization of the D2 dopamine receptor. *J Neurosci*. **22**: 8476-86.

Kakkar AK, Dahiya N (2015). Management of Parkinson´s disease: current and future pharmacotherapy. *Eur J Pharmacol*. **750**: 74-81.

Kandel ER (2001). The molecular biology of memory storage: a dialogue between genes and synapses. *Science*. **294**: 1030-1038.

Kelleher RJ 3rd, Govindarajan A, Jung HY, Kang H, Tonegawa S (2004). Translational control by MAPK signaling in long-term synaptic plasticity and memory. *Cell*. **116**: 467-479.

Kelly MA, Rubinstein M, Asa SL, Zhang G et al., (1997). Pituitary lactotroph hyperplasia and chronic hyperprolactinemia in dopamine D2 receptor-deficient mice. *Neuron.* **19**: 103-113.

Kelly MA, Rubinstein M, Phillips TJ, Lessov CN et al., (1998). Locomotor activity in D2 dopamine receptor-deficient mice is determined by gene dosage, genetic background, and developmental adaptations. *J Neurosci*. **18**: 3470-9.

Kemppainen N, Laine M, Laakso MP, Kaasinen V et al., (2003). Hippocampal dopamine D2 receptors correlate with memory functions in Alzheimer´s disease. *Eur J Neurosci*. **18**: 149-154.

Khan Zu, Gutiérrez A, Martin R, Peñafiel A et al., (2000). Dopamine D5 receptors of rat and human brain. *Neuroscience*. **100**: 689-699.

Kim BH, Hawes SL, Gillani F, Wallace LJ, Blackwell KT (2013). Signaling pathways involved in striatal synaptic plasticity are sensitive to temporal pattern and exhibit spatial specificity. *PLOS Comput Biol*. **9**:e1002953.

Kiyomi S, Arata S, Hosono T, Sano Y et al., (2006). Adiponection plays an important role in efficient energy usage under energy shortage. *Biochimica et Biophysica*. **1761**: 709-716

Knowlton BJ, Mangels JA, Squire LR (1996). A neostriatal habit learning systems in humans. *Science.* **273**: 1399-402.

Koós T, Tepper JM (2002). Dual cholinergic control of fast-spiking interneurons in the neostriatum. *J Neurosci*. **15**: 529-35.

O´Keefe J, Dostrovsky K(1971). The hippocampus as a spatial map. Preliminary evidence from unit activity in the freely-moving rat. *Brain Res.* **34**: 171-75

Kruse MS, Prémont J, Krebs MO, Jay TM (2009). Interaction of dopamine D1 with NMDA NR1 receptors in rat prefrontal cortex. *Eur Neuropsychopharmacol.* **19**: 296-304.

Le Doux J (1999). The emotional brain. New York: Simon & Schuster.

Lee FJ, Xue S, Pei L, Vukusic B et al., (2002). Dual regulation of NMDA receptor functions by direct protein-protein interactions with the dopamine D1 receptor. *Cell*. **18**:219-230.

Lee SP, So CH, Rashid AJ, Varghese G et al., (2004). Dopamine D1 and D2 receptor Co-activation generates a novel phospholipase C-mediated calcium signal. *J Biol Chem*. **279**: 35671-35678.

Leentjens AFG, Dujardin K, Marsh L, Richard IH et al., (2011). Anxiety rating scales in Parkinson´s disease: a validation study of the Hamilton Anxiety Rating Scale, the Beck Anxiety Inventory, and the Hospital Anxiety and Depression scale. *Mov Disord*. **26**: 407-415.

LeMoine C, Tison F, Bloch B (1990). D_2 dopamine receptor gene expression by cholinergic neurons in the rat striatum. *Neurosci Lett*. **117**: 248-252.

Levesque M, Bédard A, Cossette M, Parent A (2003). Novel aspects of the chemical anatomy of the striatum and is efferents projections. *J Chem Neuroanat*. **25**: 271-281.

Levin BE, Katzen HL (2005). Early cognitive changes and nondementing behavioral abnormalities in Parkinson's disease. *Adv Neurol*. **98:** 84-94.

Levitt M, Spector S, Sjoerdosma A, Udenfriend S (1965). Elucidation for the rate-limiting step in norepinephrine biosynthesis in the perfused guinea-pig heart. *J Pharmacol Exp Ther*. **148**: 1-8.

Lewis-tuffinLJ, Quinn PG, Chikaraishi DM (2004). Tyrosine hydroxylase transcription depends primarily on cAMP response element activity, regardless od the type of inducing stimulus. *Mol cell Neurosci*. **25**: 536-547.

Li SC, Lindenberger U, Sikström S (2001). Aging cognition: from neuromodulation to representation. *TRENDS Cogn Sci*. **5**: 479-486

Li SC, Sikström S (2002). Integrative neurocomputational perspectives on cognitive aging, neuromodulation and representation. *Neurosci Biobehav Rev*. **26**: 795-808.

Li S, Cullen WK, Anwyl R, Rowan MJ (2003). Dopamine-dependent facilitation of LTP induction in hippocampal CA1 by exposure to spatial novelty. *Nat Neurosci*. **6**: 526-531.

Li SC, Naveh-Benjamin M, Lindenberger U (2005). Aging neuromodulation impairs associative binding: a neurocomputational account. *Psychol Sci*. **16**: 445-50.

Lisman JE, Grace AA (2005). The hippocampal-VTA loop: controlling the entry of information into long-term memory. *Neuron*. **46**: 703-713.

Ljungberg T, Apicella P, Schultz W (1992). Responses of monkey dopamine neurons during learning of behavioral reactions. *J Neurophysiol*. **67**: 145-163.

Lopez-Real A, Rodrigez-Pallarés J, Guerra MJ, Labandeira-García JL (2003). Localization and functional significance of striatal neurons immunoreactive to aromatic L-amino acid decarboxylase or tyrosine hydroxylase in rat Parkinsonian models. *Brain Research*. **969**: 135-146.

Lovestone S, Killick R, Di Forti M, Murray R (2007). Schizophrenia as a GSK-3 dysregulation disorder. *TRENDS Neurosci*. **30**: 142-149.

Lundblad M, Picconi B, Lindgran H, Cenci MA. (2004). A model of L-DOPA-induced dyskinesia in 6-hydroxydopamine lesioned mice: relation to motor and cellular parameters of nigrostriatal function. *Neurobiol. Dis*. **16**: 110 -123.

Ma SY, Ciliax BJ, Stebbins G, Jaffar S et al., (1999). Dopamine transporter-immunoreactive neurons decrease with age in the human substantia nigra. *J Compt Neurol*. **409**: 25-37.

Madroñal N, Delgado-García JM, Gruart A (2007). Differential effects of long-term potentiation evoked at the CA3-CA1 synapse before, during, and after the acquisition of classical eyeblink conditioning in behaving mice. *J Neurosci.* **27**: 12139-12146.

Madroñal N, Gruart A, Delgado-García JM (2009). Differing presynaptic contributions to LTP and associative learning in behaving mice. *Front Behav Neurosci*. **3**:7.

Malenka RC, Bear MF (2004). LTP and LTD: an embarrassment of riches. *Neuron*. **44**: 5-21.

Mansikka H, Erbs E, Borrelli E, Pertovaara A (2005). Influence of the dopamine D2 receptor knockout on pain-related behaviour in the mouse. *Brain Research.* **1052**: 82-87.

Mao L, Lau YS, Petroske E, Wang JQ (2001). Profound astrogenesis in the striatum of adult mice following nigrostriatal dopaminergic lesion by repeated MPTP administration. *Brain Res Dev Brain Res.* **131**: 57-65.

Marder K, Levy G, Louis ED, Mejia-Santana H et al., (2003). Familial aggregation of early and late-onset parkinson´s disease. *Annals of Neurology*. **54**: 507-513.

Marin C, Jiménez A, Tolosa E, Bonastre M, Bové J (2004). Bilateral subthalamic nucleus lesión reverses L-DOPA-induced motor fluctuations and facilitates dyskinetic movements in Hemiparkinsonian rats. *Synapse*. **51**: 140-150.

Martín ED, Bruño W (2005). Stabilizing effects of extracellular ATP on synaptic efficacy and plasticity in hippocampal pyramidal neurons. *Eur J Neurosci*. **21**: 936-944.

Martin SJ, Morris RG (2002). New life in an old idea: the synaptic plasticity and memory hypothesis revisited. *Hippocampus.* **12**: 609-636.

Masuda M, Miura M, Inoue R, Imanishi M et al., (2011). Postnatal development of tyrosine hydroxylase mRNA-expressing neurons in mouse nostraitum. *Eur J Neurosci*. **34**: 1355-1367.

Matthies H, Becker A, Schröeder H, Kraus J et al., (1997). Dopamine D1-deficient mutant mice do not express the late phase of hippocampal long-term potentiation. *Neuroreport*. **8**: 3533-5

Mayr BM, Canettieri G, Montminy MR (2001). Distinct effects of cAMP and mitogenic signals on CREB-binding protein recruitment impart specificity to target gene activation via CREB. *Proc. Natl. Acad. Sci. USA*. **98**: 10936-10941.

Mazloom M, Smith Y (2006). Synaptic microcircutry of tyrosine hydroxylase-containing neurons and terminals in the striatum of 1-methyl-4-phenyl-1,2,3,6,-tetrahydropyridine-trated monkeys. *J Comp Neurol*. **495**: 453-469.

McEchron MD, Disterhoft JF (1997). Sequence of single neuron changes in CA1 hippocampus of rabbits during acquisition of trace eyeblink conditioned responses. *J Neurophysiol*. **78**: 1030-1044.

McEchron MD, Tseng W, Disterhoft JF (2003). Single neurons in CA1 hippocampus encode trace interval duration during trace heart rate (fear) conditioning in rabbit. *J Neurosci*. **23**: 1535-1547.

McGaugh JL (2015). Consolidating Memories. *Annu Rev Psychol*. **66**: 1-24.

McKinlay A, Grace RC, Dalrymple-Alford JC, Anderson TJ et al., (2008). Neuropsychiatric problems in parkinson´s disease: comparisons between self and caregiver report. *Aging & Mental Health*. **12**: 647-653.

McShane R, Keene J, Gendling K, Fairburn C et al., (1997). Do neuroleptic drugs hasten cognitive decline in dementia? Prospective study with necropsy follow up. *BMJ.* **314**: 266-70.

Meredith GE, Farrell T, Kellaghan P, Tan Y et al., (1999). Immunocytochemical characterization of catecholaminergic neurons in the rat striatum following dopamine-depletiong lesions. *Eur J Neurosci* . **11**: 3585-3596.

Messmer K, Remington MP, Skidmore F, Fishman PS (2007). Induction of tyrosine hydroxylase expression by the transcription factor Pitx3. *Int J Dev Neurosci*. **25**: 29-37.

Missale C, Nasj SR, Robinson SW, Jaber M, Caron MG (1998). Dopamine receptors: from structure to function. *Physiol Rev*. **78**: 189-225.

Mizumori SJY, Puryear CB, Martig AK (2009). Basal ganglia contributions to adaptive navigation. *Behav Brain Res*. **199**: 32-42.

Monastero R, Di Fiore P, Ventimiglia GD, Ventimiglia CC et al., (2012). Prevalence and profile of mild cognitive impairment in Parkinson´sdisease. *Neurodegener Dis*. **10**: 187-90.

Money KM, Stanwood GD (2013). Developmental origins of brain disorders: roles for dopamine. *Front Cell Neurosci*. **7**: 1-14

Moratalla R, Xu M, Tonegawa S, Graybiel AM (1996). Cellular responses to psychomotor stimulant and neuroleptic drugs are abnormal in mice lacking the D1 dopamine receptor. *Proc Natl Acad Sci USA*. **93**: 14928–14933.

Morris RGM (2006). Elements of a neurobiological theory of hippocampal function: the role of synaptic plasticity, synaptic tagging and schemas. *Eur J Neurosci*. **33**: 2829-2846.

Moser EI, Moser MB, Roudi Y (2013). Network mechanisms of grid cells. *Philos Trans R Soc Lond B Biol Sci.* **369**.

Moyer JRJ, Deyo RA, Disterhoft JF (1990). Hippocampectomy disrupts trace eye-blink conditioning in rabbits. *Behav Neurosci*. **104**: 243-252.

Müller U, von Cramon Y, Pollmann S (1998). D1 versus D2-receptor modulation of visuospatial working memory in humans. *J Neurosci*. **18**: 2720-2728.

Múnera A, Gruart A, Muñoz MD, Fernández-Más R, Delgado-García JM (2001). Discharge properties of identified CA1 and CA3 hippocampus neurons during unconditioned and conditioned eyelid responses in cats. *J Neurophysiol*. **86**: 2571-2582.

Muñoz P, Huenchuguala S, Paris I, Segura-Aguilar (2012). Dopamine oxidation and autophagy. *Parkinson´s disease*. ID: 920953.

Mura A, Jackson D, Manley MS, Young SJ, Groves PM (1995). Aromatic L-amino acid decarboxylase immunoreactive cells in the rat

striatum: a possible site for the conversion of exogenous L-Dopa to dopamine. *Brain Res*. **704**: 51-60.

Mura A, Linder jC, Young SJ, Groves PM (2000). Striatal cells containing aromatic L-Amino acid decarbosylase: an immunohisto-chemical comparison with other classes of striatal neurons. *Neuroscience*. **98**: 501-511.

Muramatsu SI, Fujimoto KI, Ikeguchi K, Shizuma N et al., (2002). Behavioral recovery in a primate model of Parkinson´s disease by triple transduction of striatal cells with adeno-associated viral vectors expressing dopamine-synthesizing enzymes. *Human gene therapy*. **13**: 345-354.

Murphy KE, Halliday GM (2014). Glucocerebrosidase deficits in sporadic Parkinson disease. *Autophagy*. **10**: 1350-1351.

Nadel L, Hupbach A, Gomez R, Newman-Smith K (2012). Memory formation, consolidation and transformation. *Neurosci Biobehav Rev*. **36**: 1640-1645.

Nader K, LeDoux JE (1999). Inhibition of the mesoamygdala dopaminergic pathway impairs the retrieval of conditioned fear associations. *Behav Neurosci*. **113**: 891-901.

Nakahara T, Yamamoto T, Endo K, Kayama H (2001). Neural ectopic expression of tyrosine hydroxylase in the mouse striatum by combined administration of 1-methyl-4-phenyl-1,2,3,6-tetrahydropyridine and 3-nitropropionic acid. *Neuroscience*. **108**: 601-610.

Nakamura T, Sato A, Kitsukawa T, Momiyama T et al., (2014). Distinct motor impairments of dopamine D1 and D2 receptor Knockout mice revealed by three types of motor behaviour. *Front Integrative Neurosci*. **8**: 1-11

Nakanishi S, Hikida T, Yawata S (2014). Distinct dopaminergic control of the direct and indirect pathways in reward-based and avoidance learning. *Neuroscience*. **282C**: 40-59.

Nakano K (2000). Neural circuits and topographic organization of the basal ganglia and related regions. *Brain & Development*. **22**: S5-S16.

Navarro G, Moreno E, Bonaventura J, Brugarolas M et al., (2013). Cocaine inhibits dopamine D_2 receptor signaling via Sigma-1-D_2 receptor heteromers. *PLOS ONE*. **8**: e1245.

Nevalainen N, Riklund K, Andersson M, Axelsson J et al., (2014). COBRA: a prospective multi-modal imaging study of dopamine, brain structure and function, and cognition. *Brain Research*. **1622:** 83-103.

Nguyen C, Tran AH, Matsumoto J, Hori E et al., (2014). Hippocampal place cell responses to distal and proximal cue manipulations in dopamine D2 receptor-knockout mice. *Brain Research*. **1567**: 13-27.

Nicola SM, Surmeier DJ, Malenka RC (2000). Dopaminergic modulation of neuronal excitability in the striatum and nucleus accumbens. *Annu Rev Neurosci*. **23**: 185-215.

Nieullon A (2002). Dopamine and the regulation of cognition and attention. Progress in *Neurobiol*. **678**: 53-83.

Nordström AL, Farde L, Halldin C (1992). Time course of D2-dopamine receptor occupancy examined by PET after single oral doses of haloperidol. *Psychopharmacology (Berl)*. **106**: 433-438

Nunes I, Tovmasian LY, Silva RM, Burke RE, Goff SP (2003). *Pitx3* is required for development of substantia nigra dopaminergic neurons. *Proc. Natl. Acad. Sci. USA*. **100**: 4245-50.

Nutt JG, Carter JH, Woodward WR (1995). Long -duration response to levodopa. *Neurology*. **45**: 1613-1616.

O'Carroll CM, Morris RG (2004). Heterosynaptic co-activation of glutamatergic and dopaminergic afferents is required to induce persistent long-term potentiation. *Neuropharmacology*. **47**: 324-332.

Okubo Y, Suhara T, Suzuki K, Kobayashi K et al., (1997). Decreased prefrontal dopamine D1 receptos in schizophrenia revealed by PET. *Nature*. **385**: 634-6.

O´Reilly R (2006). Biologically based computational models of high-level cognition. *Science*. **314**: 91-94.

Ortiz O, Delgado-García JM, Espadas I, Bahí A et al., (2010). Associative learning and CA3-CA1 synaptic plasticity are impaired in D1R null, D1R Knock-out mice and in hippocampal siRNA silenced DR1a mice. *J Neurosci.* **30**: 12288-12300.

Palfi S, Leventhal L, Chu Y, Ma SY et al., (2002). Lentivirally delivered glial cell line-derived neurotrophic factor increases the number of striatal dopaminergic neurons in primate models of nigrostriatal degeneration. *J Neurosci*. **22**: 4942-4954.

Palmiter RD (2011). Dopamine signaling as a neural correlate of consciousness. *Neuroscience.* **198**: 213-20.

Parikh V, Khan MM, Mahadik SP (2004). Olanzapine counteracts reduction of brain-derived neurotrophic factor and TrkB receptors in rat hippocampus produced by haloperidol. *Neurosci Lett*. **356**: 135-9.

Patil SS, Sunyer B, Höger H, Lubec G (2009). Evaluation of spatial memory of C57BL/6J and CD1 mice in the Barnes maze, the Multiple T-maze and in the Morris water maze. *Behav Brain Res*. **198**: 58-68.

Pavón N, Martín AB, Mendialdua A, Moratalla R (2006). ERK phosphorylation and FosB expression are associated with L-DOPA-induced dyskinesia in hemiparkinsonian mice. *Biol Psychiatry*. **59**:64-74.

Paxinos G, Franklin KBJ (2004). The Mouse Brain in Stereotaxic Coordinates. London: Academic Press.

Pei L, Lee FJ, Moszczynska A, Vukusic B, Liu F (2004). Regulation of dopamine D1 receptor function by physical interaction with the NMDA receptors. *J Neurosci*. **4**: 1149-1158.

Peterson GM (1989). Aquantitative analysis of the crossed septohippocampal projection in the rat brain. *Anat Embryol (Berl)*. **180**: 421-425

Piggott MA, Marshal EF, Thomas N, Lloyd S et al., (1999). Striatal dopaminergic markers in dementia with Lewy bodies, Alzheimer´s and Parkinson´s diseases: rostrocaudal distribution. *Brain*. **122:** 1449-68.

Piggott MA, Ballard CG, Rowan E, Holmes C et al., (2007). Selective loss of dopamine D2 receptors in temporal cortex in dementia with Lewy bodies, association with cognitive decline. *Synapse*. **61**: 903-911.

Pittenger C, Fasano S, Mazzocchi-Jones D, Dunnett SB et al., (2006). Impaired bidirectional synaptic plasticity and procedural memory formation in striatum-specific cAMP response element-binding protein-deficient mice. *J Neurosci*. **10**: 2808-2813.

Pons R, Syrengelas D, Youroukos S, Orfanou I et al., (2013). Levodopa-induced dyskinesias in tyrosine hydroxylase deficiency. *Mov Disord*. **28**: 1058-1063.

Porras-García E, Cendelin J, Domínguez-del-Toro E, Vožeh F, Delgado-García JM (2005). Purkinje cell loss affects differentially the execution, acquisition and prepulse inhibition of skeletal and facial motor responses in Lurcher mice. *Eur J Neurosci*. **21**: 979-988.

Porritt MJ, Batchelor PE, Hughes AJ, Kalnins R et al., (2000). New dopaminergic neurons in Parkinson´s disease striatum. *Lancet*. **356**: 44-45.

Porsolt RD, Bertin A, Jalfre M (1978). Behavioral despair in rats and mice: strain differences and the effects of imipramine. *Eur J of Pharmacology*. **51**: 291-294.

Puzzo D, Bizzoca A, Privitera L, Furnari D et al., (2013). F3/Contactin promotes hippocampal neurogenesis, synaptic plasticity, and memory in adult mice. *Hippocampus*. **23**: 1367-1382.

Rascol O, Brooks D, Korczyn AD, De Deyn PP et al., (2006). Development of Dyskinesias in a 5-year trial of ropinirole and L-DOPA. *Mov Disorders*. **21**: 1844-1850.

Reeves S, Bench C, Howard R (2002). Ageing and the nigrostriatal dopaminergic system. *Int J Geriatr Psychiatry*. **17**: 359-70

Reig R, Silberber G (2014). Multisensory integration in the mouse striatum. *Neuron*. **83**: 1200-12.

Rinne JO, Lönnberg P, Marjamäki P (1990). Age-dependent decline in human brain dopamine D1 and D2 receptors. *Brain Research*. **508**: 349-352.

Rivera A, Alberti I, Martin AB, Narvaez JA et al., (2002). Molecular phenotype of rat striatal neurons expressing the dopamine D5 receptor subtype. *Eur J Neurosci*. **16**: 2049-2058.

Rocchetti J, Isingrini E, Dal Bo g, Sagheby S et al., (2014). Presynaptic D2 dopamine receptors control Long-term depression expression and memory processes in the temporal hippocampus. *Biol Psychiatry*. **77**: 513-525.

Rodriguez-Oroz MC, Jahanshahi M, Krack P, Litvan I et al., (2009). Initial clinical manifestations of Parkinson´s disease: features and pathophysiologiucal mechanisms. *Lancet Neurol*. **8**: 1128-1139.

Ruiz-DeDiego I, Mellstrom B, Vallejo M, Naranjo JR, Moratalla R (2015). Activation of DREAM (downstream regulatory element antagonistic modulator), a calcium-binding protein, reduces L-DOPA-induced dyskinesias in mice. *Biol Psychiatry*. **77**: 95-105.

Ryan L, Lin CY, Ketcham K, Nadel L (2010). The role of medial temporal lobe in retrieving spatial and nonspatial relations from episodic and semantic memory. *Hippocampus.* **20:**11-8.

Saab BJ, Georgiou J, Nath A, Lee FJ et al., (2009). NCS-1 in the dentate gyrus promotes exploration, synaptic plasticity, and rapid acquisition of spatial memory. *Neuron.* **63**: 643-56.

Sacktor TC (2008). PKMzeta, LTP maintenance, and the dynamic molecular biology of memory

storage. *Prog Brain Res*. **169**: 27-40.

San Sebastián W, Guillen J, Manrique M, Belzunegui S et al., (2007). Modification of the number and phenotype of striatal dopaminergic cells by carotid body graft. *Brain*. **130**: 1306-1316.

Sarazin M, Deweer B, Merkl A, Von Poser N et al., (2002). Procedural learning and striatofrontal dysfunction in Parkinson´s disease. *Mov Disord*. **17**: 265-73.

Scatton B, Simon H, Le Moal M, Bischoff S (1980). Origin of dopaminergic innervation of the rat hippocampal formation. *Neurosci Lett*. **18**: 125-131.

Schapira AHV (2008). Mitochondrial dysfunction in neurodegenerative diseases. *Neurochem Res*. **33**: 2502-2509.

Schenider JS, Roeltgen DP (1993). Delayed matching-to-sample, object retrieval, and discrimination reversal deficits in chronic low dose MPTP- treated monkeys. *Brain Res.* **615**: 351-4.

Schultz W (2007). Multiple dopamine functions at different time courses. *Annu Rev Neurosci*. **30**: 259-88.

Schuster S, Doudnikoff E, Rylander D, Berthet A et al., (2008). Antagonizing L-type Ca^{+2} channel reduces development of abnormal involuntary movement in the rat model of L-3,4-Dihydroxyphenylalanine-induced dyskinesia. *Biol Psychiatry*. **65**: 518-526.

Schwartzkroin PA (1986). Regulation of excitability in hippocampal neurons. In: The Hippocampus. (Isacson RL, Pribram KH, eds), pp 113-136. New York, NY: Plenum Press.

Seamans JK, Yang CR (2004). The principal features and mechanisms of dopamine modulation in the prefrontal cortex. *Progress in Neurobiology*. **74**: 1-57.

Selemon LD, Goldman-Rackic PS (1990). Topographic intermingling of striatonigral and striatopallidal neurosn in the rhesus monkey. *J Comp Neurol.* **297**: 359-76.

Seligman ME, Rosellini RA, Kozak MJ (1975). Learned helplessness in the rat: time course, immunization, and reversibility. *J. Comp. Physiol. Psychol*. **88**: 542-7.

Setlow B, McGaugh JL (1999). Involvement of the posteroventral Caudate-Putamen in memory consolidation in the Morris Water Maze. *Neurobiology of Learning and Memory.* **71**: 240-247.

Setlow B, McGaugh JL (2000). D_2 dopamine receptor blockade immediately post-training enhances retention in hidden and visible platform versions of the water maze. *Learn Mem.* **7**: 187-191.

Shannon HE, Hart JC, Bymaster FP, Calligaro DO et al., (1999). Muscarinic receptor agonists, like dopamine receptor antagonist antipsychotics, inhibit conditioned avoidance response in rats. *J Pharmacol Exp Ther.* **290**: 901-907.

Slagter HA, Georgopoulou K, Frank MJ (2015). Spontaneous eye blink rate predicts learning from negative, but not positive, outcomes. *Neuropsychologia*. **71**: 126-32.

Smidth MP, Smits SM, Bouwmeester H, Hamers FPT et al., (2004). Early developmental failure of substantia nigra dopamine neurons in mice lacking the homeodomain gene *Pitx3. Development*. **131**: 1145-1155.

Smith DR, Striplin CD, Geller AM, Mailman RB et al., (1998). Behavioral assessment of mice lacking D1A dopamine receptors. *Neuroscience*. **86**: 135-146.

Smith JW, Fetsko LA, Xu R, Wang Y (2002). Dopamine D2L receptor knockout mice display deficits in positive and negative reinforcing properties of morphine and in avoidance learning. *Neuroscience*. **113**: 755-65.

Smith WB, Starck SR, Roberts RW, Schuman EM (2005). Dopaminergic stimulation of local protein synthesis enhances surface expression of GluR1 and synaptic transmission in hippocampal neurons. *Neuron*. **3**:765-779.

Solís O, Espadas I, Del-Bel EA, Moratalla R (2015). Nitric oxide synthase inhibition decreases L-DOPA-induced dyskinesia and the expression of striatal molecular markers in Pitx3-/- aphakia mice. *Neurobiol Dis*. **73**: 49-59.

Song DD, Haber SN (2000). Striatal responses to partial dopaminergic lesion: evidence for compensatory sprouting. *J Neurosci*. **20**: 5102 -14.

Sossi V, de la Fuente-Fernández, Schulzer M, Troiano AR et al., (2008). Dopamine trasnporter relation to dodpamine rurnover in Parkinson´s disease: a positrón emission tomography study. *Ann Neurol*. **62**: 468-474.

Sprengelmeyer R, Canavan AG, Lange HW, Hömberg V (1995). Associative learning in degenerative neostriatal disorders: contrasts in explicit and implicit remembering between Parkinson´s and Huntington´s diseases. *Mov Disord*. **10**: 51-65.

Squire LR, Knowlton BJ (1995). Learning about categories in the absence of memory. *Proc. Natl. Acad. Sci. USA*. **92:** 12470-12474.

Suarez LM, Solís O, Carmés JM, Taravini IR et al., (2014). L-DOPA treatment selectively restores spine density in dopamine receptor D2-expressing projection neurons in dyskinetic mice. *Biol Psychiatry*. **75**: 711-722.

Sugahara M, Shiraishi H (1998). Synaptic density of the prefrontal cortex regulated by dopamine instead of serotonin in rats. *Brain Research*. **814**: 143-156.

Sunahara RK, Guan HC, O´Dowd BF, Seeman P et al., (1991). Cloning of the gene for a human dopamine D5 receptor with higher affinity for dopamine than D1. *Nature*. **350**. 614-9.

Takamura N, Nakagawa S, Masuda T, Boku S et al., (2014). The effect of dopamine on adult hippocampal neurogenesis. *Prog Neuropsychopharmacol Biol Psychiatry*. **50**: 116-24.

Takatsuki K, Kawahara S, Kotani S, Fukunaga S et al., (2003). The hippocampus plays an important role in eyeblink conditioning with a short trace interval in glutamate receptor subunit delta 2 mutant mice. *J Neurosci*. **23**: 17-22.

Tanaka Y, Meguro K, Yamaguchi S, Ishii H et al., (2003). Decreased striatal D2 receptor density associated with severe behavioral abnormality in Alzheimer´s disease. *Ann Nucl Med*. **17**: 567 -73.

Tande D, Hoglinger G, Debeir T, Freundlieb N et al., (2006). New striatal dopamine neurons in MPTP-treated macaques result from a phenotypic shift and not neurogenesis. *Brain*. **129**: 1194-1200.

Tashiro Y, Sugimoto T, Hattori T, Uemura Y et al., (1989). Tyrosine Hydroxylase-Like Immunoreactive Neurons in the Striatum of the Rat. *Neuroscience Letters*. **97**: 6-10.

Tepper JM, Young SJ, Groves PM (1984). Autoreceptor-mediated changes in dopaminergic terminal excitability: effects of increases in impulse flow. *Brain Research*. **309**: 309-316.

Terry AV Jr, Hill WD, Parikh V, Waller JL et al., (2003). Differential effects of haloperidol, risperidone and clozapine exposure on cholinergic markers and spatial learning perm-formance in rats. *Neuropsychopharmacology*. **28**: 300-9.

Thanos PK, Roushdy K, Sarwar Z, Rice O et al., (2015). The effect of dopamine D4 receptor density on novelty, seeking, activity, social interaction, and alcohol binge drinking in adult mice. *Synapse*. **69:** 356-64.

Threlfell S, Lalic T, Platt NJ, Jennings KA et al., (2012). Striatal dopamine release is triggered by synchronized activity in cholinergic interneurons. *Neuron*. **75:** 58-64.

Trettel F, Rigamonti D, Hilditch-Maguire P, Wheeler VC et al., (2000). Dominant pehnotypes produced by the HD mutation in STHdh(Q111) striatal cells. *Hum Mol Genet*. **9**: 2799-809.

Unal B, Ibañez-Sandoval O, Shah F, Abercrombie ED, Tepper JM (2011). Distribution of tyrosine hydroxylase-expressing interneurons with respect to anatomical organization of the neostriatum. *Frontiers in systems Neuroscience*. **5**: 1-11.

Ungerstedt U (1968). 6-Hydroxy-dopamine induced degeneration of central monoamine neurons. *Eur J Pharmacol*. **5**: 107-110.

Ugrumov MV (2009). Non-dopaminergic neurons partly expressing dopaminergic phenotype: distribution in the brain development and functional significance. *J Chem Neuroanat.* **38**: 241 -256.

Vallone D, Picetti R, Borrelli E (2000). Structure and function of dopamine receptors. *Neurosci Biobehav Rev*. **24**: 125-132.

Vergaño-Vera E, Díaz-Guerra E, Rodríguez-Traver E, Méndez-Gómez HR et al., (2014). Nurr1 blocks the mitogenic effect of FGF-2 and EGF, inducing olfactory bulb neural stem cells to adopts dopaminergic and dopaminergic-GABAergic neuronal phenotypes. *Develp Neurobiol*. Doi: 10.1002/dneu.22251

Viosca J, Lopez de Armentia M, Jancic D, Barco A (2009). Enhanced CREB-dependent gene expression increases the excitability of neurons in the basal amygdala and primes the consolidation of contextual and cued fear memory. *Learm Mem*. **16**: 193-197.

Volkow ND, Gur RC, Wang GJ, Fowler JS et al.,. (1998). Association between decline in brain dopamine activity with age an cognitive and motor impairment in healthy individuals. *Am J Psychiatry*. **155**: 344-9.

Volkow ND, Logan J, Fowler JS, Wang GJ et al., (2000). Association between age-related decline in brain dopamine activity and impairment in frontal and cingulate metabolism. *Am J Psychiatry*. **157**: 75-80.

Wall VZ, Parker JG, Fadok JP, Darvas M et al., (2011). A behavioral genetics approach to understanding D1 receptor involvement in phasic dopamine signaling. *Molecular and Cellular Neuroscience* .**46**: 21-31.

Wang Y, Chan GL, Holden JE, Dobko T et al., (1998). Age-dependent decline of dopamine D1 receptors in human brain: a PET study. *Synapse*. **30**: 56-61.

Wang HD, Standwood GD, Grandy DK, Deutch AY (2009). Dystrophic dendrites in prefrontal cortical pyramidal cells of dopamine D1 and D2 but not D4 receptor knockout mice. *Brain research*. **1300**: 58-64

Watabe-Uchida M, Zhu l, Ogawa SK, Vamanrao A, Uchida N (2012). Whole-brain mapping of direct inpust to midbrain dopamine neurons. *Neuron*. **74:** 858-873.

Weihe E, Depboylu C, Schüz B, Schäfer MKH, Eiden LE (2006). Three types of tyrosine hydroxylase-positive CNS neurons distinguished by dopa decarboxylase and VMAT2 co-expression. *Cell Mol Neurobiol*. **26**: 659-678.

Weiner DM, Levey AI, Sunahara RK, Niznik HB et al., (1991). D_1 and D_2 dopamine receptor mRNA in rat brain. *Proc. Natl. Acad. Sci. USA*. **88**: 1859-1863.

Weintraub D, Comella CL, Horn S (2008). Parkinson´s disease, Part 3: Neuropsychiatric symptoms. *Am J Manag Care*. **14**: S59-69.

Weintraub D (2009). Impulse control disorders in Parkinson´s disease: prevalence and possible risk factors. *Parkinsonism Relat Disord*. **15**: S110-3.

Wells TT, Beevers CG, Knopik VS, McGeary JE (2013). Dopamine D4 receptor gene variation is associated with context-dependent attention for emotion stimuli. *Int J Neurospychopharmacol*. **16**: 525-534.

Westin JE, Vercammen L, Strome EM, Konradi C, Cenci MA (2007). Spatiotemporal pattern of striatal ERK1/2 phosphorylation in a rat model of L-DOPA-induced dyskinesia and the role of dopamine D1 receptors. *Biol Psychiatry*. **62**: 800-810.

Whishaw IQ, Dunnett SB (1985). Dopamine depletion, stimulation or blockade in the rat disrupts spatial navigation and locomotion dependent upon beacon or distal cues. *Behav Brain Res*. **18**:11-29.

White NM, Hiroi N (1998). Preferential localization of self-stimulation sites in striosomes/ patches in the rat striatum. *Proc. Natl. Acad. Sci. USA*. **95**: 6486-6491.

Wiescholleck V, Manahan-Vaughan D (2014). Antagonism of D1/D5 receptors prevents Long-term depression (LTD) and learning-facilitated LTD at the performant path dentate gyrus synapse in freely behaving rats. *Hippocampus*. **24**: 1615-1622.

Williams GV, Goldman-Rakic PS (1995). Modulation of memory fields by dopamine D1 receptors in prefrontal cortex. *Nature*. **376**: 572-575.

Winkler C, Kirik D, Björklund A, Cenci MA (2002). L-DOPA-induced dyskinesia in the intrastriatal 6-Hydroxydopamine model of Parkinson´s disease: relation to motor and cellular parameters of nigrostriatal function. *Neurobiol Disease*. **10**: 165-186.

Xie Z, Maddox WT, Knopik VS, McGeary JE, Chandrasekaran B (2015). Dopamine receptor D4 (DRD4) gene modulates the influence of information masking on speech recognition.

Neuropsychologia. **67**: 121-131.

Xing B, Kong H, Meng X, Wei SG et al., (2010). Dopamine D1 but not D3 receptor is critical for spatial learning and related signaling in the hippocampus. *Neuroscience.* **169**: 1511-9.

Xu M, Moratalla R, Gold LH, Hiroi N et al., (1994). Dopamine D1 receptor mutant mice are deficient in striatal expression of dynorphin and in dopamine-mediated behavioral responses. *Cell*. **79**: 729-742.

Xu TX, Yao WD (2010). D1 and D2 dopamine receptors in separate circuits cooperate to drive associative long-term potentiation in the prefrontal cortex. *Proc. Natl. Acad. Sci. USA*. **107**: 16366-16371.

Zalla T, Sirigu A, Pillon B, Dubois B et al., (1998). Deficit in evaluating pre-determined sequences of script events in patients with Parkinson´s disease. *Cortex*. **34**: 621-7.

Zhou QY, Pamiter RD (1995). Dopamine-Deficient mice are severely hypoactive, adipsic, and aphagic. *Cell.* **83**: 1197-1209.

Zweifel LS, Parker JG, Lobb CJ, Rainwater A et al., (2009). Disruption of NMDAR-dependent burs firing by dopamine neurons provides selective assessment of phasic dopamine-dependent behaviour. *Proc. Natl. Acad. Sci. USA*. **106**: 7281-7288.

Appendix

Associative learning and CA3-CA1 synaptic plasticity are impaired in D_1R null, *Drd1a*$^{-/-}$ and in hippocampal siRNA silenced *Drd1a* mice.

Oskar Ortiz[1,2], José María Delgado-García[3], Isabel Espadas[1,2], Amine Bahí[4], Ramón Trullas[2,5], Jean-Luc Dreyer[4], Agnés Gruart[3*] and Rosario Moratalla[1,2]

[1]Instituto Cajal, Consejo Superior de Investigaciones Científicas (CSIC), Madrid, Spain [2]Centro de Investigación Biomédica en Red sobre Enfermedades Neurodegenerativas, Instituto de Salud Carlos III, Madrid, Spain, [3]División de Neurociencias, Universidad Pablo de Olavide, Sevilla, Spain, [4]University of Fribourg, Fribourg, Switzerland, and [5]Instituto de Invest Biomédicas de Barcelona, CSIC, Barcelona, Spain

Behavioral/Systems/Cognitive

Associative Learning and CA3–CA1 Synaptic Plasticity Are Impaired in D_1R Null, *Drd1a*$^{-/-}$ Mice and in Hippocampal siRNA Silenced *Drd1a* Mice

Oskar Ortiz,[1,2] José María Delgado-García,[3] Isabel Espadas,[1,2] Amine Bahí,[4] Ramón Trullas,[2,5] Jean-Luc Dreyer,[4] Agnès Gruart,[3]* and Rosario Moratalla[1,2]*

[1]Instituto Cajal, Consejo Superior de Investigaciones Científicas (CSIC), Madrid 28002, Spain, [2]Centro de Investigación Biomédica en Red sobre Enfermedades Neurodegenerativas, Instituto de Salud Carlos III, Madrid 28002, Spain, [3]División de Neurociencias, Universidad Pablo de Olavide, Sevilla 41013, Spain, [4]University of Fribourg, Fribourg, Switzerland, and [5]Instituto de Invest Biomédicas de Barcelona, CSIC, Barcelona 08036, Spain

Associative learning depends on multiple cortical and subcortical structures, including striatum, hippocampus, and amygdala. Both glutamatergic and dopaminergic neurotransmitter systems have been implicated in learning and memory consolidation. While the role of glutamate is well established, the role of dopamine and its receptors in these processes is less clear. In this study, we used two models of dopamine D_1 receptor (D_1R, *Drd1a*) loss, D_1R knock-out mice (*Drd1a*$^{-/-}$) and mice with intrahippocampal injections of *Drd1a*-siRNA (small interfering RNA), to study the role of D_1R in different models of learning, hippocampal long-term potentiation (LTP) and associated gene expression. D_1R loss markedly reduced spatial learning, fear learning, and classical conditioning of the eyelid response, as well as the associated activity-dependent synaptic plasticity in the hippocampal CA1–CA3 synapse. These results provide the first experimental demonstration that D_1R is required for trace eyeblink conditioning and associated changes in synaptic strength in hippocampus of behaving mice. *Drd1a*-siRNA mice were indistinguishable from *Drd1a*$^{-/-}$ mice in all experiments, indicating that hippocampal knockdown was as effective as global inactivation and that the observed effects are caused by loss of D_1R and not by indirect developmental effects of *Drd1a*$^{-/-}$. Finally, *in vivo* LTP and LTP-induced expression of *Egr1* in the hippocampus were significantly reduced in *Drd1a*$^{-/-}$ and *Drd1a*-siRNA, indicating an important role for D_1R in these processes. Our data reveal a functional relationship between acquisition of associative learning, increase in synaptic strength at the CA3–CA1 synapse, and *Egr1* induction in the hippocampus by demonstrating that all three are dramatically impaired when D_1R is eliminated or reduced.

Introduction

Recent studies demonstrate that dopamine plays an important role in learning and memory. Moreover, integration of glutamate- and dopamine-mediated signals at the cellular level is required for persistent long-term potentiation (LTP) (O'Carroll and Morris, 2004), learning (Smith-Roe and Kelley, 2000; Baldwin et al., 2002), and long-term memory (O'Carroll et al., 2006). Exposure to a novel environment facilitates LTP (Li et al., 2003), linking dopamine signaling with enhanced LTP and with new information acquisition and storage (Lisman and Grace, 2005). Conversely, dopaminergic dysfunction significantly alters spatial learning and short- and long-term memory in rodents and in nonhuman primates (Whishaw and Dunnett, 1985; Williams and Goldman-Rakic, 1995). Dopamine depletion causes cognitive deficits in Parkinson's disease patients (Dubois and Pillon, 1997; Levin and Katzen, 2005), in agreement with studies in dopamine-deficient mice (Palmiter, 2008; Darvas and Palmiter, 2009), stressing the importance of dopamine in learning and associated synaptic plasticity.

The dopamine D_1 receptor (D_1R), in particular, has been implicated in mediating dopamine's effects in learning and synaptic plasticity. Pharmacological blockade of D_1/D_5 receptors significantly diminishes early and late phases of LTP in rat hippocampal slices (Otmakhova and Lisman, 1996) and blocks long-term memory storage (O'Carroll et al., 2006; Rossato et al., 2009) *in vivo*. Selective genetic inactivation of the dopamine D_1R subtype (*Drd1a*) differentiated between the roles of D_1 and D_5 receptor subtypes in LTP (Granado et al., 2008) and spatial learning (El-Ghundi et al., 1999; Granado et al., 2008). However, the role of the D_1R in associative learning and classical conditioning is less clear, as is its role in the synaptic changes that occur in hippocampal networks *in vivo* during the acquisition of new information. Most, if not all, of the electrophysiological studies involving D_1R have been performed *in vitro*.

Trace eyeblink conditioning, a form of associative learning, was recently shown to induce a progressive increase in strength at the hippocampal CA3–CA1 synapse in awake mice (Gruart et al.,

Received May 25, 2010; revised July 7, 2010; accepted July 20, 2010.

This work was supported by Grant PI071073 from Plan Nacional Sobre Drogas from the Spanish Ministerio de Sanidad y Política Social and Spanish Ministerio de Ciencia e Innovación Grants BFU2010-20664 (R.M.) and BFU2005-01024 and BFU2005-02512 (J.M.D.-G. and A.G.). O.O. was supported by a Basque Government Ph.D. fellowship. We thank M. Esteban, E. Rubio, and M. de Mesa for technical assistance and Dr. Angel Barco for help and advice with the fear-conditioning test.

*A.G. and R.M. contributed equally to this work.

Correspondence should be addressed to Dr. Rosario Moratalla, Instituto Cajal, Consejo Superior de Investigaciones Científicas, Avda Dr Arce, 37, Madrid, Spain. E-mail: moratalla@cajal.csic.es.

DOI:10.1523/JNEUROSCI.2655-10.2010

 0270-6474/10/3012288-13$15.00/0

Involvement of Cannabinoid CB1 receptor in associative learning and in hippocampal CA3-CA1 synaptic plasticity.

Noelia Madroñal[1], Agnés Gruart[1],Olga Valverde[2], Isabel Espadas[3], Rosario Moratalla[3,4] and José María Delgado-García[1]

[1]División de Neurociencias, Universidad Pablo de Olavide, Sevilla, Spain, [2] Departament de ciènces experimentals i de la salut, Grup de Recerca de Neurobiologia del comportament, Universitat Pompeu Fabra, Barcelona, Spain [3]Instituto Cajal, Consejo Superior de Investigaciones Científicas (CSIC), Madrid, Spain, [4]Centro de Investigación Biomédica en Red sobre Enfermedades Neurodegenerativas, Instituto de Salud Carlos III, Madrid, Spain.

Cerebral Cortex March 2012;22:550-566
doi:10.1093/cercor/bhr103
Advance Access publication June 14, 2011

Involvement of Cannabinoid CB1 Receptor in Associative Learning and in Hippocampal CA3–CA1 Synaptic Plasticity

Noelia Madroñal[1], Agnès Gruart[1], Olga Valverde[2], Isabel Espadas[3], Rosario Moratalla[3,4] and José M. Delgado-García[1]

[1]División de Neurociencias, Universidad Pablo de Olavide, Sevilla, [2]Departament de Ciències Experimentals i de la Salut, Grup de Recerca de Neurobiologia del Comportament, Universitat Pompeu Fabra, Barcelona, [3]Instituto Cajal, Consejo Superior de Investigaciones Científicas, Madrid, Spain and [4]Centro de Investigación Biomédica en Red sobre Enfermedades Neurodegenerativas, Instituto de Salud Carlos III, Madrid, Spain

Address correspondence to José M. Delgado-García, División de Neurociencias, Universidad Pablo de Olavide, Carretera de Utrera, Km 1, 41013-Sevilla, Spain. Email: jmdelgar@upo.es.

We studied, in behaving mice, the contribution of CB1 receptors to the activity-dependent changes induced at the hippocampal CA3–CA1 synapse by associative learning and following experimentally evoked long-term potentiation (LTP). Mice were classically conditioned to evoke eyelid responses with a trace paradigm using a tone as conditioned stimulus (CS) and an electric shock as unconditioned stimulus (US). Field excitatory postsynaptic potentials (fEPSPs) were evoked at the CA3–CA1 synapse during the CS–US interval across training. Conditioning was performed in presence of an agonist (WIN55,212-2) alone or with an antagonist (AM251) of the CB1 receptor, injected either systemically or locally. Conditioned responses (CRs) and fEPSP potentiation were depressed by WIN55,212-2. LTP was evoked by high-frequency stimulation of Schaffer collaterals after systemic or local WIN55,212-2 and AM251 injections. WIN55,212-2 affected the induction phase of LTP, mainly when injected locally. The addition of AM251 canceled out the effects of WIN55,212-2. Similar experiments were carried out in animals lacking the CB1 receptor ($CB1^{-/-}$ mice) and following silencing of hippocampal CB1 receptors (CB1R-siRNA–injected animals). In this case, CRs ($CB1^{-/-}$ mice) and LTP ($CB1^{-/-}$ and CB1R-siRNA–injected mice) reached lower values than their respective controls. Results offer new insights for understanding CB1 receptor contribution to associative learning and to CA3–CA1 synaptic plasticity.

Keywords: CB1, CB1 knockout mice, hippocampus, long-term potentiation, mice, siRNA, trace eyeblink conditioning

Introduction

Mammalian tissues contain at least 2 types of cannabinoid receptor: CB1 and CB2 (Matsuda et al. 1990; Munro et al. 1993). Both are classic G-protein–coupled receptors containing 7 transmembrane domains (Howlett 1995). The cannabinoid CB1 receptor is present in the central nervous system (CNS) and also in certain peripheral tissues, whereas CB2 has thus far been located primarily in peripheral tissues. However, recent investigations have shown CB2 receptor expression in neuronal populations (Morgan et al. 2009). CB1 receptors are expressed at nerve terminals, and an important function of these receptors is to suppress the release of a range of excitatory and inhibitory neurotransmitters (Gessa et al. 1997; Shen and Thayer 1998).

Learning and memory impairments are among the most commonly reported behavioral effects of cannabinoids (Lichtman et al. 1995; Pamplona and Takahashi 2006). These effects are thought to be associated with the hippocampus, since CB1 receptors are expressed at especially high density in the dentate gyrus, CA1, and CA3 regions (Herkenham et al. 1990, 1991; Matsuda et al. 1990; Pertwee 1997, 2001; Tsou et al. 1998; Julián et al. 2003; Martín et al. 2008). Both systemic injections (Iwasaki et al. 1992; Lichtman et al. 1995; Ferrari et al. 1999; Varvel et al. 2001; Da Silva and Takahashi 2002) and the direct administration of cannabinoid receptor agonists into the hippocampus (Lichtman et al. 1995; Egashira et al. 2002; Suenaga et al. 2008) induce deficits in various hippocampal-dependent tasks, such as the radial and water mazes. Furthermore, cannabinoid receptor activation in hippocampal slices impairs synaptic transmission and long-term potentiation (LTP) (Nowicky et al. 1987; Collins et al. 1994; Terranova et al. 1995, 1996; Serpa et al. 2009), whereas CB1 blockade enhances them (Terranova et al. 1995, 1996; Hoffman et al. 2007). Taken together, considerable evidence demonstrates that cannabinoid agonists impair, whereas cannabinoid antagonists improve memory and synaptic plasticity (Sullivan 2000; Davies et al. 2002). However, recent studies suggest that the cannabinoid system cannot be categorized into these previously described simple patterns. For example, the neural processes underlying memory formation are differentially sensitive to cannabinoid receptor activation or deactivation depending on the type of memory under examination (Abush and Akirav 2010). In addition, although initial studies using CB1-deficient mice reported increased memory performance in hippocampal-dependent tasks (Terranova et al. 1996) and enhancement of hippocampal LTP (Böhme et al. 2000), it has been reported latterly that the absence of CB1 receptors leads to an accelerated decline in cognitive functions (Bilkei-Gorzo et al. 2005).

In order to obtain a more complete perspective of cannabinoid CB1 receptor actions in alert behaving animals, we attempted to study here how the cannabinoid system contributes to several forms of in vivo hippocampal synaptic transmission processes (input/output curves, paired-pulse (PP) facilitation, and LTP induction in behaving animals), as well as to the acquisition of a well-known associative learning task—namely, the classical conditioning of eyelid responses using a trace paradigm. For this purpose, experimental manipulations at different levels were carried out: from the systemic injection of CB1 agonists and antagonists to the local silencing of hippocampal CB1 receptors (Ramiro-Fuentes et al. 2010), including the direct infusion of a cannabinoid agonist into the hippocampus and experiments carried out with mice lacking the CB1 receptor (Ledent et al. 1999; Aso et al. 2008). Results indicate a definite and complex role of cannabinoid CB1 receptors in hippocampal synaptic plasticity during experimentally evoked LTP and associative learning tasks.

L-DOPA-induced increase in TH-immunoreactive striatal neurons in parkinsonian mice: Insights into regulation and function.

Isabel Espadas[1,2], Sanja Darmopil[1,2], Eva Vergaño-Vera[1,2], Oskar Ortiz[1,2], Idaira Oliva[3], Carlos Vicario-Abejón[1,2], Eduardo D. Martón[3] and Rosario Moratalla[1,2*]

[1]Instituto Cajal, Consejo Superior de Investigaciones Científicas (CSIC), Madrid, Spain, [2]CIBENED, Instituto de Salud Carlos III, Madrid, Spain, [3]Laboratory of Neurophysiology and Syanptic plasticity, Albacete Science and Technology Park (PCyTA), Institute for Research in Neurological Disabilities (IDINE), University of Castilla-La Mancha, Albacete, Spain.

Neurobiology of Disease 48 (2012) 271–281

Contents lists available at SciVerse ScienceDirect

Neurobiology of Disease

journal homepage: www.elsevier.com/locate/ynbdi

L-DOPA-induced increase in TH-immunoreactive striatal neurons in parkinsonian mice: Insights into regulation and function

Isabel Espadas [a,b], Sanja Darmopil [a,b], Eva Vergaño-Vera [a,b], Oskar Ortiz [a,b], Idaira Oliva [c], Carlos Vicario-Abejón [a,b], Eduardo D. Martín [c], Rosario Moratalla [a,b,*]

[a] Cajal Institute, Consejo Superior de Investigaciones Científicas (CSIC), Spain
[b] CIBERNED, Instituto de Salud Carlos III, Madrid, Spain
[c] Laboratory of Neurophysiology and Synaptic Plasticity, Albacete Science and Technology Park (PCyTA), Institute for Research in Neurological Disabilities (IDINE), University of Castilla-La Mancha, Albacete, Spain

ARTICLE INFO

Article history:
Received 4 May 2012
Revised 6 July 2012
Accepted 10 July 2012
Available online 20 July 2012

Keywords:
Parkinson's disease
L-DOPA
D1 and D2 dopamine receptors
Pitx3 deficient aphakia mice
Fast scan cyclic voltammetry
Dopamine transporter (DAT)
Aromatic-L-amino acid decarboxylase (AADC)
Cylinder test
Olfactory bulb transplants

ABSTRACT

Tyrosine hydroxylase (TH)-immunoreactive (ir) neurons have been found in the striatum after dopamine depletion; however, little is known about the mechanism underlying their appearance or their functional significance. We previously showed an increase in striatal TH-ir neurons after L-DOPA treatment in mice with unilateral 6-OHDA lesions in the striatum. In the present study, we further examined the time-course and persistence of the effects of chronic L-DOPA treatment on the appearance and regulation of TH-ir neurons as well as their possible function. We found that the L-DOPA-induced increase in striatal TH-ir neurons is dose-dependent and persists for days after L-DOPA withdrawal, decreasing significantly 10 days after L-DOPA treatment ends. Using hemiparkinsonian D1 receptor knock-out ($D1R^{-/-}$) and D2 receptor knock-out ($D2R^{-/-}$) mice, we found that the D1R, but not the D2R, is required for the L-DOPA-induced appearance of TH-ir neurons in the dopamine-depleted striatum. Interestingly, our experiments in aphakia mice, which lack Pitx3 expression in the brain, indicate that the L-DOPA-dependent increase in the number of TH-ir neurons is independent of Pitx3, a transcription factor necessary for the development of mesencephalic dopaminergic neurons. To explore the possible function of L-DOPA-induced TH-ir neurons in the striatum, we examined dopamine overflow and forelimb use in L-DOPA-treated parkinsonian mice. These studies revealed a tight spatio-temporal correlation between the presence of striatal TH-ir neurons, the recovery of electrically stimulated dopamine overflow in the lesioned striatum, and the recovery of contralateral forelimb use with chronic L-DOPA treatment. Our results suggest that the presence of TH-ir neurons in the striatum may underlie the long-duration response to L-DOPA following withdrawal. Promotion of these neurons in the early stages of Parkinson's disease, when dopamine denervation is incomplete, may be beneficial for maintaining motor function.

Introduction

The central neuropathology of Parkinson's disease (PD) is the degeneration of dopaminergic neurons in the substantia nigra, leading to a dramatic decrease in dopaminergic innervation of the striatum. This loss of striatal dopamine causes the debilitating motor symptoms that characterize PD. Until recently, these nigral dopaminergic neurons were thought to be the sole source of striatal dopaminergic innervation. However, animal and human studies have demonstrated that dopaminergic neurons exist in the striatum itself (Betarbet et al., 1997; Busceti et al., 2008; Cossette et al., 2005; Huot and Parent, 2007). The number of these neurons increases significantly in animal models of Parkinson's disease (Betarbet et al., 1997; Darmopil et al., 2008; Jollivet et al., 2004; Lopez-Real et al., 2003; Mura et al., 1995, 2000).

These dopaminergic neurons in the striatum have been identified primarily based on expression of tyrosine hydroxylase (TH). Convincing evidence with BrdU experiments demonstrates that the striatal TH-immunoreactive (ir) neurons that appear in rodents and monkeys following dopaminergic denervation result from a phenotypic shift in which pre-existent GABAergic neurons begin to express TH, rather than from the birth of new neurons (Darmopil et al., 2008; Tandé et al., 2006). The existence of resident striatal TH neurons was further demonstrated using EGFP-TH BAC transgenic mice. These mice have multiple copies of a modified BAC containing the TH gene in which the TH mRNA coding sequence was replaced by sequences encoding the EGFP reporter gene (Ibáñez-Sandoval et al., 2010). In these mice, EGFP-positive neurons were evident in the striatum under basal conditions; however, TH-ir was only observed after colchicine treatment. Similarly, a more recent study in transgenic mice expressing EGFP under the control of the TH promoter reported the existence

* Corresponding author at: Cajal institute (CSIC), Avda Dr Arce 37, 28002 Madrid, Spain. Fax: +34 91 58 54 754.
E-mail address: moratalla@cajal.csic.es (R. Moratalla).
Available online on ScienceDirect (www.sciencedirect.com).

0969-9961/$ – see front matter © 2012 Elsevier Inc. All rights reserved.

Methamphetamine Causes Degeneration of Dopamine Cell Bodies and Terminals of the Nigrostriatal Pathway Evidenced by Silver Staining.

Sara Ares-Santos[1,2], Noelia Granado[1,2,3], Isabel Espadas[1,2], Ricardo Martinez-Murillo[1] and Rosario Moratalla[1,2*]

[1]Instituto Cajal, Consejo Superior de Investigaciones Científicas (CSIC), Madrid, Spain, [2]CIBENED, Instituto de Salud Carlos III, Madrid, Spain, [3]Facultad de Medicina, Universidad Complutense de Madrid, Madrid, Spain.

Neuropsychopharmacology (2014) 39, 1066–1080

www.neuropsychopharmacology.org

Methamphetamine Causes Degeneration of Dopamine Cell Bodies and Terminals of the Nigrostriatal Pathway Evidenced by Silver Staining

Sara Ares-Santos[1,2,4], Noelia Granado[1,2,3,4], Isabel Espadas[1,2], Ricardo Martinez-Murillo[1] and Rosario Moratalla*[,1,2]

[1]Instituto Cajal, Consejo Superior de Investigaciones Científicas (CSIC), Madrid, Spain; [2]CIBERNED, ISCIII, Madrid, Spain; [3]Facultad de Medicina, Universidad Complutense de Madrid, Madrid, Spain

Methamphetamine is a widely abused illicit drug. Recent epidemiological studies showed that methamphetamine increases the risk for developing Parkinson's disease (PD) in agreement with animal studies showing dopaminergic neurotoxicity. We examined the effect of repeated low and medium doses *vs* single high dose of methamphetamine on degeneration of dopaminergic terminals and cell bodies. Mice were given methamphetamine in one of the following paradigms: three injections of 5 or 10 mg/kg at 3 h intervals or a single 30 mg/kg injection. The integrity of dopaminergic fibers and cell bodies was assessed at different time points after methamphetamine by tyrosine hydroxylase immunohistochemistry and silver staining. The 3 × 10 protocol yielded the highest loss of striatal dopaminergic terminals, followed by the 3 × 5 and 1 × 30. Some degenerating axons could be followed from the striatum to the substantia nigra pars compacta (SNpc). All protocols induced similar significant degeneration of dopaminergic neurons in the SNpc, evidenced by amino-cupric-silver-stained dopaminergic neurons. These neurons died by necrosis and apoptosis. Methamphetamine also killed striatal neurons. By using D1-Tmt/D2-GFP BAC transgenic mice, we observed that degenerating striatal neurons were equally distributed between direct and indirect medium spiny neurons. Despite the reduced number of dopaminergic neurons in the SNpc at 30 days after treatment, there was a partial time-dependent recovery of dopamine terminals beginning 3 days after treatment. Locomotor activity and motor coordination were robustly decreased 1–3 days after treatment, but recovered at later times along with dopaminergic terminals. These data provide direct evidence that methamphetamine causes long-lasting loss/degeneration of dopaminergic cell bodies in the SNpc, along with destruction of dopaminergic terminals in the striatum.

Neuropsychopharmacology (2014) **39,** 1066–1080; doi:10.1038/npp.2013.307; published online 27 November 2013

Keywords: amphetamine derivatives; cell death; Parkinson's disease; psychostimulants; neurotoxicity; silver-degeneration stain

INTRODUCTION

Methamphetamine is an addictive illegal psychostimulant consumed by between 14.3 million and 53.1 million users worldwide, according to last estimations from the United Nations Office on Drugs and Crime (UNODC, 2013). Despite its high popularity, attributed to its wide availability, relative low cost, and long duration of psychoactive effects, methamphetamine is a neurotoxic drug that can produce long-lasting impairments in abusers (Krasnova and Cadet, 2009; McCann *et al*, 1998; Volkow *et al*, 2001a). Brain PET studies in human abusers showed dopamine transporter (DAT) reductions in the caudate nucleus and putamen that are associated with reduced motor skills (Volkow *et al*, 2001a,b; McCann *et al*, 1998). Furthermore, recent epidemiological studies provided evidence that the risk for developing Parkinson's disease (PD) is almost doubled in individuals with a history of methamphetamine use (Callaghan *et al*, 2012).

It is established that methamphetamine is a potent inducer of dopamine release and is toxic to dopamine neurons. Neurodegeneration of dopaminergic terminals in the striatum is evidenced by reductions in the immunoreactivity of tyrosine hydroxylase (TH), the rate-limiting enzyme for dopamine synthesis, and of DAT, accompanied by decreases in levels of dopamine and its metabolites (Ares-Santos *et al*, 2012, 2013a, b; Moratalla *et al*, 2014; Hotchkiss and Gibb, 1980; Granado *et al*, 2010, 2011a,b; Ricaurte *et al*, 1982,1984; Seiden *et al*, 1976; Wagner *et al*, 1980; Zhu *et al*, 2006a). Concomitant increases in reactive astrocytes and microglia in the striatum have also been described as indirect markers of this neurotoxicity.

However, a controversy exists regarding whether or not methamphetamine produces neurodegeneration of dopaminergic cell bodies in the substantia nigra pars compacta

*Correspondence: Dr R Moratalla, Instituto Cajal, Consejo Superior de Investigaciones Científicas (CSIC), Avda Dr Arce 37, Madrid 28002, Spain, Tel: +34 91 58 54 705, Fax: +34 91 58 54 754,
E-mail: moratalla@cajal.csic.es
[4]These authors contributed equally to this work
Received 2 September 2013; revised 21 October 2013; accepted 22 October 2013; accepted article preview online 30 October 2013

Nitric Oxide synthase inhibition decreases L-DOPA-induced dyskinesia and the expression of striatal molecular markers in Pitx3$^{-/-}$ aphakia mice.

Oscar Solís[1,2], Isabel Espadas[1,2*], Elaine A. Del-Bel[1] and Rosario Moratalla[1,2*]

[1]Instituto Cajal, Consejo Superior de Investigaciones Científicas (CSIC), Madrid, Spain, [2]CIBENED, Instituto de Salud Carlos III, Madrid, Spain, [3]Department of Morphology, Physiology and Pathology, School of Odontology, University of Sao Paulo, campus Ribeirao Preto, Brazil.

Neurobiology of Disease 73 (2015) 49–59

Contents lists available at ScienceDirect

Neurobiology of Disease

journal homepage: www.elsevier.com/locate/ynbdi

Nitric oxide synthase inhibition decreases L-DOPA-induced dyskinesia and the expression of striatal molecular markers in *Pitx3*$^{-/-}$ aphakia mice

Oscar Solís [a,b], Isabel Espadas [a,b], Elaine A. Del-Bel [c], Rosario Moratalla [a,b,*]

[a] Instituto Cajal, Consejo Superior de Investigaciones Científicas, CSIC, 28002 Madrid, Spain
[b] CIBERNED, Instituto de Salud Carlos III, Madrid, Spain
[c] Department of Morphology, Physiology and Pathology, School of Odontology, University of Sao Paulo, Campus Ribeirao Preto, Brazil

ARTICLE INFO

Article history:
Received 26 May 2014
Revised 12 September 2014
Accepted 21 September 2014
Available online 30 September 2014

Keywords:
Parkinson disease
L-DOPA
Abnormal involuntary movements
Nitrergic system
NO/cGMP
Pitx3 deficient aphakia mice
FosB
Histone3
Molsidomine
Zaprinast
Striatum

ABSTRACT

Nitric oxide (NO), a gaseous messenger molecule synthesized by nitric oxide synthase (NOS), plays a pivotal role in integrating dopamine transmission in the basal ganglia and has been implicated in the pathogenesis of Parkinson disease (PD). To study the role of the nitrergic system in L-DOPA-induced dyskinesia (LID), we assessed the effect of the pharmacological manipulation of NO levels and NO/cyclic guanosine monophosphate (cGMP) signaling on LID in the *Pitx3*$^{-/-}$ aphakia mouse, a genetic model of PD. To evaluate the effect of decreased NO signaling on the development of LID, *Pitx3*$^{-/-}$ mice were chronically treated with L-DOPA and 7-nitroindazole (7-NI, a neuronal NOS inhibitor). To evaluate its effect on the expression of established LID, 7-NI was administered acutely to dyskinetic mice. The chronic 7-NI treatment attenuated the development of LID in the *Pitx3*$^{-/-}$ mice, and the sub-acute 7-NI treatment attenuated established dyskinesia without affecting the beneficial therapeutic effect of L-DOPA. Moreover, 7-NI significantly reduced FosB and pAcH3 expression in the acutely and chronically L-DOPA-treated mice. We also examined how increasing NO/cGMP signaling affects LID expression by acutely administering molsidomine (an NO donor) or zaprinast (a cGMP phosphodiesterase 5-PDE5 inhibitor) before L-DOPA in mice with established dyskinesia. Paradoxically, the administration of either of these drugs also significantly diminished the expression of established LID; however, the effect occurred at the expense of the antiparkinsonian L-DOPA properties. We demonstrate that targeting the NO/cGMP signaling pathway reduces dyskinetic behaviors and molecular markers, but only the 7-NI treatment preserved the antiparkinsonian effect of L-DOPA, indicating that NOS inhibitors represent a potential therapy to reduce LID.

Introduction

Parkinson disease (PD) is a neurodegenerative disease with both genetic and acquired etiologies. It is characterized by the degeneration of the dopaminergic neurons of the substantia nigra and a decrease of dopamine (DA) in the dorsal striatum (Dauer and Przedborski, 2003). Despite the progress in PD research, current treatment focuses on dopamine replacement therapy through the administration of L-3,4-dihydroxyphenylalanine (L-DOPA). However, repeated treatment with L-DOPA is associated with adverse effects, including a reduction in drug efficacy ("wearing off" and "on–off" fluctuations) and the onset of dyskinesia. L-DOPA-induced dyskinesia (LID) is characterized by excessive and abnormal purposeless movements, which interfere with physiological motor activity. The prevalence of LID in PD patients increases with L-DOPA treatment duration, and once it develops, the LID severity increases over time. This LID can be debilitating and represents a major disadvantage of continued L-DOPA therapy (Gerlach et al., 2011; Jankovic, 2005; Prashanth et al., 2011).

Despite extensive investigation, the mechanisms underlying LID are not completely understood. Several lines of evidence have associated dyskinesia with the expression of FosB, phosphorylation of ERK1/2, and the phosphoacetylation of histone 3 (H3) (Andersson et al., 1999; Cenci and Konradi, 2010; Murer and Moratalla, 2011; Pavón et al., 2006; Santini et al., 2007; Westin et al., 2007). These molecular markers of dyskinesia require the D1, but not the D2, dopamine receptor (Darmopil et al., 2009). A wide range of other neurotransmitter systems and molecular mechanisms have been proposed to participate in the pathogenesis of dyskinesia, including glutamate, serotonin, adenosine, noradrenaline, and the cannabinoid receptor (González-Aparicio and Moratalla, 2014; Huot et al., 2013; Iravani and Jenner, 2011), but their precise contributions to LID remain less well understood. A growing body of evidence also suggests that nitric oxide (NO) plays a role in the maintenance of LID (Del Bel et al., 2005; Padovan-Neto et al., 2011).

The gaseous signaling molecule NO is produced by a subclass of interneurons containing the neuronal NO synthase (nNOS). NO activates the secondary messenger cyclic guanosine monophosphate (cGMP) through activation of soluble guanyl cyclase and plays a crucial role in

* Corresponding author at: Instituto Cajal, CSIC, Avd. Dr. Arce 37, 28002 Madrid, Spain. Fax: +34 91 585 4754.
E-mail address: moratalla@cajal.csic.es (R. Moratalla).
Available online on ScienceDirect (www.sciencedirect.com).

http://dx.doi.org/10.1016/j.nbd.2014.09.010
0969-9961/